Transcription Factor Regulation in Urothelial-Type Differentiation and Reprogramming

Arianna Hustler

PhD

University of York

Biology

May 2016

Abstract

For bladder tissue-engineering, there is a need for a surrogate epithelial cell source for patients whose own bladder epithelial cells (urothelial cells) are compromised by disease or cancer. Current work in the field has focused on attempting to differentiate various types of stem cells into urothelial cells using conditioned medium, co-culture or specific factors. These approaches have lacked clear focus, making it obvious that a better understanding of the transcription factors underlying urothelial lineage, development, and cell differentiation is necessary. The aim of the work presented in this thesis was to acquire specific knowledge regarding transcription factors involved in urothelial cell differentiation, which could be applied to an *in vitro* transdifferentiation approach of cell reprogramming. Since buccal mucosa is readily available, and already used as a grafted tissue for urology surgical applications, buccal epithelial cells were identified as a potential starting cell type.

An *in vitro* comparison of human buccal epithelial cells to urothelial cells revealed that buccal epithelial cells had weak transcript and protein expression of four transcription factors that play key roles in urothelial cell differentiation: ELF3, FOXA1, GATA3 and PPARγ. Since ELF3 and FOXA1 have been previously shown to act downstream of PPARγ in urothelial cells, PPARγ and GATA3 were chosen as key upstream transcription factors to overexpress in buccal epithelial cells. Investigation into PPARγ expression in human urothelial cells revealed that of the two main PPARγ protein isoforms, PPARγ1 was most critical for urothelial cell differentiation. Knockdown of GATA3 expression in urothelial cells using specific siRNA revealed an important role for GATA3 in maintaining the differentiated state of urothelium. Individual overexpression of GATA3 and PPARγ1 in human buccal epithelial cells was unable to cause complete transdifferentiation to urothelial cells, but each resulted in the upregulation of downstream genes that play critical roles in urothelial cell differentiation and barrier formation.

This work revealed key differences in transcription factor expression between buccal epithelial cells and urothelial cells, allowing for a better understanding of transcription factors involved in urothelial cell differentiation. The work provides a starting point for future urothelial-type cell reprogramming efforts which will likely require combined overexpression of several of these identified transcription factors to achieve complete transdifferentiation.

Table of Contents

List of Figures

List of Tables

Acknowledgements

I would firstly like to thank my supervisor Prof. Jenny Southgate for her advice and guidance throughout the last three years. Thanks also goes to the members of my training advisory panel, Dr. Paul Genever and Dr. Gonzalo Blanco, for their support during my project.

I would especially like to thank all members of the Jack Birch Unit for their advice and friendship. Special mention goes to Simon Baker, Jennifer Hinely, Ros Duke and Joanna Pearson for all of their help and advice. It was greatly appreciated.

I would also like to thank Mr. Ian Eardley for his help in obtaining buccal mucosa tissue samples, without which the project would not have been possible.

Most of all, I would like to that my parents for all of their support throughout my studies.

Author’s Declaration

The candidate confirms that the work presented in this thesis is her own, and that it has not been submitted for examination at this or any other institution for another award. The candidate also confirms that appropriate credit has been given where reference is made to the work of others.

Chapter 1:

Introduction

1 Introduction

1.1 Peroxisome Proliferator-Activated Receptor Gamma (PPARγ)

PPARγ is a nuclear receptor, which when bound to retinoid X receptor α (RXRα), and activated by a specific ligand, is able to act as a transcription factor to regulate gene expression. PPARγ is best known as a key transcription factor involved in adipocyte differentiation (reviewed in Lefterova et al., 2014), but it has also been shown to have important roles in other cell types including macrophages, and both prostate and bladder epithelia (Ricote et al., 1998; Varley et al., 2006; Strand et al., 2013). PPARγ is one of a family of receptors which also includes PPARα and PPARβ/δ.

1.1.1 PPARγ Transcript Variants

The most recent description of human PPARG transcript variants defines four main splice variants (PPARG1, PPARG2, PPARG3 and PPARG4), which produce two unique proteins, PPARγ1 and PPARγ2 (Aprile et al., 2014) (Figure 1.1). The PPARG1, PPARG3 and PPARG4 transcript variants differ in their 5' untranslated regions (UTRs) and promoter usage, but all produce the same protein product, PPARγ1 (Aprile et al., 2014). The PPARγ2 protein is produced from the PPARG2 transcript variant, which is generated though alternate promoter usage (Tontonoz et al., 1994). The human PPARγ2 protein contains the same protein sequence as PPARγ1, but has an additional 28 amino acids at its N-terminus; the human PPARγ1 protein is 477 amino acids, while the human PPARγ2 protein is 505 amino acids (Fajas et al., 1997).

In addition to the transcript variants mentioned above, several other PPARγ splice variants have been identified in humans (Chen et al., 2006). Various truncated isoforms have also been identified, which lack the exons necessary to produce the ligand binding domain; these transcript variants have been described to act in a dominant negative fashion, inhibiting full length PPARγ expression (Kim et al., 2006; Aprile et al., 2014).

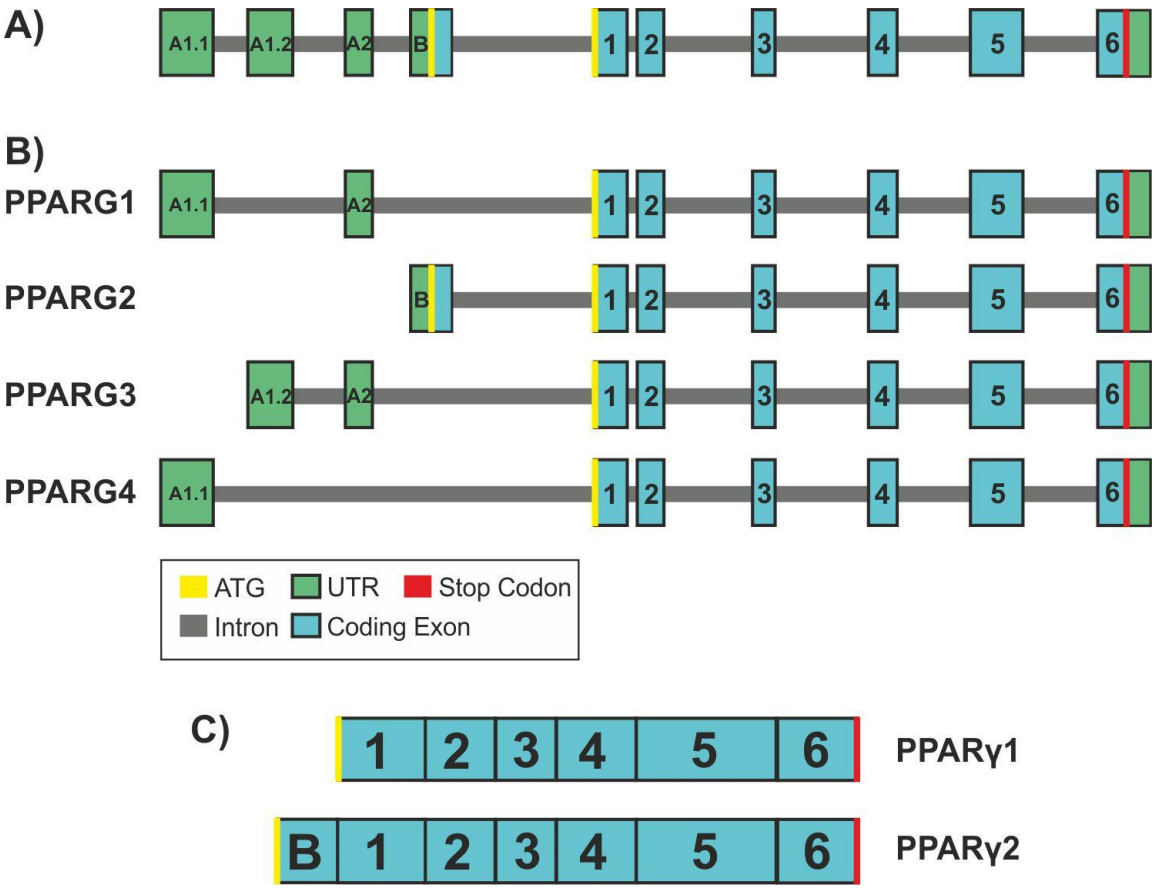

Figure 1.1 Human PPARγ Transcript Variants

A) The most recent description of the human PPARG gene structure defines ten exons: A1.1, A1.2, A2, B and 1-6 (Aprile et al., 2014). Alternative splicing of these exons results in the production of four main protein coding transcript variants, which are used to produce the PPARγ1 and PPARγ2 proteins. Several other protein coding and non-protein coding splice variants have also been described in humans (Chen et al., 2006).

B) Three PPARγ transcript variants produce PPARγ1 protein: PPARG1, PPARG3, PPARG4; these variants all differ in their 5' UTR (Aprile et al., 2014). Translation of the PPARG2 variant produces the PPARγ2 protein.

C) The PPARγ1 protein is produced from the translation of exons 1-6. The PPARγ2 protein is produced from the translation of a portion of exon B plus exons 1-6, which results in the human PPARγ2 protein having the same amino acid sequence as PPARγ1, with an additional 28 amino acids at the N-terminus (Fajas et al., 1997).

This figure is adapted from (Aprile et al., 2014).

1.1.2 PPARγ Structure, Ligand Binding and Modifications

The PPARγ proteins, like other nuclear receptors, contain four distinct regions: an N-terminal ligand-independent activation function (AF1), a DNA binding domain, a hinge domain, and a C-terminal ligand binding domain, which contains a ligand-dependent activation function (AF2) (reviewed in Jin and Li, 2010) (Figure 1.2). The AF-1 and AF-2 domains act as docking sites for coactivators and corepressors (Nolte et al., 1998; Bugge et al., 2009).

The PPARγ-RXRα heterodimer binds to a specific site in promoter regions called the PPAR response element (PPRE) (Chandra et al., 2008). It consists of two repeated sequences with a single base pair in the middle: 'AGGTCAxAGGTCA'. The DNA binding domain of PPARγ binds to the first (5') sequence, and the DNA binding domain of RXRα binds to the second sequence (Jpenberg et al., 1997) (Figure 1.3).

The majority of PPARγ-mediated transcriptional activity requires the binding of a ligand to the ligand binding domain, which causes a conformational change in the PPARγ protein structure in order to elicit gene activation (Chandra et al., 2008). There have been several natural ligands described for PPARγ, including some unsaturated and oxidized fatty acids, and prostaglandins, but they are all known to have weak binding affinities (Kliewer et al., 1995; Kliewer et al., 1997). Potent synthetic ligands have been identified which bind to and activate PPARγ at high affinity; one group of ligands, termed thiazolidinediones, includes troglitazone, pioglitazone and rosiglitazone (Lehmann et al., 1995). RXRα is also ligand mediated, with its natural ligand being 9-*cis*-retinoic acid (Heyman et al., 1992).

Several forms of PPARγ modification occur which can affect its ability to modulate gene expression; these include sumoylation, phosphorylation and ubiquitination. PPARγ has been shown to be regulated by small ubiquitin-related modifier 1 (SUMO-1) modification (Ohshima et al., 2004). Ohshima et al. demonstrated that the conjugation of SUMO-1 to PPARγ resulted in a repression of PPARγ-dependent transcription. It was later shown, by another group, that the sumoylation of PPARγ prevented the removal of corepressor proteins from PPARγ-dependent promoters, and thus inhibited gene activity (Pascual et al., 2005). Phosphorylation of PPARγ has also been shown to

reduce PPARγ activity, and several groups have demonstrated that the phosphorylation of PPARγ is mediated by mitogen activated protein (MAP) kinases (Hu et al., 1996; Zhang et al., 1996; Camp and Tafuri, 1997). Another form of modification shown to regulate PPARγ is ubiquitination, which has been shown to occur prior to PPARγ degradation by the proteasome (Hauser et al., 2000).

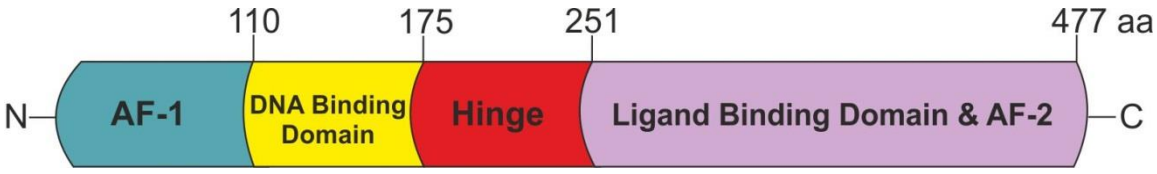

Figure 1.2 Human PPARγ1 Linear Protein Structure

The PPARγ protein structure, like other nuclear receptors, contains four main protein domains:

AF-1 Domain - Acts as a ligand independent transactivation domain and interacts with both coactivators and corepressors (Bugge et al., 2009). It is also a site where posttranslational modifications occur (Adams et al., 1997).

DNA Binding Domain - Interacts directly with PPRE sequences in promoter regions (Chandra et al., 2008).

Hinge Domain - A flexible portion of the protein between the DNA and ligand binding domains.

Ligand Binding Domain – Location where PPARγ agonist binds to allow for transcriptional activation (Chandra et al., 2008). The AF-2 domain is located at the C-terminus, and its function is dependent on ligand binding (Nolte et al., 1998).

This figure is adapted from (review by Rosen and Spiegelman, 2001; review by Jin and Li, 2010).

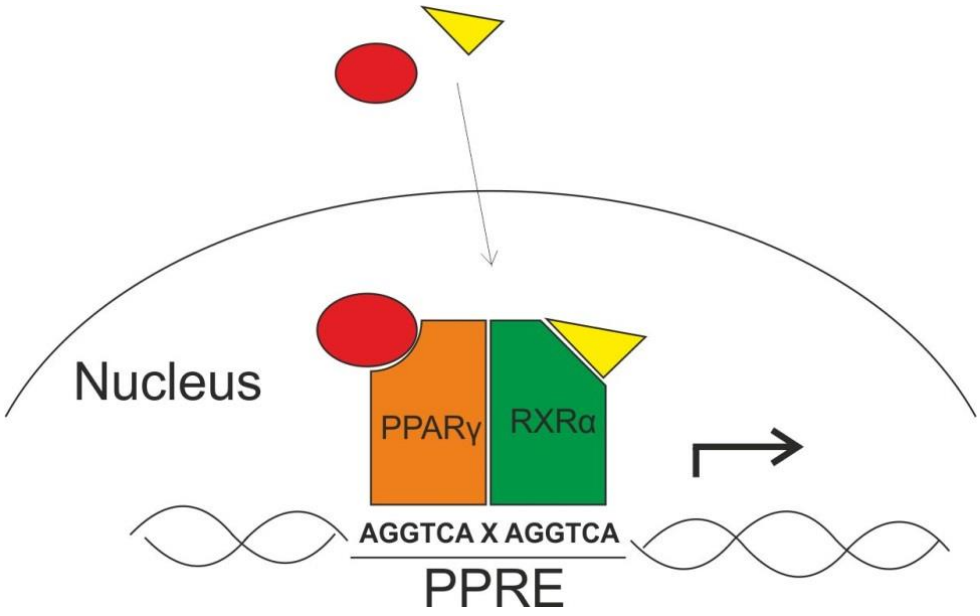

Figure 1.3 PPARγ-RXRα Binding at a PPRE

Simplified diagram showing PPARγ heterodimerisation with RXRα, and ligand binding, at a PPRE. The binding of an agonist to PPARγ causes a conformational change in the ligand binding domain, which allows for transcriptional activation to occur (Chandra et al., 2008). Common synthetic ligands used to activate PPARγ include troglitazone, pioglitazone and rosiglitazone (Lehmann et al., 1995). The common natural ligand for RXRα is 9-*cis*-retinoic acid (Heyman et al., 1992).

This figure is adapted from (review by Ahmadian et al., 2013).

1.1.3 PPARγ Knockout Mice

PPARγ knockout mice die before embryonic day 10 (E10.0) due to a defective placenta (Barak et al., 1999). In the study, the authors showed that PPARγ1 is highly expressed in the placenta from at least E8.5. To determine the effect of PPARγ beyond this early stage, a mouse was produced which was PPARγ-null, but could generate a wild-type placenta during development, allowing the embryo to be viable. The mouse was sacrificed at postnatal day 6.5 where it was shown that it had failed to develop all types of adipose tissue.

To determine the role of the different PPARγ isoforms in mouse development, PPARγ2-null mice were generated by two groups and showed some similar and differing results (Zhang et al., 2004; Medina-Gomez et al., 2005). Overall, both studies found that PPARγ2 knockout mice survived to term and displayed normal development. PPARγ2-null mice generated by Zhang et al. had reduced amounts of white adipose tissue, and histological analysis of the white adipose tissue present showed a marked difference in appearance in comparison to control mice. By contrast, Medina-Gomez et al. saw no difference in the amount or appearance of white adipose tissue between the PPARγ2-null and control mice. Both groups did demonstrate that the expression of several genes (LPL, aP2, Leptin, Resistin) known to play important roles in adipocytes were significantly downregulated in PPARγ2-null white adipose tissue. They also both demonstrated that when preadipocyte cells were taken from PPARγ2-null mice and induced to differentiate *in vitro*, their differentiation capacity was greatly impaired. These results whilst indicating a potential role for PPARγ2 in white adipose tissue development *in vivo*, suggested its involvement was not essential, since adipose tissue was still generated in both instances.

1.1.4 PPARγ in Adipogenesis

Adipogenesis is the process of generating mature adipocytes. Much of the work done to investigate adipocyte differentiation has been completed *in vitro* using a mouse embryonic fibroblast cell line, called NIH 3T3-L1, which is predisposed to adipocyte differentiation. Using this model system, among others, PPARγ was identified as an important regulator of both adipogenesis and maintenance of the adipocyte phenotype; PPARγ-null fibroblasts were incapable of undergoing adipocyte differentiation (Rosen et al., 2002), and mature NIH 3T3-L1 adipocytes, which were transduced to overexpress a dominant negative form of PPARγ, displayed impairment of the adipocyte phenotype (Tamori et al., 2002).

Adipogenesis is thought to occur through a two-stage transcription factor activation cascade (Lefterova et al., 2014). During the first part of adipogenesis, following initiation by blocking proliferation and cyclin D1 expression (Fu et al., 2005), two key transcription factors are upregulated, C/EBPβ and C/EBPδ (Wu et al., 1995b; Tanaka et al., 1997). The upregulation of these transcription factors causes the second stage of adipogenesis, where upregulation of PPARγ and C/EBPα expression occurs (Rosen et al., 2002). The expression of C/EBPα is thought to play a role in the maintenance of PPARγ expression; C/EBPα has been shown to directly bind to, and activate expression of PPARγ2 in adipocytes (Rosen et al., 2002).

Using *in vitro* models, both PPARγ1 and PPARγ2 have been shown to play important roles during adipogenesis. Mueller et al. used a PPARγ-null murine fibroblast cell line to demonstrate that the independent overexpression of PPARγ1 or PPARγ2 was able to induce adipocyte differentiation when the appropriate ligands were present. In low ligand concentrations, PPARγ2 overexpression was found to be better at inducing adipocyte differentiation than PPARγ1 overexpression (Mueller et al., 2002).

1.2 GATA Binding Protein 3 (GATA3)

GATA3 is a member of the GATA family of transcription factors. All six GATA transcription factors (GATA1-6) contain two zinc finger domains (C-terminal and N-terminal) which can bind directly to the DNA of target genes. Binding of the C-terminal zinc finger to '(A/T)GATA(A/G)' sequences of promoter regions is able to either activate or repress gene expression (Ko and Engel, 1993; Bates et al., 2008). The binding of the N-terminal zinc finger in GATA-2 and -3 to 'GATC' is also able to elicit gene activity (Pedone et al., 1997). GATA transcription factors are considered to be 'pioneer factors', with the ability to bind to areas of condensed chromatin, allowing access to silenced genes (reviewed in Zaret and Carroll, 2011).

Knockout of GATA3 in mice is embryonically lethal, with death occurring at embryonic day 11 or 12. This occurs as a result of several factors which include internal bleeding, growth retardation, malformations of the brain and spinal cord, and abnormal liver haematopoiesis. GATA3 is best studied for its important regulatory role in T cell

commitment and differentiation (reviewed in Wan, 2014). Depending on the T cell type, GATA3 binds to and regulates a wide range of target genes (Wei et al., 2011). In T helper 2 cells, GATA3 was shown to both bind to and positively regulate PPARγ gene expression in mice (Wei et al., 2011).

GATA3 has a well-documented role in breast epithelial cell differentiation and cancer progression. In normal mammary epithelium, GATA3 is expressed in the luminal epithelial cells, but not in the basal epithelial cells (Kouros-Mehr et al., 2006). Mammary epithelium-specific knockout of GATA3 in mice resulted in reduced mammary gland branching and bud formation (Kouros-Mehr et al., 2006). The mammary epithelium was also affected, and formed areas of multi-layered epithelium, which was caused by the expansion of undifferentiated luminal cells.

The expression of GATA3 is also strongly associated with breast cancer, where low GATA3 expression is indicative of poor prognosis (Mehra et al., 2005). GATA3 expression varies among metastatic and non-metastatic breast cancers, with metastatic breast cancers having low GATA3 expression. In contrast, the non-metastatic breast carcinoma-derived cell line, MCF-7, has high GATA3 expression (Kouros-Mehr et al., 2008). GATA3 has been shown to act upstream of, and directly regulate the expression of another key transcription factor involved in breast cancer development, forkhead box protein A1 (FOXA1) (Kouros-Mehr et al., 2006; Theodorou et al., 2013).

In human epidermis, GATA3 is expressed in both the basal and suprabasal layers (Chikh et al., 2007). It has been suggested that GATA3 may be regulated in part by p63 in the skin, and it has been shown that both the Tap63 and ΔNp63 isoforms are able to bind to the GATA3 promoter to activate gene expression (Candi et al., 2006; Chikh et al., 2007). Epidermal-specific deletion of GATA3 in mice resulted in death shortly after birth due to a defective skin barrier (de Guzman Strong et al., 2006). Mice had desiccated skin at birth, and the rate of water loss across the epidermis was significant in comparison to control mice. The authors identified that the cause of the barrier impairment was as a result of abnormal lipid synthesis, with tight junctions and the cornified cell envelope appearing normal.

1.3 Urothelium

The renal pelvis, ureters, bladder and upper portion of the urethra are lined on their luminal surfaces by a specialised epithelium called urothelium. The primary role of the urothelium is to act as a permeability barrier to the toxins present in urine, preventing them from re-entering the body. Urothelium is classified as a transitional type of epithelium. It is derived from the embryonic endoderm layer in the bladder and urethra, and the embryonic mesoderm layer in the renal pelvis and ureters (review by Staack et al., 2005). It consists of three main epithelial cell zones: basal, intermediate and superficial (Figure 1.4), and in general averages approximately 4-5 cell layers thick (Jost et al., 1989).

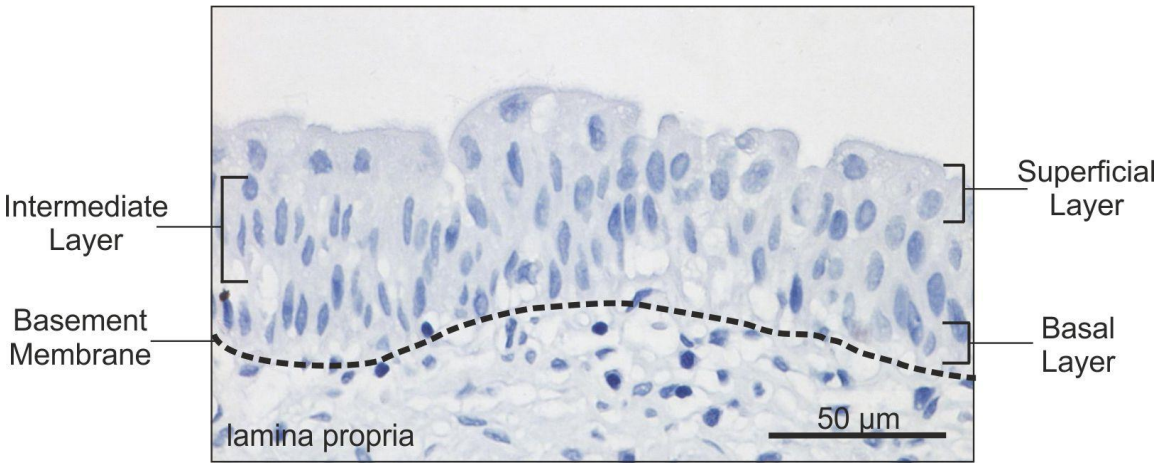

Figure 1.4 Human Urothelium

Haematoxylin stained human bladder epithelium section. The three epithelial zones of the transitional epithelium are shown: the basal layer, intermediate layer and superficial layer. The dashed line represents the basement membrane, which separates the epithelium from the underlying connective tissue.

Urothelium is a largely quiescent tissue, with a very low cell turnover rate (Limas, 1993); when urothelium sections are analysed for Ki67 expression, a marker of proliferating cells, the expression is either absent or limited to a few cells (Varley et al., 2005). In response to insult or injury, the quiescent nature of urothelium changes to a highly regenerative phenotype, which allows for rapid repair of the epithelium (Pust et al., 1976). Like other multi-layered epithelia, urothelium has a hierarchical structure; the

least differentiated cells make up the basal cell layer and the most specialised cells reside at the luminal/superficial side of the epithelium.

Various stem cell populations have been described in urothelium in animal and human models, but no consensus has been reached as to the exact identity of the cells. Several groups have described the bladder urothelium as having different clonogenic cell populations, and these have been observed in rat, porcine and human systems (Nguyen et al., 2007; Thangappan and Kurzrock, 2009; Larsson et al., 2014). Several lineage tracing experiments have also been performed using mouse and rat models, but they have had differing results; two groups found that BrdU or EdU labelled cells could be observed in all layers of the urothelium (Zhang et al., 2012; Sun et al., 2014), while a third group demonstrated label retaining cells were restricted to the basal cells of the urothelium (Kurzrock et al., 2008). Several specific stem cell populations have also been described in the bladder urothelium, these include CK5-expressing basal cells (Shin et al., 2011), p63-expressing cells (Pignon et al., 2013), specific intermediate cells (Gandhi et al., 2013) and combinations of CK5-expressing basal cells and specific intermediate cells (Colopy et al., 2014). None of these specific stem cell populations have been described in the human system. This area of research remains controversial. Much more work is needed to determine whether a specific stem cell population does exist in the urothelium, and if it does, then what are the true characteristics that define the cells.

As with all epithelia, the urothelium can be classified by its specific expression of epithelial cell–specific intermediate filament forming proteins called cytokeratins (CK), which act to support the epithelial cell cytoskeletal structure. Urothelium is characterised as being CK5, CK7, CK8, CK13, CK18, CK19, and CK20 positive (reviewed in Southgate et al., 1999). CK20 expression is restricted to the superficial cells of the urothelium, and as a result is a useful marker of urothelial cell differentiation.

1.3.1 Urothelial Barrier Function

Urothelium is one of the tightest barrier epithelia in the body, with skin being the only other epithelium type of comparable barrier function (reviewed in Powell, 1981). The tight barrier of the urothelium is attributed to two groups of proteins: the uroplakin proteins and tight junction-associated proteins (reviewed in Khandelwal et al., 2009). The uroplakin proteins play a role in inhibiting transcellular function (movement of ions or molecules through a cell) (Hu et al., 2000; Hu et al., 2002) (Figure 1.5 A), whilst the tight junction contributes to the paracellular barrier function (movement of molecules or ions in between cells) (Varley et al., 2006; Smith et al., 2015) (Figure 1.5 B).

The barrier function of epithelia is measured using two main methods: permeability assays (a measure of the movement of water, ions or molecules) or transepithelial electrical resistance (TER) (Negrete et al., 1996). An epithelium which is considered to be leaky has a TER of less than 1000 $\Omega.cm^2$, while epithelia which are considered to have tight barriers have TER values greater than or equal to 1000 $\Omega.cm^2$ (review by Powell, 1981).

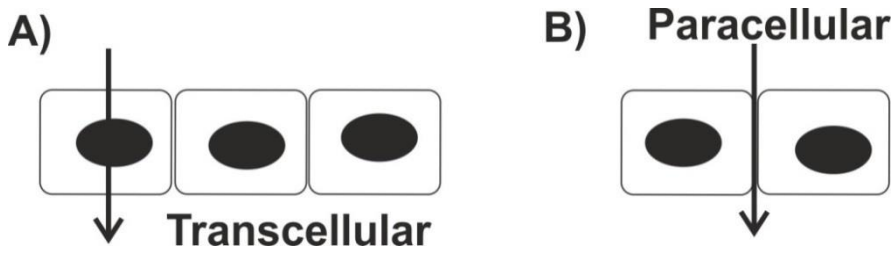

Figure 1.5 Barrier Function - Cell Transport

Barrier function in epithelia regulates two types of cellular transport:

A) Transcellular transport is the movement of ions or molecules through a cell. In urothelium the apical-most cells form specialised plaques from interacting uroplakin proteins to prevent transcellular transport of unwanted molecules or ions (Hu et al., 2002).

B) Paracellular transport is the movement of ions or molecules between cells. In urothelium, tight junctions regulate this form of transport (Varley et al., 2006; Smith et al., 2015).

This figure was adapted from (review by Tsukita et al., 2001).

1.3.1.1 Uroplakin Proteins

The superficial cell layer of urothelium contains a single layer of specialised cells called 'superficial' or 'umbrella' cells. On the apical (luminal) surface of these cells exists specialised plaques which form the urothelium-specific asymmetric unit membrane (AUM) (Sun et al., 1996). The AUM is considered to play key roles in stabilizing the urothelium surface during bladder filling, and in the transcellular barrier function of the urothelium.

The main protein components of the AUM are a group of proteins called the uroplakins (UPKs): UPK1A, UPK1B, UPK2, UPK3A, and UPK3B (Sun et al., 1996; Deng et al., 2002). UPK2, UPK3A and UPK3B are single-span transmembrane proteins (Wu and Sun, 1993; Lin et al., 1994; Deng et al., 2002), while UPK1A and UPK1B are tetraspanins (Yu et al., 1994). The uroplakins are integral membrane proteins, which form specific heterodimers with one another; UPK1A dimerises with UPK2, while UPK1B dimerises with UPK3A or UPK3B (Wu et al., 1995a; Liang et al., 2001; Deng et al., 2002). UPK1A, UPK2 and UPK3A are specifically expressed in the superficial cells of urothelium, while UPK1B and UPK3B are less specific to urothelium, and can also be found expressed in other tissues, including corneal epithelium (Adachi et al., 2000) and mesothelium (Kanamori-Katayama et al., 2011; Rudat et al., 2014), respectively.

To investigate the role of uroplakin proteins, knockout mice were generated for UPK2, UPK3A and UPK3B (Hu et al., 2000; Hu et al., 2002; Kong et al., 2004; Rudat et al., 2014). UPK2 deficient mice displayed smaller superficial cells of the urothelium and had a complete loss of plaque formation, which indicated that both sets of heterodimer pairs are required for successful plaque formation (Kong et al., 2004). The urothelium also became hyperplastic and demonstrated increased BrdU uptake (Kong et al., 2004), indicating a more proliferative phenotype of the epithelium. UPK3A knockout mice had abnormal superficial cells, and plaque size was reduced (Hu et al., 2000). The barrier function of the urothelium was also affected, with increased permeability to methylene blue (Hu et al., 2000), water, and urea (Hu et al., 2002), although TER values remained normal at approximately 2000 $\Omega.cm^2$ (Hu et al., 2002). UPK3B knockout mice

displayed no abnormalities in urothelium or plaque formation (Rudat et al., 2014). These results suggest a likely essential role for UPK2 and UPK3A in the barrier function of the urothelium, while UPK3B appears to have a non-essential role.

1.3.1.2 Tight Junction Proteins

Tight junctions are found at the apical surface of two adjacent epithelial cells, where they act to regulate the paracellular passage of water, molecules and ions across an epithelium. Tight junctions are formed through the interaction of many different proteins, of which the major protein components are the claudin (CLDN) proteins, occludin, and the zonula occludens (ZO) proteins (ZO-1, ZO-2 and ZO-3) (reviewed in Van Itallie and Anderson, 2014) (Figure 1.6). Occludin and the claudin proteins are tetraspan transmembrane proteins, which act to form the tight junction between two cells, while the ZO proteins anchor these transmembrane proteins on the cytoplasmic surface of the cell (reviewed in Van Itallie and Anderson, 2014).

The claudin proteins are a critical component of the tight junction; it is believed that the interaction between opposing extracellular claudin loops regulates the tightness of a given epithelial barrier (Furuse et al., 1999). Each epithelium relies on a unique combination of claudin proteins in order to control the tightness of the epithelial barrier, with different claudin proteins being associated with either tight or leaky epithelia (reviewed in Krug et al., 2014). For example, the presence of claudin 2 protein in an epithelial tight junction is associated with leaky barrier epithelia, like that of the kidney proximal tubule (Amasheh et al., 2002; Muto et al., 2010); when claudin 2 was overexpressed in a kidney distal tubule cell type known to produce a high TER, the cells completely failed to form a functional barrier (Amasheh et al., 2002).

Claudin proteins can have both *cis*- and *trans*- interactions: *cis*- interactions occur between adjacent claudin proteins in the same cell membrane, while *trans*- interactions occur between claudins across the intercellular space of neighbouring cells (Blasig et al., 2006; Piontek et al., 2008). Claudin proteins are also known to interact in both homo- and heterotypic fashions, with either like or differing claudins respectively (Furuse et al., 1999).

The ZO proteins are the main intracellular component of tight junctions. All three of the ZO proteins (ZO-1, ZO-2 and ZO-3) bind the C-terminal domain of claudin and occludin proteins to act as a link to the actin cytoskeleton in the cell (Itoh et al., 1999; Li et al., 2005). ZO-1 and ZO-2 are believed to be critical for organisation and placement of the claudin proteins in the tight junction (Umeda et al., 2006). Both ZO-1 and ZO-2 knockout mice are embryonically lethal (Katsuno et al., 2008; Xu et al., 2008), while ZO-3 knockout mice are viable, with no obvious defects (Xu et al., 2008), suggesting a more essential role for ZO-1 and ZO-2.

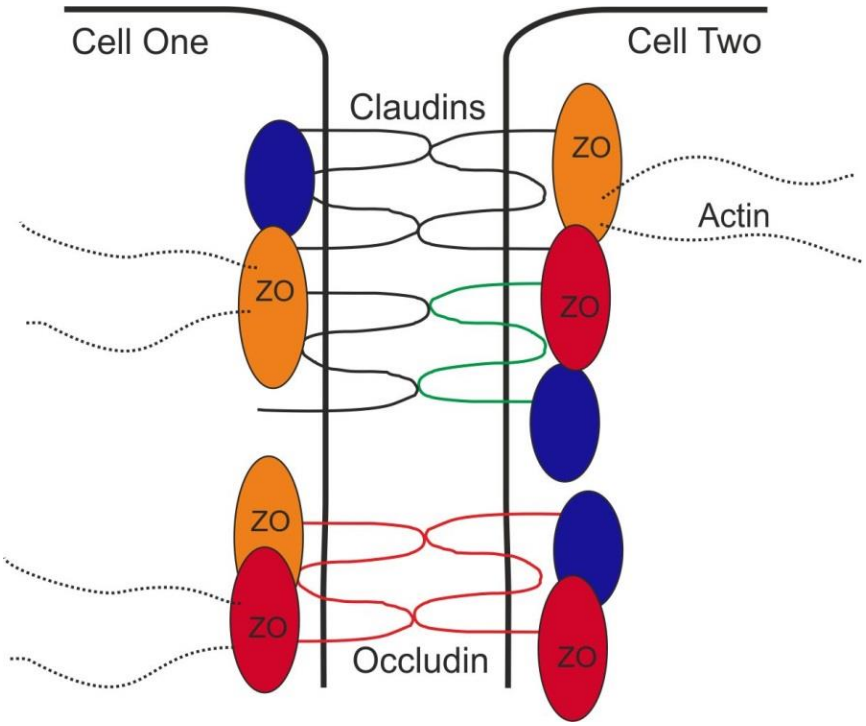

Figure 1.6 Main Protein Components of a Tight Junction

The main protein components of tight junctions are the claudin proteins, occludin and the zonula occludens proteins (reviewed in Van Itallie and Anderson, 2014). The claudin proteins and occludin are tetraspan transmembrane proteins, which interact with claudins and occludins, respectively, from neighbouring cells to facilitate paracellular barrier function. The ZO proteins act on the inner surface of the cell and bind to the C-terminal portion of the claudins and occludins. ZO proteins act as a link to the actin cytoskeleton. This figure is adapted from (review by Matter et al., 2005; review by Steed et al., 2010).

Only little work has been completed to investigate the expression or role of tight junction proteins in urothelium. In human urothelium, claudins 3, 4, 5 and 7 have been shown to be expressed, along with ZO-1 and occludin (Varley et al., 2006), while in mice, claudins 3, 4, 7, 8, and 12, as well as ZO-1 and occludin have been shown to be expressed (Acharya et al., 2004; Fujita et al., 2012). In order to investigate the role of claudin 4 in the urinary system, claudin 4 knockout mice were generated (Fujita et al., 2012). These mice displayed a slightly hyperplastic urothelium, but there was no obvious effect on urothelial barrier function or the expression of other tight junction proteins, like claudins 3 or 7 (Fujita et al., 2012). This study indicated a non-crucial role for claudin 4 in urothelial barrier function.

An *in vitro* system was used to examine the role of claudin 3 in the barrier function of human urothelium (Smith et al., 2015). Human urothelial cells with knocked-down claudin 3 expression were generated, and the barrier function of these cells was measured following differentiation to form a biomimetic urothelium equivalent (Smith et al., 2015). Interestingly, knockdown of claudin 3 caused a complete lack of barrier function, as measured by the TER (Smith et al., 2015). This indicated an essential role for claudin 3 in urothelial barrier function. The authors also overexpressed claudin 3 in human urothelial cells, but found that this was unable to improve barrier function when cells were induced to stratify (Smith et al., 2015). This demonstrated that the barrier function of urothelium is most likely reliant on the combined expression of several tight junction-associated proteins as opposed to primarily being reliant on the expression of a single claudin protein. The authors also identified the gain of ZO-$1^{\alpha+}$ protein expression, an alternative ZO-1 isoform, which occurred only as a result of urothelial cell differentiation (Smith et al., 2015). This result could suggest a possible important role for ZO-$1^{\alpha+}$ in urothelial barrier function.

1.3.2 Urothelial Cell Proliferation and Differentiation in Vitro

When human urothelial cells are isolated from native urothelium and grown *in vitro*, in serum-free, low calcium (0.09 mM) conditions, they are highly proliferative (Southgate et al., 1994). Southgate et al. described the growth of normal human urothelial (NHU) cells in keratinocyte serum-free medium (KSFM) with added bovine pituitary extract, epidermal growth factor and cholera toxin (KSFMc). Under these conditions, NHU cells adopted a more basal-like phenotype; many of the typical markers of urothelial cell differentiation were lost, including the expression of tight junction proteins, CK13, CK20, and several of the uroplakin genes (Figure 1.7). The cells also became squamous in nature, and began to express CK14, a squamous epithelial cell-associated cytokeratin. Upon reaching confluence, the cells became contact inhibited, but they could be subcultured, maintaining the basal-like, proliferative phenotype for in excess of 10 passages, before reaching senescence (Southgate et al., 1994).

The proliferative and regenerative nature of urothelial cells is thought to be largely attributed to epidermal growth factor receptor (EGFR) signalling (Bindels et al., 2002; Daher et al., 2003; Varley et al., 2005). Treatment of proliferating NHU cells with an EGFR tyrosine kinase inhibitor, PD153035, which blocks EGFR activation, resulted in the cells arresting in G1 phase, and failure to reach confluence (Varley et al., 2005).

Southgate et al. also demonstrated that increasing the calcium concentration of the medium to 2 mM caused NHU cells to stratify, forming a multi-layered tissue, although this failed to cause differentiation of the cells. Sugasi et al. used a similar serum-free technique to generate stratified human urothelial cell sheets. The authors also demonstrated increased calcium concentrations alone failed to completely differentiate the cells, but that the cell sheets did possess some barrier function (Sugasi et al., 2000). Cross et al. later showed that it was the combined addition of adult bovine serum (ABS) and an increased calcium concentration to 2 mM (termed ABS/Ca^{2+} protocol in this thesis), which was able to cause NHU cells to both stratify and differentiate. Using this method, NHU cells formed a multi-layered, biomimetic urothelium equivalent (Cross et al., 2005). The cells lost expression of CK14, and gained expression of CK13 (Figure 1.7). The cells also formed tight junctions, and developed a tight barrier, as measured by electrical resistance and permeability assays (Cross et al., 2005). The exact components

of adult bovine serum that cause NHU cells to differentiate *in vitro* are not yet known, but signalling through PPARγ and the retinoic acid receptors (RARs) may play a major role. The involvement of PPARγ and the RARs in urothelial cell differentiation is described in more detail in sections *1.3.3.1* and *1.3.4*, respectively.

An interesting feature of urothelium is that all cells of the epithelium appear to be capable of becoming more or less differentiated (ie. differentiation is not irreversible) (Wezel et al., 2014). When urothelial cells are isolated from native tissue, nearly all of the cells survive and contribute to the culture (Southgate et al., 1994). Work by Wezel et al. showed that when urothelial cells were separated into basal and suprabasal fractions at isolation, both cell populations were able to be propagated *in vitro*, and they were both able to be differentiated to form functional barrier epithelia with a basal cell compartment. This work suggested that unlike other epithelia (eg. skin) where cell fate is unidirectional, in urothelium, cell fate appears to be much more plastic in nature.

	A) Native Urothelium	B) Serum-Free, Low Ca^{2+} (0.09 mM)	C) 5% ABS and 2 mM Ca^{2+}
CK13	++	+	++
CK14	-	++	-
CK20	++	-	-
UPKs	++	-/+	+
Tight Junctions	++	-	++
Barrier Function	++	-	++
Regeneration	++	++	++

Figure 1.7 Basic Characteristics of NHU Cells *in Vitro* Compared to Native Human Urothelium

a) Native human urothelium exhibits expression of CK13, and the superficial cell-associated cytokeratin, CK20. All five of the uroplakin genes are expressed, as well as an array of tight junction (TJ) proteins, which contribute to native urothelium having one of the tightest barriers in the human body. Urothelium is normally quiescent, but in response to injury adopts a regenerative phenotype (Pust et al., 1976).

b) NHU cells grown in serum-free, low calcium (0.09 mM) medium (KSFMc) adopt a monolayer squamous phenotype, expressing CK14, and are highly proliferative (Southgate et al., 1994). The cells lose expression of differentiation-associated genes.

c) Following use of 5% ABS and 2 mM Ca^{2+}, NHU cells form a multilayered urothelium, which expresses many differentiation-associated genes (Cross et al., 2005). They also gain barrier function, and are highly regenerative following scratch wounding.

(-) Negative/ Does not occur, (+) Weak Expression, (++) Strong Expression/Does occur. This table was adapted from (Cross et al., 2005).

1.3.3 Transcription Factors Involved in Urothelial Cell Differentiation

In cell culture systems, differentiation of urothelial cells is controlled by a tightly regulated cascade of transcription factor activation and repression, which leads to the differentiation of the cells. Several key transcription factors have been shown to be involved in the differentiation of urothelial cells, but the full hierarchical network is still far from being elucidated. Upregulation of the transcription factors PPARγ, interferon regulatory factor 1 (IRF1), forkhead box protein A1 (FOXA1) and E74-like factor 3 (ELF3), has been shown to prequel the upregulation and *de novo* induction of expression of multiple differentiation markers in NHU cells *in vitro* (CK20, the uroplakin genes, and tight junction-associated genes) (Varley et al., 2004a; Varley et al., 2004b; Varley et al., 2006; Varley et al., 2009; Böck et al., 2014).

Other transcription factors that have been shown to be involved in the development and differentiation of urothelium include Kruppel-like factor 5 (KLF5) (Bell et al., 2011), grainyhead-like 3 (GRHL3) (Yu et al., 2009), GATA4 (Mauney et al., 2010) and GATA6 (Mauney et al., 2010); all of these studies were completed in mice, or using mouse cells. Studies investigating KLF5 have shown that targeted germ cell deletion prevents the urothelium from being able to stratify and differentiate; the mice had a single layer bladder epithelium (Bell et al., 2011). GRHL3 has been shown to play a key role in the differentiation of urothelium and the formation of the superficial cell layer (Yu et al., 2009). It has also been suggested that UPK2 is a direct target of GRHL3 (Yu et al., 2009). GATA4 and GATA6 have also been implicated in urothelial cell differentiation (Mauney et al., 2010). Both transcription factors were shown to be upregulated during the differentiation of mouse embryonic stem cells (ESCs) into urothelial-like cells. The authors also demonstrated that mouse ESCs which were null for either GATA4 or GATA6 had significantly reduced expression of UPK1A, UPK1B, UPK2, and UPK3A following differentiation.

1.3.3.1 PPARγ

Activation of PPARγ has been shown to play an important role in the differentiation program of urothelial cells (reviewed in Varley and Southgate, 2008)(Figure 1.8). Urothelial cells treated with both the PPARγ agonist, troglitazone (TZ), and the EGFR tyrosine kinase inhibitor, PD153035 (PD) (treatment protocol termed TZ/PD in this thesis), have been shown to downregulate CK14 expression and upregulate CK13 expression (Varley et al., 2004b). Use of the TZ/PD protocol has also been shown to upregulate expression of urothelial differentiation markers: CK20 (Varley et al., 2004b) and the uroplakins (Varley et al., 2004a). Additionally, activation of PPARγ has been shown to upregulate the expression of several tight junction proteins, including claudin 3, claudin 4 and claudin 5, which are all implicated in maintaining the tight barrier function of the urothelium (Varley et al., 2006). In all cases, the effects of the TZ/PD protocol were shown to be specific to PPARγ activation using specific PPARγ antagonists, GW9662 or T0070907, or PPARγ knockdown, which abrogated the effect.

In terms of identifying a transcription factor hierarchy involved in the differentiation of urothelial cells, PPARγ has been shown to act upstream of the transcription factors, ELF3, FOXA1 and IRF1 (Varley et al., 2009; Böck et al., 2014). These three transcription factors were identified using gene chip microarray data generated from NHU cells which had been treated with and without the TZ/PD or ABS/Ca^{2+} protocols. FOXA1 and IRF1 were shown to be upregulated as a result of TZ/PD treatment at all of the time points assessed. Likewise, ELF3 was shown to be upregulated during both the TZ/PD and ABS/Ca^{2+} protocols. The upregulation of these transcription factors was shown to be directly as a result of PPARγ activation using the PPARγ-specific antagonists, GW9662 or T0070907.

PPARγ is highly associated with bladder cancer, and in particular luminal muscle invasive bladder cancers (Biton et al., 2014; Cancer Genome Atlas Research, 2014; Choi et al., 2014). Luminal bladder cancers have a more differentiated urothelial cell phenotype, and exhibit high levels of PPARγ gene expression (Biton et al., 2014; Choi et al., 2014). A recent large scale study of muscle invasive, high-grade urothelial tumours demonstrated that 17% of the specimens examined exhibited gene amplification of PPARγ (Cancer Genome Atlas Research, 2014). Using *in vitro* models,

Biton et al. demonstrated that knockdown of PPARγ, by the use of specific siRNA, in bladder carcinoma-derived cell lines (SD48, UMUC9 and MGHU3) caused a significant decrease in cell viability. For the SD48 and UMUC9 cell lines, it also caused a significant reduction in colony formation. This work suggested a role for PPARγ in maintaining a pathway of urothelial cancer cell growth and viability.

Research has also indicated that the use of thiazolidinediones (synthetic PPAR ligands, with specificity to PPARγ), some of which were prescribed to treat type 2 diabetes in humans, leads to a significant increase in bladder cancer incidence (Azoulay et al., 2012; Neumann et al., 2013). These studies suggest a possible role for sustained PPARγ activation in bladder cancer development.

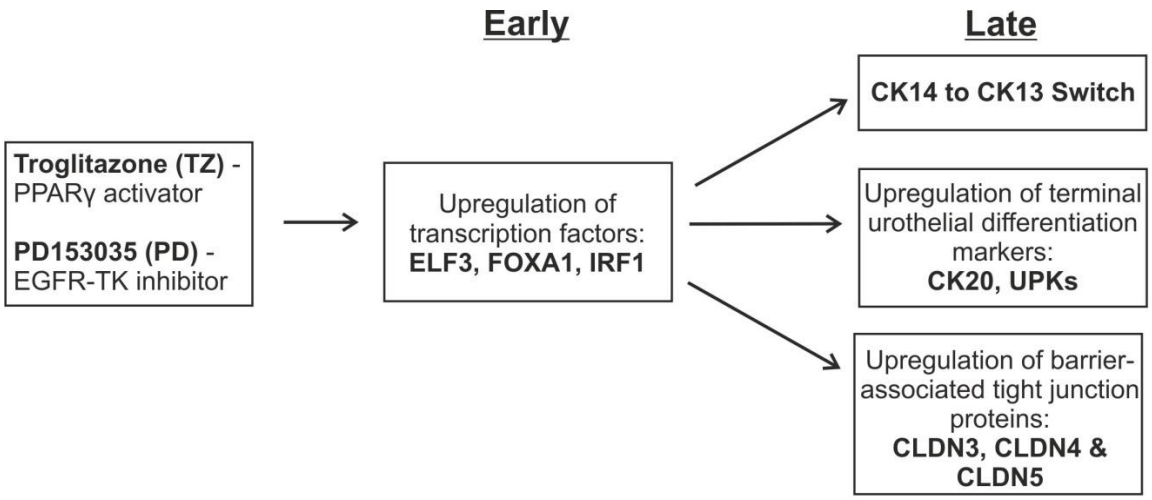

Figure 1.8 Activation of PPARγ in NHU Cells Using the TZ/PD Protocol
Combined treatment of NHU cells with troglitazone and PD153035 results in the upregulation of transcription factors ELF3, FOXA1, and IRF1 within 24-48 hours (Varley et al., 2009; Böck et al., 2014). Within six days, the cells express CK13, and upregulate the urothelial terminal differentiation associated genes CK20 and the UPKs (Varley et al., 2004a; Varley et al., 2004b). Several tight junction proteins are also upregulated as a result of PPARγ activation, including CLDN3, CLDN4 and CLDN5, although the cells do not form a functional barrier epithelium (Varley et al., 2006).

1.3.3.2 GATA3

GATA3 is a zinc finger, pioneer transcription factor. In the urinary bladder, GATA3 has been identified as both a key diagnostic (Higgins et al., 2007; Zhao et al., 2013), and prognostic marker of bladder cancer (Miyamoto et al., 2012). In general, decreased GATA3 expression is associated with bladder cancer, when compared to normal urothelium (Miyamoto et al., 2012). This has also been demonstrated using an *in vitro* model, where it was shown that urothelial carcinoma-derived cell lines (5637, TCC-SUP, J82 and UMUC3) expressed less GATA3 than normal urothelial cells (Li et al., 2014a). The authors also showed that when GATA3 expression was further decreased in these bladder carcinoma-derived cell lines by GATA3 knockdown, it caused an increase in cell migration and invasion (Li et al., 2014a). As a result, this work suggested that decreased GATA3 expression may be necessary for either instigating or maintaining essential bladder tumour cell characteristics.

It has been suggested that the decreased GATA3 expression in urothelial carcinomas may be as a result of androgen receptor activation (Li et al., 2014b). Li et al. demonstrated that treatment of an immortalised non-neoplastic urothelial cell line with a specific androgen receptor agonist caused a concentration-dependent downregulation of GATA3 expression.

GATA3, among other factors, is also useful for distinguishing different subtypes of urothelium-derived cancers. For examples, upregulated GATA3 expression is associated with the luminal muscle invasive bladder cancer subtype (Damrauer et al., 2014). It can also be used to identify squamous cell carcinoma of the bladder, which is associated with low/absent GATA3 expression (Eriksson et al., 2015).

The role of GATA3 in normal urothelial cell differentiation has yet to be elucidated.

1.3.3.3 FOXA1

FOXA1 is a transcription factor that has been shown to have important roles in many cell types, in particular cells of endodermal origin (reviewed in Bernardo and Keri, 2012). FOXA1, like GATA3, is considered to be a pioneer transcription factor, and therefore it is able to act in areas of heterochromatin (reviewed in Zaret and Carroll, 2011).

FOXA1 has been shown to have important roles in the development and differentiation of urothelium (Oottamasathien et al., 2007; Thomas et al., 2008; Varley et al., 2009). Studies in mouse have found that both FOXA1 and FOXA2 are expressed during the early development of the urothelium (Oottamasathien et al., 2007; Thomas et al., 2008). When urothelium begins to mature to its fully differentiated state, FOXA2 expression becomes absent as the uroplakin proteins begin to be expressed (Oottamasathien et al., 2007). FOXA1 expression was shown to be present during both embryonic development and in the mature adult murine urothelium (Oottamasathien et al., 2007).

To investigate the effect of FOXA1 loss in urothelium, mice with urothelium-specific FOXA1 knockout were generated (Reddy et al., 2015). Reddy et al. demonstrated that FOXA1 knockout resulted in changes to the urothelium which were gender-specific. Male mice displayed areas of hyperplastic urothelium with increased expression of CK14 in basal cells. Female mice, by contrast, developed areas of keratinising squamous metaplasia, which had significant CK14 expression. This work demonstrated a role for FOXA1 in maintaining urothelial-type differentiation, and specifically in preventing squamous-type differentiation.

In vitro study has shown that FOXA1 acts downstream of PPARγ in urothelial cell differentiation (Varley et al., 2009). The authors also demonstrated that knockdown of FOXA1 expression in NHU cells, during treatment with the TZ/PD protocol, resulted in the downregulation of several urothelial differentiation genes, including CLDN3, CK13, UPK1A, UPK2 and UPK3A. The knockdown also resulted in the slight upregulation of UPK1B and UPK3B. This work demonstrated the importance of FOXA1 as a key regulator of several aspects of urothelial cell differentiation.

FOXA1 has also been shown to be involved in bladder cancer. Loss of FOXA1 in bladder cancer is significantly associated with poor patient prognosis (Reddy et al., 2015). In general, decreased FOXA1 expression correlates with both increased stage and grade of bladder cancer (DeGraff et al., 2012). *In vitro* studies completed to investigate the role of FOXA1 in bladder cancer demonstrated that FOXA1 knockdown in a bladder carcinoma-derived cell line, with high FOXA1 expression (RT4 cells), resulted in significantly increased cell proliferation (DeGraff et al., 2012). By contrast, overexpression of FOXA1 in a bladder carcinoma-derived cell line with low FOXA1 expression (T24 cells) resulted in a significant decrease in both cell proliferation and invasion (DeGraff et al., 2012). This work supported the important role of FOXA1 loss in bladder carcinoma progression.

Recent work has demonstrated the presence of FOXA1 mutations in bladder cancers; the authors demonstrated that 5% of the bladder cancer specimens examined had either a frameshift or missense mutation (Cancer Genome Atlas Research, 2014). It has also been shown that FOXA1 expression differs between the bladder cancer subtypes. Upregulated FOXA1 expression is associated with the luminal muscle invasive bladder cancer subtype (Damrauer et al., 2014), while low/absent FOXA1 expression is associated with squamous cell carcinoma of the bladder (DeGraff et al., 2012; Eriksson et al., 2015).

1.3.4 Role of Retinoic Acid Receptors in Urothelial Cell Differentiation

The retinoic acid receptors (RARs) are nuclear receptors which have been shown to have important roles in the development and differentiation of many cell types (reviewed in Duester, 2008). There are three retinoic acid receptors, RARα, RARβ and RARγ. Similar to PPARγ signalling, the RARs must form heterodimers with RXRs, and upon ligand binding the complex can activate transcription at specific sequences in promoter regions called retinoic acid response elements (RAREs) (Mader et al., 1993).

Early evidence of the importance of retinoic acid receptor signalling in urothelium was demonstrated in mice fed vitamin-A deficient diets; in these mice, keratinising squamous metaplasia of the bladder occurred (Molloy and Laskin, 1988; Liang et al., 2005). When pregnant mice were fed a vitamin-A deficient diet, and their resulting offspring were also fed a vitamin-A deficient diet, female offspring displayed evidence of squamous metaplasia of the bladder as early as 8 weeks of age (Liang et al., 2005). Male offspring, in the same study, took much longer for the squamous metaplasia to occur, with the phenomenon not occurring until approximately 48 weeks of age.

Mouse models have subsequently been used to demonstrate an important regulatory role of retinoic acid in the development and differentiation of urothelium (Gandhi et al., 2013). Gandhi et al. demonstrated, using a RARE-LacZ system in mice, that RAR activity was present predominantly in urothelial progenitor cells at E12. By E14, the RAR activity was much more prevalent in the intermediate and superficial cells of the developing urothelium. Adult urothelium, by contrast, showed only little RARE-LacZ activity, with the authors suggesting that less retinoic acid signalling was necessary to maintain the mature urothelial phenotype. When retinoic acid signalling was blocked using a dominant negative RAR mutant, it prevented differentiation of urothelium, with the mice displaying only a single layered basal epithelium, and nearly absent superficial cells (Gandhi et al., 2013).

Retinoic acid signalling has also been investigated in urothelial cells *in vitro*. In proliferating NHU cell cultures, treatment of the cells with 13-*cis*-retinoic acid was shown to inhibit CK14 expression, a squamous epithelial cell marker, and increase CK13 expression (Southgate et al., 1994). Retinoic acid treatment has also been shown to have potential roles in the conversion of stem cells into urothelial cells, where it has been demonstrated that treatment of pluripotent stem cells (human ESCs and iPSCs, and murine ESCs) with retinoic acid was able to cause upregulation of uroplakin gene expression (Mauney et al., 2010; Kang et al., 2014b).

1.4 Buccal Epithelium

Buccal epithelium is a non-cornified, stratified squamous epithelium which is found on the inner surface of the cheek and lips (Figure 1.9). It averages 20-30 cell layers thick, functions as a barrier epithelium, and is derived from the embryonic ectoderm (reviewed in Winning and Townsend, 2000). Buccal epithelial cells express cytokeratin 14, the squamous-associated epithelial cell protein, as well as several other cytokeratins (CK4, CK5, CK13 and CK19), which can be used to characterise the epithelium (reviewed in Presland and Dale, 2000).

Buccal epithelium has four epithelial cell layers: the basal layer, spinous layer, intermediate layer and superficial layer (Landay and Schroeder, 1979). It is a non-cornified stratified squamous epithelium, and as a result lacks layers of dead cells on its surface, which is associated with cornified epithelia like the epidermis. Buccal epithelial cells commit to terminal differentiation in the basal and spinous layers and later migrate up through the epithelial cell layers undergoing a progressive differentiation process similar to that observed in skin. Protein markers which can be used to identify terminal differentiation in stratified squamous epithelia include transglutaminases (TGMs) and small proline rich proteins (SPRRs), which are expressed only in the upper layers of the epithelium (reviewed in Presland and Dale, 2000). Absence of loricrin (LOR) can be used to distinguish a non-cornified, stratified squamous epithelium from a cornified epithelium (Gibbs and Ponec, 2000).

Much of the work completed to investigate the differentiation and barrier function properties of stratified squamous epithelia has been completed using epidermis, and particularly using mouse models. Very little work of this nature has been focused on oral epithelial cells.

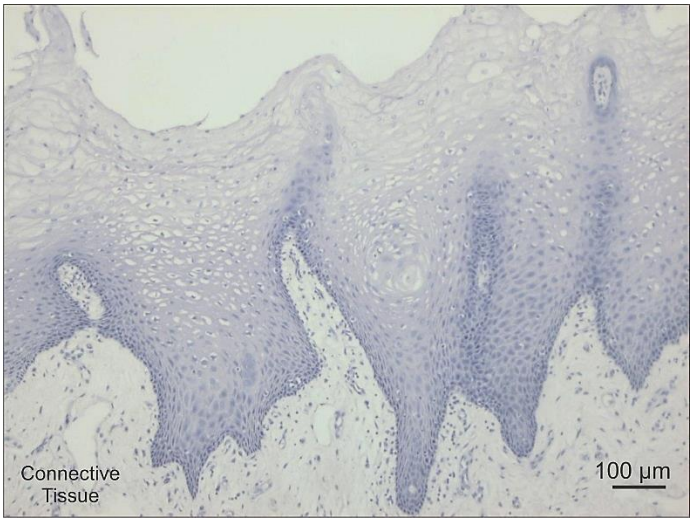

Figure 1.9 Human Buccal Mucosa

Haematoxylin and Eosin stained section of human buccal mucosa. Buccal mucosa consists of a non-cornified, stratified squamous epithelium, and an underlying connective tissue layer.

1.4.1 Differentiation of Oral Epithelia

The differentiation process of oral epithelia is thought to be similar to that of skin (reviewed in Jones and Klein, 2013). There are believed to be at least two populations of cells in stratified squamous epithelia: a mitotically-active population of stem/progenitor cells found in the basal most layers, and mitotically-inactive, terminally differentiating cells in the suprabasal layers. (reviewed in Mascre et al., 2012; reviewed in Jones and Klein, 2013). Committed progenitor cells become terminally differentiating and migrate through the layers of the epithelium undergoing a progressive differentiation process (reviewed in Jones and Klein, 2013). This process leads to cell death in cornified epithelia, with complete loss of organelles, including the nucleus. In non-cornified stratified squamous epithelia, superficial cells remain alive and still contain their nuclei (Landay and Schroeder, 1979). Ultimately, cells of the superficial layer of both the cornified and non-cornified oral epithelia are sloughed off and replaced by new terminally differentiating cells (reviewed in Presland and Dale, 2000).

For the differentiation of stratified squamous epithelia, much of the work to determine the transcription factors involved in development and differentiation has been performed in mouse epidermis (reviewed in Dai and Segre, 2004). Example transcription factors which have been found to play a key role in mouse epidermal terminal differentiation and barrier formation include p63, KLF4 and GRHL3 (Segre et al., 1999; Yang et al., 1999; Ting et al., 2005). Mice lacking p63 failed to form a stratified epithelium, and instead formed only a single layered epidermis, which expressed several terminal differentiation-associated proteins including, loricrin, involucrin and filaggrin (Yang et al., 1999). p63 is suspected to play a role in the maintenance of the basal/progenitor cell population of stratified squamous epithelia (Yang et al., 1999). Both KLF4-deficient and GRHL3-deficient mice die due to defects in barrier function, which was attributed to both an imbalance in barrier-associated lipids and proteins (Segre et al., 1999; Ting et al., 2005).

In the culture of squamous epithelial cells from skin, treatment of the cells with PPARγ agonists has been shown to increase the expression of squamous differentiation-associated genes, involucrin and transglutaminase-1 (Westergaard et al., 2001; Mao-Qiang et al., 2004), as well as inhibit proliferation (Ellis et al., 2000). Targeted knockout of PPARγ in the skin of mice showed only a slight thickening of the epithelium, but was not associated with any functional abnormalities (Mao-Qiang et al., 2004). The study suggested a non-crucial role of PPARγ in mouse skin differentiation and barrier function.

The effect of retinoic acid on oral epithelial cells has been investigated. In an immortalised mouse gingival epithelial cell line it was shown that treatment of the cells with retinoic acid caused downregulation of both CK13 and CK14 expression (Hatakeyama et al., 2004), as well as downregulated expression of the tight junction-associated genes, claudins 1 and 5 (Hatakeyama et al., 2010). In primary human oral epithelial cells (obtained from cornified oral epithelia), retinoic acid treatment abrogated the cells' ability to form a cornified cell layer (Kautsky et al., 1995; Kato et al., 2013), and reduced the overall epithelium thickness (Chung et al., 1997) when cells were induced to differentiate with fetal bovine serum. Retinoic acid also caused decreased expression of the terminal squamous

differentiation markers, profilaggrin and keratin 1 (Kautsky et al., 1995; Chung et al., 1997). In general, it appears that retinoic acid treatment of oral epithelial cells has a negative effect on squamous-type differentiation of the cells.

1.4.2 Barrier Function of Oral Epithelia

The barrier function of stratified squamous epithelia is attributed to two main components: the presence of a cross-linked protein meshwork on the inside of the plasma membrane, and the presence of a unique composition of lipids on the outer surface of the cells of the most superficial cell layers (reviewed in Kalinin et al., 2002).

As cells commit to terminal differentiation, they begin to produce a new set of proteins, including filaggrin, involucrin, loricrin, and small proline rich region (SPRR) proteins (reviewed in Presland and Dale, 2000). By the time the cells reach the superficial layer, these proteins are cross-linked by a group of enzymes, the transglutaminases, to form the cornified cell envelope (reviewed in Candi et al., 2005). This cornified cell envelope eventually replaces the cell membrane of the cells of the stratum corneum in cornified oral epithelia. In non-cornified oral epithelia, the process is less well organised, with not all of these proteins being produced (loricrin is absent in buccal epithelium), and the cell membrane remains intact (Gibbs and Ponec, 2000).

As the cells migrate through the epithelium, the committed differentiating cells produce a new type of organelle called membrane coating granules, which occurs in the upper spinous layers (Squier, 1977). These granules contain glycolipids and as the cells reach the superficial layer the granules bind to the plasma membrane and release their lipid contents into the intercellular space. The lipids form a water-tight barrier. The particular combination of lipids released by the membrane coating granules differs among the types of oral epithelia (Wertz et al., 1986). This differing combination of lipids gives each type of oral epithelium a unique permeability to water; in order of increasing permeability to water are hard palate > buccal mucosa > the floor of the mouth (Lesch et al., 1989).

1.5 Bladder Tissue Engineering

Tissue engineering is the concept of generating functional tissue replacements *in vitro* for patients whose tissues or organs are affected by injury, disease, or cancer. For patients with end-stage diseased bladders or bladder cancer, bladder tissue engineering aims to provide an alternative to the current surgical approaches, which can have many associated complications.

Bladder augmentation (enlargement of the bladder) and reconstruction following cystectomy (part or full removal of the bladder) are the two main surgical procedures where bladder tissue engineering could be useful. The current widely used clinical method for enlarging or creating an entirely new bladder involves taking a vascularised segment of the patients own intestine and either grafting it into the bladder (method called enterocystoplasty) to increase its size, or using a portion of the intestine to form a bag-like structure to act as a neo-bladder (reviewed in Biers et al., 2012). While these types of surgical procedures are widely used with success, a variety of complications arise as a result of the inherent nature of the intestinal epithelium (it is an absorptive epithelium): metabolic imbalance, mucus production, infection, and risk of stones (reviewed in Gilbert and Hensle, 2005).

Tissue engineering-based alternatives to using gastrointestinal grafts have been the subject of active research since the mid-1990's (reviewed in Lam Van Ba et al., 2015). An early study involved seeding autologous, *in vitro* cultivated urothelial cells onto the luminal side of an allogeneic piece of bladder submucosa and autologous smooth muscle cells on the opposite surface (Yoo et al., 1998). The tissue construct was allowed to grow for up to ten days *in vitro*, and then used to augment the bladder of dogs. Following 3 months of implantation, the grafted tissue was reported to display a full thickness urothelium on the luminal surface, and smooth muscle with an angiogenic response on the opposite surface. The bladders were successfully increased in capacity by up to 99%, and had maintained a normal compliance.

Subsequent studies by the same group attempted full bladder replacement, first using an animal model (Oberpenning et al., 1999), and later in humans (Atala et al., 2006). This method of bladder tissue engineering involved the use of a biodegradable scaffold (made from collagen and/or polyglycolic acid) formed in the shape of the bladder. Autologous, *in vitro* grown urothelial cells were seeded on the luminal surface of the scaffold, and autologous smooth muscle cells were seeded on the external surface. The cells were allowed to grow *in vitro* for several days before the construct was used for surgical replacement of the bladder. While results were quite successful in the animal model, initial positive hype from the human study was later called in to question by a subsequent clinical trial by another group (Joseph et al., 2014). The follow-up clinical trial concluded that the bladder tissue-engineering technique resulted in high risk of complication and harm to patients. This prompted a call for further basic bladder research before any other similar human studies were carried out (Cheng, 2014; Farhat, 2014).

The other main approach to bladder tissue engineering, termed "composite cystoplasty", involves using a vascularised, demucosalised segment of the patients' intestine, which is lined by an autologous, *in vitro* produced, urothelium (Fraser et al., 2004; Turner et al., 2011). The resulting construct eliminates the harm-causing component of a pedicle intestinal graft, by replacing the intestinal epithelial layer with a layer of cultured bladder epithelium. Early work in this area saw the use of autologous islets of urothelium (not *in vitro* produced) placed on a de-epithelialised bowel, which resulted in decreased shrinkage of the grafts in comparison to grafts which contained no urothelium patches (Lutz and Frey, 1995). This work showed initial promise for the technique. More recent work has shown this method of bladder tissue engineering to be much simpler than others, as only the epithelial layer must be produced *in vitro*, and it adapts current gold standard surgical procedures, making it potentially less risk-associated for patients. The method has been tested successfully in autologous pig surgical models (Fraser et al., 2004; Turner et al., 2011), and waits further animal-based model testing before possible translation to human patients.

1.5.1 Epithelial Cells for Bladder Tissue Engineering

The production of epithelia i*n vitro* for use in tissue-engineering applications is well advanced. However, the vast majority of these epithelia are produced using epithelial cells isolated from the donor tissue of healthy organs, and the pre-clinical surgical studies are completed using healthy animal models. A problem can arise when attempting to translate these models into patients with chronically diseased tissues or organs.

All clinically relevant bladder tissue engineering techniques require the use of *in vitro* cultured, autologous epithelial cells; the most ideal epithelial cell type for this being the patient's own bladder epithelial cells. More recent work has intimated that the use of autologous urothelial cells may not be possible for some patients with bladder disease; urothelial cells isolated from patients with neuropathic bladders senesced much earlier in culture, and were less likely to form a functional barrier epithelium when induced to differentiate, in comparison to urothelial cells from healthy bladders (Subramaniam et al., 2011). This work suggested that urothelial cells were affected by the disease environment, and could not be considered normal, healthy urothelial cells.

The main research strategy for generating other autologous epithelial cells for bladder tissue engineering has been to differentiate various types of multipotent or pluripotent stem cells into urothelial cells (reviewed in Osborn and Kurzrock, 2015) (Figure 1.10 A). Aside from this, others have suggested simply using another autologous barrier-forming epithelial cell type, such as buccal epithelial cells (Lu et al., 2010; Watanabe et al., 2011) (Figure 1.10 B). The other plausible method of generating surrogate autologous epithelial cells is via *in vitro* transdifferentiation (Figure 1.10 C).

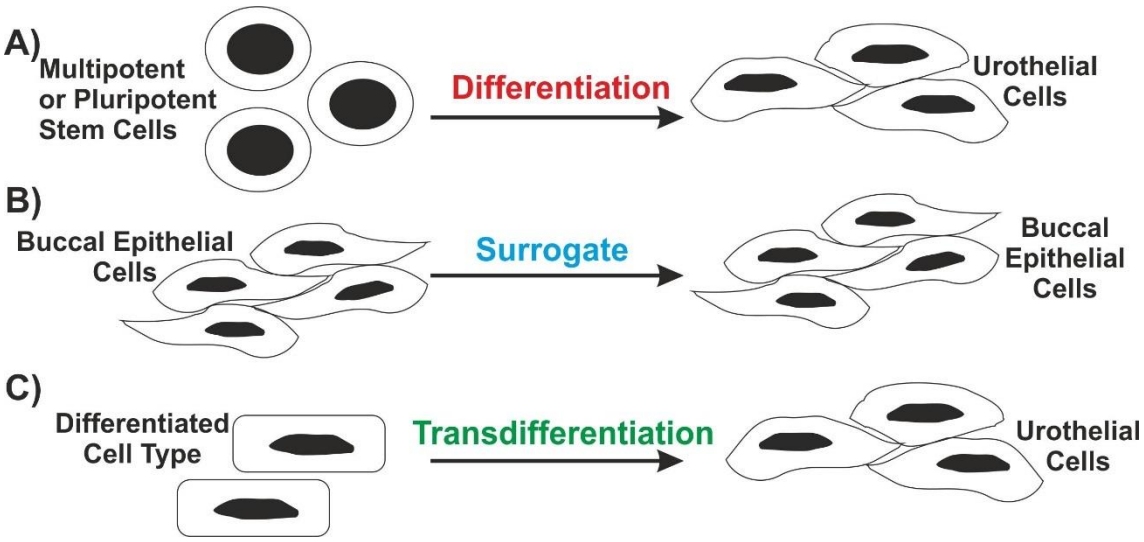

Figure 1.10 Methods of Generating Epithelial Cells for Bladder Tissue Engineering

A) Differentiation of autologous multipotent or pluripotent stem cells into urothelial cells using growth factors and agonists.

B) Use of another easily harvestable and expandable autologous barrier-forming epithelial cell type.

C) Transdifferentiation using direct transcription factor reprogramming of one autologous differentiated cell type into urothelial cells.

1.5.1.1 Differentiation of Multipotent and Pluripotent Stem Cells into Urothelial Cells

In recent years, there have been a number of attempts to differentiate various types of multipotent and pluripotent stem cells into urothelial cells, with the aim of providing a possible alternate autologous cell source for bladder tissue engineering. In order to do this, three main methods have been employed: the use of conditioned medium (Shi et al., 2012; Moad et al., 2013; Wu et al., 2013; Kang et al., 2014a; Zhao et al., 2014), co-culture (Liu et al., 2009; Tian et al., 2010; Ning et al., 2011; Chung and Koh, 2013), and the use of a specific medium/specific agonists (Bharadwaj et al., 2013; Lang et al., 2013; Kang et al., 2014b; Osborn et al., 2014). All of the methods have produced a similar outcome, the production of a population of cells which had upregulated expression of some epithelial and urothelial-associated genes – best classified as 'urothelial-like' cells.

One of the first reports of multipotent stem cell to urothelial-like cell differentiation used human bone marrow derived mesenchymal stem cells; this was performed by the use of indirect co-culture, and also by urothelial cell-derived conditioned medium (Tian et al., 2010). The authors demonstrated an upregulation of UPK1A, CK7 and CK13 expression by RT-PCR as a result of the culture conditions. Others have shown the differentiation of human adipose-derived stem cells (Shi et al., 2012), amniotic fluid stem cells (Kang et al., 2014a), and umbilical cord stem cells (Wu et al., 2013) into urothelial-like cells using conditioned medium (generated from human urothelial cells, a bladder cancer cell line, or an immortalised urothelial cell line), and observed an upregulation of CK18 and UPK2 expression. Induced pluripotent stem cells (iPSCs), derived from urinary tract stromal cells, have also been shown to have upregulated UPK1B, UPK2, UPK3A and UPK3B expression as a result of growth in human urothelial cell-derived conditioned medium (Moad et al., 2013).

The notion that urothelial cell conditioned medium or co-culture with urothelial cells alone should have the ability to completely differentiate stem cells into urothelial cells is unsupported. While the use of these techniques in the work described above appeared to have some ability to upregulate both epithelial cell-specific and urothelial cell-specific genes, their ability to cause complete conversion to a functional urothelium was not shown. This work is likely more important for its demonstration that human urothelial cells appear to be excreting factor/s which are able to induce expression of epithelial cell and urothelial cell-specific genes. Identification of these excreted factors could be beneficial for the understanding of how urothelial cells *in vivo* maintain their differentiated state.

The discovery of multipotent stem cells collected from voided urine (Zhang et al., 2008), and the subsequent attempt to convert these cells into urothelial cells (Bharadwaj et al., 2013) provided another possible surrogate urothelial cell source. Following growth in a specific medium (a combination of KSFM and embryonic fibroblast medium) with added EGF and 2 % FBS, the cells had increased expression of UPK1A, UPK3 and CK20 (shown by RT-PCR and/or immunofluorescence microscopy) (Bharadwaj et al., 2013). The authors were also able to demonstrate an increase in barrier function (decreased permeability to FITC-dextran) of these cells in comparison to non-differentiated cells.

The idea that simply culturing multipotent or pluripotent stem cells in a generic epithelial cell medium should have the ability to induce urothelial cell-specific differentiation is unfounded. This work must suggest that these urine-derived stem cells were pre-primed for urothelial-type differentiation above all other epithelial cell types. This notion was shown by another group (Moad et al., 2013), who compared the urothelial differentiation potential of human dermal-derived iPSCs and human urinary tract stroma-derived iPSCs; when both cell types were treated with human urothelial cell-derived conditioned medium, the urinary tract stroma-derived iPSCs had significantly greater upregulation of UPK1B, UPK2, UPK3A, UPK3B, CLDN1, CLDN5 and CK7, than the dermal-derived iPSCs.

More recently, attempts at a more 'directed' approach have been undertaken, using a two-step process whereby pluripotent stem cells are first differentiated into definitive endoderm-type (DE) cells, and then further differentiated into a urothelial cell lineage (Kang et al., 2014b; Osborn et al., 2014). Osborn et al. used this method starting with human embryonic stem cells. For urothelial-type differentiation, the DE cells were cultured in 'Uromedium' for 21 days, with PPARγ activation, by use of Troglitazone, at day 18. The authors demonstrated upregulated expression of all five of the uroplakin genes. In addition to this report, Kang et al. demonstrated differentiation of iPSCs using this two-step method, choosing to use KSFM with added retinoic acid for urothelial-type differentiation. The authors showed upregulated expression of UPK1B, UPK2, UPK3A and CK20, as well as increased barrier function (decreased permeability to FITC-dextran) in comparison to non-urothelial differentiated cells (definitive endoderm-type cells). The authors also demonstrated upregulation of epithelial cell-associated genes including CK7, CLDN5, ZO-1, and E-cadherin.

While the two-step directed approach to cell conversion applies a more logical approach, the actual urothelial cell differentiation step in both studies still lacked clear foundation. In both cases, the authors' primary method for demonstrating urothelial cell specification, over any other epithelial cell type, was to show fold change increase in uroplakin gene expression. It is well established that other epithelial cell types can at the very minimum express UPK1B and UPK3B (Adachi et al., 2000; Rudat et al., 2014). Therefore, the use of uroplakin gene expression as the sole basis for demonstrating

successful conversion to urothelial cells is not enough. More work is still necessary to determine useful sets of markers that can more fully distinguish urothelial cells from other epithelial cell types.

1.5.1.2 Use of Buccal Epithelial Cells for Bladder Tissue Engineering

Two forms (free graft and tissue-engineered graft) of buccal mucosa have been used and investigated for use in the urinary system. Currently, buccal mucosa is used commonly for urethroplasty, where a buccal mucosa graft is taken from the mouth, and directly transplanted to fix a urethral defect; this occurs in cases where tissue local to the urethra is not usable (reviewed in Markiewicz et al., 2007). Tissue-engineered versions of buccal mucosa have also been produced for urethroplasty patients who would need larger portions of buccal mucosa than are attainable via an intact free graft. While several healthy animal model-based studies have shown success (Li et al., 2008; Mikami et al., 2012), a clinical trial in human patients revealed poor outcomes, with two of the five patients needing full or part removal of the graft due to fibrosis (Bhargava et al., 2008).

Investigation into the use of buccal mucosa or buccal epithelial cells in the bladder is limited, with only a few animal studies having been performed; two studies have examined the effect of urine on buccal mucosa tissue for use in urethroplasty (Filipas et al., 1999; Xu et al., 2005), while a further two studies investigated the potential use of buccal epithelial cells for bladder tissue engineering (Lu et al., 2010; Watanabe et al., 2011).

A study published in 1999 compared the robustness of full-skin grafts and buccal mucosa grafts in the bladder of pigs (Filipas et al., 1999). Following 7 months of implantation, a histological analysis was completed which found that the buccal mucosa grafts fared better in the bladder than the full skin grafts following long-term exposure to urine; buccal mucosa grafts showed only little inflammation, while the majority of the skin grafts showed significant inflammation or necrosis.

The presence of buccal mucosa and colonic mucosa in the bladder has also been compared (Xu et al., 2005). Autologous buccal mucosa and colonic mucosa grafts were transplanted into opposite sides of the bladder in dogs. Upon histological analysis, following 6-10 months of the grafts' implantation, both the buccal mucosa and colonic mucosa grafts survived with only minimal inflammation present. The authors observed transitional-type epithelium on top of portions of some of the buccal mucosa and colonic mucosa grafts, likely indicating that overgrowth of adjacent urothelium had occurred.

More recently, autologous buccal mucosa grafts have been transplanted into the bladders of pigs, to determine their possible use for bladder tissue engineering (Lu et al., 2010). Following 3 and 6 months of implantation, the grafts displayed a normal non-cornified, stratified squamous epithelium. Following 12 months of implantation, the authors noted some histological changes to the grafted epithelium, which began to look less stratified squamous. The authors observed CK14 expression by immunohistochemical and transcript analysis at all of time points, indicating that the epithelium maintained its squamous phenotype throughout. UPK2 expression was observed by both immunohistochemical and transcript analysis at the 6 and 12 month time points. The authors suggested that this finding could highlight the transdifferentiation potential of buccal epithelial cells towards a more transitional epithelial cell phenotype.

Previous work has shown that patients with urine-deprived bladders display a normal urothelium phenotype, as characterised by morphology, and the expression of UPK1A, UPK1B, UPK3A, CK20, PPARγ and RXRα (Stahlschmidt et al., 2005). The work suggested that urine plays little or no role in maintaining the differentiation state of urothelial cells. Therefore, it is unlikely that urine should be able to cause any sort of urothelial-type differentiation of buccal epithelial cells. Changes observed in the studies described above were more likely attributed to urothelial cell ingrowth as opposed to transdifferentiation or metaplasia, as suggested by the authors. The other possible cause for the changes observed could be due to signalling from the underlying bladder stroma.

A tissue-engineered version of buccal mucosa has also been produced, where epithelial cell sheets were grown from autologous oral keratinocytes, then grafted onto gastric flaps and transplanted to augment the bladder of dogs (Watanabe et al., 2011). The epithelial cell sheets were produced using a serum and feeder layer-based cell culture method and appeared 2-5 cell layers thick. Following 3 weeks of implantation in the bladder, the grafts had an absence of oral epithelium and instead an ingrowth of urothelium on 20-30% of the grafts, with the other 70% of the grafts containing no epithelium. The authors also attempted a two-part surgery, where first the gastric flaps with buccal epithelial cell sheets where placed into a protective latex pouch in the abdomen for 5 days, and then they were transferred to augment the bladder for a duration of 3 weeks. Upon histological analysis, all of the grafts had a multi-layered stratified squamous epithelium similar to native buccal epithelium. The authors noted significant contraction of the grafts (up to 70 %) had occurred in all of the cases. This work demonstrated that oral epithelial cells directly implanted into the bladder are unable to survive. In order to survive and function in the bladder, they required pre-implantation in the body away from the bladder microenvironment. A much longer term study needs to be completed to assess the true long term potential of these cells in the bladder.

1.6 Transdifferentiation

Transdifferentiation (also termed lineage reprogramming) is the conversion of one differentiated cell type into another differentiated cell type, without reversion back to the pluripotent state (reviewed in Slack, 2007). Directed transdifferentiation is traditionally performed *in vitro* by the forced, exogenous expression of one or more critical transcription factors. This is typically fulfilled by using either lentiviral or retroviral-based transduction. More recently the use of microRNAs (miRNAs) and small molecules has also been employed (reviewed in Xu et al., 2015).

The first example of transdifferentiation was demonstrated in 1987, where it was shown that exogenous expression of the transcription factor, MyoD, in fibroblasts, could lead to conversion to myoblast-type cells. Since then, many groups have reported *in vitro* transdifferentiations of numerous cell types (reviewed in Xu et al., 2015). Much of the

transdifferentiations reported have been completed through conversion of cells of the same embryonic germ layer derivation. These include the conversion of myoblasts to adipocytes (Hu et al., 1995), B lymphocytes to macrophages (Xie et al., 2004), fibroblasts to myoblasts (Davis et al., 1987), and fibroblasts to cardiomyocytes (Ieda et al., 2010), which are all mesoderm to mesoderm cell conversions. Transdifferentiation of cell types across different embryonic lineages has also been shown to be possible: the conversion of fibroblasts to neurons is a mesoderm to ectoderm conversion (Vierbuchen et al., 2010). Work in the field of transdifferentiation has led to the new idea that differentiated cells are not lineage restricted, and can likely be converted into any other cell type by reprogramming once the key transcription factors are known.

The choice of transcription factors used for transdifferentiation is almost always derived from transcription factors known to play an important role in the embryonic development of the cell type. It has also been shown that a combination of both embryonic development-associated and mature differentiation-associated transcription factors can be required for the full transdifferentiation of some cell types (ie. the conversion of human fibroblasts into hepatocytes (Du et al., 2014)).

The main perceived advantage of transdifferentiation over the use of differentiated stem cells or induced pluripotent stem cells (iPSCs) is that transdifferentiated cells theoretically have no propensity to form teratomas, while cells derived from embryonic stem cells and iPSCs do form teratomas by definition (Miura et al., 2009).

1.6.1 Conversion of Fibroblasts to Cardiomyocytes and Neurons *in vitro*

Two of the most well studied types of transdifferentiation are the conversion of fibroblasts to cardiomyocytes, and the conversion of fibroblasts to neurons.

Direct reprogramming of fibroblasts into cardiomyocyte-like cells was first completed in 2010 by Ieda et al. using murine fibroblasts; three transcription factors, GATA4, Mef2c and Tbx5 were required (Ieda et al., 2010). Subsequent groups reported that the addition of up to four additional transcription factors, to the originally discovered three,

could lead to improved conversion to cardiomyocytes (Addis et al., 2013; Christoforou et al., 2013). In the attempt to translate these findings in the murine system to that of the human system, it was found that the original set of three transcription factors discovered in the mouse model (GATA4, Mef2c and Tbx5) was unable to cause successful transdifferentiation of human fibroblasts; additional genes were required for a more complete transdifferentiation (Fu et al., 2013; Wada et al., 2013). Another group discovered that murine fibroblasts could be converted to cardiomyocytes using four microRNAs (miR-1, miR-33, miR-208, and miR-499) (Jayawardena et al., 2012). They also found that the combined use of the microRNAs with a specific inhibitor was able to enhance the reprogramming 10-fold.

The first report of directed conversion of fibroblasts into functional neurons was published in 2010, where it was demonstrated that a combination of three transcription factors, Ascl1, Brn2, and Myt1l, could convert mouse fibroblasts into neuron-like cells (Vierbuchen et al., 2010). The authors originally started with 19 candidate genes known to have a role in neuron development and maintenance, before narrowing it down to the final three factors. The same group later demonstrated that when these three factors were combined with a fourth factor, NeuroD1, that fetal and postnatal human fibroblasts could be successfully converted into neurons (Pang et al., 2011). More recently this group further showed that neuron-like cells could be generated from both mouse and human fibroblasts using the overexpression of the transcription factor, Ascl1, alone (Chanda et al., 2014). Other groups have also shown the conversion of fibroblasts into neuron-like cells using various methods, including single gene knockdown (Xue et al., 2013), combined use of microRNA and transcription factor overexpression (Yoo et al., 2011), and the combined use of transcription factor overexpression with small molecule-based inhibition (Ladewig et al., 2012). A problem that arose with neuronal conversions, was that the final neuronal cells produced were post-mitotic, and therefore unable to be expanded further *in vitro*. As a result, several groups have worked on the transdifferentiation of fibroblasts into neural stem/progenitor cells, which can be propagated *in vitro* for many passages, and later induced to differentiate into multiple neuronal lineages (Han et al., 2012; Lujan et al., 2012; Ring et al., 2012; Thier et al., 2012; Cheng et al., 2014).

The main issue with all types of reprogramming and transdifferentiation-type experiments is being able to demonstrate complete conversion to the new cell type (ie. is the epigenetic signature from the starting cell type completely overwritten?). In many cases, authors are quick to make claims of achieved full conversion, without providing adequate evidence. Recently, Cahan et al. studied whether the reported transdifferentiations of fibroblasts to neurons or cardiomyocytes was complete. Unsurprisingly, they demonstrated that the generated cells failed to silence all of the fibroblast gene regulatory networks (Cahan et al., 2014), and as a result, the cells were likely in a much more immature state than they were originally described. This work demonstrated the need for much more rigorous testing in order to show true transdifferentiation to the new cell type. This notion is very much applicable to stem cell differentiation experiments. It is clear that a change in the reporting of results in this field needs to occur. Authors need to be a much more cautious in their description of findings, rather than the current trend of being overly acclamatory.

1.6.2 Transdifferentiation to Urothelial Cells

The only demonstration of possible transdifferentiation of a cell type into urothelial cells was demonstrated by Strand et al. The authors were investigating the role of PPARγ in prostate epithelium and found that the knockdown of PPARγ2 in benign human prostatic epithelial cells caused them to transdifferentiate into urothelial-like cells (Strand et al., 2013). Human prostate epithelial cells expressed both PPARγ1 and PPARγ2. Using shRNA, the authors demonstrated that PPARγ2 knockdown resulted in *de novo* CK20 protein expression, and increased p63 expression. When the PPARγ2 knockdown cells were grown on rat embryonic bladder mesenchyme, and transplanted under the renal capsule of immunocompromised mice, approximately 40% of the resulting epithelium was positive for pan-uroplakin protein expression. Portions of the epithelium also had CK14 expression in the basal cells. When both PPARγ1 and PPARγ2 were knocked down, there was no uroplakin protein expression, and increased CK14 expression. Although this work failed to fully demonstrate complete transdifferentiation to urothelial cells, it identified an essential role of PPARγ1 urothelial cell differentiation. It also demonstrated that loss of the PPARγ2 isoform was necessary for urothelial-type differentiation.

1.7 Thesis Aims

The overall aim of this research project was to investigate the potential use of oral epithelial cells as a surrogate epithelial cell source for bladder tissue engineering. More specifically, the aim was to attempt to transdifferentiate buccal epithelial cells into urothelial-like cells; the hypothesis being that there existed the ability to reprogramme one epithelial cell type to have the function of another epithelial cell type. In order to achieve this, the project had three key objectives:

1. Perform an *in vitro* characterisation of buccal epithelial cells with reference to urothelial cells, and in doing so determine a set of transcription factors which could be used to transdifferentiate buccal epithelial cells into urothelial-like cells (Chapter 3).

2. Investigate the expression and role of these determined transcription factors in maintaining urothelial cell identity and differentiation (Chapter 4).

3. Overexpress the determined transcription factors in buccal epithelial cells and determine their propensity to cause successful transdifferentiation (Chapter 5).

Chapter 2:
Materials and Methods

2 Materials and Methods

2.1 Practical Work

All laboratory work was carried out in the Department of Biology at the University of York in York, UK. Day-to-day laboratory work was carried out in the Jack Birch Unit of Molecular Carcinogenesis under the supervision of Professor Jennifer Southgate.

2.2 H_2O and Buffers

All water used for experiments and making buffers was ultrapure water (ELGA purified water), with a water purity of 18.2 MΩ-cm, which was generated using a type 1 ultrapure water purification system (ELGA, PURELAB® Ultra). Any water used for tissue culture was autoclaved (121 ^{o}C for 20 minutes) (Priorclave, 60L compact Priorclave) prior to use.

For molecular biology-based experiments, where nuclease-free water was required, diethylpyrocarbonate (DEPC) -treated ELGA purified water was used. To generate, DEPC-treated water, DEPC (Sigma-Aldrich, D5758) was added to ELGA purified water to a final concentration of 0.1 %, and then autoclaved (121 ^{o}C for 20 minutes).

Various buffer and solution recipes can be found in Appendix 7.1. All buffers and solutions were prepared using ELGA-purified water unless indicated (by use of a reference to see the Appendix).

2.3 Ethical Approval

Buccal mucosa and urological (renal pelvis and ureter) samples were obtained with National Health Service (NHS) Research Ethics Committee (REC) approval, from consented patients where applicable. Only the patients' age and gender were collected for the purpose of the research. The samples were sent unlinked and anonymised to the laboratory. Local ethical approval was also obtained from the University of York Biology Ethics Committee. Upon arrival to the laboratory, urological tissue specimens were given a unique 'Y' number (eg. Y1400) (Table 2.1). Buccal mucosa tissue specimens were given either a 'Y' number, or an 'AS' number (eg. AS001b)

(Table 2.2). When the epithelial cells were isolated from the tissue samples they retained their unique identifier, and thus were each defined as named distinct finite cell lines after serial passage.

Table 2.1 List of 'Y' Numbers Pertaining to Urological Tissue Samples

Sample ID Number	Type of Operation	Tissue Type	Age (yr.)/Sex
Y938	Nephrectomy	Ureter	?/?
Y939	Pyeloplasty	Renal Pelvis	?/?
Y1153	Nephrectomy	Ureter	?/?
Y1156	Nephrectomy	Ureter	?/?
Y1281	Nephrectomy	Ureter	79/F
Y1282	Nephrectomy	Ureter	55/M
Y1288	Nephrectomy	Ureter	57/M
Y1289	Nephrectomy	Ureter	54/F
Y1334	Renal Transplant	Ureter	24/M
Y1336	Nephrectomy	Ureter	63/F
Y1356	Renal Transplant	Ureter	63/M
Y1358	Pyeloplasty	Renal Pelvis	51/F
Y1361	Nephrectomy	Ureter	52/M
Y1390	Renal Transplant	Ureter	31/F
Y1393	Renal Transplant	Ureter	60/M
Y1453	Renal Transplant	Ureter	?/?
Y1541	Renal Transplant	Ureter	59/F
Y1642	Nephrectomy	Ureter	63/M
Y1677	Pyeloplasty	Renal Pelvis	1/M
Y1691	Nephrectomy	Ureter	59/F
Y1752	Renal Transplant	Ureter	41/M
Y1772	Renal Transplant	Ureter	50/M
Y1773	Renal Transplant	Ureter	46/M
Y1774	Pyeloplasty	Renal Pelvis	26/F
Y1815	Renal Transplant	Ureter	23/?

'?' means information not known.

Table 2.2 List of 'AS' and 'Y' Numbers Pertaining to Buccal Mucosa Tissue Samples

Sample ID Number	Type of Operation	Tissue Type	Age (yr.)/Sex
AS001b	Urethroplasty	Buccal Mucosa	37/M
AS003b	Urethroplasty	Buccal Mucosa	47/M
AS005b	Urethroplasty	Buccal Mucosa	40/M
AS006b	Urethroplasty	Buccal Mucosa	?/M
AS007b	Urethroplasty	Buccal Mucosa	62/M
AS008b	Urethroplasty	Buccal Mucosa	50/M
AS010b	Urethroplasty	Buccal Mucosa	65/M
AS011b	Urethroplasty	Buccal Mucosa	52/M
AS021b	Urethroplasty	Buccal Mucosa	24/M
AS027b	Urethroplasty	Buccal Mucosa	54/M
Y1590	Urethroplasty	Buccal Mucosa	13/M
Y1595	Urethroplasty	Buccal Mucosa	3/M
Y1600	Urethroplasty	Buccal Mucosa	5/M
Y1656	Urethroplasty	Buccal Mucosa	4/M
Y1721	Urethroplasty	Buccal Mucosa	3/M
Y1778	Urethroplasty	Buccal Mucosa	6/M

'?' means information not known.

2.4 Tissue Culture

2.4.1 General

Cell culture work was performed under aseptic working conditions, in BioMat^2 laminar recirculating airflow, class 2 safety cabinets (Contained Air Solutions Ltd.). Any cell culture work which involved the use of viruses was performed in an externally vented, Bio2+ laminar airflow, class 2 safety cabinet (Envair Ltd.).

All normal human buccal (NHB) epithelial cells and normal human urothelial (NHU) cells were maintained in Keratinocyte Serum Free Medium (KSFM) (Gibco®, 17005-034) containing 0.05 mg/ml bovine pituitary extract (Gibco®, 37000-015), 5 ng/ml epidermal growth factor (Gibco®, 37000-015) and 30 ng/ml cholera toxin, which was referred to as KSFM-complete (KSFMc) in this thesis.

Cultures were incubated in humidified HERAcell™ 240 CO_2 incubators (Thermo Scientific, 51026331). Buccal epithelial cells and urothelial cells were grown at 37 ºC in 5% CO_2 in air, in Cell+ tissue culture plasticware (Sarstedt Ltd., Cell+).

For cell counting, cell suspension was pipetted into each chamber of an Improved Neubauer haemocytometer (Hawksley, AC1000). The total number of cells present in 0.0001 cm^3 volume (1 mm^2 area) was counted for each chamber. The average number of cells was calculated from the two chambers, and then multiplied by 1.0×10^4 to obtain the number of cells/ml in the cell suspension.

All cell culture centrifugation steps were performed using a benchtop Sigma-Aldrich 2-6E centrifuge (SciQuip, 10223) at 250 g for 4 minutes.

All solutions required for tissue culture were either filter-sterilised using a 0.2 µm syringe filter (Appleton Woods, BC694) or, if heat stable, were autoclaved (121 ºC for 20 minutes), prior to use.

Phase contrast images of cells were taken using an EVOS® XL Core cell imaging system (Life Technologies) microscope.

2.4.2 Tissue Sample Collection

In order to ensure that the cells present in the tissue samples remained viable once removed from the patient, the tissue samples were placed into a transport medium shortly after removal from the patient in theatre. The transport medium was made using Hanks' Balanced Salt Solution (HBSS) (containing Ca^{2+} and Mg^{2+}) (Gibco®, 24020-091) with 10 mM HEPES (Gibco®, 15630-056), and 20 KIU/ml aprotonin (Nordic Pharma Ltd.) (Southgate et al., 1994). 100 U/mL penicillin-streptomycin (Gibco®, 15140-122) was added to the transport medium for collection of buccal mucosa tissue samples. The tissue samples were kept at 4 ºC for up to five days until they were processed for epithelial cell isolation and histology.

2.4.3 Epithelial Cell Isolation

Prior to epithelial cell isolation from the tissue samples, a small representative piece of tissue (<0.5 cm^2), from each sample, was cut and fixed in a 10 % (v/v) formalin solution (see Appendix) for 48 hours. The tissue was then stored in 70 % (v/v) ethanol (Fisher Scientific, E/0650DF/P17) for later histological analysis.

2.4.3.1 Buccal Epithelial Cells

The isolation protocol for NHB epithelial cells was adapted from (Oda and Watson, 1990). Buccal mucosa tissue samples were cut, using scissors (World Precision Instruments, 14394), into 0.5 cm^2 pieces, and incubated in 10 ml of 0.5 % (w/v) Dispase® II (Roche, 04942078001) solution (see Appendix) at 37ºC for 3-4 hours. The epithelium was separated from the underlying connective tissue using forceps (World Precision Instruments, 501976 & 504156), and each 0.5 cm^2 portion of buccal epithelium was cut into approximately 10-15 pieces. The tissue pieces were incubated in 2 ml of trypsin versene (TV) (see Appendix) at 37 ºC for 5 minutes to disaggregate the cells. 200 µl of 20 mg/ml trypsin inhibitor (TI) (see Appendix) was added to 5 mL of KSFMc, and the 5.2 ml solution was added to the disaggregated cell suspension. The cell suspension was centrifuged, and the cells were resuspended in 2 ml of 100 U/ml collagenase (see Appendix) for 20 minutes at 37 ºC, before centrifugation and

resuspension in KSFMc. The cells were counted, and seeded into Cell+ cell culture plasticware at a seeding density of 4.0 x 10^4 cells/cm^2. 1 % (v/v) penicillin-streptomycin was added to the medium for the initial 24 hours after seeding.

2.4.3.2 Urothelial Cells

NHU cells were isolated from patient tissue samples as previously described (Southgate et al., 1994). Tissue samples were cut into 0.5-1.0 cm^2 pieces using scissors, and placed in 'stripper medium' (see Appendix) for 4 hours at 37 ^oC. The epithelium was separated from the underlying connective tissue using forceps, and collected by centrifugation. The cells were resuspended in 2 ml of 100 U/ml collagenase for 20 minutes at 37 ^oC, before being centrifuged, and resuspended in KSFMc. The cells were counted using a haemocytometer, and seeded at a density of 4.0 x 10^4 cells/cm^2 into Cell+ cell culture plasticware.

2.4.4 Maintenance and Subculture (Passage) of Finite Epithelial Cell Lines

NHB epithelial cell and NHU cell cultures were maintained in KSFMc, and the medium was changed every 2-3 days. Upon reaching confluence, the cultures were passaged and reseeded into new flasks. To passage, cultures were treated with 0.1 % (w/v) EDTA (BDH, 100935V) for 5-10 minutes at 37^oC until the cells started to separate from one another, and become rounded in appearance. The EDTA solution was removed, and 1 ml of TV was added for approximately 1 minute at 37 ^oC, until cells detached from the plasticware upon tapping. 100 µl of 20 mg/ml TI in 5 mL of KSFMc was added to the cells. The resulting cell suspension was centrifuged to pellet, and the cells were resuspended in KSFMc. The cells were seeded onto plasticware at a minimum seeding density of 1.0 x 10^4 cells/cm^2. Normal human buccal epithelial and urothelial cell lines were used for experiments between passages 1-5 (P1-P5). Experiments were replicated using up to four independent donor finite cell lines.

2.4.5 Freezing and Thawing Cells

Cell lines were cryopreserved and stored in liquid nitrogen-containing dewars (Taylor-Wharton, LS6000). Cells were harvested as described in section 2.4.4, and the cell pellet was resuspended in 'freeze mix' made using KSFMc with 10 % (v/v) FBS and 10 % (v/v) DMSO (Sigma-Aldrich, D2650). 1 ml of 'freeze mix' with cells was pipetted into each 2 ml cryo vial (Sarstedt, 73.380.992). The vials were placed at -80 ^{o}C in a Mr. Frosty™ Freezing Container (Thermo Scientific, 5100-0001) for 24 hours in order to allow for controlled reduction of the temperature at a rate of -1 ^{o}C/min. The vials were transferred to liquid nitrogen-containing dewars for long term storage.

To recover cells from frozen, vials were removed from the liquid nitrogen dewars, and thawed rapidly in a 37 ^{o}C water bath. The contents of the vial were resuspended in 10 ml of KSFMc, and centrifuged to pellet. The cells were resuspended in KSFMc, and seeded as required.

2.4.6 ABS/Ca^{2+} Protocol

The ABS/Ca^{2+} protocol has been previously described to cause differentiation of NHU cells, and generation of biomimetic urothelium equivalents (cell sheets) (Cross et al., 2005) (Figure 2.1). Cells were grown to 80-90 % confluence, and the medium was changed to KSFMc containing 5 % adult bovine serum (ABS) (SeraLab, S-202) for 4-5 days. Cultures were harvested, and seeded onto either 12 mm Snapwell membranes (pore size 0.4 μm) (Fisher Scientific, TKT-541-030W) or 12-well Thincert™ cell culture inserts (Greiner Bio-One, 665640). 5.0 x 10^5 cells were seeded per membrane in a volume of 500 μl. The cells were grown in KSFMc with 5 % ABS for 24 hours, and then the medium was changed to KSFMc with 5 % ABS and 2 mM [Ca^{2+}]. The calcium concentration of the medium was increased to 2 mM (near physiological levels) by adding the appropriate amount of a sterile 1 M $CaCl_2$ stock solution; it was taken into account that KSFMc contains approximately 0.09 mM [Ca^{2+}] and ABS contains approximately 2.2 mM [Ca^{2+}]. The cultures were maintained in the 5 % ABS and 2 mM [Ca^{2+}] medium for 7 days, with the medium changed every 2-3 days. 0.5 ml of medium was placed on top of the cells (in the upper well) and 2 ml of medium was placed underneath the cells (in the lower well).

To differentiate cell cultures for the purpose of taking protein lysates, the cells were established as above in 6-well plates, but the passage step, and subsequent seeding onto the membranes was omitted; following 5 days in KSFMc containing 5 % ABS, the medium was changed to KSFMc containing 5 % ABS and 2 mM [Ca^{2+}]. The cultures were medium changed every 2-3 days.

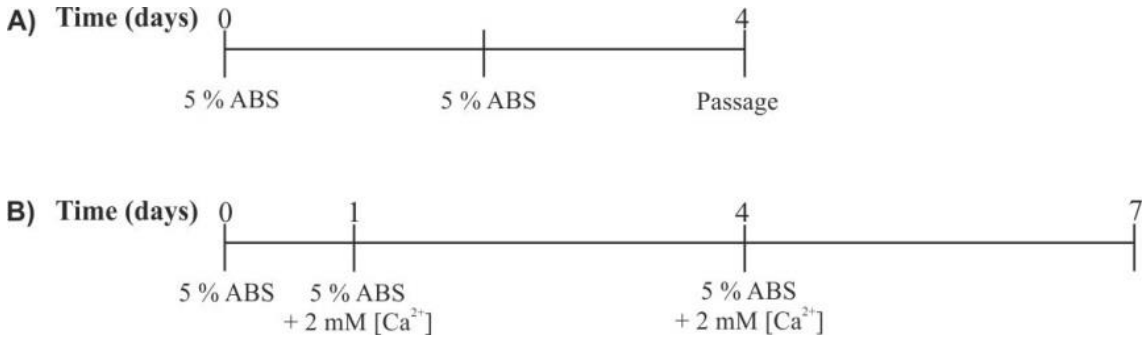

Figure 2.1 ABS/Ca^{2+} Differentiation Protocol

A) 5% ABS pre-treatment of the cells for 4 days.

B) 7 day differentiation with near physiological calcium concentrations (2 mM).

2.4.7 Measurement of Transepithelial Electrical Resistance (TER)

The transepithelial electrical resistance (TER) was used as a measurement of the barrier function of cell sheets produced on Snapwell and ThinCert™ membranes. For the TER measurement, chopstick electrodes (World Precision Instruments, STX2) and an Epithelial Voltohmmeter X (World Precision Instruments, EVOMX) were used. The electrode was first disinfected using Cidex Plus solution (World Precision Instruments, 7364) and then equilibrated in 37 ^{o}C pre-warmed medium (KSFMc) for 10 minutes. To take the TER measurement, the electrode was placed so that the shorter prong was just above the cell surface in the inner well, and the longer prong of the electrode was placed in the medium in the outer well. The electrode was held in place for up to 30 seconds, and the TER value was recorded. The TER of Snapwell and ThinCert™ membranes containing medium only (ie. no cells) was taken, and subtracted from all recorded values.

2.4.8 Dispase Lifting of Cell Sheets

Cell sheets (created as described above in section 2.4.6) were harvested from Snapwell and ThinCert™ membranes, by incubating the cultures in a 2 % (w/v) dispase solution for 30 minutes at 37 ºC; 0.5 ml of dispase solution was placed on top of the cells, and 2 ml of dispase solution was placed in the well below the cells. The lifted cell sheet was carefully floated into a CellSafe+ biopsy capsule (CellPath, EBE-0301-02A). The capsules were placed into System III Hex embedding cassettes (CellPath, EAI-0106-10A), and labelled appropriately. Cell sheets were fixed in 10 % (v/v) formalin for 24 hours. The cassettes were transferred into 70 % (v/v) ethanol for storage before processing for histological analysis (see section 2.5.2.1).

2.4.9 TZ/PD Protocol

To investigate the response of cultures to PPARγ activation, the protocol described by Varley et al., termed TZ/PD in this thesis, was used (Figure 2.2). The combined use of troglitazone (a PPARγ agonist) and PD153035 (an EGFR-TK inhibitor) has been shown to cause the upregulation of urothelial differentiation-associated genes, including the uroplakins, CK20, and several tight junction-associated proteins, in NHU cells (Varley et al., 2004a; Varley et al., 2004b; Varley et al., 2006).

Cultures were grown to 70-80 % confluence, and treated with 1 μM troglitazone (TZ) (Tocris, 3114) and 1 μM PD153035 (PD) (Merck Millipore, 234490) in KSFMc for 24 hours. The medium was then changed to KSFMc containing 1 μM of PD153035 only. The cultures were maintained as such for up to 6 days, with the medium changed on the 3rd day. Cultures grown in KSFMc containing 0.1 % dimethyl sulphoxide (DMSO) acted as a vehicle control. The amount of vehicle solution (DMSO) used for drug treatments was kept constant at 0.1 %.

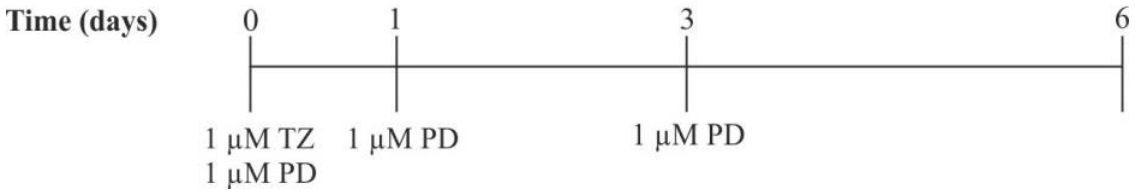

Figure 2.2 TZ/PD Protocol.
NHB epithelial cell cultures and NHU cell cultures were grown in KSFMc containing 1 μM troglitazone (TZ) and 1 μM PD153035 (PD) for 24 hours. The medium was then changed to contain only 1 μM PD153035 for all subsequent medium changes.

2.4.10 atRA/PD Protocol

Retinoic acid receptor (RAR) activation has been implicated as a key regulator in the maintenance of the urothelial cell identity, with a particular role in preventing squamous metaplasia (Southgate et al., 1994; Liang et al., 2005; Gandhi et al., 2013). To investigate the effect of RAR activation on regulating urothelial-associated genes in NHB epithelial cells, a combination of all-trans retinoic acid (atRA), a RAR ligand, and PD153035 were used. The protocol employed was based on the already established TZ/PD protocol, and was developed by Dr. Simon Baker, a post-doctoral researcher at the Jack Birch Unit.

Cultures were grown to approximately 70 % confluence, and the medium was changed to either KSFMc containing 1 μM PD153035 (control), or KSFMc containing 1 μM PD15035 and atRA (10 nM, 100 nM and/or 1 μM) for 72 hours (Figure 2.3). Some treatments also included 1 μM TZ to investigate the effect of simultaneous PPARγ and RAR activation. If TZ was being used, then the medium was changed after 24 hours to remove TZ from any cultures which contained it, in keeping with the standard TZ/PD protocol. The amount of vehicle solution (DMSO) used for drug treatments was kept constant at 0.1 %.

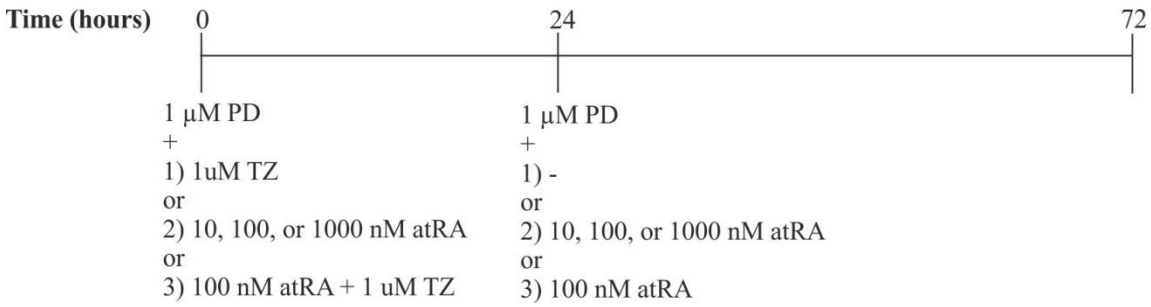

Figure 2.3 atRA/PD Protocol

NHB epithelial cells were grown to approximately 70 % confluence. The medium was changed to either KSFMc containing 1 μM PD153035 or KSFMc containing 1 μM PD153035 plus atRA (10 nM, 100 nM or 1 μM) for 72 hours. Some treatments also included 1 μM Troglitazone. The medium was changed after 24 hours to remove TZ from any cultures which contained it, in keeping with the standard TZ/PD protocol

2.4.11 Culture of Immortalised Cell Lines

Three immortalised cell lines (MCF-7, UMUC9 and PT67) were cultured, and used for experiments in this thesis; MCF-7 cells are a breast carcinoma-derived cell line, UMUC9 cells are a bladder carcinoma-derived cell line, and PT67 cells are a retroviral packaging cell line (3T3 variant). Cells were maintained in Dulbecco's Modified Eagle's Medium (DMEM) (Gibco®, 21969-035) with 10 % Fetal Bovine Serum (FBS) (SeraLab, EU-000) (batch selected) and 1 % L-glutamine (LG) (Gibco®, 25030-024), which was referred to as DMEM10% medium. Cultures were grown at 37 ^{o}C in 10 % CO_2 in air, in Corning® cell culture plasticware (Sigma-Aldrich).

For the subculture of immortalised cell lines, the same protocol as described in section 2.4.4 was employed, except DMEM10% medium was used in place of KSFMc. The use of trypsin inhibitor was omitted, due to the presence of serum in the medium, which also has the capacity to inhibit trypsin activity.

Immortalised cell lines were frozen, as previously described in section 2.4.5, except 'Freeze mix' was made using DMEM with 10 % (v/v) FBS and 10 % (v/v) DMSO (Sigma-Aldrich, D2650).

2.5 Protein Analysis

2.5.1 Indirect Immunofluorescence Microscopy

Indirect immunofluorescence (IF) is a technique used to determine the localisation of a protein in cultured cells or tissue samples. It relies on the use of fluorescently-labelled secondary antibodies, which bind to the protein-specific primary antibodies. Cells or tissue are first fixed, and then permeabilised by lipid extraction or detergent, in order to allow for detection of the intracellular antigens.

2.5.1.1 Slide Preparation

Cells were seeded and grown on 12-well glass slides (C A Hendley Essex Ltd., PH-057 Royal blue) in quadriPERM® 4-well slide boxes (Sarstedt, 94.6077.308). Upon completion of the cell growth or treatment protocol, slides were washed twice with phosphate buffered saline (PBS) (see Appendix). Cells were fixed with either methanol:acetone (50:50) (Fisher Chemical, M/4000/PC17 & A/0600/PC17) for 30 seconds, or 10 % (v/v) formalin solution for 10 minutes. Slides fixed with methanol:acetone were air dried for 10 minutes, and stored desiccated at -20 ^{o}C until use. Slides fixed with formalin were washed twice with PBS to remove any remaining formalin solution, and stored in PBS at 4 ^{o}C for up to one week. Directly prior to antibody labelling, formalin-fixed slides were incubated in PBS containing 0.5 % Triton X-100 (SLS, 93443) for 30 minutes to permeabilise the cells. The slides were washed once with PBS.

2.5.1.2 Antibody Labelling

Slides were brought to ambient temperature, and an ImmEdge hydrophobic barrier pen (Vector, H-4000) was used to outline each well to prevent antibody movement. 20 µl of primary antibody, diluted (as required) in Tris Buffered Saline (TBS), pH 7.6 with 0.1 % NaN_3 (Sigma-Aldrich, S8032) and 0.1% bovine serum albumin (BSA) (Thermo Fisher Scientific, 37520) was pipetted onto wells of the 12-well slides. Cells were incubated with the primary antibody (see Table 2.3) overnight (16 hours) at 4 ^{o}C. Negative control wells were incubated with the antibody diluent only. Primary antibody was removed by 4x 5 minute washes with PBS on an orbital shaker (Jencons-PLS,

R100T/W). 20 µl of the appropriate secondary antibody (see Table 2.4) (diluted in TBS pH 7.6 with 0.1 % NaN_3 and 0.1% BSA) was applied to each well for 1 hour at ambient temperature. Slides were protected from light to prevent bleaching of the fluorescence. For red fluorescent labelling, a secondary antibody conjugated to Alexa Fluor 594 was used, and for green fluorescent labelling, a secondary antibody conjugated to Alexa Fluor 488 was used. The slides were washed with PBS, on the orbital shaker, for 2x 5 minutes to remove excess secondary antibody. Each slide was incubated in 5 mL of PBS with 0.1 µg/ml Hoechst 33258 (fluorescent DNA stain) (Sigma-Aldrich, 861405) to label the nuclei, which fluoresced blue. The slides were mounted with an antifade mountant (see Appendix), and a 22x64 mm coverslip (SLS, MIC3208). Coverslips were sealed to the slide using clear nail varnish around the coverslip edge.

For every immunofluorescence experiment, additional slides were generated and used as positive controls; slides contained cells that were known to express the protein of interest. Positive control slides typically contained NHU cells treated with TZ/PD for either 72 hours or 6 days. Slides seeded with MCF-7 cells or UMUC9 cells were also used in some instances.

Negative control wells (no primary antibody) were included on each slide, for each secondary antibody used, to determine if non-specific absorption of the secondary antibody had occurred.

Table 2.3 List of Primary Antibodies used for Indirect Immunofluorescence

Antigen	**Antibody Clone or Catalogue #**	**Host (Production)**	**Supplier**	**Dilution***
CK5	PH607	Sh	The Binding Site	1:100
CK7	OV-TL12/30	M (monoclonal)	Novocastra	1:40
CK13	1C7	M (monoclonal)	abnova	1:500
CK14	LL001	M (monoclonal)	ICRF (gift)	1:5
CK18	CY-90	M (monoclonal)	Sigma-Aldrich	1:1000
CK19	LP2K	M (monoclonal)	ICRF (gift)	1:5
CK20.3	IT–Ks20.3	M (monclonal)	Cymbus Bioscience Ltd.	1:100
ELF3	EPESER1	Rb (monoclonal)	Abcam	1:1000
GATA3	D13C9	Rb (monoclonal)	Cell Signaling	1:800
HNF-3 α (FOXA1)	Q6	M (monoclonal)	Santa Cruz	1:200
HNF-3α/β (FOXA1/2)	C-20	Gt (polyclonal)	Santa Cruz	1:200
PPARγ	E-8	M (monoclonal)	Santa Cruz	1:200
PPARγ	81B8	Rb (monoclonal)	Cell Signalling	1:100
PPARγ	D69	Rb (polyclonal)	Cell Signalling	1:100
PPARγ	P&A53.25	M (monoclonal)	GSK (gift)	1:400

Sh – Sheep, M – Mouse, Rb- Rabbit, ICRF – Imperial Cancer Research Fund

* Dilution previously determined by titration.

Table 2.4 List of Secondary Antibodies used for Indirect Immunofluorescence

2º Antibody	**Conjugated Alexa Fluor®**	**Company, Code**	**Dilution***
Goat anti Rabbit (IgG)	594 (red)	Life Technologies, A11012	1:700
Goat anti Rabbit (IgG)	488 (green)	Life Technologies, A11008	1:400
Goat anti Mouse (IgG)	594 (red)	Life Technologies, A11005	1:500
Goat anti Mouse (IgG)	488 (green)	Life Technologies, A11001	1:500
Donkey anti Goat (IgG)	594 (red)	Life Technologies, A11058	1:500

* Dilutions previously determined by titration.

2.5.2 Immunohistochemistry

Immunohistochemistry is an antibody-based labelling method used to determine the localisation of a protein of interest in a tissue sample or cell sheet. It relies on the use of secondary antibodies that are conjugated to horseradish peroxidase. Horseradish peroxidase reacts with the substrate, diaminobenzidine (DAB), to produce an insoluble product that can be used to visualise the protein of interest.

2.5.2.1 Embedding Tissue Samples and Cell Sheets

Prior to embedding, all tissue samples and cell sheets were fixed in a 10 % (v/v) formalin solution for 24-48 hours. Samples were transferred to a 70 % (v/v) ethanol solution for long term storage at ambient temperature.

Tissue samples were cut into pieces less than 0.5 cm^2. The tissue samples and cell sheets (in CellSafe+ biopsy capsule) were placed into System III Hex embedding cassettes (CellPath, EAI-0106-10A). To dehydrate the samples, which allows for the paraffin wax to fully penetrate the tissue/cell sheets, the samples underwent a series of washes as follows: 70 % ethanol for 10 minutes, 4x 10 minute washes in 100 % ethanol

(Fisher Chemical, E/0650DF/P17), 2x 10 minute washes in isopropanol (Sigma-Aldrich, 33539) and 4x 10 minute washes in xylene (Fisher, X/0250/PB17). Excess xylene was removed from the cassettes by blotting, and they were incubated in melted paraffin wax (Thermo Scientific, 6774060) for 4x 15 minutes at 65 ^{o}C. The samples were embedded in fresh paraffin wax using metal embedding moulds (Leica Biosystems, 38VSP58167), and left to harden on a cold block (RA Lamb, E6613) at -12 ^{o}C. Once set, the wax blocks were removed from the moulds and stored at ambient temperature until use.

2.5.2.2 Sectioning of Samples and Slide Preparation

Prior to sectioning of samples, the wax blocks were cooled to -12 ^{o}C on a cold block for approximately 1 hour. 5 µm sections were prepared using a rotary microtome (Leica Biosystems, RM2135). The sections were transferred to a paraffin section floatation water bath set to 40 ^{o}C (RA Lamb, E66.2), before being collected onto Superfrost™ Plus microscope slides (Thermo Scientific, 4951PLUS4). The slides were left to air dry overnight, and then placed on a 50 ^{o}C slide drying heat block (RA Lamb, E18.1) for 1 hour to adhere the tissue/cell sheet to the slide. Slides were stored at ambient temperature until use.

Sections were dewaxed by: 2 x 10 minute washes in xylene, 2 x 1 minute washes in xylene, 4 x 1 minute washes in 100 % ethanol, 1 x 1 minute wash in 70 % ethanol. The slides were washed for 1 minute in running tap water to remove any remaining ethanol. Tissue sections were blocked using 3 % (v/v) hydrogen peroxide (Fisher, H/1800/15) for 10 minutes (this blocking step was used to prevent background signal from any red blood cells present in the tissue), and washed with running tap water for 10 minutes.

To reverse the cross-linking of proteins caused by formalin fixation, and allow for the epitope of interest to be more easily accessible to the primary antibody, one of four antigen retrieval methods was used (see Table 2.5). The antigen retrieval method used was specific to each primary antibody, and was determined prior to starting experiments.

Following antigen retrieval, slides were washed in distilled water, and loaded into Shandon Sequenza® slide racks (Fisher Scientific, 73310017) using Coverplates™ (Fisher Scientific, 11927774). Slides were rinsed with TBS. Depending on the primary antibody, either the standard immunohistochemistry procedure (described in section 2.5.2.3) was used, or a more sensitive polymer staining kit (described in section 2.5.2.4) was used.

Positive control slides, containing tissue known to express the protein of interest, were included as part of every immunohistochemistry experiment. Negative control slides (no primary antibody) for each type of secondary antibody, were also included as part of every experiment; this was used to identify if any non-specific interactions had occurred. Example positive and negative control images for immunohistochemistry are shown in the Appendix.

Table 2.5 Antigen Retrieval Methods used for Immunohistochemistry

Name	Method
Trypsinization (**Tr**)	The slides were incubated in 0.1 % (w/v) trypsin (Sigma-Aldrich, T7409) at 37 ^{o}C for 10 minutes.
Citric Acid (**CA**)	The slides were placed in a 21 x 21 cm glass Pyrex dish, covered with 10 mM citric acid buffer, pH 6.0 (Fisher Scientific, c/6200/53), and microwaved to boil for 10 minutes.
Trypsin and Citric Acid (**Tr/CA**)	The slides were incubated in 0.1 % (w/v) trypsin at 37 ^{o}C for 1 minute, and then washed in distilled water. The slides were microwaved in 10 mM citric acid buffer, pH 6.0 as described above in the citric acid antigen retrieval method.
EDTA	The slides were placed in a 21 x 21 cm glass Pyrex dish, covered in 1 mM EDTA buffer, pH 8.0, and microwaved to boil for 10 minutes

2.5.2.3 Standard Immunohistochemistry

To block any endogenous biotin in the cells, the slides were incubated with avidin (Vector, sp-2001) for 10 minutes. The slides were washed twice with TBS to remove any excess. The slides were then incubated with biotin (Vector, sp-2001) for 10 minutes to bind to any remaining avidin binding sites. Excess biotin was removed by washing the slides twice with TBS. To block any non-specific binding of the secondary antibody, the slides were incubated with serum derived from the animal in which the secondary antibody was raised (Table 2.7), for 5 minutes. The slides were incubated with the primary antibody at 4 ^{o}C overnight (Table 2.6). Negative control slides were incubated with the antibody diluent only. The next day, slides were washed three times with TBS to remove excess primary antibody, and an appropriate biotinylated secondary antibody was applied for 30 minutes (Table 2.7). The slides were washed twice with TBS, and a streptavidin-biotinylated/horseradish peroxidase complex (StrepAB/HRP) (Vector, PK-6100) was applied for 30 min; this complex binds to the biotin conjugated to the secondary antibody, in order to amplify the visible signal. The slides were washed again to remove excess StrepAB/HRP, and incubated with diaminobenzidine (DAB) (Sigma-Aldrich, D4293) for 10 minutes. DAB reacts with the horseradish peroxidase to produce a brown precipitate, which identifies the protein of interest. Slides were washed with distilled water, and placed into metal slide racks before being counterstained and mounted (see section 2.5.2.5).

2.5.2.4 Polymer Staining Kit-based Immunohistochemistry

The ImmPRESS™ Excel Immunolabelling kit (Vector Laboratories, MP-7601 & MP-7602) was used as a more sensitive technique for certain primary antibodies which failed to work using the standard immunohistochemistry protocol. All reagents described in the method below were supplied in the kit. To block any non-specific binding, 100 µl of 2.5 % horse serum was applied to each slide, and incubated at ambient temperature for 20 minutes. 100 µl of primary antibody (Table 2.8) was applied to each slide, and incubated overnight (approximately 16 hours) at 4 ^{o}C. Primary antibodies were diluted as required in TBS-T (0.05 M Tris-HCl pH 7.6, 0.3 M NaCl and 0.1 % Tween 20). The slides were washed three times with TBS-T to remove any unbound primary antibody. The appropriate ‘amplifier’ (secondary) antibody was applied to the slides, and incubated at ambient temperature for 15 minutes. The slides

were washed twice with TBS-T to remove excess 'amplifier' antibody. Next, 100 µl of a third antibody (called the ImmPRESS Excel Reagent in the kit), which is conjugated with horseradish peroxidase, was applied to the slides, and incubated for 30 minutes at ambient temperature. The slides were washed twice with TBS-T, and once with distilled water to remove any excess antibody. 100 µl of 50:50 Immpact DAB reagent 1:reagent 2 was applied to the slides for 5 minutes at ambient temperature. The slides were washed once with distilled water to remove excess DAB, and placed into metal slide racks before being counterstained and mounted (see section 2.5.2.5).

Table 2.6 List of Primary Antibodies used for Standard Immunohistochemistry

Antigen	**Antibody Clone or Catalogue #**	**Host (Production)**	**Supplier**	**Dilution* (Retrieval Method)**
CK5	SP27	Rb (monoclonal)	Abcam	1:100 (CA)
CK7	OV-TL12/30	M (monoclonal)	Novocastra	1:400 (CA)
CK13	1C7	M (monoclonal)	abnova	1:500 (Tr/CA)
CK14	LL002	M (monoclonal)	Serotec	1:1200 (Tr/CA)
CK20.8	Ks20.8	M (monoclonal)	Novocastra	1:200 (Tr)
Claudin 4	3E2C1	M (monoclonal)	Zymed	1:500 (CA)
Claudin 5	4C3C2	M (monoclonal)	Invitrogen	1:50 (CA)
Claudin 7	34-9100	Rb (polyclonal)	Zymed	1:200 (CA)
Occludin	71-1500	Rb (polyclonal)	Zymed	1:100 (CA)
ZO-1	ZO1-1A12	M (monoclonal)	Life Technologies	1:100 (CA)
ZO-2	2847	Rb (polyclonal)	Cell Signaling	1:250 (EDTA)
ZO-3	D57G7	Rb (monoclonal)	Cell Signaling	1:200 (Tr/CA)
HNF-3α/β (FOXA1/2)	C-20	Gt (polyclonal)	Santa Cruz	1:150 (CA)

M – Mouse, Rb- Rabbit, Gt – Goat

* Dilution previously determined by titration.

Table 2.7 List of Sera and Corresponding Secondary Antibodies used for Standard Immunohistochemistry

Serum	**Company, Code**	**Dilution**	**2º Antibody**	**Company, Code**	**Dilution***
Rabbit Serum	Dako, X0902	1:10	Biotinylated Rabbit anti Mouse (Ig)	Dako, E0354	1:200
Goat Serum	Dako, X0907	1:10	Biotinylated Goat anti Rabbit (Ig)	Dako, E0466	1:600

* Dilution previously determined by titration.

Table 2.8 List of Primary Antibodies used for the Polymer Staining Kit-Based Immunohistochemistry

Antigen	**Antibody Clone or Catalogue #**	**Host (Production)**	**Supplier**	**Dilution* (Retrieval Method)**
GATA3	D13C9	Rb (monoclonal)	Cell Signalling	1:800 (Mw)
PPARγ	81B8	Rb (monoclonal)	Cell Signalling	1:250 (EDTA)
RXRα	K8508	M (monoclonal)	R&D Systems	1:600 (Mw)

M – Mouse, Rb- Rabbit

* Dilution previously determined by titration.

2.5.2.5 Slide Counterstaining and Mounting

Slides were incubated in haematoxylin (stains nuclei) (see Appendix) for up to 10 seconds, and washed in running tap water to remove excess haematoxylin. The slides were dehydrated by: 1 x 1 minute wash in 70% ethanol, 3 x 1 minute washes in 100 % ethanol, and 2 x 1 minute washes in xylene, and mounted with a coverslip (SLS, MIC3104) using DPX (CellPath, SEA-1304-00A).

2.5.3 Imaging Immunofluorescence and Immunohistochemistry Slides

Slides generated from immunohistochemistry and immunofluorescence-based experiments were imaged using a brightfield/epifluorescence microscope (Olympus, BX60) equipped with x10 (dry), x20 (oil) x40 (oil) and x60 (oil) objective lenses and emission and excitation filters for DAPI (Hoechst 33258), FITC and Texas Red. Images were taken using a digital camera (Olympus, DP50) attached to the microscope, and analysed using Image-Pro Plus Software (Media Cybernetics, Image-Pro Plus version 4.5.1.29).

For immunofluorescence experiments, optimal exposures were chosen for each antibody at the time of imaging, in order to best demonstrate the localisation of the protein of interest. In cases were protein expression was examined across a treatment time course, the optimal exposure for one of the middle time points was picked, and used for all of the time points. In cases where absent or very weak expression was observed, the optimal exposure of the positive control was used. Negative control wells were imaged at the same exposure as the primary antibody labelled wells. Example negative control images for IF are shown in Figure 2.4.

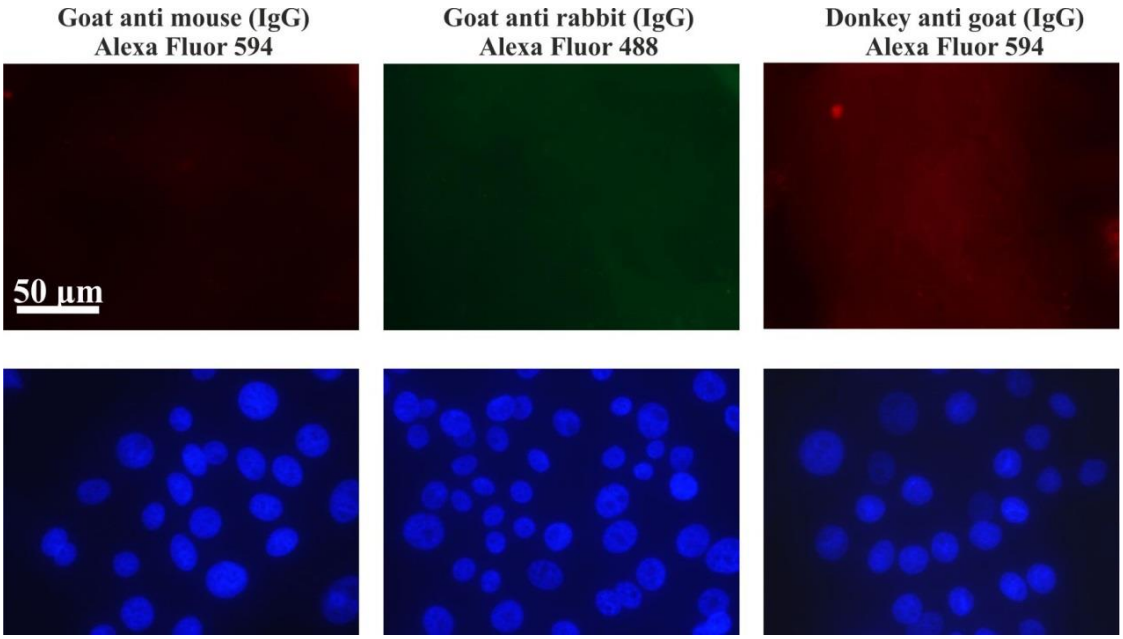

Figure 2.4 Example Negative Control Images – Indirect Immunofluorescence Microscopy

Example negative control (secondary antibody only) images are shown. The corresponding Hoechst 33258 images for each are shown below. Weak background signal was observed with all of the secondary antibodies used for IF.

2.5.4 Western Blotting

Western blotting is a process whereby proteins extracted from a population of cells are first separated, based on molecular weight, by electrophoresis through a polyacrylamide gel. The proteins are then transferred, by electroblotting, onto a Polyvinylidene fluoride (PVDF) membrane. The membrane is first blocked, and then probed using antibodies to detect the presence of a protein of interest. This technique allows for relative analysis of a specific protein between different protein extracts.

2.5.4.1 Protein Lysates

Prior to taking the lysate, cell cultures were washed twice with cold 1x PBS. Whole protein lysates were generated using an SDS lysate buffer (2x sodium dodecyl sulfate (SDS) sample buffer (see Appendix) containing 0.013 M DTT (Sigma-Aldrich, D0632) and 1 % protease inhibitor (Sigma-Aldrich, P8340)), which were combined at the time of taking the lysates. SDS lysate buffer was pipetted onto the cells (100 µl for each well of a 6-well plate). Cells were scraped into the lysis buffer using a cell scraper (Sarstedt, 83.1830), and collected into a 1.5 ml microfuge tube on ice. The lysates were sonicated (2.5 W, 40% amplitude) on ice for 10 seconds, followed by a 10 second rest, and then another 10 second burst of sonication. Lysates were rested on ice for 30 minutes, and centrifuged (Hettich Lab Technologies, MIKRO 200 R) at 18,000 g for 30 minutes at 4 ^{o}C. The supernatant (protein containing portion) was collected, and transferred to a fresh 1.5 ml microfuge tube. Lysates were stored at -20 ^{o}C for up to several months, or were stored at -80 ^{o}C for longer term storage.

2.5.4.2 Coomassie Assay

A Coomassie assay was used to measure the approximate amount of protein present in each protein lysate. This allowed for an equal amount of each protein lysate to be loaded for comparison by western blotting. For the Coomassie assay, first a standard curve was generated by pipetting equal amounts (10 µl) of bovine serum albumin (BSA) (Thermo Scientific, 23209) at the following concentrations, in duplicate, into a 96 well plate: 0 (dH2O), 25, 125, 250, 500, 750, 1000 µg/ml. 200 µl of Coomassie reagent (Thermo Scientific, 23236), warmed to ambient temperature, was added to each well.

The absorbance of each sample well was measured at 570 nm using a Multiskan™ Ascent™ microplate photometer (Thermo Scientific, 51118300), and a standard curve was generated using the accompanying Ascent™ software.

To measure the concentration in each protein lysate, 2 µl of each protein lysate was diluted in 23 µl of DEPC-treated water, and pipetted in duplicate into the wells below the standards. 200 µl of Coomassie reagent was added to each protein lysate well. The absorbance of each well was measured using the microplate photometer, and the concentration of each lysate was calculated using the standard curve. The average protein concentration of the duplicate sample wells was taken to give the final protein concentration for each lysate.

2.5.4.3 SDS-PAGE and Western Blot

To prepare the protein lysates for SDS-PAGE, each sample (typically 20-25 µg of protein) was combined with 4x LDS (Novex®, NP0007) to a final concentration of 1x, 10x Reducing Agent (Novex®, NP0005) to a final concentration of 1x, and DEPC-treated water to a final volume of 20 µl. The sample was heated at 70 ºC for 10 minutes. The combined use of LDS, reducing agent, and near boiling results in denaturation of the proteins. The use of LDS also gives the proteins a negative charge, which is proportional to the proteins mass; this allows for the linearised proteins to be separated based on molecular weight using an electric field.

The samples were loaded into a 4-12% Bis-Tris gel (Novex®, NP0321BOX) or a 3-8% Tris-Acetate gel (Novex®, EA0375BOX) set up in an XCell Surelock™ Mini-Cell Electrophoresis system (Invitrogen, EI0002). 20x MOPs SDS buffer (Novex®, NP0001) or 20x Tris-Acetate SDS buffer (Novex®, LA0041) were diluted to 1x in ELGA-treated water, and used as the running buffer. The electrophoresis was performed at 200 V for approximately 1 hour, which allowed for the proteins to be sufficiently separated.

The proteins were then transferred, by electroblotting, to an Immobilon-FL 0.45 μm PVDF membrane (Fisher Scientific, 10113432), which had been activated by incubating in methanol briefly prior to its use. The PVDF membrane was placed on top of the gel, and between Whatman Grade 1, 150 mM filter paper (Sigma-Aldrich, WHA1001150) and blotting pads (Invitrogen, EI9052). The transfer was completed using an XCell II™ Blot Module (Invitrogen, EI0002), and 30 V for 2.5 hours in transfer buffer (see Appendix), on ice.

The membrane was blocked using 50:50 Odyssey Blocking Buffer (Li-Cor, 927-40000):TBS or 5% (w/v) milk powder in TBS, for 1 hour, to prevent non-specific binding of the antibodies. As a negative control, membranes were incubated with the fluorescently-labelled secondary antibody (Table 2.9), which was diluted 50:50 in Odyssey Blocking Buffer:TBS-T, for 1 hour at ambient temperature. Membranes were washed for 4x five minutes with TBS-T, to remove excess secondary antibody. Membranes were then scanned using an Odyssey® infrared imaging system (Li-Cor, CLx or Sa), to identify whether any non-specific binding of the secondary antibody had occurred. Example negative control western blots are shown in Figure 2.5.

Membranes were incubated with primary antibody (Table 2.10) (diluted 1:1 in Odyssey Blocking Buffer:TBS-T pH 7.4 or 5% (w/v) milk powder in TBS-T) overnight (approximately 16 hours) at 4 ^{o}C. The membranes were washed in TBS-T (see Appendix) to remove excess primary antibody, and the secondary antibody was applied at ambient temperature for 1 hour. The membrane was washed 4x 5 minutes in TBS-T to remove excess secondary antibody, and imaged using the Odyssey® infrared imaging system. Membranes were stored in TBS at 4 ^{o}C until further use.

If multiple proteins of similar size were being examined on the same membrane, antibodies were stripped from the membrane using a 10x antibody stripping solution (Source Bioscience, 90100), diluted 1:10 in dH_2O, for 20-30 minutes at ambient temperature. To ensure that all of the primary antibody had been removed, appropriate secondary antibody was reapplied, washed, and imaged as above. The next primary antibody was incubated on the membrane overnight at 4 ^{o}C, and the protocol followed as above.

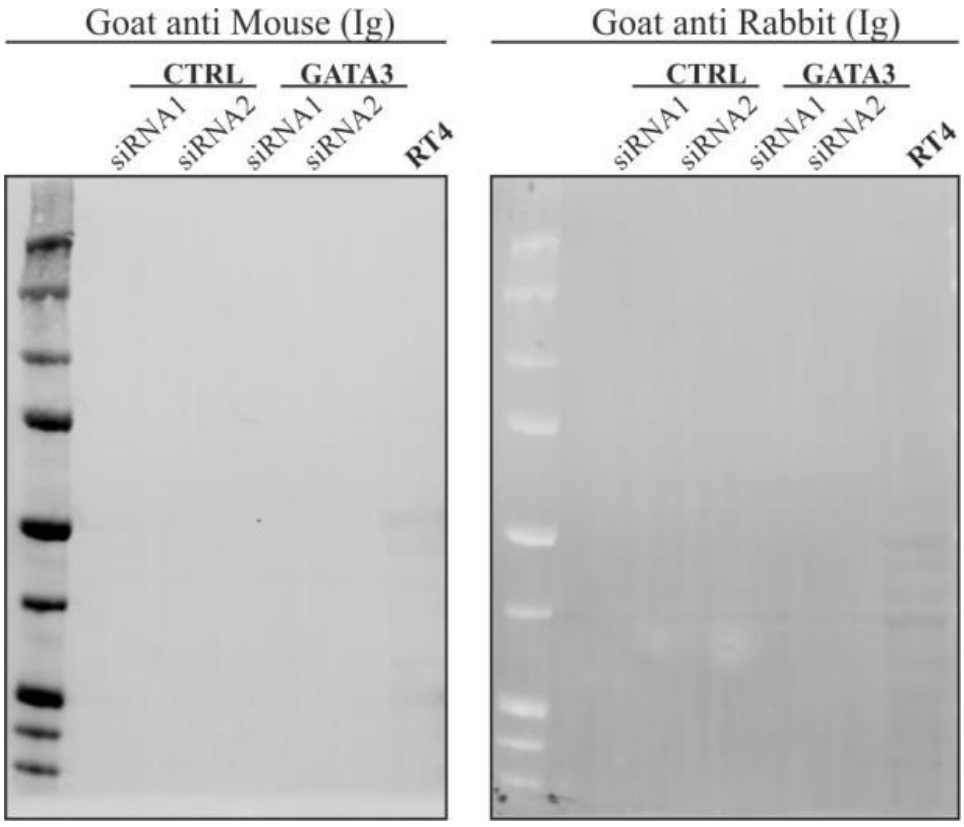

Figure 2.5 Example Negative Control Western Blots

Negative control western blots (secondary antibody only) are shown for NHU cells (Y938) which were treated with control (CTRL) or GATA3 siRNA as described in section 2.10. An RT4 cell lysate was also included on the blots. 30 µg of protein was loaded into each well.

Western blots were probed with β-actin or histone H3, which were used as loading controls for comparison.

Densitometry analysis was completed using the accompanying Li-Cor software (Li-Cor, Odyssey version 1.2 or Image Studio Lite version 5.0). Equivalent boxes were drawn around each protein band, and the corresponding optical density was calculated. The background was measured for each box, as the median intensity above and below each box, and subtracted from each densitometry measurement. Densitometry analysis was also completed for β-actin expression, and this was used to normalise the amount of protein loaded into each lane.

Table 2.9 List of Secondary Antibodies used for Western Blotting.

2º Antibody	Conjugated Fluorescent Dye	Company, Code	Dilution*
Goat anti Rabbit Ig	IRDye® 800CW	Rockland, 611-131-122	1:10,000
Goat anti Mouse Ig	Alexa Fluor® 680	Life Technologies, A21057	1:10,000
Donkey anti Goat Ig	Alexa Fluor® 680	Life Technologies, A21084	1:10,000

* Dilution determined by titration.

Table 2.10 List of Primary Antibodies used for Western Blotting.

Antigen	Antibody Clone or Catalogue #	Host (Production)	Supplier	Dilution*
CK13	1C7	M (monoclonal)	abnova	1:1000
CK14	LL002	M (monoclonal)	Serotec	1:1000
ELF3	EPESER1	Rb (monoclonal)	Abcam	1:20,000
Histone H3	ab1791	Rb (polyclonal)	Abcam	1:10,000
FOXA1	Q-6	M (monoclonal)	Santa Cruz	1:500
GATA3	D13C9	Rb (monoclonal)	Cell Signalling	1:1000
PPARγ	E-8	M (monoclonal)	Santa Cruz	1:500
PPARγ	81B8	Rb (monoclonal)	Cell Signalling	1:500
PPARγ	D69	Rb (polyclonal)	Cell Signalling	1:500
PPARγ2	N-19	Gt (polyclonal)	Santa Cruz	1:500
β-actin	AC-15	M (monoclonal)	Sigma-Aldrich	1:250,000

M – Mouse, Rb- Rabbit, Gt-Goat

* Dilution determined by titration.

2.6 Analysis of Gene Expression

In order to assess the relative gene (transcript) expression between various cell types or treatments, polymerase chain reaction (PCR) was used. To do this, total RNA was extracted from the cells, and then treated with DNase to remove any genomic DNA contamination of the samples. cDNA was generated using reverse transcriptase, and PCR was performed. All steps were performed at ambient temperature unless otherwise stated.

For non-quantitative analysis, standard PCR was performed using a thermal cycler machine, while for a quantitative analysis of gene expression, quantitative PCR (qPCR) was performed using a SYBR® Green-based reporter method.

2.6.1 RNA Extraction

Total RNA was extracted from cell cultures using TRIzol™ reagent (Fisher Scientific, 10227212). The medium was removed, and cultures were incubated in 1 ml of TRIzol™ (approximately 100 µl/cm^2) for 2-5 minutes. The lysate was scraped from the substrate using a cell scraper (Sarstedt, 83.1830), and transferred into an RNase/DNase-free 1.5 mL microfuge tube (Ambion, AM12400). Samples were stored at -80 ^{o}C until the RNA extraction took place.

For the RNA extraction, samples were thawed to ambient temperature, and 0.2 ml of chloroform (VWR, 22711.290) was added. The mixture was vortexed using a Vortex-Genie® 1 (Scientific Industries, G-560-E) for 15 seconds. The sample was incubated for 2-3 minutes, followed by centrifugation in a refrigerated centrifuge (Hettich Lab Technologies, MIKRO 200 R) at 12500 g for 15 minutes at 4 ^{o}C. The centrifugation caused the mixture to separate into a lower phenol-chloroform phase (containing DNA and protein), a cloudy interphase and a clear upper aqueous phase (containing RNA). The upper aqueous phase was carefully pipetted off, and transferred to a new RNase/DNase-free 1.5 ml microfuge tube. 0.5 ml of isopropanol (Sigma-Aldrich, 33539) was added to the aqueous phase solution and the tube was turned end-over-end to mix. The samples were incubated for 10 minutes and then centrifuged at 12500 g for

20 minutes at 4 ºC to pellet the RNA. The sample was washed to remove any excess salts by adding 1 ml of 75% (v/v) ethanol to the pellet and centrifuging at 7700 g for 5 minutes at 4 ºC. This wash was repeated once. The final RNA pellet was left to air dry. The RNA was resuspended in 30 µl of nuclease-free DEPC-treated water and transferred to a 0.5 ml RNase/DNase-free microfuge tube (Ambion, AM12300). Samples were stored at -80 ºC until DNase treatment.

2.6.2 DNase Treatment

Any DNA contamination was removed from the RNA samples using the DNA-free™ DNA removal kit and accompanying protocol (Ambion®, AM1906). 0.1 volume of 10X DNase 1 Buffer and 1 µl of rDNase were added to the 30 µl RNA sample and incubated at 37 ºC for 30 minutes. 0.1 volume of the DNase Inactivation Reagent was added and the RNA was incubated for 2 minutes, with vortexing every 30 seconds. The mixture was centrifuged (Sigma-Aldrich, 1-13) at 7000 g for 90 seconds. The aqueous phase (which contained the RNA) was collected and transferred to a new 0.5 ml RNase/DNase-free microfuge tube. RNA samples were stored at -80 ºC. The RNA concentration for each sample was determined using a NanoDrop® spectrophotometer and its accompanying software (Thermo Scientific, ND-1000). The NanoDrop measures the absorbance of the sample at 260 nm to determine the concentration. A260/A280 ratios were used to assess the RNA sample purity, where values of approximately 2.0 were accepted as pure.

2.6.3 cDNA Synthesis

For cDNA synthesis, 1 µg of each RNA sample was used. For each RNA sample, two cDNA synthesis reactions were performed: one which contained the reverse transcriptase (RT) enzyme to produce the cDNA, and one which did not (RT-negative control used to check for genomic DNA contamination). For cDNA synthesis, random primers were annealed to the RNA by combining 1 µg of RNA with 1 µl of 50 ng/µl random hexamers (Fisher, SO142) and DEPC-treated water, to a final volume of 12 µl. The mixture was incubated at 65 ºC for 10 minutes, and rested on ice for at least 1 minute. 4 µl of 5x First Strand Buffer (Invitrogen, Y02321), 2 µl of 0.1 M DTT

(Invitrogen, Y00147), and 1 µl of a deoxynucleotide triphosphate (dNTP) (Promega, U1240) mix containing 10 mM of each of the four dNTPs (diluted in DEPC-treated water) (see Appendix), were added to each of the reaction mixtures and incubated at 25 ^{o}C for 2 minutes. 50 units of the enzyme, Superscript II Reverse Transcriptase (Invitrogen, 100004925), was added to only one of the two cDNA synthesis reactions (called RT-positive) for each RNA sample. All samples were incubated at 25 ^{o}C for a further 10 minutes. The reaction tubes were incubated at 42 ^{o}C for 50 minutes, where cDNA synthesis took place. The enzyme was inactivated by incubating the samples at 70 ^{o}C for 15 minutes. cDNA samples were stored at -20 ^{o}C for short term storage (up to several months) or -80 ^{o}C for longer term storage.

2.6.4 PCR

Standard PCR is a technique which is used to amplify DNA. It relies on the use of forward and reverse primers which allow for amplification of a target sequence. A list of the forward and reverse primers used for standard PCR can be found in section 2.6.7.

Standard, non-quantitative PCR was performed using a T100™ Thermal Cycler machine (Bio Rad, 186-1096). To make the PCR master mix for 1x reaction, the following were combined: 4 µl of 5x GoTaq® Flexi buffer (Promega, M891A), 0.4 µl of dNTP mix, 2 µl of 25 mM $MgCl_2$ (Promega, A351H), 2 µl of the forward primer (10 µM), 2 ul of the reverse primer (10 µM), 0.1 µl of 5 U/ul GoTaq® G2 flexi DNA Polymerase (Promega, M7808) and 8.5 µl of DEPC-treated water (total volume 19 µl). 19 µl of master mix (equivalent to 1x reaction mix) was pipetted into each well of an 8-well PCR tube (Starlab, I1400-0800). To this, either 1 µl of test sample cDNA (RT-positive), 1 µl of DEPC-treated water (negative control), or 1 µl of genomic/control DNA (Promega, G304A) was added. PCR was performed as follows: 95^{o}C for 2 minutes, and then 25-35 cycles of: 95^{o}C for 30 seconds (denaturation step), annealing temperature (^{o}C) for 30 seconds (annealing step), and 72^{o}C for 30-90 seconds (extension time: 30 seconds/500 base pairs) (extension step). The appropriate annealing temperature and extension times were determined prior to running the PCR by performing a gradient PCR (see section 2.6.7.3). Genomic DNA was used as a positive control where possible; otherwise cDNA generated from the total RNA of a cell type known to express the target gene was used.

GAPDH was used as an internal loading control for all experiments. Samples were checked for DNA contamination by running a standard GAPDH PCR on the RT-negative samples to ensure that no PCR product was generated. The resulting PCR product was resolved on an agarose gel by electrophoresis as described below in section 2.6.5. An example GAPDH PCR performed on corresponding RT-positive and RT-negative samples is shown in Figure 2.6.

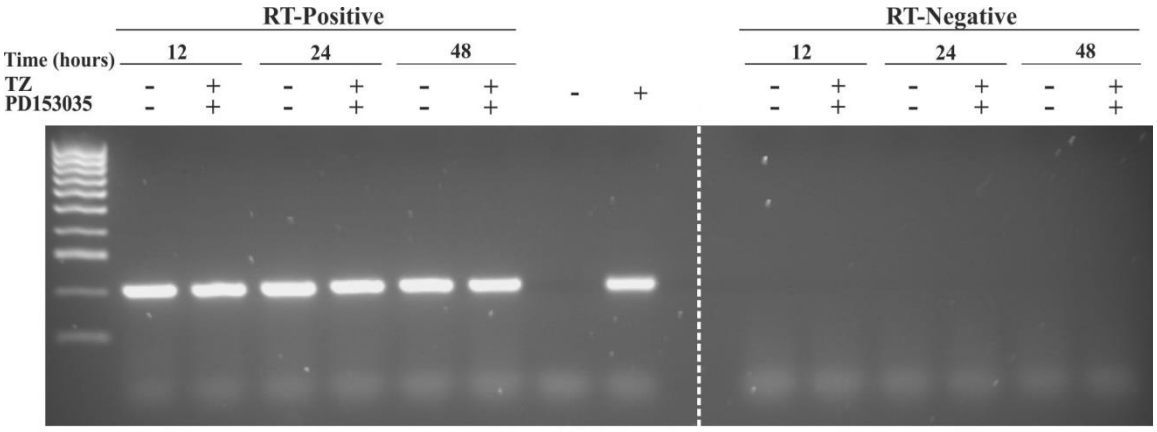

Figure 2.6 Example GAPDH PCR on Reverse Transcriptase Positive and Negative cDNA Samples

The TZ/PD protocol was used to activate PPARγ expression in NHU Cells (Y1281). 0.1 % DMSO was used as a vehicle control. GAPDH PCR was performed on RT-positive and RT-negative samples generated as part of the cDNA synthesis protocol. PCR was performed using 25 cycles. H_2O (no template) was used as the negative control. Genomic DNA was used as a positive control for the PCR. No PCR product could be shown in the RT-negative samples, demonstrating that DNA contamination had not occurred during the cDNA synthesis.

2.6.5 Gel Electrophoresis

Gel electrophoresis can be used to separate PCR products through an agarose gel. An electric field is applied across the gel, causing the negatively charged nucleic acids to move towards the cathode. Smaller fragments are able to travel more quickly through the gel than larger fragments, which allows for separation based on size (base pairs)

The PCR products were separated in 1-3% (w/v) agarose (Melford, MB1200) gels. The agarose gels were created by adding the appropriate amount of agarose to ELGA-treated water, and heated (by microwave) until dissolved. 1x SYBER® safe DNA gel stain (Invitrogen, S33102) (a DNA intercalating, fluorescent stain) was added to the gels to allow for later visualisation of the DNA bands by ultraviolet (UV) detection. The agarose was cast into trays, with an appropriate comb, and allowed to solidify. PCR products were loaded into the wells of the gel. An appropriate DNA ladder, typically Hyperladder IV (Bioline, BIO-33056), was also run on every gel. Gel electrophoresis was performed in horizontal gel tanks (SCI-PLAS, HU13 Midi), at approximately 100 volts using an OmniPAC power supply (Cleaver Scientific Ltd., MP-300V), until the DNA had been appropriately separated. DNA bands were visualised, and imaged using a Gene Genius Bio imaging System (Syngene, Gene Genius), and accompanying software (Syngene, GeneSnap version 7.12).

2.6.6 qPCR

qPCR allows for a quantitative analysis of gene expression. It relies on the use of forward and reverse primers which allow for amplification of a short portion of the target gene (up to100 bp). A list of the forward and reverse primers used for qPCR can be found in section 2.6.7. qPCR was performed using a SYBR® Green-based detection method. For every cycle of the PCR, SYBR® Green dye binds to the double-stranded PCR product produced, and fluoresces. The amount of fluorescence detected during each cycle is measured, and used to calculate the amount of DNA present in a sample relative to a housekeeping gene. GAPDH was used as the housekeeping gene for comparison in all qPCR experiments.

qPCR was performed using a StepOne™ Real-Time PCR machine (Life Technologies, 4376357) and accompanying StepOne™ Software (Life Technologies, Version 2.2.2). To set up the qPCRs, cDNA (as generated in section 2.6.3) was diluted 1:5 in DEPC-treated water. qPCR master mix was created by combining: 10 µl of 2x Fast SYBR® Green master mix (Applied Biosystems, 4385612), 0.6 µl each of the 10 µM forward and reverse primer stocks, and 3.8 µl of DEPC-treated water to a final volume of 15 µl. The master mix was pipetted in triplicate into MicroAmp® Fast optical 96-well reaction plates (Applied Biosystems, 4346906). 5 µl of cDNA was added to each well in triplicate. A single replicate of RT-negative cDNA for each sample was used to ensure there was no DNA contamination during the cDNA synthesis reaction. GAPDH was used as the internal control for comparison on every plate. To analyse the resulting data, cycle threshold (C_T) values were extracted, and normalised to GAPDH expression. Fold change was calculated relative to a calibrator value (ie. the control sample).

2.6.7 PCR Primer Design and Optimisation

All PCR primers were ordered from Eurofins Genomics and diluted using DEPC-treated water to a working stock of 10 µM.

2.6.7.1 PCR Primers

Standard PCR primers were designed using NCBI Primer-BLAST (http://www.ncbi.nlm.nih.gov/tools/primer-blast) to be between 19-22 base pairs (bp) long and have a GC content of approximately 50%. The primers were tested prior to their use for experiments by running a gradient PCR to determine the appropriate annealing temperature for the primers, and to ensure that the correct PCR product size was produced (see section 2.6.7.3 for gradient PCR protocol). See Table 2.11 for a list of PCR primers used.

2.6.7.2 qPCR Primers

qPCR primers were designed using Primer Express software (Applied Biosciences, version 3.0). To test the efficiency of the qPCR primers, qPCR (see section 2.6.6 for protocol) was completed using serially diluted (1:5, 1:10, 1:100, 1:1000) genomic DNA or cDNA, known to express the target gene, as the template. A standard curve was generated using the StepOne™ Software (Life Technologies, Version 2.2.2). Primers with an R^2 value greater than 0.95, and a single, large peak generated on a melt curve, were deemed to be acceptable for use. See for Table 2.12 a list of qPCR primers used.

2.6.7.3 Gradient PCR

Gradient PCR was used to determine the correct annealing temperature for the primers used for standard PCR. A standard PCR master mix was generated using genomic DNA, or cDNA generated from the total RNA of cells known to express the target gene, as the template. For gradient PCR, the reactions were completed as follows using the gradient setting on the PCR machine: 95^{o}C for 2 minutes, and then 30 cycles of: 95^{o}C for 10 seconds (denaturation step), 56-66 ^{o}C (annealing temperature) for 30 seconds (annealing step), and 72^{o}C for 30-90 seconds (extension time: 30 seconds/500 base pairs) (extension step). The resulting PCR product was resolved on an agarose gel and the PCR product was visualised as described in section 2.6.5. The annealing temperature that produced a single band of the correct height PCR product was selected.

Table 2.11 List of Primers used for Standard PCR.

Gene Name	Forward Primer (5'-3')	Reverse Primer (5'-3')
CLDN1	TTTACTCCTATGCCGGCGAC	ACTTTGCACTGGATCTGCCC
CLDN10	TTATTGGATGGGCAGGAGCC	AGATGTGGCCCCGTTGTATG
CLDN2	CCTGGGATTCATTCCTGTTG	AGTTGGAGCGATTTCTCTGG
CLDN3	TGGTCGGCCAACACCATTAT	CCGTGTACTTCTTCTCGCGT
CLDN4	CTGGGAAGTGCAGAGTGGAT	AAGGAAGAGGAAAAACCCCA
CLDN5	CTGTTTCCATAGGCAGAGCG	AAGCAGATTCTTAGCCTTCC
CLDN6	CTCTCACTTAGGCTCTGCTG	AAATGTGAGTGTAAAGGGGG
CLDN7	CGAGCCCTAATGGTGGTCTC	ACGGGCCTTCTTCACTTTGT
CLDN8	TCTTCTCCCAGAGGCTTTTT	TTTGACTCAGGTACCCACAT
ELF3	GTTCATCCGGGACATCCTC	GCTCAGCTTCTCGTAGGTC
ESR1	CCATGACCATGACCCTCCAC	CCTCGGGGTAGTTGTACACG
ESR2	CATCTTACCCCTGGAGCACG	CATTTGGGCTTGTGGTCTGC
FOXA1	CAAGAGTTGCTTGACCGAAAGTT	TGTTCCCAGGGCCATCTGT
GATA3	TCCAGACACATGTCCTCCCT	TGGTGTGGTCCAAAGGACAG
GRHL3	GTGACAAGGGAGCTGAGAGG	CAGTCTCTGGCCGAAGGTAG
IRF1	GCTGGGACATCAACAAGGAT	GTGGAAGCATCCGGTACACT
KLF5	GACACCTCAGCTTCCTCCAG	ACTCTGGTGGCTGAAAATGG
LOR	GCGAAGGAGTTGGAGGTGTT	CTGGGGTTGGGAGGTAGTTG
PPARA	GACACGGAAAGCCCACTCTG	TTCCAGAACTATCCTCGCCG
PPARB	GGCTGAGAAGAGGAAGCTGG	TGAAGCTGGGGATGCTCTTG
PPARG*	AGACAACCTGCTACAAGCCC	GGAAATGTTGGCAGTGGCTC
PPARG$^{\#}$	ACTTTGGGATCAGCTCCGTG	GGGCTTGTAGCAGGTTGTCT
PPARG2$^{\sim}$	TCCTTCACTGATACACTGTCTGC	GGGCTTGTAGCAGGTTGTCT
RARA	GAAACCTTCCCTGCCCTCTG	GGATCAGGATGTCCAGGCAG
RARB	GCCTCCAAGGCAGAAACACT	CTTGGCATCAAGAAGGCTGG
RARG	GCAAAGCCCATCAGGAGACT	CTGCTCTGGGGTGTACCTTG
RXRA	CTCAATGGCGTCCTCAAGGT	TGTTTGCCTCCACGTAGGTC
RXRB	ACTGCCGCTATCAGAAGTGC	CCCTGGTCACTCTTCTGTTCC
RXRG	TTCAAGCTCATCGGGGACAC	AGCCCTGTAGACAGCAAAGC
SPRR4	GGCTCACCTGTTCCTAGAGC	GTTTACTCTTGGAGGCTTGC

Table 2.11 Continued.

Gene Name	Forward Primer (5'-3')	Reverse Primer (5'-3')
TGM1	GACCTGTTCCATCTCAGCCC	TCTGGAGATGGCGTGGTAGG
UPK1A	GGGGTATCTCGTGGTTTGGG	CGTAAGGGCTAGGGACGTTG
UPK1B	TTGAAGCCACCGACAACGAT	AACAGACAGGCAGAAGAGGC
UPK2	CTCCCGCAAGTAAGGAGGT	GAAGGATGGGGGAATTGTTA
UPK3A	ATGGGGAGTTCTGATGGGGA	TGCTGGAATACACCTCAGCC
UPK3B	CCTCCTGCTTCACTCTCTCTGTCT	GAAACTGACAATCACGGCAGAA

* Both primers are in exon 6.
# Forward primer is in exon 1 and reverse primer is in exon 6.
~ PPARG2 specific primers. Forward primer is in exon B and reverse primer is in exon 6.

Table 2.12 List of Primers used for qPCR.

Gene Name	Forward Primer (5'-3')	Reverse Primer (5'-3')
ELF3	TCAACGAGGGCCTCATGAA	TCGGAGCGCAGGAACTTG
FOXA1	CAAGAGTTGCTTGACCGAAAGTT	TGTTCCCAGGGCCATCTGT
GAPDH	CAAGGTCATCCATGACAACTTTG	GGGCCATCCACAGTCTTCTG
GATA3	TCTATCACAAAATGAACGGACA GAA	TGTGGTTGTGGTGGTCTGACA
PPARG	GAACAGATCCAGTGGTTGCAG	CAGGCTCCACTTTGATTGCAC
TGM1	GAGCGGAAGGCAGTAGAGACA	CCCCGGTTGGCATACACA
UPK1A	CATTCTTGCTGAACCGTTTGTG	GTGACCGTGACAGAACTCTCATG
UPK1B	CGCTTGCCTTCAGCTTGTG	GGCCCTGGAAGCAACGA
UPK2	CAGTGCCTCACCTTCCAACA	TGGTAAAATGGGAGGAAAGTCAA
UPK3A	CGGAGGCATGATCGTCATC	CAGCAAAACCCACAAGTAGAAAGA
UPK3B	CCTCCTGCTTCACTCTCTCTGTCT	GAAACTGACAATCACGGCAGAA

2.7 Molecular Cloning and Microbiology

Various molecular cloning and microbiology-based techniques were used to generate a retroviral vector, which was used to overexpress one of the human GATA3 coding sequences. A plasmid containing the selected GATA3 coding sequence (Ensembl Transcript ID – ENST00000379328) was obtained from Mr. Felix Wezel, a previous clinical research fellow at the Jack Birch Unit. The coding sequence was amplified from this vector using PCR, and ligated into a shuttle vector, pGEM (Promega, A1360). The pGEM-GATA3 vector was then transformed into competent bacteria. Colony PCR was used to determine the correctly transformed bacteria. A single colony containing the pGEM-GATA3 was amplified using liquid culture. Miniprep of the plasmid DNA was performed, and the GATA3 coding sequence was checked for its accuracy by sequencing. The GATA3 coding sequence was cut from the pGEM vector using restriction enzymes, gel purified, and then ligated into the retroviral vector, pLXSN. The pLXSN-GATA3 vector was used to transfect retroviral packaging cells (PT67 cells), for later production of retrovirus.

The techniques used for the generation of the pLXSN-GATA3 vector are outlined below. For all molecular cloning experiments, a table top micro centrifuge (Eppendorf, 5415c) was used for centrifugation steps.

2.7.1 PCR Amplification of a Gene for Cloning

PCR amplification for gene cloning was used to generate large amounts of the GATA3 coding sequence from an initial plasmid (plasmid obtained from Felix Wezel). Primers were designed to add useful restriction sites, and a Kozak sequence (necessary for protein translation in mammalian cells) to either end of the gene sequence (an example of PCR primers which were used to amplify the GATA3 gene sequence for cloning can be found in Figure 2.7). To ensure accurate amplification of the sequence, a high fidelity DNA polymerase, called Q5® (New England BioLabs, M0491S), was used with its accompanying protocol.

To set up a 25 µl PCR reaction, the following items were combined: 5 µl of 5x Q5 reaction buffer, 0.5 µl of 10 mM dNTP mix, 1.25 µl of the forward primer (10 µM), 1.25 µl of the reverse primer (10 µM), 0.1 ng plasmid DNA, 0.25 µl of Q5 high-fidelity DNA polymerase and DEPC-treated water to 25 µl. The PCR reaction was run in a T100™ Thermal Cycler machine (Bio Rad, 186-1096) with the following conditions: 98 ^{o}C for 30 seconds, and then 30 cycles of: 98 ^{o}C for 10 seconds (denaturation step), annealing temperature for 30 seconds (annealing step), and 72 ^{o}C for 30 seconds/kb (extension step). The annealing temperature was determined prior to the PCR by running a gradient PCR (see section 2.6.7.3) using cDNA generated from the total RNA of a cell type known to express the GATA3 sequence, as the template.

2.7.2 PCR Purification

PCR purification was performed to purify the GATA3 sequence product from the rest of the contents of the PCR master mix, on completion of the PCR reaction. PCR purification was completed using a QIAGEN QIAquick® PCR Purification kit, and the accompanying protocol (QIAGEN, 28104). 5 volumes of Buffer PB was added for every volume of PCR reaction, and the mixture was pipetted into a QIAquick column. The column was centrifuged at 13,800 g for 60 seconds. This caused excess liquid to pass through the column, while leaving the PCR product bound to the column. The flow-through was discarded. The column was washed once by adding 750 µl of Buffer PE and centrifuged at 13,800 g for another 60 seconds. The resulting flow-through was discarded. To elute the PCR product from the column, the column was placed into a 1.5 ml microfuge tube, and 30 µl of elution buffer was added to the column. The column was left to stand for 1 minute, and centrifuged for 60 seconds. The concentration of the resulting PCR product was determined using a NanoDrop® spectrophotometer and its accompanying software.

pLXSN Multiple Cloning Site (MCS):

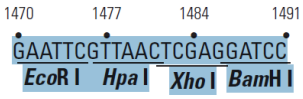

Add 5' EcoR1 = GAATTC and Kozac sequence = ACC

Add 3' Xho1= CTCGAG

GATA3 Forward Primer 5' - 3':

5' AAAAAAGAATTCACCATGGAGGTGACGGCGGACC **3'**

GATA3 Reverse Primer 5'-3':

5' AAAAAACTCGAGCTAACCCATGGCGGTGACC **3'**

Blue = GATA3 sequence

Figure 2.7. PCR Primers Used to Generate GATA3 Coding Sequence for Later Insertion into the pLXSN Plasmid.

These primers included a 5' poly A tail which was used for ligation of the PCR product into pGEM. The GATA3 gene was cut from the pGEM plasmid using the added restriction sites and ligated to the pLXSN plasmid (cut using the same restriction enzymes). The pLXSN-GATA3 construct was later used for transfection into retroviral packaging cells (PT67). The pLXSN MSC image was obtained from the pLXSN Retroviral Information Sheet (Clontech).

2.7.3 Ligation

Ligation is the process of joining two DNA segments together (ie. joining an insert and vector). To determine the amount of insert DNA necessary for the ligation reaction, the following formula was used:

$$\frac{100 \text{ ng vector} \cdot \text{insert size (kb)}}{\text{vector size (kb)}} \cdot \frac{3}{1} = \text{x ng insert}$$

The following components were combined for the ligation reaction: 1 µl of 10x T4 DNA ligase buffer (Promega, C126B), 100 ng vector, x ng insert (as calculated above), 1 µl of T4 DNA Ligase (Promega, M1801) and DEPC-treated water to a final volume of 10 µl. The ligation mixture was incubated at 4 ^{o}C overnight (approx. 16 hours). A negative control reaction was carried out, where the insert sequence was omitted, in order to account for possible vector re-ligation.

2.7.4 Transformation

The process whereby bacteria take up plasmid DNA is called transformation. Transformations were completed using a strain of competent E. coli called, XL1-Blue subcloning-grade competent cells (Agilent Technologies, 200249). For each transformation, a positive control transformation, using the plasmid pUC18 (Agilent, 200231-42), and a negative control transformation, using dH_20, were performed. The competent cells were thawed on ice, and 50 µl of the competent cells was pipetted into chilled Corning® 15 ml centrifuge tubes (Sigma-Aldrich, CLS430791). 0.1-50 ng of experimental DNA (5 µl of ligation mix reaction), or 1 µl of pUC18 or 1 µl of dH_20 was added to the competent cells. The tubes were incubated on ice for 20 minutes. The tubes were put into a 42 ^{o}C water bath for 45 seconds (where the plasmid DNA enters the bacteria cells), and then returned to ice for a further 2 minutes. 900 µl of SOC medium (Invitrogen, 15544-034), prewarmed to 37 ^{o}C, was added to the cells and they were incubated at 37 ^{o}C, with shaking, for 30 minutes. 50 – 200 µl was spread onto LB-agar (see Appendix) plates (with appropriate antibiotics). The plates were allowed to dry and placed inverted at 37 ^{o}C overnight (approx. 16 hours).

2.7.5 Colony PCR

To determine which colonies from a ligation, and subsequent transformation were successful, colonies grown from the transformation were dabbed into PCR mix containing primers for the GATA3 sequence. The PCR was performed as described in section 2.6.4, and the products were separated on an agarose gel (see section 2.6.5). Based on the size and/or presence of PCR product bands, it was determined which of the selected colonies had taken up the plasmid with a successful ligation of the insert and plasmid DNA.

2.7.6 LB Broth Cultures

Luria-Bertani (LB) broth cultures were used to generate large amounts of a single colony of successfully transformed bacteria; these cultures were used to extract the plasmid DNA by miniprep, or to freeze the cells for later use. A single colony grown on an LB-agar plate was picked up using a sterile pipette tip and swirled into 6 ml of LB broth (with appropriate antibiotics) (see Appendix) in a universal tube. The tubes were incubated in a 37 ^{o}C incubator, with shaking, overnight (approx. 16 hr).

2.7.7 Miniprep of Plasmid DNA

The miniprep of plasmid DNA is a process used to extract plasmid DNA from bacterial cells. The miniprep of plasmid DNA from liquid LB broth cultures was performed using the QIAprep Spin Miniprep Kit (QiaGen, 27104), and its accompanying protocol. The bacteria from a 6 ml LB broth culture were pelleted by centrifuging for 15 minutes at 3000 g at 4 ^{o}C. The cells were resuspended in 250 µl of Buffer P1, before being transferred to a 1.5 ml microfuge tube. 350 µl of Buffer P2 was added to the tube and the contents were mixed by inverting 4-6 times. 350 µl of Buffer N3 was added and again, the tubes were inverted 4-6 times to mix. The tubes were centrifuged at 13,800 g. The resulting supernatant was put into the QIAprep spin column, and the columns were centrifuged at 13,800 g for 1 minute. (At this point, the plasmid DNA binds to the column). The resulting flow-through was discarded. The columns were washed once

with Buffer PB, and once with Buffer PE, with centrifugation at 13,800 g for 1 minute after each wash. The flow-through was discarded, and the tubes were centrifuged once more to remove any remaining liquid from the column. To elute the plasmid DNA from the column, the column was placed into a new 1.5 ml microfuge tube. 50 µl of elution Buffer EB was applied to the column, and it was allowed to stand for 1 minute. The tube was centrifuged at 13,800 g for 1 minute. The column was discarded, and the concentration of the resulting plasmid DNA was determined by using a NanoDrop® spectrophotometer.

2.7.8 Sequencing

To confirm that the GATA3 sequence was correct, and no errors had been introduced by the PCR amplification step, sequencing was performed following miniprep of the pGEM-GATA3 vector. All sequencing of DNA was performed using the sequencing service provided by the Genomics Department of the Technology Facility in the Department of Biology at the University of York, York, UK. Sequencing results were analysed using Sequence Scanner v2.0 software (Applied Biosystems).

2.7.9 Restriction Digest of Plasmid DNA

Restriction digest is a process used to cut double stranded DNA at designated restriction cut sites. It relies on the use of restriction enzymes, which are able to recognize specific, short sequences of DNA and make a single cut at that site. Restriction digest was used to cut the GATA3 sequence out of the shuttle vector (pGEM). It was also used to linearise the pLXSN vector, for later ligation of the GATA3 sequence and pLXSN vector.

For restriction digests, 1 µg of plasmid DNA was combined with 2 µl of 10x Promega Restriction Digest Buffer (used Buffer H) (Promega, R008A), 0.2 µl of 10 mg/ml acetylated BSA (Promega, R396D), 1 µl of each the two required restriction enzymes (Promega), and DEPC-treated water to 20 µl. The mixture was incubated in a 37 ^{o}C water bath for 4 hours. To inactivate the enzymes, the mixture was incubated at 65 ^{o}C for 15 min.

2.7.10 Gel Extraction and Purification

Gel extraction is a method used to purify DNA fragments of varying sizes from a mixture (ie. an insert from a plasmid backbone following a restriction digest); the DNA fragments are separated by electrophoresis on an agarose gel, then cut out of the gel, and purified. Gel extraction was used to separate the GATA3 sequence from the pGEM vector backbone after restriction digest. It was also used to resolve the digested pLXSN vector backbone.

Gel extraction was used following restriction digest of plasmid DNA. Prior to gel electrophoresis, 5x loading buffer (Qiagen, 239901) was added to the restriction digest mixture to a final concentration of 1x. Once the DNA bands had been separated on the gel by electrophoresis, the required bands (GATA3 sequence and linearised pLXSN backbone) were cut out of the gel. To do this, the DNA bands were quickly visualised (to prevent UV-induced mutagenesis) using a UV transilluminator, and cut out using a scalpel. The gel pieces were put into 1.5 ml microfuge tubes, and the contents of the tubes were weighed using a bench top balance.

To purify DNA fragments from agarose gel, a QiaQuick Gel Extraction kit and its accompanying protocol (QiaGen, 28704) were used. 3 volumes of Buffer QG was added to each volume of gel. The gel mixture was incubated at 50 ^{o}C for approximately 10 minutes, or until the gel had melted. The mixture was vortexed briefly to combine. 1 volume of isopropanol was added to the tubes and mixed. The mixture was placed into a spin column, and the sample was centrifuged at 13,800 g for 1 min (at this point, the DNA binds to the column.) The flow-through was discarded and any remaining gel mixture was loaded into the column and centrifuged as previous. The column was washed using 500 µl of Buffer QG, and centrifuged at 13,800 g for 1 min. The flow through was discarded. The column was washed using 750 µl of Buffer PE, and again centrifuged for 1 min, and the flow-through discarded. The column was centrifuged again, and any remaining flow-through was discarded. The column was placed into a 1.5 ml microfuge tube, and 30 µl of Buffer EB was applied to the column to elute the DNA. The column was allowed to stand for up to 4 minutes before being centrifuged. The concentration of the resulting eluted DNA was measured using a NanoDrop® spectrophotometer.

2.7.11 Plasmid Dephosphorylation

Plasmid dephosphorylation is used to remove the 5' phosphate group from the end of a restriction digested plasmid DNA segment; this prevents the digested plasmid from re-ligating back together during a ligation reaction. Plasmid deposphorylation was performed on the gel purified pLXSN vector backbone, prior to ligation with the GATA3 coding sequence.

Plasmid dephosphorylation was completed using the FastAP Thermosensitive Alkaline Phosphatase kit (Thermo Scientific, EF0651), and accompanying protocol. Up to 1 μg of the digested, and purified plasmid back bone was combined with 2 μl of 10x Reaction Buffer for AP and 1 μl of FastAP Alkaline Phosphatase. Using a PCR machine, the mixture was heated to 37 ºC for 10 minutes. It was incubated at 75 ºC for 5 minutes to inactivate the enzyme.

Following, plasmid dephorphorylation, the GATA3 sequence and linearised pLXSN vector were ligated together, and then transformed into competent bacteria. Colony PCR was performed to confirm successful ligation and transformation. A single, successfully transformed colony was expanded by liquid culture, and then the pLXSN-GATA3 plasmid DNA was extracted by miniprep. This plasmid was used for transfection of PT67 cells, as described in below in section 2.8.

2.7.12 Freezing and Thawing Bacteria

For long term storage of specific bacteria, cells were frozen as glycerol stocks. 750 μl of a 6 ml overnight LB broth culture was mixed with 250 μl of sterile 80% (w/v) glycerol and put into a 1.5 ml cryo vial (Sarstedt, 73.380.992). The vials were stored at -80 ºC for future use.

In order to thaw bacteria from a frozen glycerol stock, a sterile pipette tip was used to pick up some of the frozen culture, and it was streaked out onto a LB agar plate (containing the appropriate antibiotics). The plates were incubated at 37 ºC overnight.

2.8 Transfection of Retroviral Packaging Cells

Transfection is the process whereby mammalian cells take up naked DNA. It was used to introduce the pLXSN-GATA3 vector into retroviral packaging cells. The pLXSN plasmid (see Figure 2.8 for a plasmid diagram) contains a neomycin resistance gene, which allows for selection of successfully transfected cells with the antibiotic, G418 (Sigma-Aldrich, A1720). PT67 retroviral packaging cells were used (Clontech, 631510), which are a cell line derived from mouse 3T3 cells. The PT67 packaging cells contain the necessary GAG, POL and ENV genes, which are required for the production of the virus particles.

PT67 cells were grown in T25 flasks, in DMEM with 10% fetal bovine serum (FBS) and 1% L-glutamine (LG) (DMEM10%), at 37 ^{o}C and 10% CO_2 in air until they reached approximately 60% confluence. One extra flask of PT67s was used during every transfection to act as a 'mock' transfection; the exact protocol was followed as below, but no plasmid DNA was added. These 'mock' transfected cells die under antibiotic selection because they do not contain the plasmid. This allowed for an approximate determination of the successful selection of the transfected cells.

At the point of transfection, 3 μg of plasmid DNA was mixed, by pipetting, with 90 μl of Buffer EC (Qiagen, 301425) and 24 μl of 1 mg/ml Enhancer (Qiagen, 301425) in a 1.5 ml microfuge tube and incubated at ambient temperature for 5 minutes. 30 μl of 1 mg/ml Effectene (Qiagen, 301425) (used to aid transfection) was added to the mixture, and incubated at ambient temperature for a further 10 minutes. The plasmid solution was combined with 5 ml of DMEM10%, and incubated on the PT67 cells for approximately 16 hr at 37 ^{o}C and 10 % CO_2 in air. Following the 16 hour incubation, the medium was changed to DMEM10%. 48 hours after transfection, the cells were passaged (split at a 1:3 ratio), and grown in DMEM10% with 0.5 mg/ml G418, for antibiotic selection of the transfected cells. Flasks were passaged as required if they became confluent before all the cells in the 'mock' flask had died. The cells were medium changed every 2-3 days, and maintained in antibiotic selection as above. Once all of the cells in the 'mock' flask had died, the remaining flasks were considered as

containing only successfully transfected cells. Successful transfection of the pLXSN-GATA3 vector was confirmed by PCR and immunofluorescence (data shown in Chapter 3). Transfected cells were frozen for future use as described in section 2.4.11.

The transfection protocol and appropriate antibiotic concentrations required for selection, were previously optimised by members of the Jack Birch Unit.

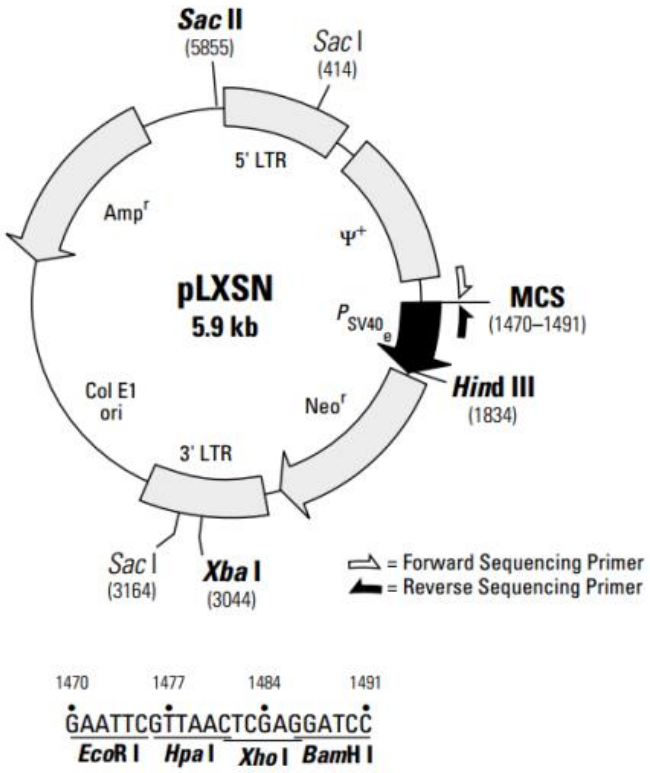

Figure 2.8 pLXSN Plasmid Diagram

The pLXSN plasmid diagram was obtained from the pLXSN retroviral vector information sheet (Clontech). The pLXSN plasmid contains the neomycin resistance gene for selection of successfully transduced mammalian cells. The 0.5 mg/ml G418 (antibiotic) was used for selection of the packaging cells.

2.9 Transduction of Epithelial Cells using Retrovirus

Retroviral transduction is the process whereby a retrovirus is used to stably integrate genes of interest into the genome of dividing mammalian cells. In order to produce retrovirus for transduction of epithelial cells, transfected PT67 cells were used. Upon successful retroviral transduction of epithelial cells, the gene of interest, under a constitutively active promoter, plus the neomycin resistance gene were incorporated into the cells' genome. The transduction protocol used was previously optimised by members of the Jack Birch Unit.

The transfected PT67 cells were grown to over 100% confluence. The medium was changed to DMEM:RPMI 1640 (Gibco, 31870-025) (50:50) plus 5% FBS and 1% LG, and they were incubated for 16 hours at 37 ^{o}C and 10% CO_2 in air. The medium containing the retrovirus particles was collected from the cells, filtered using a 0.45 μm filter (Corning, 431220), to remove any cell debris, and 8 μg/ml Polybrene (Sigma-Aldrich, H9268) was added to aid in transduction efficiency.

In addition to growing the transfected PT67 cells, equivalently sized flasks of epithelial cells were grown so they reached approximately 70% confluence at the time of the transduction. An equivalent, extra flask of epithelial cells was grown to act as a 'mock' transduced flask. The 'mock' flask was treated identically to the other flasks, but the cells were not incubated with retrovirus. These cells were used to determine successful selection of the transduced cells; the mock cells should all die under antibiotic selection.

At the time of transduction, the epithelial cells were incubated in the virus containing medium, described above, for 6 hours at 37 ^{o}C and 5% CO_2. After 6 hours, the medium of the epithelial cells was changed to KSFMc, and the cells were incubated for a further 48 hours. After 48 hours, the cells were passaged and split at a 1:2 ratio. The cells were then grown under antibiotic selection (G418). The concentration of antibiotic necessary for selection was pre-determined to cause complete death of the mock transduced flask within approximately 5 days; in general, buccal epithelial cells required a concentration of 0.5 mg/ml G418 for this to occur. Cells were grown using the above antibiotic

concentrations until all cells in the mock flask had completely died. The successfully transduced cells were then grown in medium containing a maintenance dose of antibiotic (0.025 mg/ml G418).

For transduction of the breast carcinoma-derived cell line, MCF-7, the same protocol as above was followed, but DMEM10% medium was used in place of KSFMc medium , and the cells were grown at 37 ^{o}C and 10% CO_2 in air.

2.10Transfection of Urothelial Cells with siRNA

Transfection of epithelial cells with siRNA is a technique used to transiently knock down a gene of interest. It relies on the use of specific siRNA sequences, which are short (20-25 bp) RNA sequences designed to a region of a gene of interest. The siRNA enters the cell as a double stranded sequence where it binds to the RNA-induced silencing complex (RISC). The siRNA sequences are separated, allowing the activated RISC, and single siRNA sequence to specifically bind to mRNA of the targeted gene. This causes the mRNA sequence to be cleaved, preventing it from carrying on to protein translation.

Urothelial cells were seeded into 6-well plates at a density of $4x10^5$ cells/well in KSFMc, and incubated at 37^{o}C in 5% CO_2 in air overnight. This seeding density allowed for the cells to be approximately 80 % confluent at the time of transfection the next day. 1.5 µl of Lipofectamine RNAiMAX reagent (used to mediate transfection) (Invitrogen, 13778-075) was added to 248.5 µl of KSFM (no supplements) for a final volume of 250 µl. The siRNA was added to a final volume of 250 µl of KSFM (no supplements) so that the final siRNA concentration would be correct in the 500 µl total volume that was added to the cells. The two 250 µl solutions (diluted Lipofectamine and siRNA) were combined to a total volume of 500 µl, and incubated at ambient temperature for 20 minutes. The cells were washed once with KSFM (no supplements) to remove any trace of supplements from the cells, which could affect the transfection efficiency. The 500 µl transfection mixture was added to the cells, and they were incubated for 4 hr at 37 ^{o}C at 5% CO_2 in air. 500 µl of KSFM (no supplements) was added to each well, as well as 500µl of KSFM containing 0.15 mg/ml bovine pituitary

extract (Gibco®, 37000-015), 15 ng/ml epidermal growth factor (Gibco®, 37000-015), 90 ng/ml cholera toxin, 1 μM PD153035 and 1 μM troglitazone (KSFM with 3x supplements plus TZ plus PD). The cells were incubated as such for 24 hours at 37 ºC at 5% CO_2 in air. The medium was changed to KSFMc plus 1 μM PD153035 (1.5 ml of medium per well) and the cells were incubated at 37 ºC at 5% CO_2 in air for a further 24 hours. RNA and protein were harvested.

The siRNA transfection protocol used was generated and optimised by previous members of the Jack Birch Unit.

All siRNA was purchased from Thermo Fisher Scientific from their Silencer® Select pre-designed and validated siRNA product range. A list of the control and GATA3 siRNA used can be found in Table 2.13.

Table 2.13. siRNA Information

siRNA Name (Catalogue #)	siRNA Name in Thesis
Silencer® Select Negative Control #1 siRNA (4390843)	CTRL-siRNA1
Silencer® Select Negative Control #2 siRNA (4390846)	CTRL-siRNA2
GATA3 Silencer® Select siRNA (S5600)	GATA3-siRNA1
GATA3 Silencer® Select siRNA (S5601)	GATA3-siRNA2

GATA3-siRNA1 (S5600) targeted a sequence in exon 5 of the human GATA3 transcripts, while GATA3-siRNA2 (S5601) targeted a sequence in exon 6 of the human GATA3 transcripts. The negative control siRNAs were predesigned as to not target any gene product.

2.11 Statistics

Statistical analysis of the data was performed using GraphPad Prism 6 (GraphPad Software Inc.) Where two data sets were being analysed (ie. treatment vs control), for three or more independent cell lines, a paired t-test was used. When three for more data sets were being compared, a one-way ANOVA test was performed. A Dunnett's multiple comparisons post-hoc test was performed if statistical significance was shown by the one-way ANOVA test. The Dunnett's test was used to compare multiple treatments to a single control sample.

Chapter 3:

In Vitro Characterisation of Buccal Epithelial Cells with Reference to Urothelial Cells

3 In Vitro Characterisation of Buccal Epithelial Cells with Reference to Urothelial Cells

3.1 Aims and Hypothesis

The aim of this chapter was to perform an *in vitro* characterisation of NHB cells with reference to NHU cells in terms of the expression of urothelium-associated transcription factors and differentiation-associated genes. In doing the characterisation, the goal was to:

1. Identify a set of transcription factors which could be useful for urothelial-type cell reprogramming, and in particular, be useful for the transdifferentiation of human buccal epithelial cells into urothelial cells.
2. Determine a set of criteria which could be used to validate successful conversion of human buccal epithelial cells into urothelial cells.

The hypothesis was that there exist fundamental differences in the expression of transcription factors and differentiation markers between normal human buccal epithelial cells and urothelial cells. Further to this, that these differences could be identified by comparing the two cell types in three different well characterised urothelial cell *in vitro* model systems.

3.2 Experimental Approach

NHU cells have been well characterised *in vitro*. In particular, three cell culture systems (termed KSFMc, TZ/PD and ABS/Ca^{2+} in this thesis) have been previously published, and NHU cells characterised for their expression of specific cytokeratin proteins, nuclear receptors, transcription factors, uroplakins, and tight junction-associated proteins. These three protocols are described in detail in the Introduction and Methods chapters of this thesis. Due to their ability to produce highly reproducible, yet varied results in NHU cells, the KSFMc, TZ/PD and ABS/Ca^{2+} protocols were chosen as ideal *in vitro* model systems for comparison of NHB cells to NHU cells to identify fundamental differences.

NHB cells (from 2-3 independent finite cell lines) were cultured in each of the three urothelial cell *in vitro* systems described above (KSFMc, TZ/PD and ABS/Ca^{2+}) and evaluated for their expression of nuclear receptors, cytokeratin proteins, transcription factors, and urothelium differentiation-associated genes. The ABS/Ca^{2+} protocol was also used to examine the ability of NHB cells to form a functional barrier epithelium, as measured by the TER. In all cases, a single NHU cell line was evaluated, which had been treated identically, and was used for comparison and/or as a positive control.

In addition to the three systems described above, examination of NHB cells in response to the atRA/PD protocol (see methods section 2.4.10) was also examined to determine whether RAR activation could lead to the upregulation of urothelium-associated genes in NHB cells. Retinoic acid has been implicated as a key regulator in the maintenance of the urothelial cell identity, with a particular role in preventing squamous metaplasia (Southgate et al., 1994; Liang et al., 2005; Gandhi et al., 2013). NHB cells were evaluated for their expression of urothelial cell-associated transcription factors, as well as for their expression of the uroplakin genes, following use of the atRA/PD protocol.

Phase contrast images of buccal epithelial cells and urothelial cells cultured in KSFMc, and during treatment with the TZ/PD, ABS/Ca^{2+} and atRA/PD protocols can be found in the Appendix.

3.2.1 Cell Line Nomenclature

As described in Chapter 2, upon arrival of the human tissue samples to the laboratory, each sample was given a unique coded number. Urological tissue specimens were given a unique ‘Y’ number (eg. Y1281). Buccal mucosa tissue specimens were given either a unique ‘AS’ number (eg. AS001b) or ‘Y’ number (eg. Y1600). When the epithelial cells were isolated from these tissue samples they retained their unique identifier, and thus were each defined as named, distinct finite cell lines after serial passage.

To make the data easier to follow in this chapter, where the two cell types were being compared, a specific cell line nomenclature was used for this chapter only. Finite normal human buccal epithelial (NHB) cell lines, which were originally identified as 'AS' and 'Y' numbers, were renamed to 'NHB' numbers. Finite normal human urothelial (NHU) cell lines, which were originally identified as 'Y' numbers, were renamed to 'NHU' numbers. A table of the independent finite cell lines used to generate results for this chapter, and their corresponding 'NHB' and 'NHU' numbers can be found in Table 3.1.

Table 3.1 List of Independent Finite NHB and NHU Cell Lines, and their Corresponding New Identification Numbers used in Chapter 4

Buccal Epithelial Cell Lines		**Urothelial Cell Lines**	
Original Identifier	**New Identifier**	**Original Identifier**	**New Identifier**
AS001b	NHB1	Y1281	NHU1
AS003b	NHB2	Y1288	NHU2
AS005b	NHB3	Y1334	NHU3
AS006b	NHB4	Y1358	NHU4
AS007b	NHB5	Y1453	NHU5
AS010b	NHB6	Y1642	NHU6
AS011b	NHB7	Y1677	NHU7
Y1778	NHB8	Y1691	NHU8

3.2.2 Differentiation and Barrier-Associated Gene Expression

The expression of a panel of genes was used to assess either urothelial-type differentiation, stratified squamous-type differentiation, or barrier phenotype in NHB cells following use of the KSFMc, TZ/PD, ABS/Ca^{2+} and/or atRA/PD protocols.

To identify transcription factors which could be useful for transdifferentiation-type experiments, a set of transcription factors (ELF3, FOXA1, GATA3, GRHL3, IRF1, KLF5, and PPARγ) was chosen for their known importance in regulating urothelial cell identity and differentiation, and evaluated for their expression in NHB cells.

To evaluate urothelial-type differentiation capacity of NHB cells, the expression of the five uroplakin genes (UPK1A, UPK1B, UPK2, UPK3A and UPK3B) was investigated. The uroplakin genes are highly associated with the superficial cells of the urothelium, and the formation of AUM plaques. Expression of CK13 was evaluated for its association with transitional-type differentiation (Varley et al., 2004b).

For stratified squamous-type differentiation, the expression of genes associated with the formation of the cornified cell envelope was investigated in NHB cells and NHU cells. These included LOR and SPRR4, which encode for proteins that are crosslinked to form the cornfield cell envelope of stratified squamous epithelia. The expression of TGM1 was also examined, which encodes an enzyme responsible for crosslinking the proteins that form the cornified cell envelope. The expression of CK14 was assessed as a squamous epithelial cell-associated marker (Harnden and Southgate, 1997).

The expression of a number of claudin genes (CLDN 1-10) was assessed in NHB cells as tight junction components associated with paracellular barrier function (Varley et al., 2006).

3.3 Results

3.3.1 RT-PCR Screen to Determine the Expression of Nuclear Receptors in NHB Cells Grown in KSFMc

Buccal epithelial cells from three independent NHB cell lines (NHB1, NHB3 and NHB4) expressed all three retinoic acid receptors (*RARA, RARAB* and *RARG*) and all three of the peroxisome proliferator-activated receptors (*PPARA, PPARD*, and *PPARG*) (Figure 3.1). Only two of the retinoid X receptors were expressed, *RXRA* and *RXRB*, and only *ESR1* was expressed of the oestrogen receptors. RT-PCR for a single NHU cell line (NHU2) was performed for comparison, and a similar expression profile was observed. The main difference in expression was seen with *PPARG,* where it appeared that buccal epithelial cells had potentially lower expression than urothelial cells.

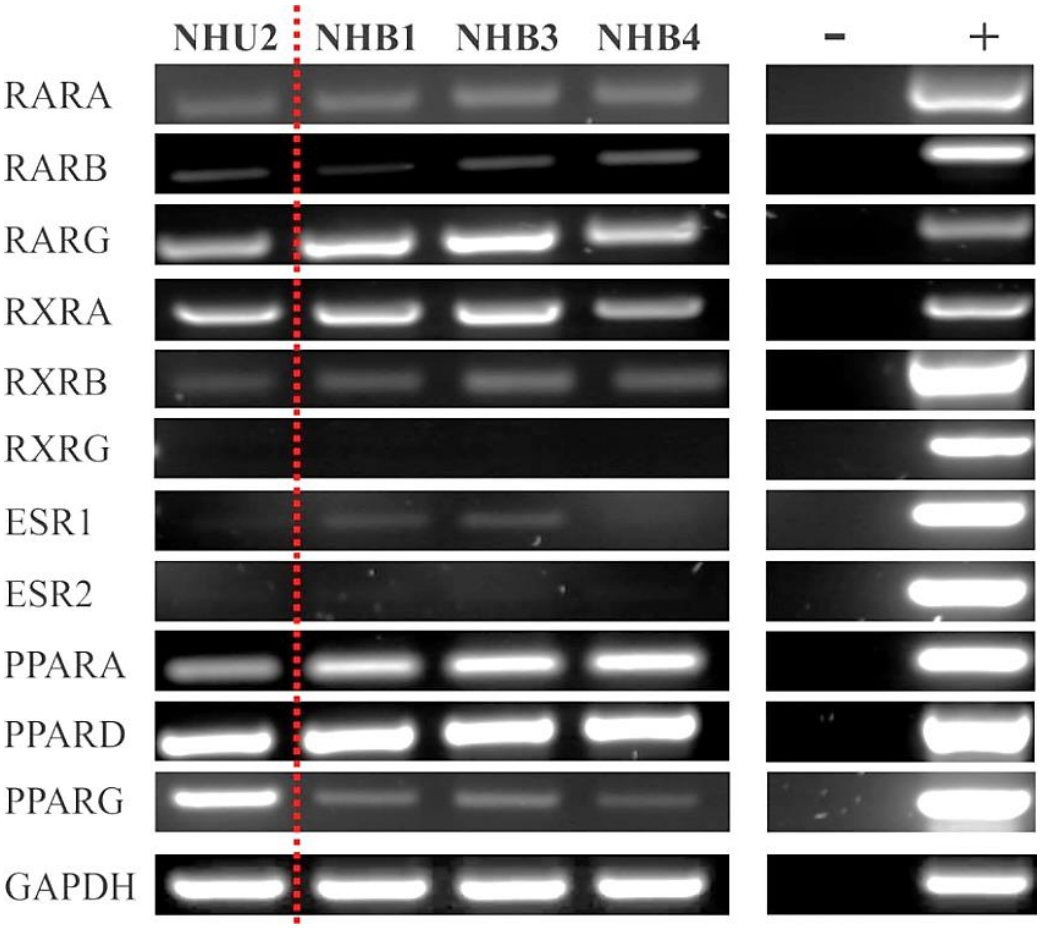

Figure 3.1 Nuclear Receptor Gene Expression in NHB Cells and NHU Cells Grown in Serum-Free, Low Calcium Medium (KSFMc) by RT-PCR

Buccal epithelial cells (NHB1, NHB3 and NHB4) and urothelial cells (NHU2) were grown in serum-free, low calcium medium (KSFMc) to confluence. PCR was performed using 30 cycles for all target genes. GAPDH was used as a loading control (25 cycles). H_2O (no template) was used as the negative control (-). Genomic DNA or cDNA generated from the total RNA of cells known to express the gene of interest was used as a positive control for the PCR (+). PPARG PCR was performed using forward and reverse primers designed to sequences in exon 6 of the PPARG coding sequence. Note similar expression of nearly all of the nuclear receptors assessed between NHU cells and NHB cells. A possible difference in expression was observed with PPARG, were NHB cells appeared to have weaker expression than NHU cells.

3.3.2 Cytokeratin Protein Expression

3.3.2.1 Expression of Cytokeratin Proteins in NHB Cells Grown in Serum-Free, Low Calcium Medium (KSFMc)

In serum-free, low calcium (0.09 mM) medium (KSFMc), buccal epithelial cells from three independent NHB cell lines (NHB2, NHB3 and NHB4) expressed CK5, CK14 and CK18 in all cells (Figure 3.2). CK7, CK13 and CK19 had mixed expression, with some cells positive and other cells negative. Expression of CK20 was absent. In NHU cells (NHU4), CK5, CK7, CK18 and CK19 were expressed in all cells. CK13 and CK14 were expressed in some of the cells and had weak expression in others. CK20 expression was absent in all cells.

3.3.2.2 Effect of PD and TZ/PD Treatment on the Expression of CK13 in NHB Cells

CK13 expression was weak to absent in control (0.1 % DMSO) NHB cells (Figure 3.3). Upon treatment with either 1 μM PD or combined TZ/PD, CK13 expression noticeably increased. Comparable amounts of CK13 expression were observed in both the PD only, and TZ/PD treated cells.

3.3.2.3 Expression of Cytokeratin Proteins in NHB Cell Sheets Generated using the ABS/Ca^{2+} Protocol

Assessment of cell sheets generated from three independent NHB cell lines (NHB1, NHB2 and NHB3) using the ABS/Ca^{2+} protocol, saw cytoplasmic CK5 and CK14 expression throughout all cell layers of the cell sheets (Figure 3.4). CK7 expression was also present throughout the cell sheets, but only in two of the three NHB cell lines (NHB1 and NHB3). CK13 expression was specifically restricted to only the upper portion of the NHB cell sheets. In NHU cell sheets, CK5, CK7 and CK13 expression was observed throughout the entire cell sheet. CK14 expression was absent, as expected in NHU cells differentiated with the ABS/Ca^{2+} protocol.

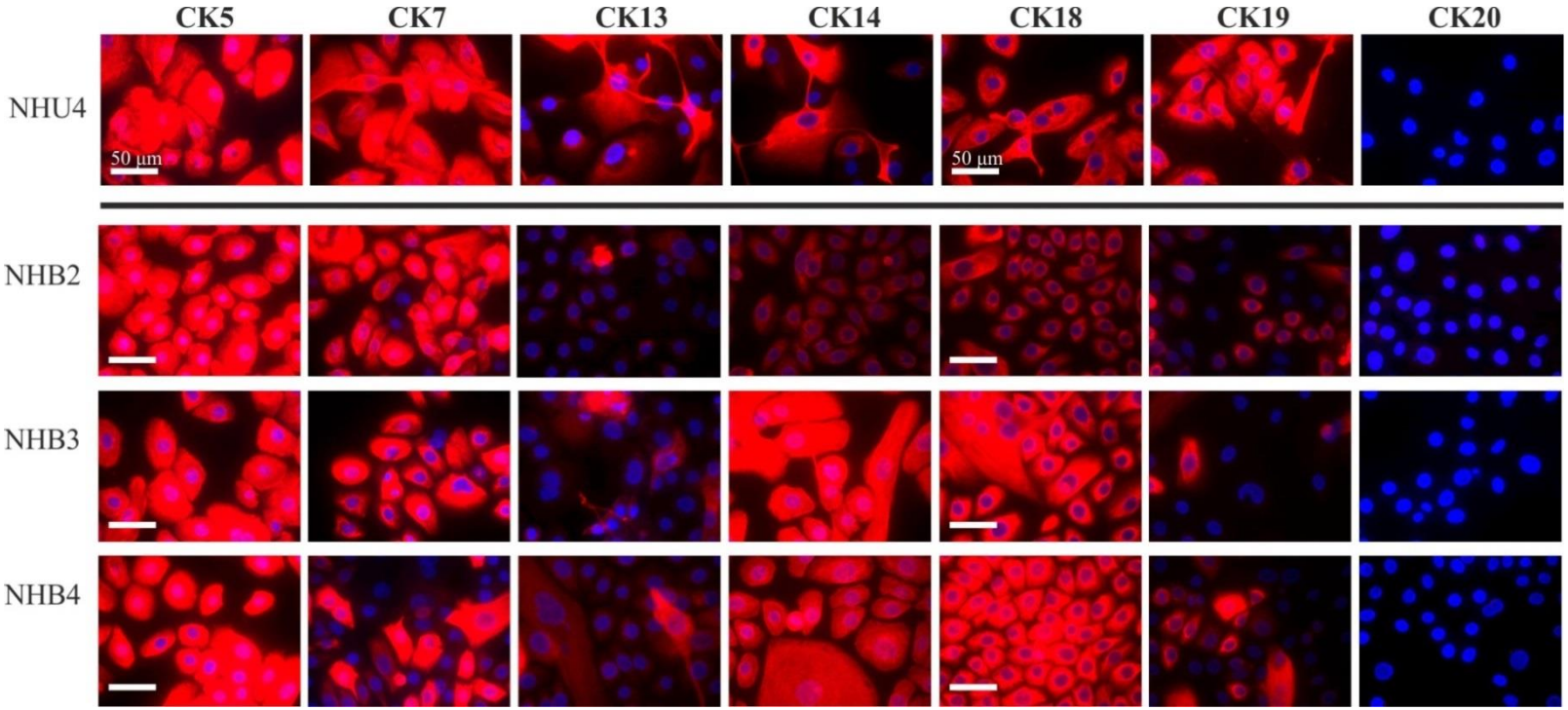

Figure 3.2 Cytokeratin Protein Expression in NHB Cells and NHU Cells Grown in Serum-Free, Low Calcium Medium (KSFMc) by Indirect Immunofluorescence Microscopy

Expression of CK5, CK7, CK13, CK14, CK18, CK19 and CK20 in three independent NHB cell lines (NHB2, NHB3 and NHB4) and a single NHU cell line (NHU4). Cells were grown on 12 well glass slides and fixed using 50:50 methanol acetone. Red labelling represents the specified cytokeratin. Nuclei were counterstained with Hoechst 33258. NHU cells which had been treated with TZ/PD for 6 days were used as a positive control for CK20 expression; the positive control image for CK20 can be seen in Appendix 7.4. Note NHB cells express CK5, CK14, and CK18 in all cells. CK7, CK13 and CK19 expression in NHB cells was mixed, with some cells positive and others negative. CK20 expression was absent.

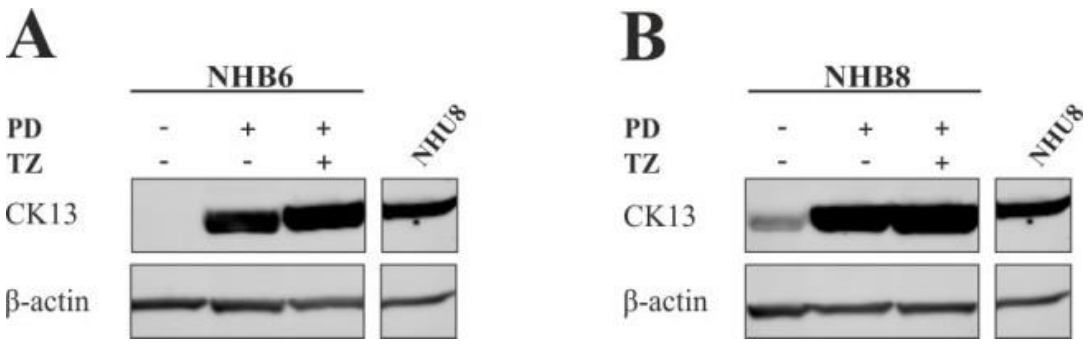

Figure 3.3 CK13 Expression in NHB Cells Following Treatment with DMSO, PD or TZ/PD for 72 hours by Western Blotting

Two independent NHB cell lines **A)** NHB6 and **B)** NHB8 were treated with either 0.1 % DMSO (vehicle control), 1 μM PD or the TZ/PD protocol for 72 hours. CK13 protein expression was assessed by western blotting. β-actin was used as a loading control. 25 μg of protein was loaded into each well. A single NHU cell line (NHU8) which had been treated with TZ/PD for 72 hours was included on the blot to act as a positive control/for comparison. NHB6 and NHB8 were carried out on the same western blot, and therefore have the same NHU positive control. Note increased CK13 expression in NHB cells as a result of PD treatment and combined TZ/PD treatment.

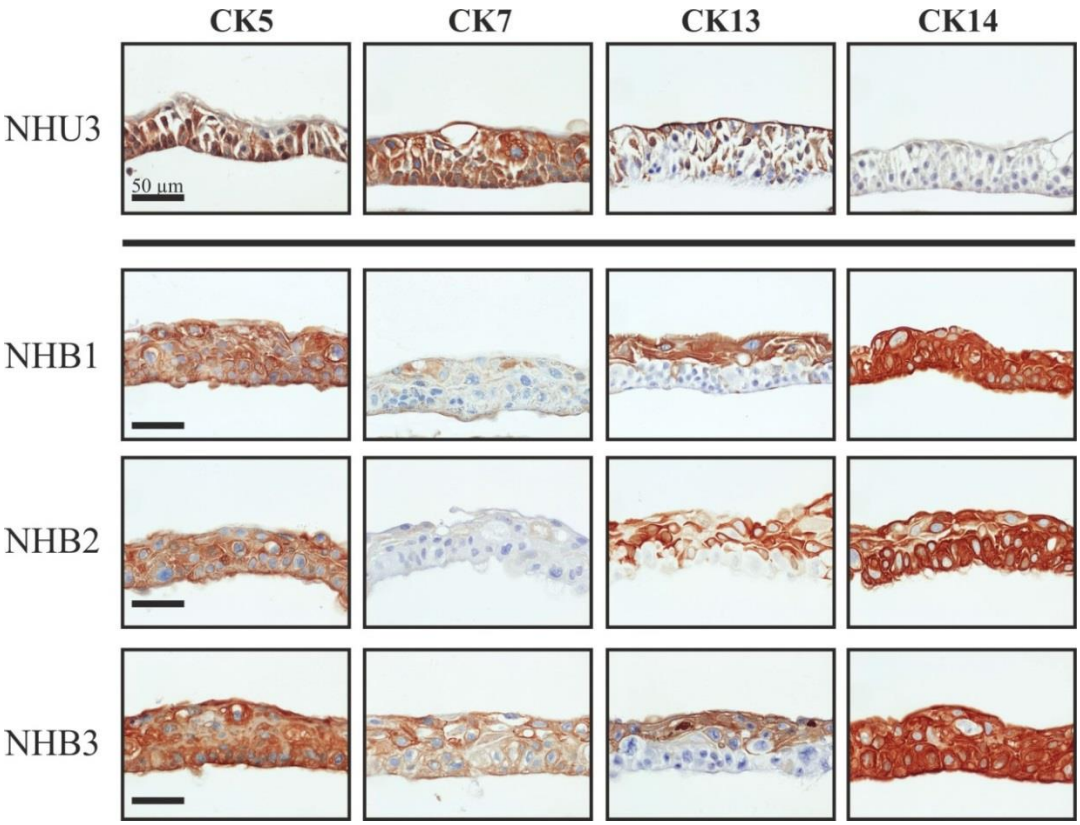

Figure 3.4 Evaluation of Cytokeratin Protein Expression by Immunohistochemistry in NHB and NHU Cell Sheets Generated Using the ABS/Ca^{2+} Protocol

The expression of cytokeratins 5, 7, 13 and 14 was assessed by immunohistochemistry. Cell sheets from a single NHU cell line (NHU3) and three independent NHB cell lines (NHB1, NHB2 and NHB3) are shown. Cell sheets were generated on Snapwell membranes using the ABS/Ca^{2+} protocol for seven days. All images are shown with the apical surface of the epithelial cell sheet at the top. Positive control and example negative control (no primary antibody) images can be found in Appendix 7.4. Note expression of CK14 throughout the whole of the NHB cell sheets, and absent in the NHU cell sheet. Also note CK13 expression is restricted to only the upper portion of the NHB cell sheets.

3.3.3 Assessment of Urothelial Cell Differentiation-Associated Transcription Factor Expression

3.3.3.1 Expression of Urothelium Differentiation-Associated Transcription Factors in NHB Cells Treated with TZ/PD

Buccal epithelial cells from two independent NHB cell lines (NHB4 and NHB5) were assessed for their expression of the transcription factors, ELF3, FOXA1, GATA3, GRHL3, IRF1, and KLF5 and PPARγ (all transcript variants), by RT-PCR (Figure 3.5). GRHL3 and KLF5 displayed high levels of gene expression throughout all of the time points (12 hr., 24 hr., and 48 hr.) in both control and TZ/PD treated cells. ELF3 and IRF1 gene expression appeared potentially upregulated by TZ/PD, with expression being observed at all time points. FOXA1 and GATA3 gene expression was noticeably weak to absent at all of the time points. Both of the NHB cell lines investigated showed similar results for all genes, at all time points. A single NHU cell line (NHU1), evaluated for comparison, displayed clear gene expression for all seven of the transcription factors, at all of the control and TZ/PD time points (12 hr., 24 hr., and 48 hr.), as was expected.

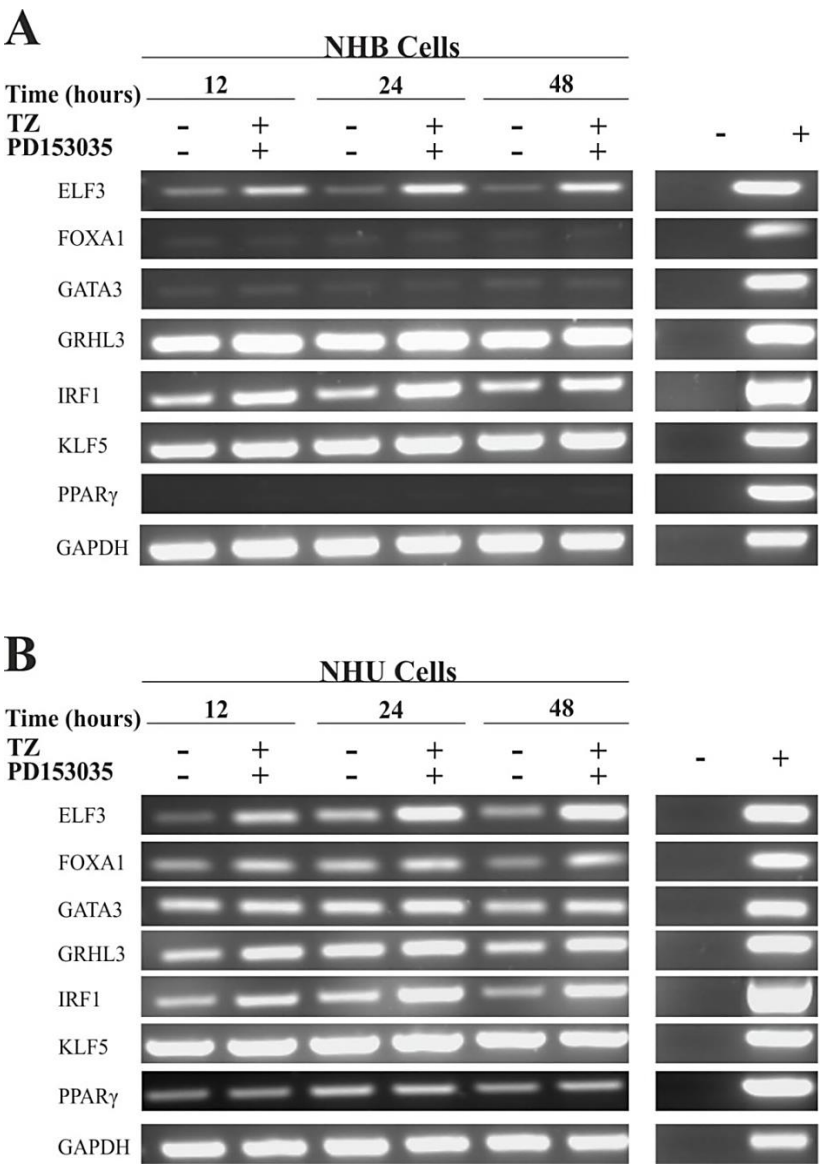

Figure 3.5 Evaluation of Transcript Expression of Urothelium-Associated Transcription Factors by RT-PCR in NHB Cells and NHU Cells Following TZ/PD Treatment

Buccal epithelial cells **A)** (NHB4) and urothelial cells **B)** (NHU1) were treated with TZ/PD for 24, 48 and 72 hours. The expression of ELF3, FOXA1, GATA3, GRHL3, IRF1, KLF5 and PPARγ (forward and reverse primers designed to sequences in exon 6) was assessed by RT-PCR. PCR was performed using 30 cycles. GAPDH was used as a loading control (25 cycles). H_2O (no template) was used as a negative control (-). Genomic DNA was used as the positive control for the PCR (+). A second buccal epithelial cell line (NHB5), which showed similar results, was also completed for this experiment, and the figure can be found in Appendix 7.4. Note the weak/absent expression of FOXA1, GATA3 and PPARγ expression in NHB cells. Also note the possible upregulation of ELF3 in NHB cells as a result of TZ/PD.

From the original set of seven transcription factors, ELF3, FOXA1, GATA3 and PPARγ were chosen to investigate in NHB cells further by RT-qPCR, western blotting and immunofluorescence. ELF3 was chosen due to its apparent upregulation as a result of the using the TZ/PD protocol. FOXA1, GATA3 and PPARγ were chosen due to their apparent weak gene expression in NHB cells in comparison to NHU cells.

Buccal epithelial cells from three independent NBH cell lines (NHB6, NHB7 and NHB8) had weak constitutive expression of FOXA1, GATA3 and PPARγ (all transcript variants), and there was no significant upregulation of expression as a result of 72 hour TZ/PD treatment by RT-qPCR analysis (Figure 3.6). ELF3 expression was significantly ($P = 0.006$) upregulated as a result of using the TZ/PD protocol (72 hour). These results confirmed the previous results obtained using RT-PCR. In comparison to a single NHU cell line (NHU6), NHB cells had lower transcript abundance of all four of the transcription factors (ELF3, FOXA1, GATA3 and PPARγ) in response to TZ/PD.

By western blotting, buccal epithelial cells from three independent NHB cell lines (NHB6, NHB7 and NHB8) had weak to absent protein expression of GATA3 and PPARγ1 even following use of the TZ/PD protocol for 72 hours (Figure 3.7). ELF3 protein expression varied between the cell lines; two NHB cell lines (NHB6 and NHB8) showed increased ELF3 expression as a result of TZ/PD, while a third cell line (NHB7) was negative. FOXA1 expression also varied; one NHB cell line (NHB6) was negative, another had expression in control and TZ/PD treated cells (NHB8), and a third cell line (NHB7) only showed expression in control cells.

By immunofluorescence, the expression of ELF3 varied among the three NHB cell lines (NHB6, NHB7 and NHB8), but in general it was weakly expressed, becoming more strongly nuclear at the 144 hr TZ/PD time point (Figure 3.8). FOXA1, GATA3 and PPARγ expression was weakly nuclear to absent at all time points (24 hr, 72 hr, and 144 hr). In NHU cells (NHU6 and NHU7) used for comparison, an obvious upregulation of expression, and nuclear localisation was observed as a result of the TZ/PD protocol (72 hour), as was expected.

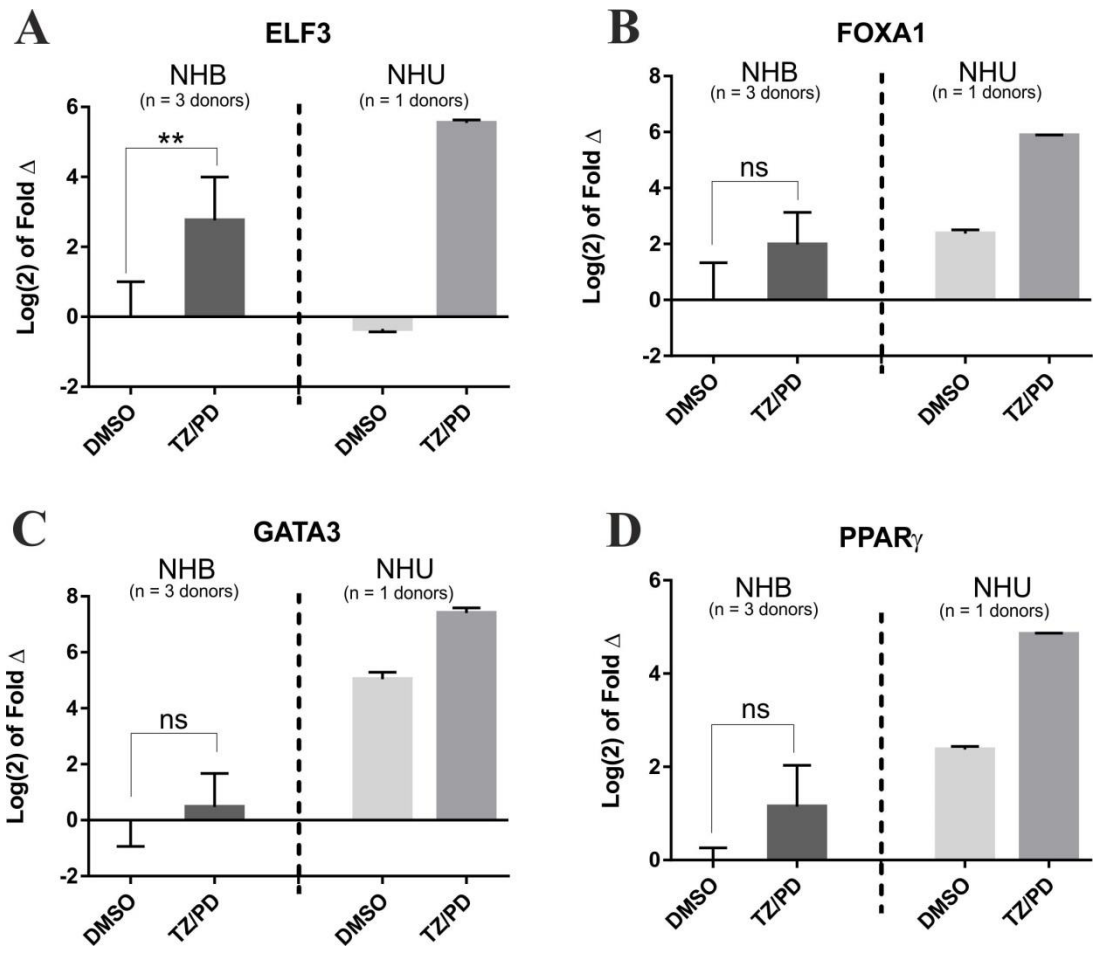

Figure 3.6 Assessment of ELF3, FOXA1, GATA3 and PPARγ Transcript Expression in NHB Cells and NHU Cells by RT-qPCR Following use of the TZ/PD Protocol for 72 hour

RT-qPCR data was generated for **A)** ELF3, **B)** FOXA1, **C)** GATA3 and **D)** PPARγ (forward primer in exon 1 and reverse primer in exon 3) using three independent NHB cell lines (NHB6, NHB7 and NHB8), and a single NHU cell line (NHU6) for comparison. Cultures were treated with either 0.1% DMSO (vehicle control) or TZ/PD for 72 hours. All values are shown relative to the mean of the 0.1% DMSO treated buccal epithelial cells for each gene. For NHB cells, error bars represent the standard deviation of the mean of the Log(2) fold change of the three independent NHB cell lines (n=3). For NHU cells, error bars represent the standard deviation of three technical replicates (n=1). All values were first normalised to GAPDH. Statistical analysis was performed using a two-tailed, paired t-test to determine whether there was a significant change in gene expression as a result of using the TZ/PD protocol. ns = non-significant. ** represents $P \leq 0.01$. Note the significant upregulation of ELF3 expression in NHB cells as a result of TZ/PD treatment. Also note weak expression of FOXA1, GATA3 and PPARγ in NHB cells even following the use of the TZ/PD protocol.

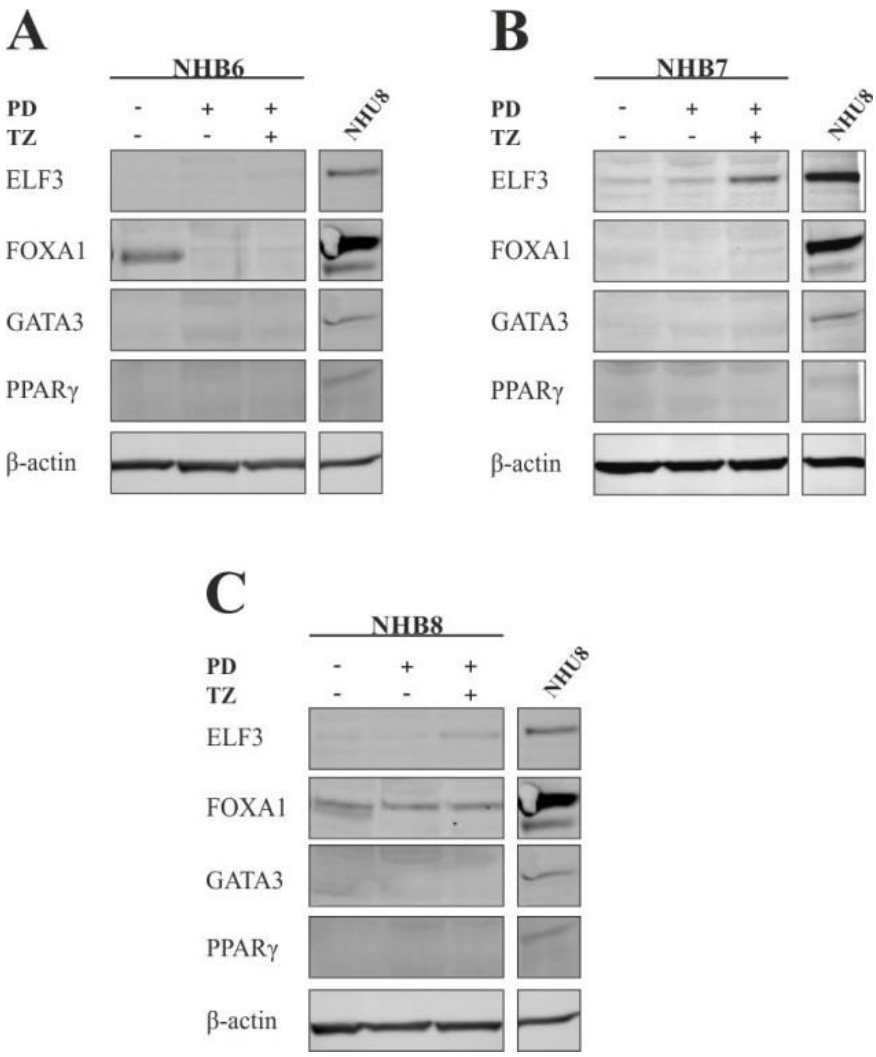

Figure 3.7 Assessment of ELF3, FOXA1, GATA3 and PPARγ Protein Expression by Western Blotting in Buccal Epithelial Cells Following 72 hour DMSO, PD and TZ/PD Treatment

Buccal epithelial cells from three independent NHB cell lines, **A)** NHB6, **B)** NHB7 and **C)** NBH8 were treated with either 0.1% DMSO (vehicle control), 1 μM PD or TZ/PD for 72 hours. ELF3, FOXA1 (Santa Cruz, Q-6), GATA3 and PPARγ (Cell Signaling, D69) expression was assessed by western blotting. The band corresponding to PPARγ1 (approximately 52 kDa) is shown. A full length blot showing all PPARγ reactive bands in NHB cells can be found in Appendix 7.4. A single NHU cell line (NHU8) which had been treated with TZ/PD for 72 hours was included on all blots to act as a positive control/for comparison. NHB6 and NHB8 were carried out on the same western blots, and therefore have the same NHU positive control. 25 μg of protein was loaded into each well and β-actin was used as a loading control. Note weak/absent expression of GATA3 and PPARγ1 in NHB cells. Expression of ELF3 and FOXA1 protein was variable.

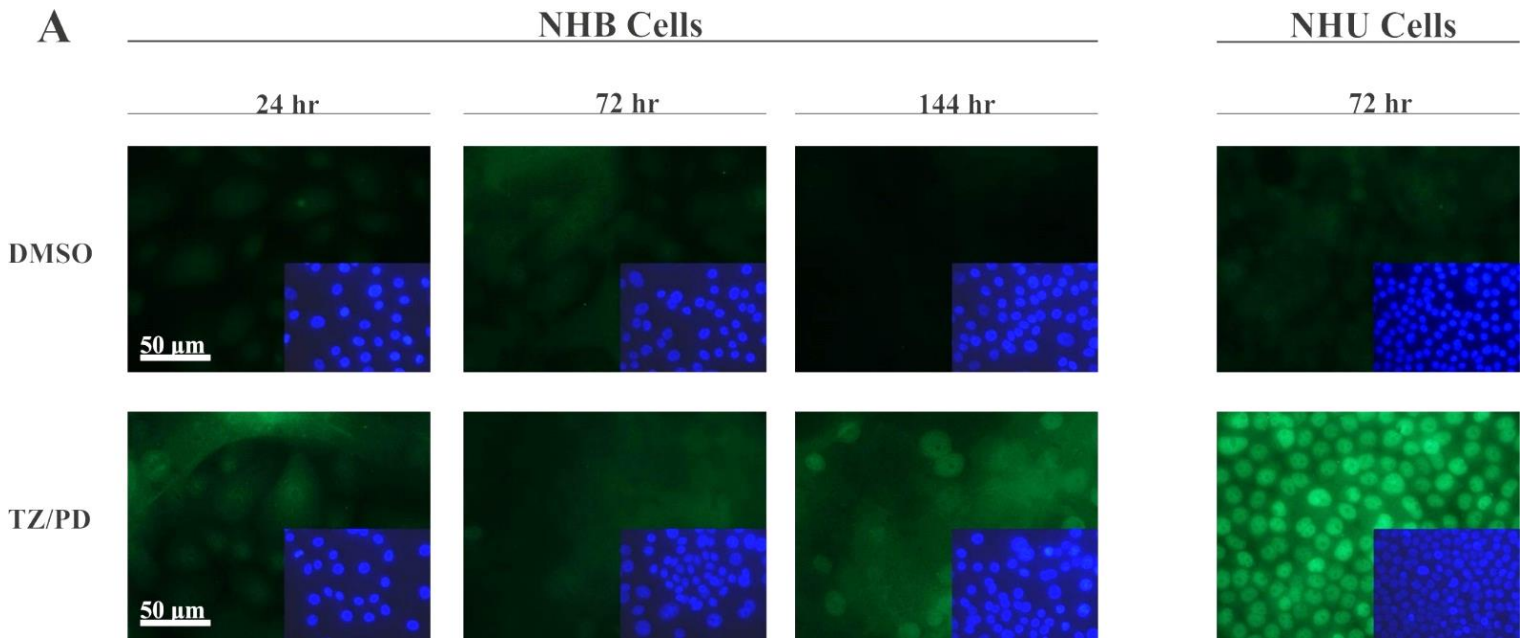

Figure 3.8 Evaluation of Transcription Factor Protein Expression in NHB Cells and NHU Cells Following use of the TZ/PD Protocol for 24, 72 and 144 hours by Indirect Immunofluorescence Microscopy – A) ELF3

NHB cells (NHB7) were treated with either 0.1% DMSO (vehicle control) or TZ/PD for 24, 72 and 144 hours. A single NHU cell line (NHU7) which had been treated with either 0.1% DMSO or TZ/PD for 72 hours was used as a positive control for comparison. **A)** ELF3, **B)** FOXA1/2 (Santa Cruz, C-20), **C)** GATA3, and **D)** PPARγ (Cell Signaling, D69) expression was assessed by immunofluorescence on formalin-fixed slides which had been permeabilised using Triton X-100. Inset images show the corresponding Hoechst 33258 staining to demonstrate cell density and nuclei location. All antibody-labelled images were taken at the same exposure for both NHB cells and NHU cells. Hoechst 33258 images were taken at optimal exposures. Two additional NHB cell lines (NHB6 and NHB8) were evaluated for the purpose of this experiment, and their figures can be found in Appendix 7.4.

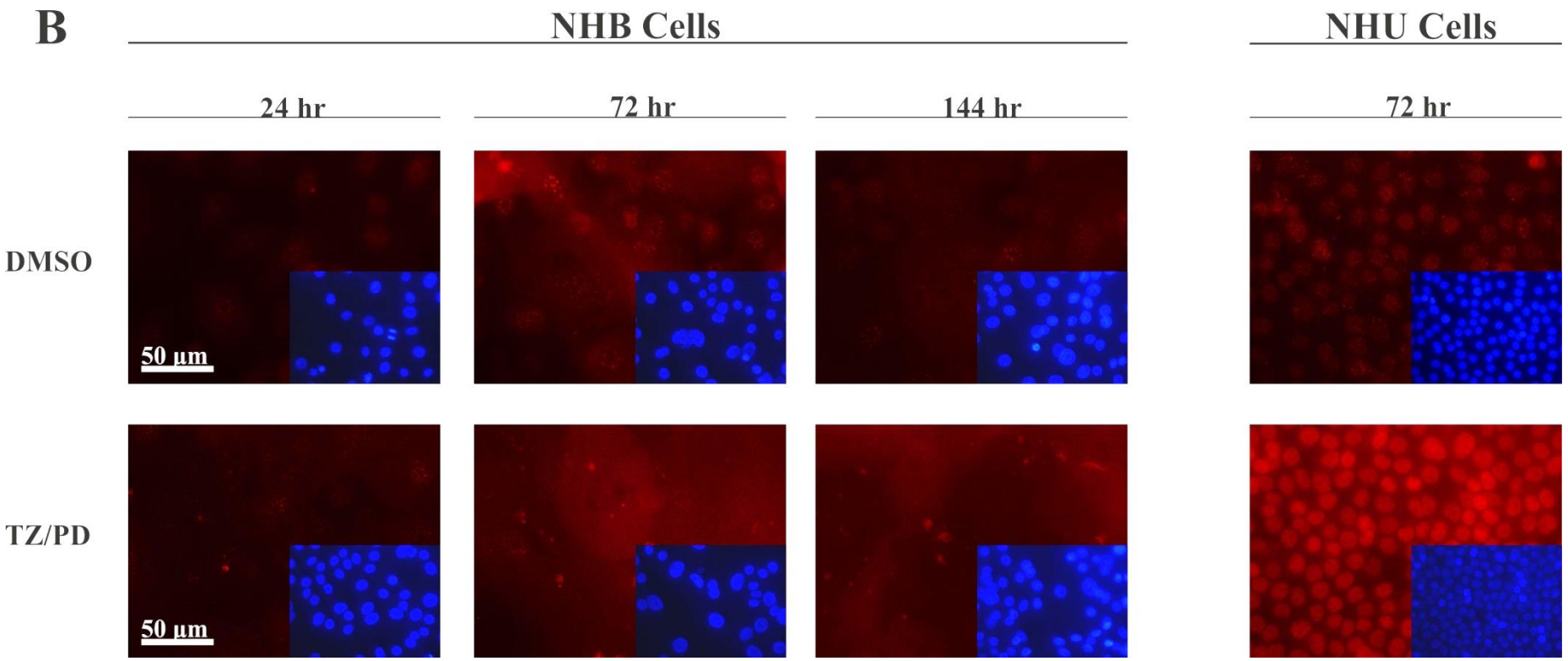

Figure 3.8 Evaluation of Transcription Factor Protein Expression in NHB Cells and NHU Cells Following use of the TZ/PD Protocol for 24, 72 and 144 hours by Indirect Immunofluorescence Microscopy – B) FOXA1/2

See main caption on page 136. Note weak/absent expression of FOXA1/2 in NHB cells even following use of the TZ/PD protocol for up to 144 hours.

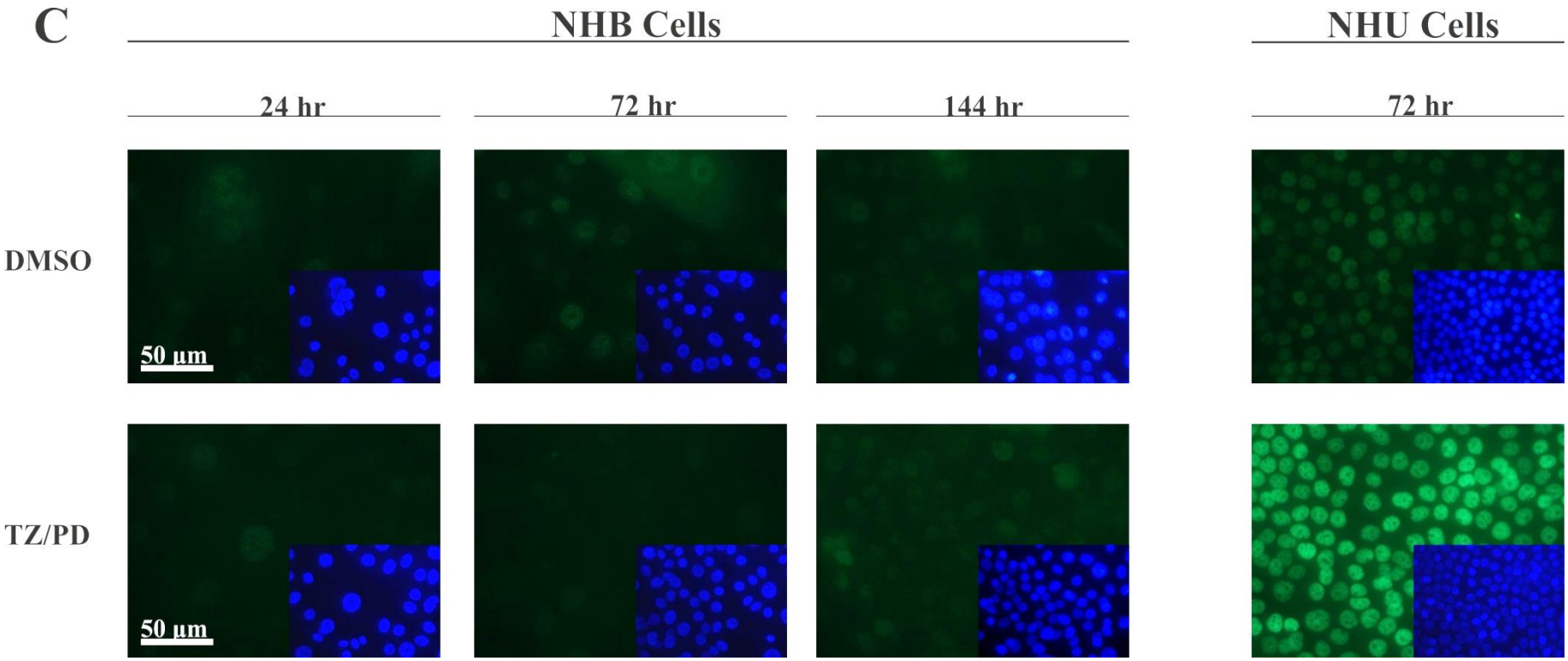

Figure 3.8 Evaluation of Transcription Factor Protein Expression in NHB Cells and NHU Cells Following use of the TZ/PD Protocol for 24, 72 and 144 hours by Indirect Immunofluorescence Microscopy – C) GATA3

See main caption on page 136. Note weak/absent expression of GATA3 in NHB cells even following use of the TZ/PD protocol for up to 144 hours.

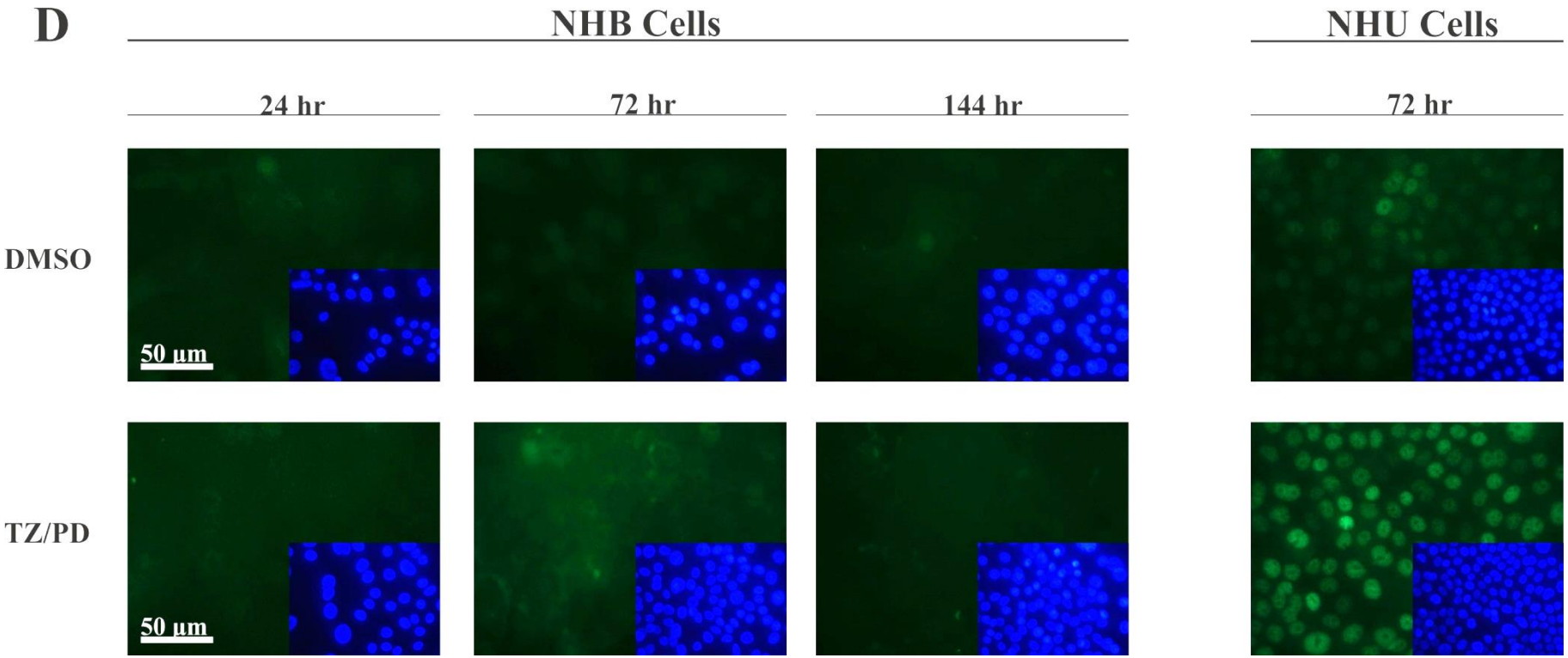

Figure 3.8 Evaluation of Transcription Factor Protein Expression in NHB Cells and NHU Cells Following use of the TZ/PD Protocol for 24, 72 and 144 hours by Indirect Immunofluorescence Microscopy – D) PPARγ

See main caption on page 136. Note weak/absent expression of PPARγ in NHB cells even following use of the TZ/PD protocol for up to 144 hours.

3.3.3.2 Expression of FOXA1 and GATA3 Following use of the atRA/PD Protocol

The effect of RAR activation on the expression of transcription factors FOXA1 and GATA3 was assessed by RT-PCR using a single NHB cell line (NHB4) (Figure 3.9). FOXA1 gene expression was weak, but appeared induced by the all-trans retinoic acid treatment in a dose-dependent manner. GATA3 expression was weak in all of the treatments.

Three independent NHB cell lines (NHB8, NHB6 and NHB7) were used to investigate the effect of all-trans retinoic acid on the protein expression of FOXA1 and GATA3, by western blotting (Figure 3.10). FOXA1 expression was upregulated, but weak in all three cell lines, as a result of all-trans retinoic acid treatment. GATA3 expression remained absent in all three cell lines.

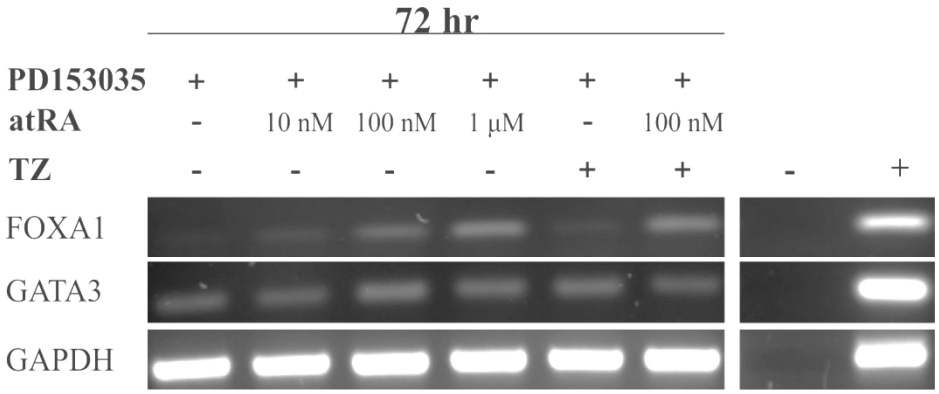

Figure 3.9 Evaluation of FOXA1 and GATA3 Transcript Expression by RT-PCR in NHB Cells Following use of the atRA/PD Protocol for 72 hours

Buccal epithelial cells (NHB4) were treated with 1 μM PD153035 and varying concentrations of atRA (10 nM, 100 nM, and 1 μM). Additional cell treatments included TZ/PD with and without 100 nM atRA. The treatment time course lasted 72 hours. PCR was performed using 30 cycles for all target genes. GAPDH was used as a loading control (25 cycles). H_2O (no template) was used as the negative control (-). Genomic DNA was used as the positive control (+). Note an upregulation of FOXA1 expression as a result of increased concentrations of atRA. GATA3 expression appeared weak and unaffected by atRA.

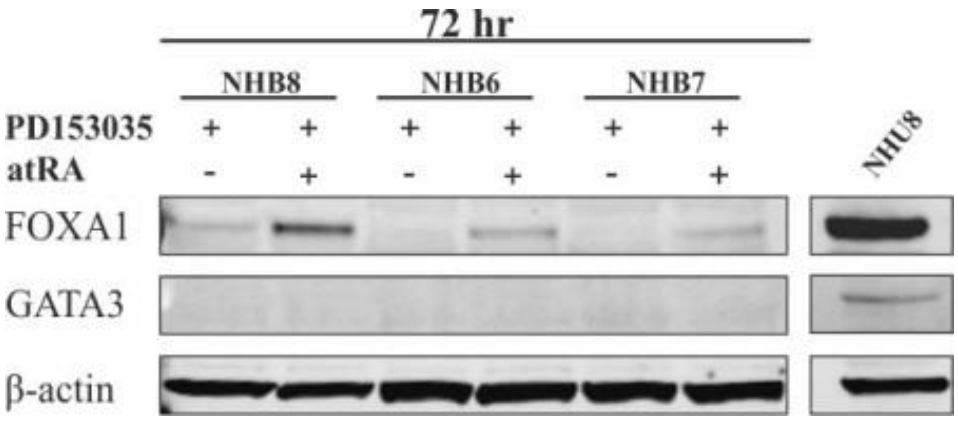

Figure 3.10 Evaluation of FOXA1 and GATA3 Protein Expression by Western Blotting in NHB Cells Following use of the atRA/PD Protocol for 72 hours

Three independent NHB cell lines (NHB8, NHB6 and NHB7) were treated with either 1 μM of PD (control) or 1 μM PD with 100 nM atRA for 72 hours. GATA3 and FOXA1 (Q-6, Santa Cruz) protein expression was assessed by western blotting. β-actin was used as a loading control. Protein taken from a single NHU cell line (NHU8), which had been treated with TZ/PD for 72 hours, was included on the same blot, and used as a positive control for each antibody. 25 μg of protein was loaded into each well. Note increased FOXA1 protein expression in all three NHB cell lines as a result of atRA treatment. GATA3 expression remained absent in all three of the NHB cell lines.

3.3.3.3 Assessment of Urothelial Differentiation-Associated Nuclear Receptor and Transcription Factor Expression in NHB and NHU Cell Sheets Generated Using the ABS/Ca^{2+} Protocol

The expression of transcription factors, FOXA1/2 and GATA3, and nuclear receptors, RXRα and PPARγ, was evaluated in NHB cell sheets which had been generated using the ABS/Ca^{2+} protocol (Figure 3.11). In buccal epithelial cell sheets, generated from three independent NHB cell lines (NHB1, NHB2 and NHB3), FOXA1/2 expression was nuclear, but restricted to only a portion of the nuclei. GATA3 expression was negative in all NHB cell lines, while PPARγ expression appeared as both cytoplasmic and nuclear. RXRα expression was nuclear in all cells. In the urothelial cell sheets, generated using a single NHU cell line (NHU3), clear nuclear expression was observed for RXRα, PPARγ, FOXA1 and GATA3.

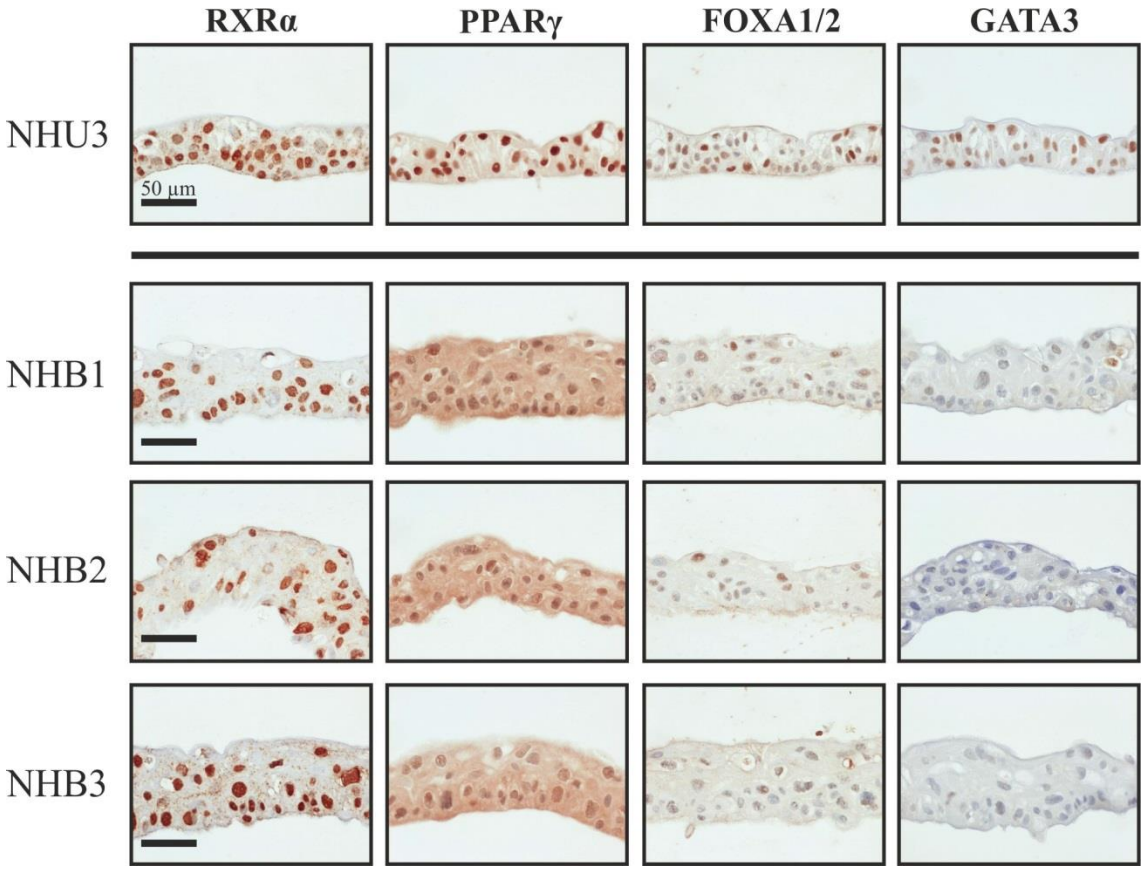

Figure 3.11 Assessment of Transcription Factor and Nuclear Receptor Protein Expression in NHB and NHU Cell Sheets Generated Using the ABS/Ca^{2+} Protocol by Immunohistochemistry

The expression of RXRα, PPARγ (Cell Signaling, 81B8), FOXA1/2 (Santa Cruz, C-20) and GATA3 was assessed by immunohistochemistry. Cell sheets from a single NHU cell line (NHU3) and three independent buccal epithelial cell lines (NHB1, NHB2 and NHB3) are shown. Cell sheets were generated on Snapwell membranes using the ABS/Ca^{2+} protocol for seven days. All images are shown with the apical surface of the epithelial cell sheet at the top. Positive control and example negative control (no primary antibody) images can be found in Appendix 7.4. Note weak nuclear expression of FOXA1/2 in NHB cells. Also note absence of GATA3 expression in NHB cells. PPARγ expression appeared both cytoplasmic and nuclear in NHB cell sheets, which differed from the strongly nuclear expression observed in NHU cell sheets.

3.3.4 Assessment of Urothelium Differentiation-Associated Genes

3.3.4.1 Uroplakin Gene Expression in NHB Cells Following use of the TZ/PD Protocol

Buccal epithelial cells from two independent NHB cell lines (NHB3 and NHB4) were assessed for their expression of the five uroplakin genes following use of the TZ/PD protocol for up to 6 days, by RT-PCR (Figure 3.12). UPK1A transcript expression was weak/absent in one of the NHB cell lines (NHB3), while in the other (NHB4) it was weakly detected at all of the time points. UPK2 transcript was weakly detected at all of the TZ/PD time points (0.5, 3 and 6 days). UPK3A expression was absent at all time points. UPK1B and UPK3B were expressed at all of the time points assessed. The single NHU cell line (NHU5) examined expressed UPK1B and UPK3B at all time points. UPK1A, UPK2 and UPK3A expression was most obvious at the 3 and 6 day TZ/PD time points in NHU cells.

To determine whether the expression of any of the five uroplakin genes was significantly upregulated as a result of using the TZ/PD protocol, RT-qPCR was performed for three independent buccal epithelial cell lines (NHB6, NHB7 and NHB8) which had been treated with either 0.1% DMSO or the TZ/PD for 72 hours (Figure 3.13). cDNA generated from a single urothelial cell line (NHU6), which had undergone the same TZ/PD protocol for 72 hours, was used for comparison. In NHB cells, the expression of UPK1A, UPK1B, UPK2 and UPK3B was detected and upregulated as a result of TZ/PD, with UPK2 and UPK3B expression being significantly upregulated. Expression of UPK3A was undetectable in all of the NHB cell lines. These results agreed with the results observed by RT-PCR.

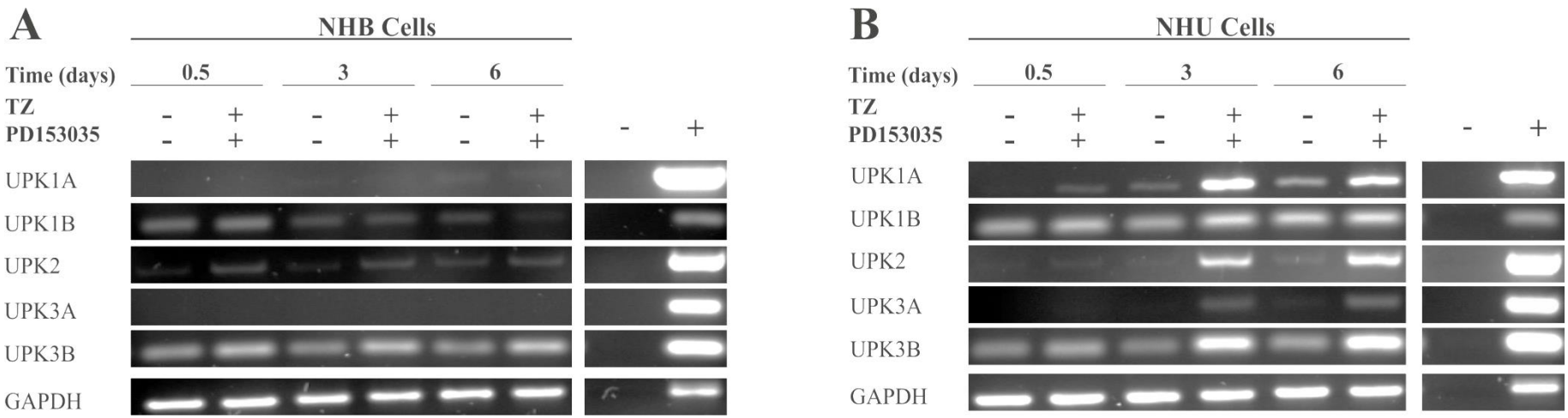

Figure 3.12 Assessment of Uroplakin Gene Expression in Buccal Epithelial Cells and Urothelial Cells by RT-PCR Following TZ/PD Treatment

A) Buccal epithelial cells (NHB3) and **B)** urothelial cells (NHU5) were treated with either 0.1% DMSO or TZ/PD for 0.5, 3 or 6 days. The gene expression of the five uroplakin genes (UPK1A, UPK1B, UPK2, UPK3A, UPK3B) is shown by RT-PCR. PCR was performed using 30 cycles. GAPDH was used as a loading control (25 cycles). H_2O (no template) was used as a negative control (-). Genomic DNA was used as the positive control for the PCR (+). A second buccal epithelial cell line (NHB4) was also completed for this experiment, and the figure can be found in Appendix 7.4. Note weak expression of UPK1A, UPK1B and UPK2 in NHB cells. Also note abundant expression of UPK3B in NHB cells. UPK3A was absent in both NHB cell lines assessed.

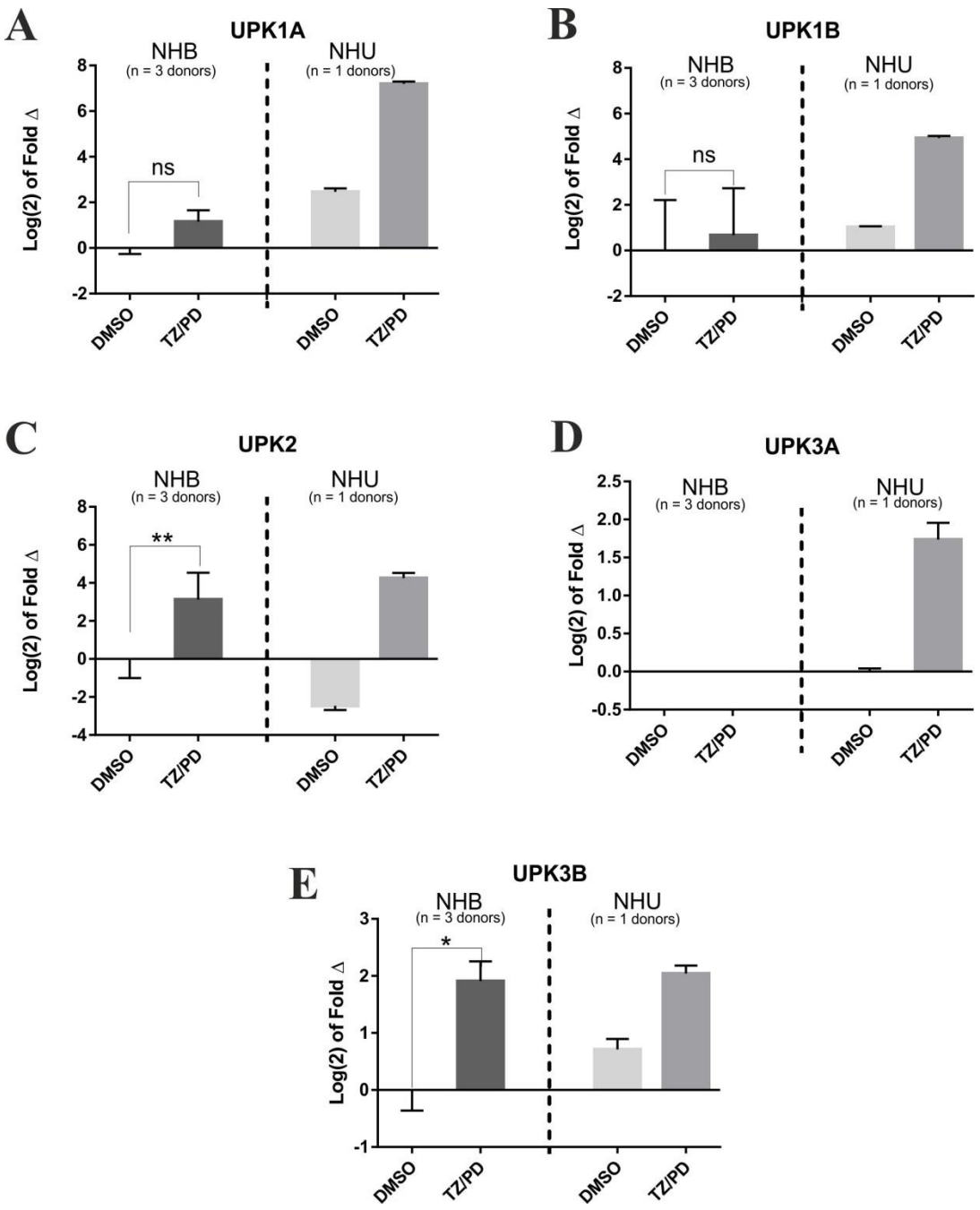

Figure 3.13 Evaluation of Uroplakin Gene Expression in Buccal Epithelial Cells and Urothelial Cells by RT-qPCR Following 72 hour TZ/PD Treatment

Figure 3.13 Evaluation of Uroplakin Gene Expression in Buccal Epithelial Cells and Urothelial Cells by RT-qPCR Following 72 hour TZ/PD Treatment

RT-qPCR data was generated for the five uroplakin genes, **A)** UPK1A, **B)** UPK1B, **C)** UPK2, **D)** UPK3A, and **E)** UPK3B, using three independent NHB cell lines (NHB6, NHB7 and NHB8), and a single NHU cell line (NHU6) for comparison. Cells were treated with either 0.1% DMSO (control) or TZ/PD for 72 hours. For NHB cells, error bars represent the standard deviation of the mean of the Log(2) fold change of the three independent NHB cell lines (n=3). For NHU cells, error bars represent the standard deviation of three technical replicates (n=1). Since UPK3A was not detected in NHB cells, UPK3A is shown relative to the DMSO treated NHU cells. Gene expression was first normalised to GAPDH expression. Statistical analysis was performed using a two-tailed, paired t-test to assess whether there was any significant change in gene expression as a result of TZ/PD. ns = non-significant. * represents $P \leq 0.05$. ** represents $P \leq 0.01$. Note weak expression of UPK1A, UPK1B and UPK2 in NHB cells. Also note the significant upregulation of UPK2 and UPK3B expression in NHB cells as a result of TZ/PD treatment.

3.3.4.2 Effect of All-Trans Retinoic Acid on Uroplakin Gene Expression

The effect of RAR activation on the expression of the five uroplakin genes (UPK1A, UPK1B, UPK2, UPK3A, and UPK3B), was assessed by RT-PCR in a single NHB cell line (NHB4) (Figure 3.14). UPK1A gene expression appeared possibly downregulated as a result of the atRA treatment, while expression of UPK1B, UPK2 and UPK3B was maintained. UPK3A expression was absent in all cases.

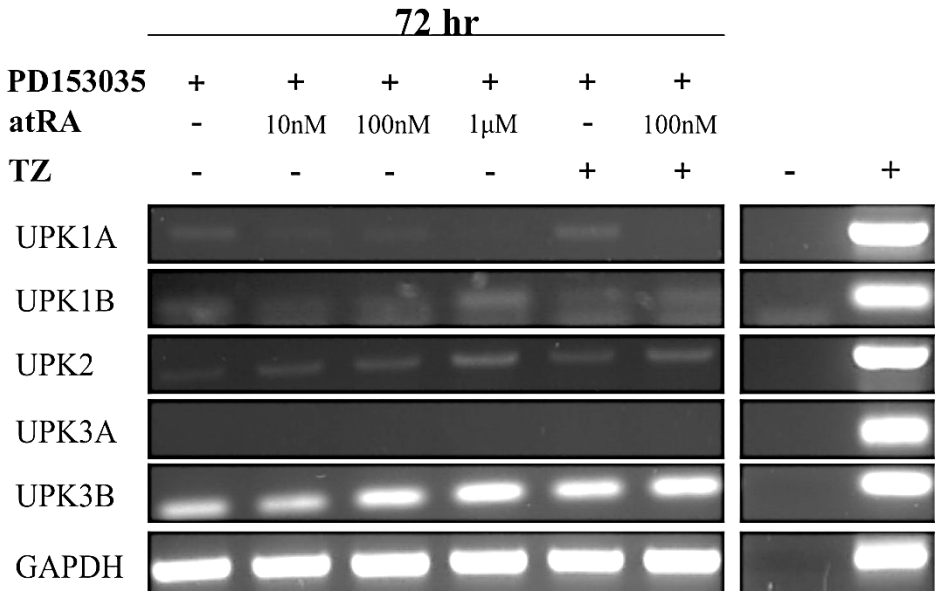

Figure 3.14 Evaluation of Uroplakin Gene Expression by RT-PCR Following use of the atRA/PD Protocol in NHB Cells

Buccal epithelial cells (NHB4) were treated with 1 μM PD and varying concentrations of atRA (10 nM, 100 nM, and 1 μM). Additional treatments included TZ/PD with and without 100 nM atRA. The treatment time course lasted 72 hours. PCR was performed using 30 cycles for all target genes. GAPDH was used as a loading control (25 cycles). H_2O (no template) was used as the negative control (-). Genomic DNA was used as the positive control (+). Note no obvious changes in uroplakin gene expression in NHB cells following treatment with either PD or atRA/PD.

3.3.4.3 Expression of Selected Claudin Genes in NHB Cells Treated with TZ/PD

Buccal epithelial cells from two independent NHB cell lines (NHB3 and NHB4) displayed expression of claudin 1, 2, 4, and 7 transcript at all of the time points assessed during the TZ/PD protocol (12 hr, 72 hr and 144 hr) (Figure 3.15). Claudin 6, 8 and 10 gene expression was absent at all of the time points. Claudin 3 and 5 gene expression was variable between the two cell lines evaluated. In one of the cell lines (NHB4) CLDN3 expression was absent at all of the time points, while in the other cell line (NHB3) CLDN3 was expressed at all time points. CLDN5 was expressed only at day 0.5 in one cell line (NHB3) while it was expressed only at day 6 in the other cell line (NHB4). In a single NHU cell line (NHU5), assessed for comparison, gene expression for claudins 1, 3, 4 and 7 was observed at all of the time points. Claudin 5 expression was restricted to only the TZ/PD treated cells at days 3 and 6. Claudin 2 was expressed only in the day 6, untreated cells. Expression of claudins 6, 8 and 10 was absent in urothelial cells.

3.3.4.4 Assessment of Selected Tight Junction Proteins in NHB and NHU Cell Sheets Generated Using the ABS/Ca^{2+} Protocol

The expression of several tight junction-associated proteins was assessed in cell sheets generated from three independent NHB cell lines (NHB1, NHB2 and NHB3) and a single NHU cell line (NHU3) using the ABS/Ca^{2+} protocol. The expression of claudins (CLDNs) -4, -5 and -7 was present at the intercellular borders and restricted to only the upper half of the NHB cell sheets (Figure 3.16). This was in contrast to the expression observed in the NHU cell sheets, where claudins -4, -5 and -7 were expressed at the intercellular borders, but throughout the whole of the cell sheets. Occludin (OCLN) expression was observed throughout the entire cell sheet in both the NHB and NHU cell sheets. The expression of the claudin proteins was observed at the cell borders/contact points in all of the cell lines. Occludin expression was cytoplasmic throughout all of the cell sheets, with expression also present at intercellular borders.

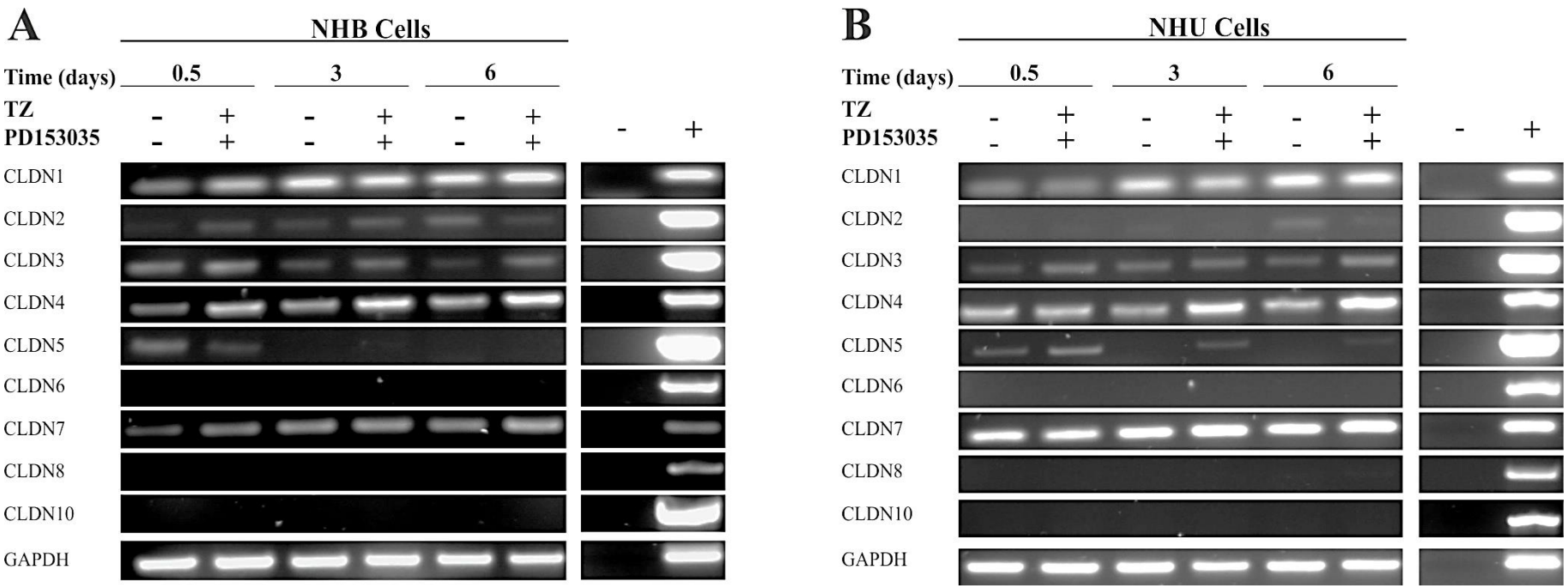

Figure 3.15 Evaluation of Claudin Gene Expression in NHB Cells and NHU Cells by RT-PCR Following TZ/PD Treatment

A) NHB cells (NHB3) and **B**) NHU cells (NHU5) were treated with either 0.1% DMSO or TZ/PD for 0.5, 3 or 6 days. The gene expression of claudins (CLDNs) 1-10 is shown by RT-PCR. PCR was performed using either 30 or 35 cycles for a given gene. GAPDH was used as a loading control (25 cycles). H_2O (no template) was used as a negative control (-). Genomic DNA was used as the positive control for the PCR (+). A second buccal epithelial cell line (NHB4) was also completed for this experiment, and the figure can be found in Appendix 7.4. Note the similar expression of the CLDN genes in NHB cells and NHU cells during use of the TZ/PD protocol.

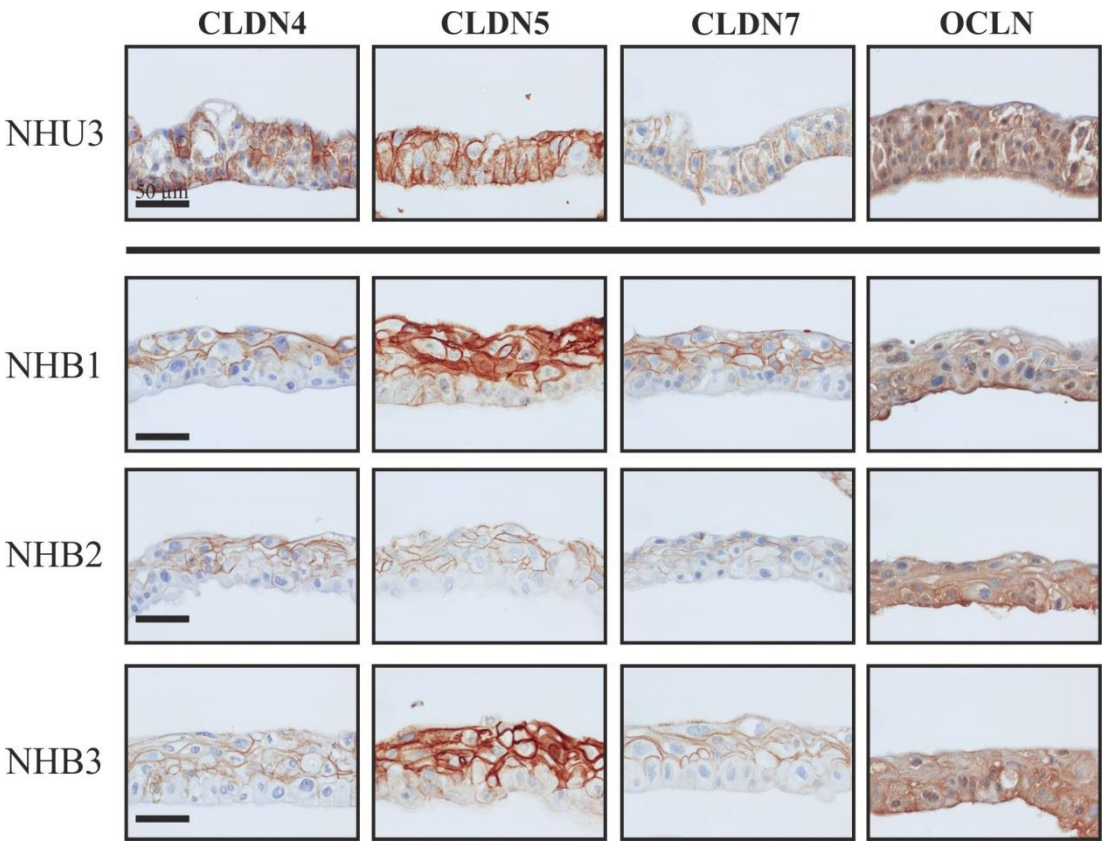

Figure 3.16 Evaluation of Tight Junction Protein Expression in NHB and NHU Cell Sheets Generated Using the ABS/Ca^{2+} Protocol by Immunohistochemistry

The expression of tight junction-associated proteins, CLDN4, CLDN5, CLDN7 and OCLN, was assessed by immunohistochemistry. Cell sheets from a single NHU cell line (NHU3) and three independent NHB cell lines (NHB1, NHB2 and NHB3) are shown. Cell sheets were generated on Snapwell membranes using the ABS/Ca^{2+} protocol for seven days. All images are shown with the apical surface of the epithelial cell sheet at the top. Positive control and example negative control (no primary antibody) images can be found in Appendix 7.4. Note expression of CLDN4, CLDN5 and CLDN7 in only the upper half of the NHB cell sheets, while NHU cell sheets displayed expression of the claudin proteins in all of the cell layers.

3.3.5 Assessment of Squamous Differentiation-Associated Genes

3.3.5.1 Assessment of Stratified Squamous Differentiation-Associated Transcript Expression in NHB Cells and NHU Cells Following use of the TZ/PD Protocol

By RT-PCR analysis, NHB cells from two independent cell lines (NHB3 and NHB4) showed varied results (Figure 3.17). One NHB cell line (NHB3) had negative expression of LOR and SPRR4. The other cell line (NHB4) had weak transcript expression of LOR and SPRR4 at the 3 and 6 day TZ/PD treated time points. TGM1 was expressed at all of the time points assessed in both NHB cell lines, with a possible upregulation of expression at the 3 and 6 day TZ/PD time points. The single NHU cell line, evaluated for comparison, showed weak expression of LOR in the control cells at day 6. Expression of SPRR4 and TGM1 was absent at all of the time points.

The expression of TGM1 was further assessed by RT-qPCR in three independent NHB cell lines (NHB6, NHB7 and NHB8), and demonstrated a significant upregulation in expression as a result of TZ/PD treatment at 72 hours (Figure 3.18). The single NHU cell line (NHU6) assessed for comparison, demonstrated weak expression, which was downregulated as a result of using the TZ/PD protocol.

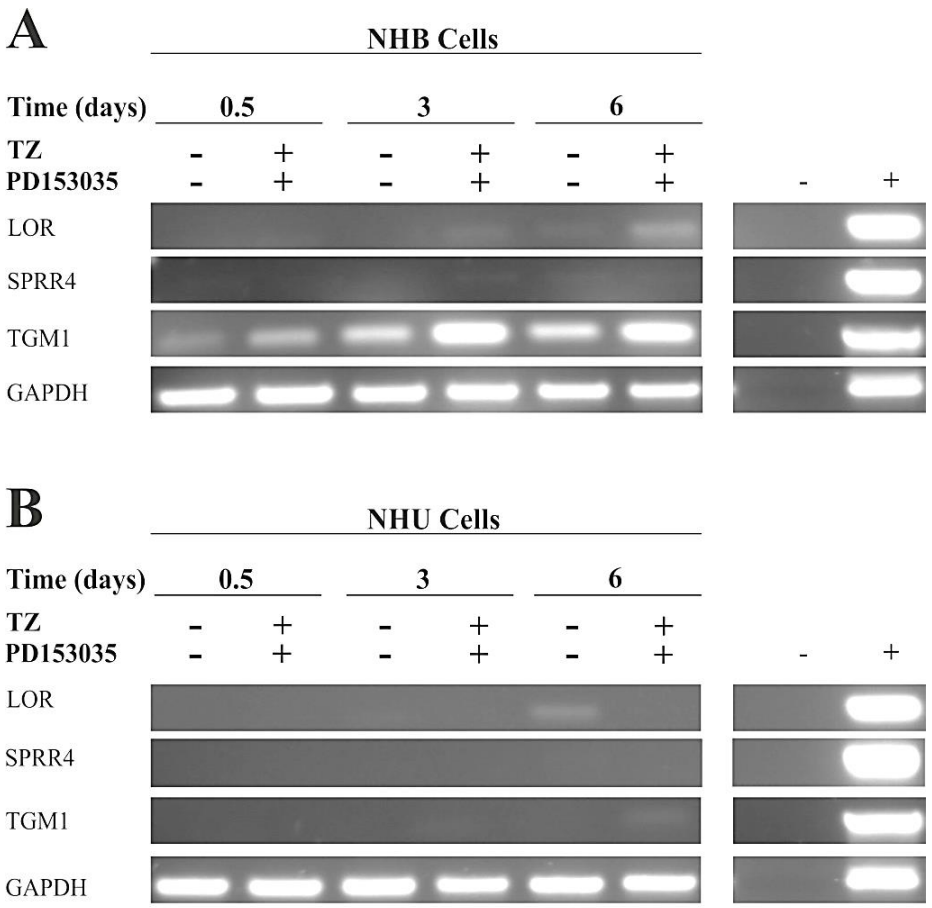

Figure 3.17 Assessment of Stratified Squamous-Associated Gene Expression in NHB Cells and NHU Cells by RT-PCR Following TZ/PD Treatment

Buccal epithelial cells **A)** (NHB3) and urothelial cells **B)** (NHU5) were treated with either 0.1 % DMSO (vehicle control) or TZ/PD for 0.5, 3 or 6 days. The transcript expression of several stratified sqaumous differentiation-associated genes (LOR, SPRR4 and TGM1) is shown by RT-PCR. PCR was performed using either 25 or 30 cycles for a given gene. GAPDH was used as a loading control (25 cycles). H_2O was used as a negative control (-). Genomic DNA was used as the positive control for the PCR (+). A second buccal epithelial cell line (NHB4), was also completed for this experiment and the figure can be found in Appendix 7.4. Note strong expression of TGM1 in NHB cells, and an absence of expression in NHU cells.

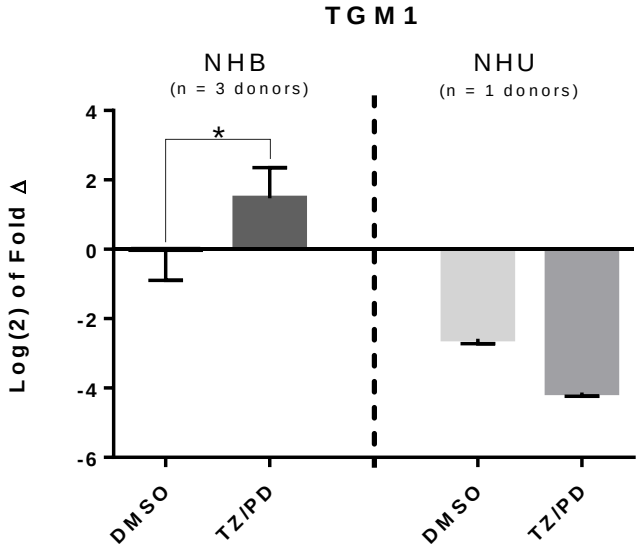

Figure 3.18 RT-qPCR Analysis of TGM1 Gene Expression in NHB Cells Following 72 hour TZ/PD Treatment

RT-qPCR data was generated for TGM1 expression in three independent NHB cell lines (NHB6, NHB7 and NHB8), and a single NHU cell line (NHU6) for comparison. Cultures were treated with either 0.1% DMSO (vehicle control) or TZ/PD for 72 hours. Values are shown relative to the mean of the 0.1% DMSO treated NHB cells for each gene. All values were first normalised to GAPDH. For NHB cells, error bars represent the standard deviation of the mean of the Log(2) fold change of the three independent NHB cell lines (n=3). For NHU cells, error bars represent the standard deviation of three technical replicates (n=1). Statistical analysis was performed using a two-tailed, paired t-test to assess whether there was a significant change in gene expression as a result of TZ/PD. * represents $P \leq 0.05$. Note significantly upregulated expression of TGM1 in NHB cells as a result of TZ/PD treatment. In NHU cells TGM1 expression is weak and downregulated as a result of TZ/PD.

3.3.6 Assessment of Barrier Function During use of the ABS/Ca^{2+} Protocol

Buccal epithelial cells from three independent cell lines (NHB1, NHB2 and NHB3) were unable to form a functional barrier at any time during the seven day ABS/Ca^{2+} differentiation protocol on Snapwell inserts (Figure 3.19). The TER values were maintained below 200 $\Omega \cdot cm^2$ in all three of the cell lines at all of the time points assessed. An NHU cell line (NHU3), used for comparison, displayed characteristic barrier formation, surpassing a TER of 1000 $\Omega \cdot cm^2$ two days after the calcium concentration was increased to 2 mM. This barrier function was maintained throughout the rest of the time course, with a maximum TER achieved on day 7.

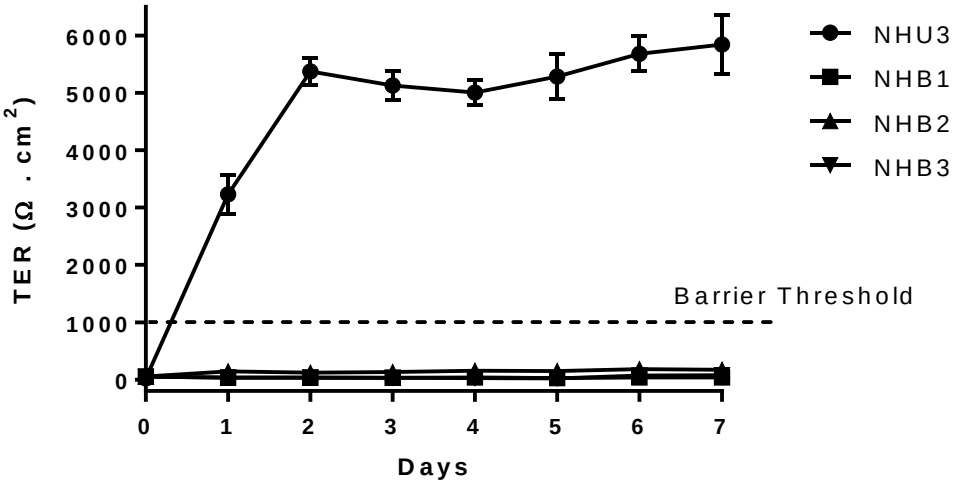

Figure 3.19 Measurement of Barrier Function for NHB Cells and NHU Cells During the ABS/Ca^{2+} Protocol - TER

NHB cells and NHU cells were pre-treated with 5% ABS for 5 days and then passaged and seeded onto Snapwell inserts. The calcium concentration was increased to 2 mM after 24 hours. The TER was measured every day for seven days. Three independent NHB cell lines (NHB1, NHB2, and NHB3) and a single NHU cell line (NHU3) were evaluated. Error bars represent the standard deviation of the mean of n=3 replicates of each cell line. Note NHB cells did not gain barrier function during use of the ABS/Ca^{2+} protocol, something that is reproducibly observed in NHU cells.

3.4 Summary of Results

- NHB cells expressed cytokeratin proteins, CK5, CK7, CK13, CK14, CK18 and CK19 when grown in KSFMc. Expression of CK13 could be upregulated in NHB cells by treatment with either PD or TZ/PD, suggesting that CK13 expression may not be mediated by PPARγ in NHB cells. Use of the ABS/Ca^{2+} protocol maintained expression of the squamous epithelial cell-associated protein, CK14, in NHB cell sheets. In urothelial cells sheets, CK14 expression was absent as a result of ABS/Ca^{2+} differentiation.

- NHB cells had weak to absent expression of the urothelial differentiation-associated transcription factors, ELF3, FOXA1, GATA3, and PPARγ1. This was observed at both the transcript and protein levels, and there was no significant upregulation or increased nuclear localisation as a result of using the TZ/PD protocol. ELF3 was significantly upregulated at the transcript level as a result of TZ/PD in NHB cells. NHB cell sheets generated using the ABS/Ca^{2+} protocol, were absent for GATA3 expression. FOXA1/2 and PPARγ showed weak nuclear expression in the NHB cell sheets.

- NHB cells expressed three of the five uroplakin genes (UPK1A, UPK1B, and UPK2) at low transcript abundance, and their expression was upregulated as a result of TZ/PD. UPK3B expression in NHB cells was comparable to that of NHU cells. Expression of UPK2 and UPK3B was significantly upregulated as a result of using the TZ/PD protocol in NHB cells.

- In NHB cell sheets, expression of the claudin proteins assessed was restricted to only the upper half of the cell sheets. This differed from urothelial cells sheets which expressed CLDN4, -5 and -7 throughout the whole of the cell sheet.

- All-trans retinoic acid treatment of NHB cells caused an upregulation of both FOXA1 transcript and protein expression, but did not obviously affect GATA3 expression, or the expression of the five uroplakin genes.

- *In vitro* maintained NHB cells were unable to form a functional barrier using the ABS/Ca^{2+} protocol, which differed from what is consistently observed with NHU cells.

3.5 Summary Table of Key Differences Between NHB Cells and NHU Cells

Table 3.2 Summary Table of Results Comparing the Expression of Markers Genes Assessed in Chapter 4 Between NHB Cells and NHU Cells *in Vitro*

Protocol	**Makers Assessed**		**NHB Cells**	**NHU Cells**
KSFMc	Cytokeratins	CK7	Some cells	All cells
		CK13	Some cells	Some cells
		CK14	All cells	Some cells
		CK20	Absent	Absent
	Transcription Factors	ELF3	Weak/Absent	Weak
		FOXA1	Weak/Absent	Weak
		GATA3	Weak/Absent	Weak
		PPARγ	Weak/Absent	Weak
TZ/PD	Transcription Factors	ELF3	Weak	Strong
		FOXA1	Weak	Strong
		GATA3	Weak/Absent	Strong
		PPARγ	Weak/Absent	Strong
	Uroplakin Genes	UPK1A	Weak	Strong
		UPK1B	Weak	Strong
		UPK2	Weak	Strong
		UPK3A	Absent	Strong
		UPK3B	Strong	Strong
atRA/PD	Transcription Factors	FOXA1	Weak	Not assessed
		GATA3	Weak/Absent	Not assessed
ABS/Ca^{2+}	Transcription Factors	GATA3	Weak/Absent	Strong Nuclear
		FOXA1	Weak Nuclear	Strong Nuclear
		PPARγ	Weak Nuclear	Strong Nuclear
	Tight Junction Proteins	CLDN4	Upper half of sheet	All layers of sheet
		CLDN5	Upper half of sheet	All layers of sheet
		CLDN7	Upper half of sheet	All layers of sheet
	Cytokeratins	CK7	Weak/Absent	All layers of sheet
		CK14	All layers of sheet	Absent
	Barrier Function	TER	No: $< 200\ \Omega \cdot cm^2$	Yes: $> 1000\ \Omega \cdot cm^2$

Chapter 4:
Expression of PPARγ and GATA3 in Urothelial Cell Differentiation

4 Expression of PPARγ and GATA3 in Urothelial Cell Differentiation

4.1 Background

4.1.1 PPARγ Expression in Urothelial Cells

PPARγ has been identified as a key regulator of normal human urothelial cell differentiation, although the specific PPARγ isoform which most contributes to the differentiation has yet to be elucidated. Of the few reports of PPARγ protein expression in urothelial cells grown *in vitro,* none have identified which of the two isoforms is involved. Two groups have demonstrated the expression of PPARγ in NHU cells grown in KSFMc by western blotting (Kawakami et al., 2002; Varley et al., 2004a); both groups used the E-8 antibody clone produced by Santa Cruz Biotechnology Inc., and demonstrated the expression of a single PPARγ band. Georgopolous et al. later demonstrated the expression of three E-8 reactive bands by western blotting, in NHU cells which had been transduced to overexpress human telomerase reverse transcriptase (hTERT). The authors also showed that there were changes in the expression of the three bands following PPARγ activation using the TZ/PD protocol (Georgopoulos et al., 2011). The corresponding molecular weight of the protein bands observed was not reported in any of the three papers described above, making it difficult to infer which of the PPARγ isoforms was being recognised.

More recently, Strand et al. investigated the expression of PPARγ in human prostate epithelial cells. The authors demonstrated that the prostate epithelial cells expressed both the PPARγ1 and PPARγ2 isoforms by western blotting, and showed that when PPARγ2 was knocked down using shRNA, the cells upregulated the expression of CK20, a urothelial superficial cell-associated marker (Strand et al., 2013). This work suggested that it was the expression of PPARγ1, and not PPARγ2 which was important for urothelial-type differentiation, although the work was completed using prostate epithelial cells.

Another important aspect of PPARγ expression in urothelial cells *in vitro* is defining the localisation of the protein in the cells, which has only minimally been investigated (Varley et al., 2004a; Varley et al., 2004b). Varley et al. demonstrated that at low density, when NHU cells were grown in KSFMc, they displayed primarily cytoplasmic PPARγ expression. This was also shown to be the case when cells were treated with the PPARγ agonist, troglitazone (TZ). The localisation of PPARγ changed when the cells were treated with PD153035 (PD), where the expression became nuclear. When the cells were treated with both TZ and PD, PPARγ expression was also nuclear. The E-8 antibody from Santa Cruz Biotechnology Inc. was used for the immunofluorescence in this instance. This work suggested that when the proliferative phenotype of NHU cells was blocked, by using an EGFR tyrosine kinase inhibitor, PPARγ translocates to the nucleus. The authors further showed that use of PD153035 resulted in a reduction of phosphorylated PPARγ, and suggested that dephosphorylation of PPARγ was associated with its subsequent translocation to the nucleus (Varley et al., 2004a).

4.1.2 Role and Expression of GATA3 in Urothelial Cells

The transcription factor, GATA3, has been identified as an important diagnostic and prognostic marker of bladder cancer (Miyamoto et al., 2012), but its role in normal healthy human urothelial cells has not yet been investigated. Other potentially related transcription factors like PPARγ, FOXA1 and ELF3, have been shown to have key roles in both bladder cancer (Biton et al., 2014; Cancer Genome Atlas Research, 2014; Eriksson et al., 2015), as well as important roles in the differentiation of normal human urothelial cells (Varley et al., 2004a; Varley et al., 2009; Böck et al., 2014). Questions have arisen as to whether GATA3 may also hold a regulatory role in the differentiation of normal urothelial cells given that it has been shown to be expressed in urothelial cells (Böck et al., 2014; Li et al., 2014b), and its noted role in bladder cancer.

4.2 Aim

Based on the results presented in Chapter 3, were GATA3 and PPARγ expression was shown to be weak/absent in NHB cells in comparison to NHU cells, the aim of this chapter was to:

- Investigate the expression and role of the transcription factors, PPARγ and GATA3, in normal human urothelial cell identity and differentiation.

4.3 Experimental Objectives

The objectives of this chapter were to:

- Assess GATA3 transcript expression following PPARγ activation using the TZ/PD protocol.
- Examine the expression of the PPARγ1 and PPARγ2 transcript variants in urothelial cells.
- Determine which of the two PPARγ protein isoforms is important for normal human urothelial cell differentiation.
- Examine the protein expression of GATA3, PPARγ, FOXA1 and ELF3 in urothelial cells following PPARγ activation by using the TZ/PD protocol.
- Investigate the effect of GATA3 knockdown on the expression of urothelial differentiation-associated genes.

4.4 Experimental Approach

4.4.1 PPARγ Transcript Variants and Protein Isoforms

Gene expression of PPARγ was evaluated by RT-PCR in NHU cells to assess which of the PPARγ transcript variants was expressed. PCR was performed using two sets of primers, which used the same reverse primer (Table 4.1). Since all four of the main PPARγ transcript variants contain exons 1-6 (Figure 4.1), 'total PPARγ' gene expression was evaluated using a forward PCR primer designed to a sequence in exon 1, and reverse PCR primer designed to a sequence in exon 6. The full length PCR product size generated using the exon 1 and exon 6 primers was 1209 bp. To evaluate PPARγ2-specific expression, a forward PCR primer was designed to a sequence in exon B, and the same reverse primer as above, designed to a sequence in exon 6, was used; exon B is specific to the PPARγ2 protein coding transcript variant. The full length PCR product size generated using the exon B and exon 6 primers was 1288 bp.

NHU cells used for this experiment were grown and differentiated by Mrs. Ros Duke, a research technician at the Jack Birch Unit. The subsequent RNA extraction, cDNA synthesis, and PCR was performed by Dr. Joanna Pearson, who is also a research technician at the Jack Birch Unit.

Table 4.1 PPARG-Specific Primer Sequences

Target	Forward Primer (5'-3')	Reverse Primer (5'-3')
Total PPARG	ACTTTGGGATCAGCTCCGTG	GGGCTTGTAGCAGGTTGTCT
PPARG2	TCCTTCACTGATACACTGTCTGC	GGGCTTGTAGCAGGTTGTCT

The forward 'total PPARG' primer is designed to sequence in exon 1. The forward PPARG2 primer is designed to a sequence in exon B. Both primer sets have the same reverse primer which is designed to a sequence in exon 6.

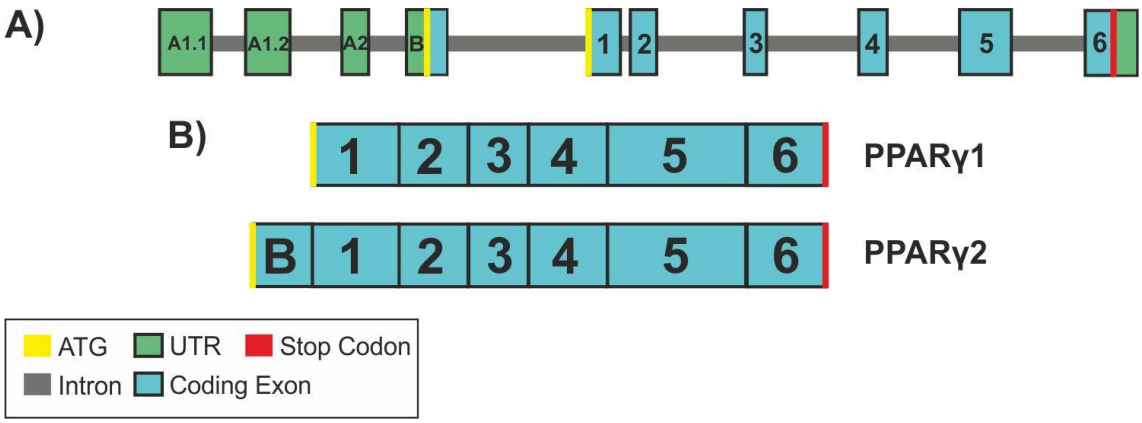

Figure 4.1 PPARγ Gene Structure and Main Protein Isoforms

A) The most recent description of the human PPARG gene structure defines ten exons: A1.1, A1.2, A2, B and 1-6 (Aprile et al., 2014). Alternative splicing of these exons results in the production of four main protein coding transcript variants, which are used to produce the PPARγ1 and PPARγ2 proteins.

B) The PPARγ1 protein is produced from the translation of exons 1-6. The PPARγ2 protein is produced from the translation of a portion of exon B plus exons 1-6, which results in the human PPARγ2 protein having the same amino acid sequence as PPARγ1, with an additional 28 amino acids at the N terminus (Fajas et al., 1997).

This figure is adapted from (Aprile et al., 2014).

To investigate which of the two PPARγ protein isoforms was expressed in NHU cells, whole protein lysates were generated from NHU cells following growth in KSFMc, and following use of the TZ/PD and ABS/Ca^{2+} protocols. Protein expression was assessed by western blotting using the 'total PPARγ' antibodies E-8 (Santa Cruz), 81B8 (Cell Signaling), D69 (Cell Signaling), and the PPARγ2-specific antibody, N-19 (Santa Cruz).

4.4.2 Peroxisome Proliferator-Activated Receptor Gamma (PPARγ) Activation and Inhibition

The TZ/PD protocol was used throughout this chapter as a means of activating PPARγ in NHU cells. Use of the TZ/PD protocol with NHU cells has been previously shown to cause upregulation of the transcription factors, ELF3, FOXA1 and IRF1 (Varley et al., 2009; Böck et al., 2014), as well as upregulation of urothelial differentiation-associated genes like CK20, the uroplakins, and several claudins (Varley et al., 2004a; Varley et al., 2006). In all of the cases, the upregulation was demonstrated to be specifically as a result of PPARγ activation by use of the PPARγ-specific antagonists, GW9662 or T0070907, which abrogated the upregulation.

To determine whether PPARγ activation had any effect on GATA3 or PPARγ gene expression, NHU cells were subjected to the TZ/PD protocol. In one set of experiments, the protein expression of transcription factors, PPARγ, GATA3, FOXA1 and ELF3 was evaluated in NHU cells treated with TZ/PD for 12, 24, 48, 72 or 166 hours. All cultures, including controls, contained 0.1 % DMSO as the vehicle. Protein expression was investigated by western blotting and immunofluorescence. FOXA1 and ELF3 were investigated due to their known upregulation as a result of PPARγ activation in NHU cells, as verification of successful use of the TZ/PD protocol. The expression of the nuclear receptor, RXRα, was also investigated by western blotting due to its known role as a dimerization partner required for PPARγ function. To demonstrate successful transitional-type differentiation of the NHU cells using TZ/PD, CK13 expression was assessed in immunoblotting experiments, and CK20 expression was assessed in immunofluorescence experiments.

To investigate whether gene upregulation caused in response to TZ/PD was specifically as a result of PPARγ activation, NHU cells (Y1153) were pretreated with 1 μM of the non-competitive PPARγ antagonist, T0070907 (IC_{50} = 1 nM) (Cambridge Bioscience, CAY10026), for 3 hours prior to the start of the TZ/PD protocol. The use of the inhibitor prior to TZ/PD treatment was based on previously published work (Varley et al., 2006). Total RNA was isolated following subsequent use of the TZ/PD protocol for 6, 24, 48 and 72 hours. Control cells were treated with 0.1 % DMSO (vehicle control). Cell culture, cell treatment, and RNA extraction for this experiment was carried out by

Tom Wahlicht as part of an undergraduate research project at the Jack Birch Unit. The RNA generated from this experiment was used to produce cDNA, and perform the subsequent PCR shown in this chapter.

4.4.3 Urothelial Carcinoma-Derived Cell Lines

The expression of PPARγ was investigated in various human bladder carcinoma-derived cell lines by western blotting. The protein lysates used to generate the western blot were originally produced by either Shu Guo (MPhil student in the Jack Birch Unit) or Ros Duke (research technician at the Jack Birch Unit). All cell lines were previously genotyped and mycoplasma tested upon arrival to the Jack Birch Unit. A list of the cell lines investigated with relevant information pertaining to their derivation and culture conditions can be found below in Table 4.2:

Table 4.2 Bladder Carcinoma-Derived Cell Lines

Cell Line	Derivation	Growth Medium (% Serum)
5637	Grade II carcinoma	RPMI (5% FBS) (Standard) or KSFM (Adapted)*
UMUC9	Grade III carcinoma	DMEM (10% FBS)
RT4	Grade I carcinoma	DMEM:RPMI (50:50) (5% FBS)
EJ	Grade III carcinoma	DMEM:RPMI (50:50) (5% FBS)
RT112	Grade II carcinoma	DMEM:RPMI (50:50) (5% FBS)

* The standard growth medium for 5637 cells is Roswell Park Memorial Institute (RPMI) medium - 1640 with 5% FBS. The cells were adapted for growth in KSFM with no serum by Shu Guo as part of her MPhil project.

4.4.4 Proteasome Inhibition

MG132 (Sigma, C2211) is a potent proteasome inhibitor. Previous work in adipocyte-cells (murine fibroblasts differentiated to adipocytes) revealed that treatment of the cells with MG132 resulted in an upregulation of PPARγ protein expression, suggesting that PPARγ was being degraded by the proteasome (Hauser et al., 2000).

The use of MG132 was employed to investigate whether PPARγ protein was being degraded by the proteasome in NHU cells. PPARγ activation was induced in NHU cells by using the TZ/PD protocol for 72 hours. Control cells were treated with 0.1 % DMSO (vehicle control). The medium was then changed, and the cells were either treated with 0.1 % DMSO (vehicle control) or 12.5 μM MG132 for 6 hours. The concentration of MG132 used was based on previously published work in NHU cells (Varley et al., 2006).

4.4.5 GATA3 Knockdown Using siRNA

Transfection of NHU cells with GATA3 siRNA was used to investigate the effect of GATA3 knockdown on the expression of urothelium-associated transcription factors and differentiation-associated genes.

GATA3 siRNA was titrated before use to determine an optimal concentration which provided knockdown of GATA3 expression, with minimal associated cell death. NHU cells (Y1752) were transfected with either 50 nM or 100 nM of each of the GATA3 siRNAs, and then PPARγ was activated using the TZ/PD protocol for 48 hours to induce differentiation-associated genes. Control cells were treated with the transfection reagent only, followed by use of the TZ/PD protocol for 48 hours.

Using the optimal siRNA concentration determined, two independent NHU cell lines, (Y1356 and Y938) were transfected with either CTRL-siRNA1, CTRL-siRNA2, GATA3-siRNA1 or GATA3-siRNA2 for 4 hours, and then PPARγ was activated using the TZ/PD protocol for 48 hours. A third NHU cell line (Y1815) was transfected with either CTRL-siRNA1, GATA3-siRNA1 or GATA3-siRNA2, and the protocol was followed as above.

4.5 Results

4.5.1 GATA3 Transcript Expression in NHU Cells Following PPARγ Activation and Inhibition

GATA3 transcript expression could be shown in NHU cells (Y1153) by RT-PCR (Figure 4.2). Treatment of the cells with TZ/PD upregulated GATA3 expression after 48 and 72 hours. Use of the PPARγ antagonist, T0070907, abrogated the upregulation caused by TZ/PD.

Using RT-qPCR, some of the results obtained using RT-PCR were confirmed. GATA3 transcript expression was upregulated upon treatment of NHU cells (Y1281) with TZ/PD at the 12, 24 and 48 hour time points, in comparison to control cells (Figure 4.3 A). GATA3 expression also increased in control cells as time progressed. FOXA1 expression was evaluated as a control for comparison, due to its known upregulation in NHU cells in response to TZ/PD (Figure 4.3).

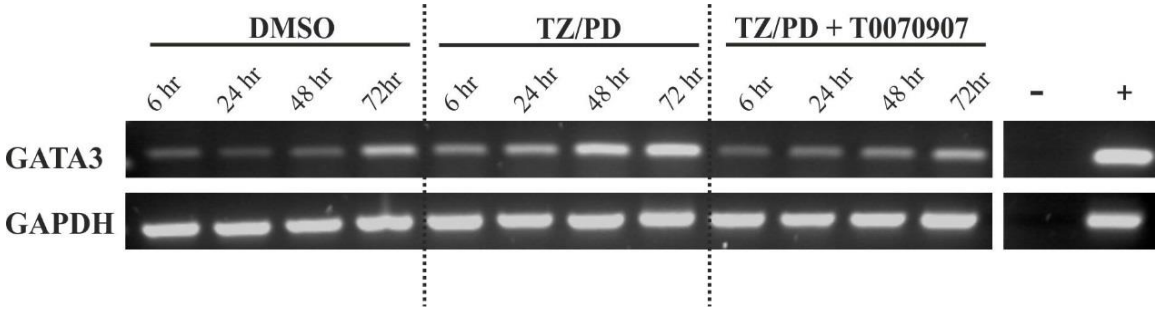

Figure 4.2. Evaluation of GATA3 Transcript Expression by RT-PCR in Urothelial Cells Following PPARγ Activation and Inhibition

NHU cells (Y1153) were treated with either the vehicle control (0.1 % DMSO), TZ/PD or 1 μM T0070907 plus TZ/PD for either 6, 24, 48 or 72 hours. Total RNA was extracted and cDNA produced. GATA3 expression was assessed by PCR (27 cycles). GAPDH was used as a loading control (25 cycles). H_2O (no template) was used as a negative control (-). Genomic DNA was used as the positive control for the PCR (+). Note upregulation of GATA3 transcript expression as a result of TZ/PD at 48 and 72 hours. Treatment with the PPARγ antagonist, T0070907, appears to abrogate this upregulation.

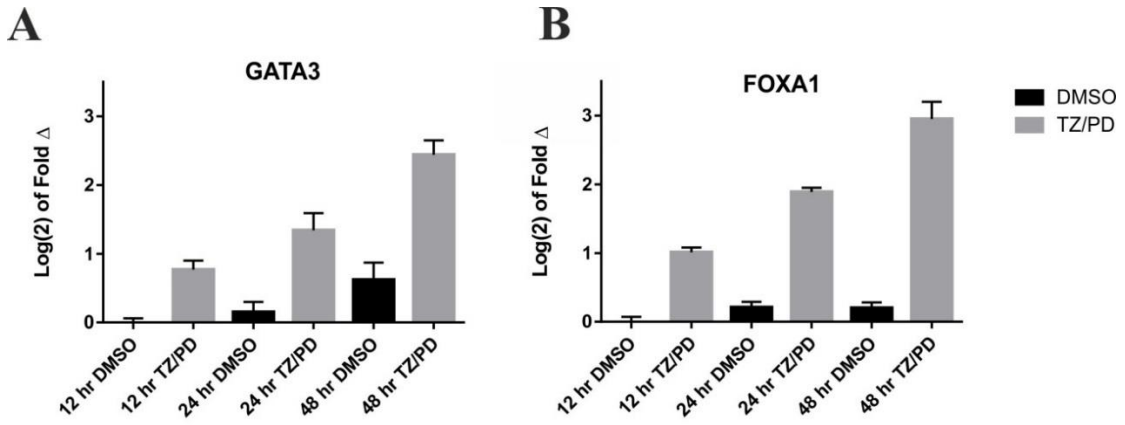

Figure 4.3. RT-qPCR analysis of GATA3 and FOXA1 Transcript Expression in NHU Cells Following PPARγ Activation using the TZ/PD Protocol

NHU cells (Y1281) were treated with either 0.1% DMSO (vehicle control) or TZ/PD for 12, 24 or 48 hours. Total RNA was extracted and cDNA produced. The expression of **A)** GATA3 and **B)** FOXA1 was evaluated by qPCR. All values were normalised to GAPDH expression, and are shown relative to the 12 hour DMSO time point. Error bars represent the standard deviation of the three technical replicates. Note upregulation of GATA3 transcript expression as a result of TZ/PD treatment at all time points assessed in NHU cells.

4.5.2 PPARγ Transcript Expression in NHU Cells

The expression of PPARγ transcript in NHU cells was assessed by RT-PCR. In three independent NHU cell lines (Y1361, Y1393 and Y1289) PPARγ expression was observed in both control cells (0.1 % DMSO), and in cells where PPARγ had been activated using the TZ/PD protocol. Using the 'total PPARγ' primers (primers designed to sequences in exon 1 and exon 6) a large band corresponding to the full length PCR product could be observed at approximately 1200 bp in all of the samples (Figure 4.4). A number of smaller PCR products were also produced using these primers, which could possibly correspond to alternate splice variants that are missing internal exons. PPARγ expression could also be shown in UMUC9 cells, which acted as a positive control due to their known PPARγ expression.

The expression of PPARγ2 was also evaluated in NHU cells at the transcript level by RT-PCR using the PPARγ2-specific primers (primers designed to sequences in exon B and exon 6) (Figure 4.5 A). PPARγ2 expression was weak/absent in the single NHU cell line (Y939) assessed, under all conditions (0.1 % DMSO, TZ/PD and ABS/Ca^{2+}). PPARγ2 expression was also evaluated in UMUC9 cells, and an obvious PCR product was observed. The expression of UPK2 was evaluated for this experiment to demonstrate successful differentiation of the NHU cells using both the TZ/PD and ABS/Ca^{2+} protocols; a clear upregulation of UPK2 expression could be observed using both protocols (Figure 4.5 B).

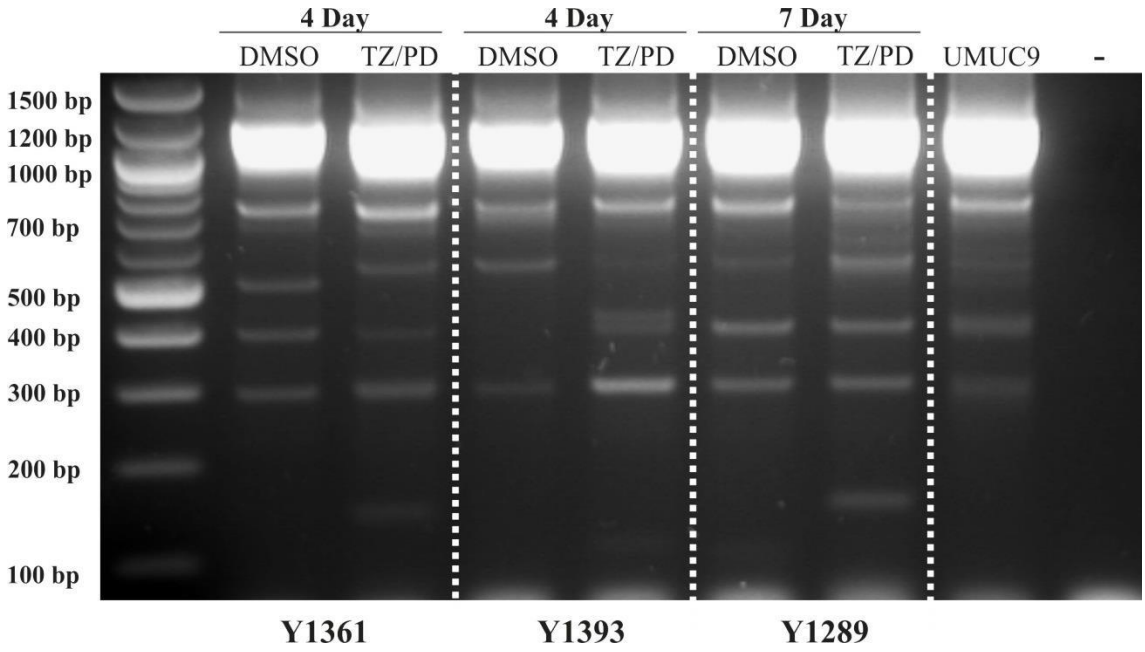

Figure 4.4 Analysis of PPARγ Transcript Expression by RT-PCR in Three Independent NHU Cell Lines Following PPARγ Activation Using the TZ/PD Protocol

Three independent NHU cell lines (Y1361, Y1393, Y1289) were treated with either the vehicle control (0.1% DMSO), or TZ/PD for either 4 or 7 Days. Total RNA was extracted and cDNA produced. Total PPARγ (forward primer in exon 1 and reverse primer in exon 6) expression was assessed by PCR (35 cycles). H_2O (no template) was used as a negative control (-). Expression of PPARγ in UMUC9 cells, was used as a positive control (+). The full length PCR product size produced using these primers should be 1209 bp. Note the clear full length PPARγ PCR product in all samples except for the negative control (-). Possible alternate PPARγ splice variants, missing internal exons, were also observed as distinct smaller PCR products.

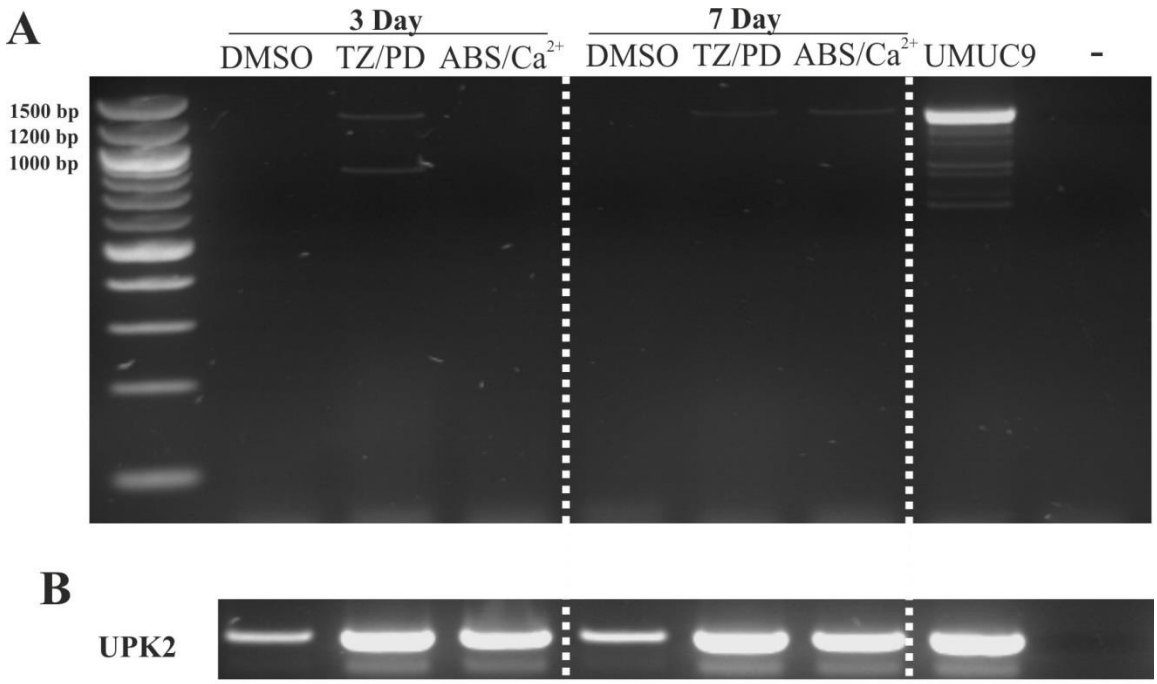

Figure 4.5 Analysis of PPARγ2 Transcript Expression in NHU Cells by RT-PCR

NHU cells (Y939) were treated with either the vehicle control (0.1% DMSO), or TZ/PD, or ABS/Ca^{2+} for 3 or 7 Days. Total RNA was extracted and cDNA produced.

A) PPARγ2 (forward primer in exon B and reverse primer in exon 6) expression was assessed by RT-PCR (35 cycles).

B) UPK2 expression was evaluated to demonstrate differentiation of the cells.

H_2O (no template) was used as a negative control (-). cDNA generated from the total RNA of UMUC9 cells, was used as a positive control (+). The full length PCR product size produced using these primers should be 1288 bp. Note the absence of PPARγ2 PCR product in all NHU samples.

4.5.3 PPARγ Protein Expression in NHU Cells Evaluated Using Different PPARγ Antibodies

PPARγ protein expression was assessed in NHU cells using the four different PPARγ antibodies (antibodies outlined in detail in the Appendix) (E-8, 81B8, D69 and N-19) (Figure 4.6). Using the three 'total PPARγ' antibodies (E-8, 81B8 and D69), PPARγ1 expression was shown to be weak/absent in the control cells (0.1% DMSO). When PPARγ was activated using the TZ/PD protocol, a band corresponding to PPARγ1 expression (approximately 52 kDa) was observed. NHU cells treated with the ABS/Ca^{2+} protocol for 12 days also displayed PPARγ1 protein expression.

As was observed with the MCF-7 cells (see Appendix), use of the E-8 antibody identified a number of additional protein bands, including a band directly below the PPARγ1-associated band (Figure 4.6 A). In NHU cells, a band corresponding to the approximate size of the PPARγ2 protein (57 kDa) was also observed using the E-8 antibody, but was not observed using either the 81B8 or D69 antibodies.

The PPARγ2-specific antibody (N-19) was used to determine if PPARγ2 protein was expressed in NHU cells (Y1390 and Y1230) (Figure 4.6 D). No band corresponding to PPARγ2 could be observed in any of the NHU cell samples, although a number of additional bands were observed in the ABS/Ca^{2+} differentiated cells, including a doublet of bands at approximately (52-54 kDa). These bands were not observed using any of the 'total PPARγ' antibodies, and are therefore unlikely to be associated with PPARγ2 protein.

PPARγ2 protein expression was further examined in another NHU cell line (Y1691), following PPARγ activation using the TZ/PD protocol for 72 or 144 hours (Figure 4.7). No obvious PPARγ2 protein expression could be observed in the control or TZ/PD treated cells at either of the time points assessed.

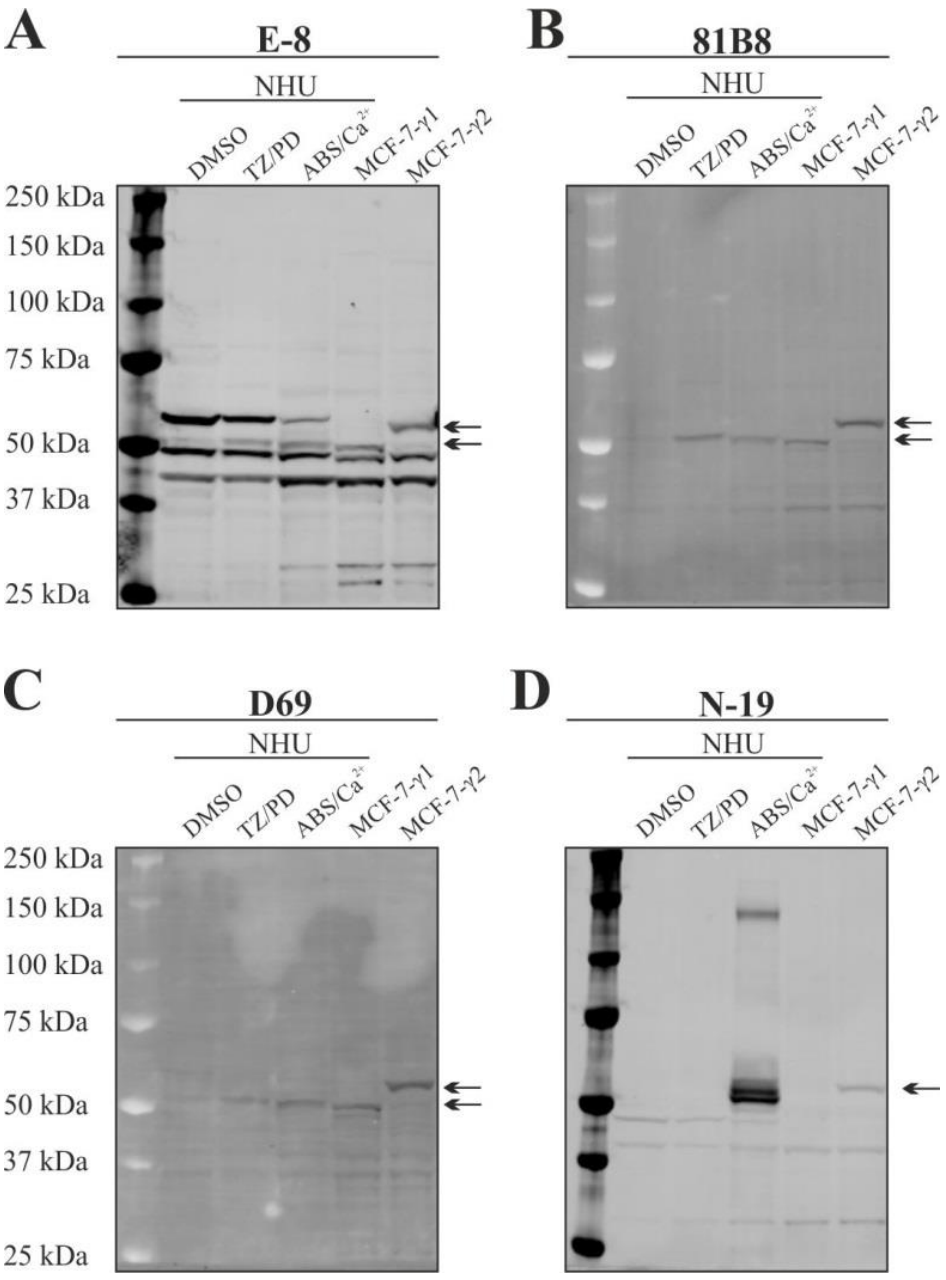

Figure 4.6 Assessment of PPARγ Protein Expression in NHU Cells Evaluated Using Several Different PPARγ Antibodies by Western Blotting

NHU cells (Y1390) were treated with either 0.1% DMSO or TZ/PD for 72 hours. A further NHU cell line, Y1230, was differentiated using ABS/Ca^{2+} for 12 days. Total PPARγ expression was assessed, by western blotting, using the **(A)** E-8 (Santa Cruz), **(B)** 81B8 (Cell Signaling), and **(C)** D69 (Cell Signaling) antibodies. PPARγ2 expression was assessed using the **(D)** N-19 (Santa Cruz) antibody. MCF-7 cells overexpressing either PPARγ1 or PPARγ2 were included as positive controls. 25 μg of protein was loaded into each well. Arrows indicate the positions of the PPARγ1 and PPARγ2 bands. Note clear PPARγ1 protein expression in the TZ/PD and ABS/Ca^{2+} samples using the E-8, 81B8 and D69 antibodies.

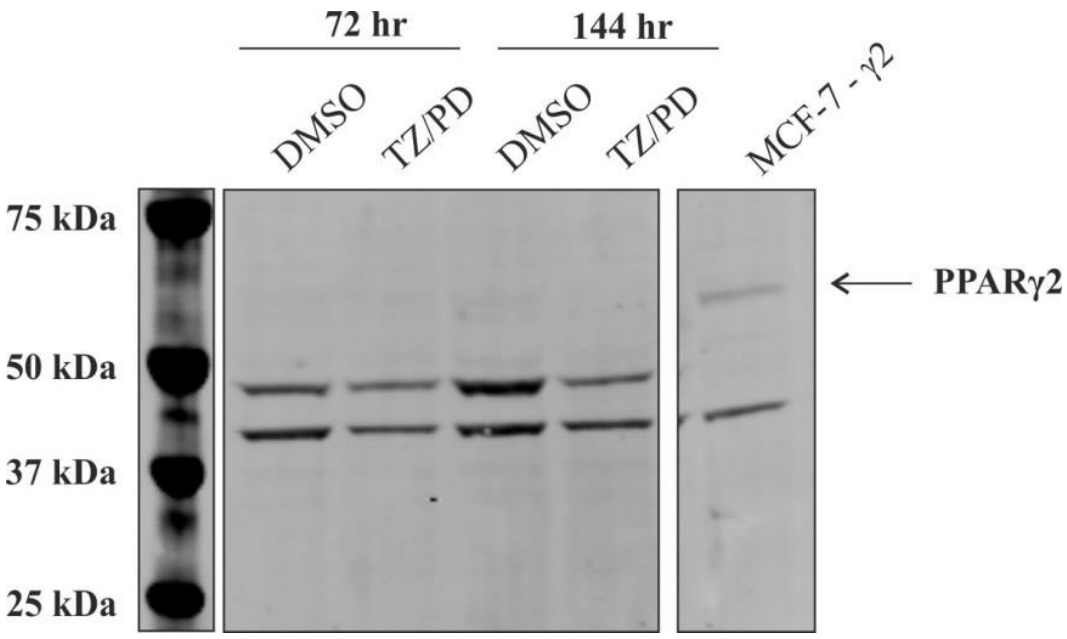

Figure 4.7 Examination of PPARγ2 Expression by Western Blotting in NHU Cells Following PPARγ Activation using the TZ/PD Protocol

NHU cells (Y1691) were treated with either 0.1% DMSO or TZ/PD for 72 and 144 hours. PPARγ2 expression was assessed by western blotting using the N-19 (Santa Cruz) antibody. MCF-7 cells overexpressing PPARγ2 were included as positive control. 20 μg of protein was loaded into each well. Note absent PPARγ2 expression in the NHU cells.

4.5.4 Expression of ELF3, FOXA1, GATA3 and PPARγ in NHU Cells Following PPARγ Activation using the TZ/PD Protocol

The expression of PPARγ and GATA3 was evaluated in NHU cells following PPARγ activation (by use of the TZ/PD protocol) for 24, 48, 72 and 144 hours. Transcription factors, ELF3 and FOXA1, were also evaluated as controls due to their known role downstream of PPARγ in urothelial cell differentiation. CK13 expression was evaluated as an internal control to demonstrate successful induction of differentiation using TZ/PD. CK13 expression became noticeably upregulated starting at the 48 hour TZ/PD time point.

By western blotting, NHU cells from two independent cell lines (Y1642 and Y1677) displayed considerable upregulation of ELF3 and FOXA1 expression as a result of PPARγ activation, as would be expected (Figure 4.8). PPARγ1 was weakly expressed at all of the time points assessed, but became upregulated starting at the 48 hour TZ/PD time point. GATA3 expression was very weak at all of the time points, although there was an obvious upregulation following 72 and 144 hours of TZ/PD treatment. RXRα expression was also evaluated, and was expressed at all of the time points in both control and treated cells.

By indirect immunofluorescence, NHU cells from three independent cell lines (Y1642, Y1677, and Y1541) displayed nuclear expression of ELF3 which appeared upregulated as a result of PPARγ activation at all of the time points assessed (Figure 4.9 A). FOXA1/2 expression was clearly nuclear in both control and TZ/PD treated cells, but a noticeable upregulation was observed as a result of PPARγ activation (Figure 4.9 B). GATA3 expression was nuclear in all cases, with a clear upregulation in control cells at the 144 hour time point (Figure 4.9 C). GATA3 expression also appeared upregulated as a result of PPARγ activation at all of the time points assessed. PPARγ expression was nuclear in control and TZ/PD treated cells (Figure 4.9 D). A clear upregulation of expression could be observed starting at the 48 hour TZ/PD time point.

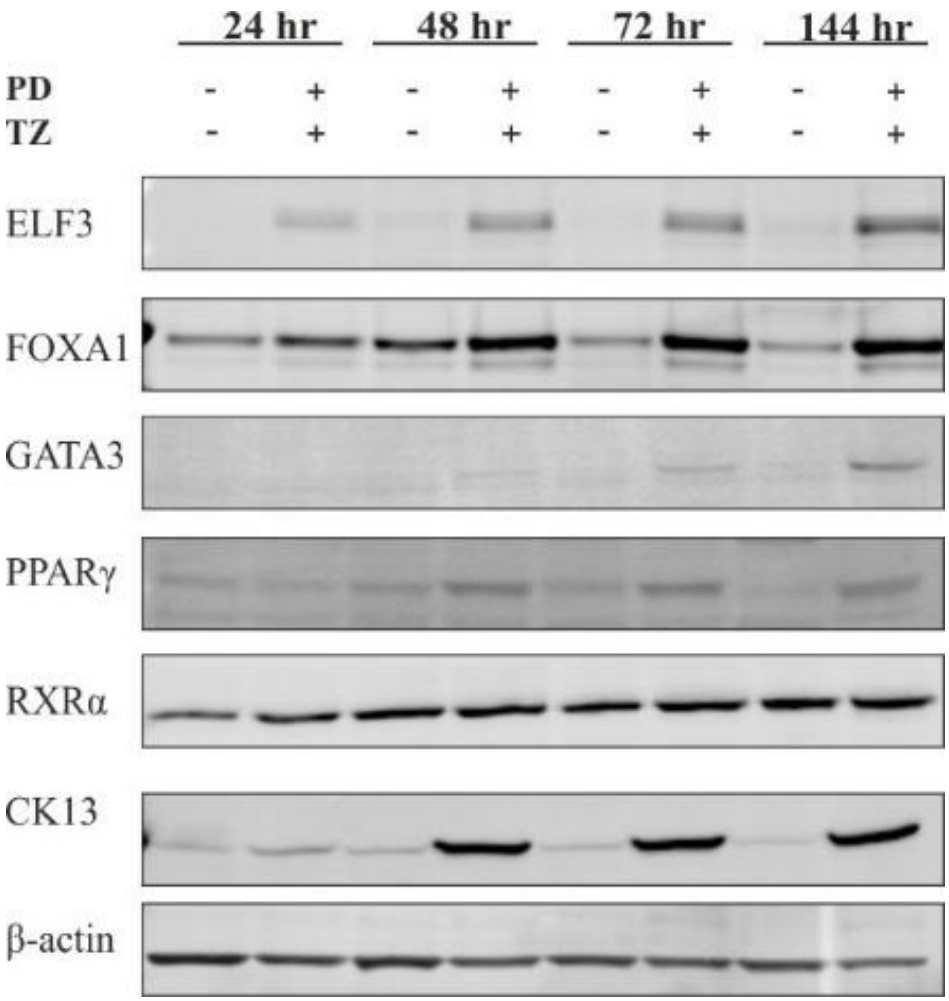

Figure 4.8. Evaluation of Transcription Factor, and Other Urothelial Cell-Associated Protein Expression by Western Blotting in NHU Cells Following PPARγ Activation

NHU cells (Y1677) were treated with either 0.1% DMSO (vehicle control) or TZ/PD for 24, 48, 72 or 144 hours. ELF3, FOXA1 (Santa Cruz, Q-6), GATA3, PPARγ (Cell Signaling, D69), and RXRα protein expression was assessed by western blotting. For PPARγ expression, the band corresponding to PPARγ1 (approximately 52 kDa) is shown. β-actin was used as a loading control. CK13 expression was evaluated to demonstrate induction of transitional-type differentiation. An additional NHU cell line (Y1642) was also evaluated for this experiment, and its figure can be found in Appendix 7.6. 25 μg of protein was loaded into each well. Note the clear upregulation of ELF3, FOXA1, GATA3 and PPARγ expression following use of the TZ/PD protocol.

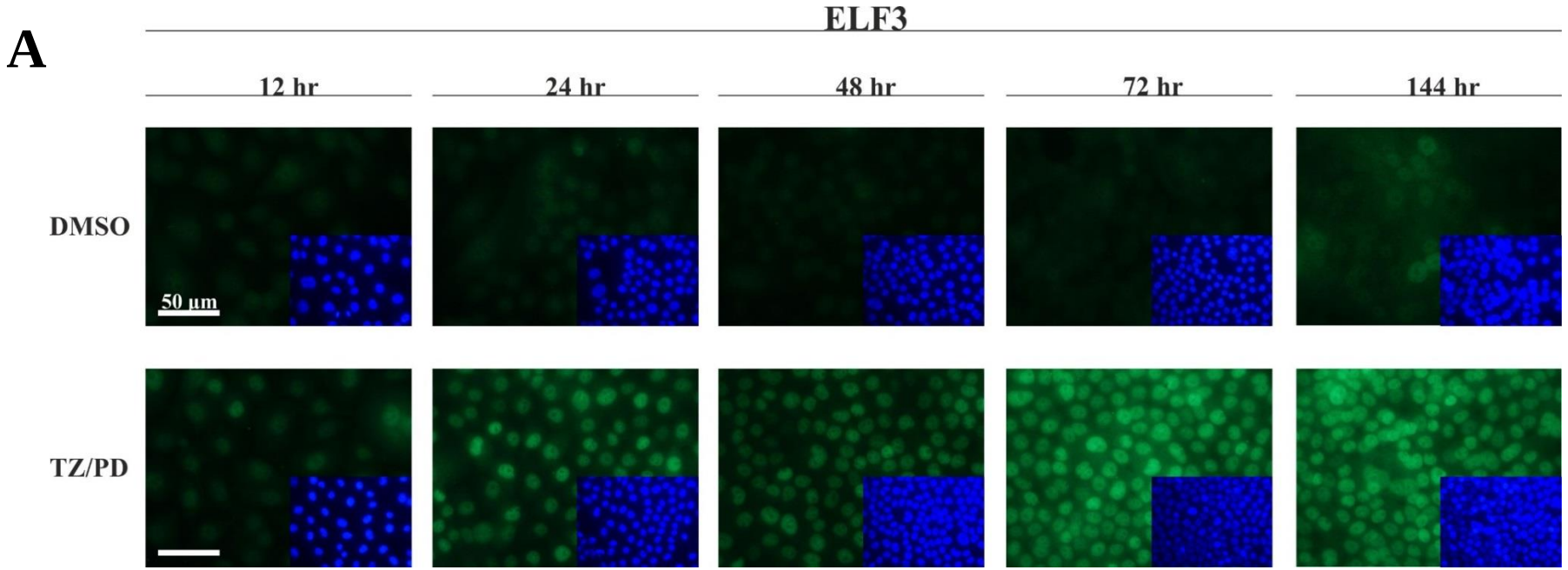

Figure 4.9. Evaluation of Transcription Factor Protein Expression in NHU Cells Following PPARγ Activation using the TZ/PD Protocol for 12, 24, 48, 72 and 144 hours by Indirect Immunofluorescence Microscopy – A) ELF3

NHU cells (Y1677) were treated with either 0.1% DMSO (vehicle control) or TZ/PD for 12, 24, 48, 72 and 144 hours. Immunofluorescence labelling for **(A)** ELF3, **(B)** FOXA1/2 (Santa Cruz, C-20), **(C)** GATA3 and **(D)** PPARγ (Cell Signaling, D69) was performed on formalin-fixed slides which had been permeabilised with Triton X-100. Inset images represent the corresponding Hoechst 33258 staining to demonstrate cell density and nuclei location. All antibody labelled images were taken at the same exposure to enable for comparison of expression between the untreated and treated cells, and between the different time points. Hoechst 33258 images were taken at optimal exposures. Two additional NHU cell lines (Y1642 and Y1541) were evaluated for the purpose of this experiment, and their figures can be found in Appendix 7.6. CK20 expression was assessed to demonstrate successful TZ/PD differentiation at the 144 hour time point; an example of this can be found in Appendix 7.6.

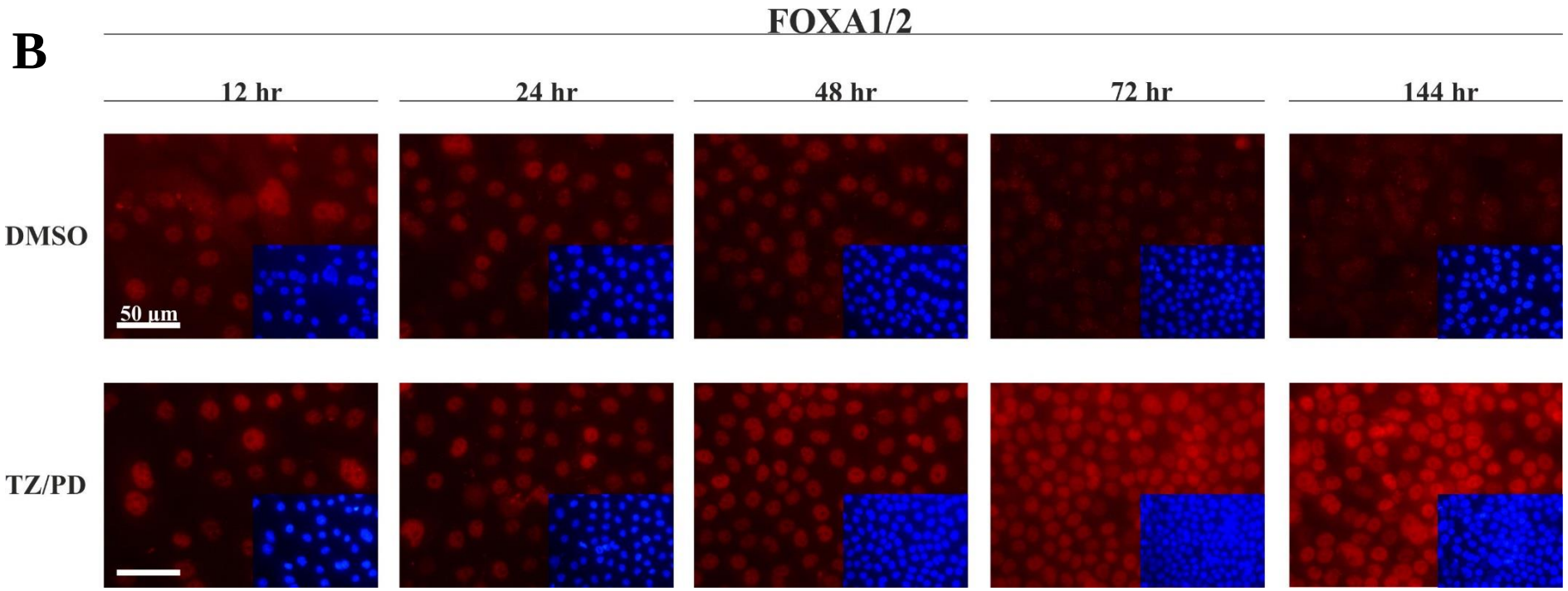

Figure 4.9. Evaluation of Transcription Factor Protein Expression in NHU Cells Following PPARγ Activation using the TZ/PD Protocol for 12, 24, 48, 72 and 144 hours by Indirect Immunofluorescence Microscopy – A) FOXA1/2

See main caption on page 177. Note nuclear expression of FOXA1/2 in NHU cells, with upregulated expression associated with PPARγ activation.

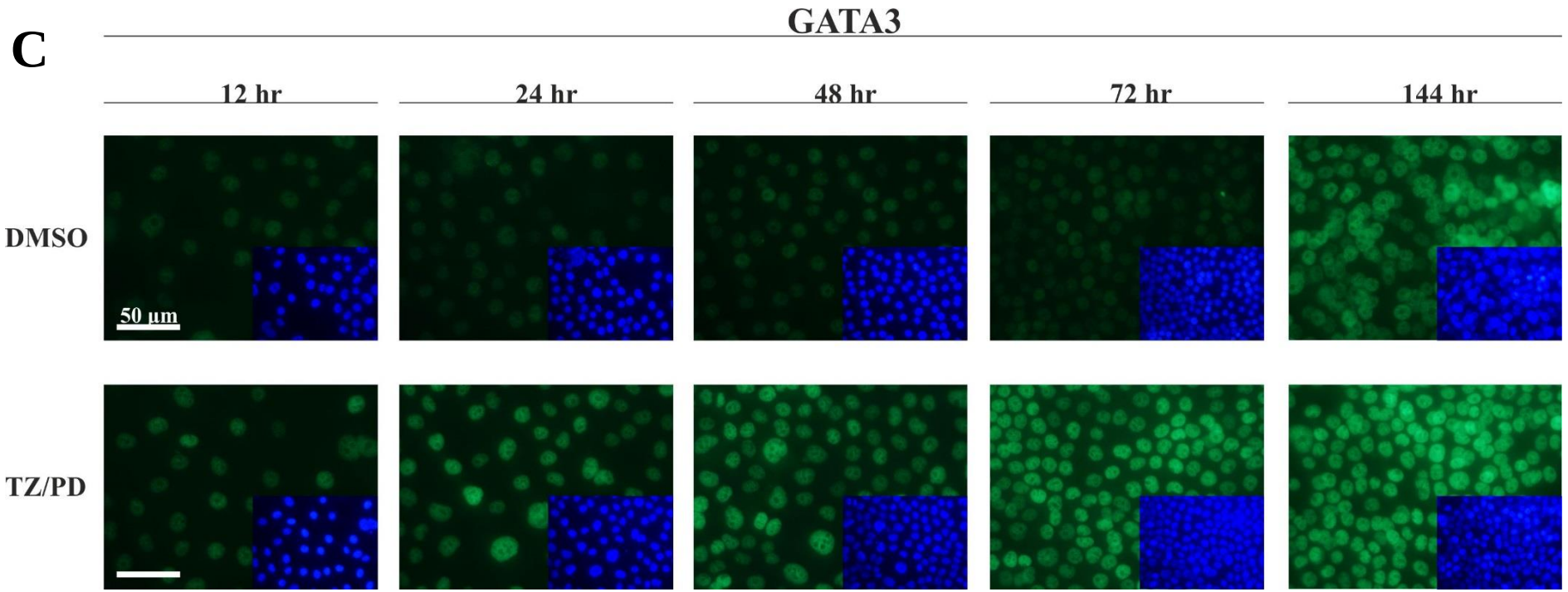

Figure 4.9. Evaluation of Transcription Factor Protein Expression in NHU Cells Following PPARγ Activation using the TZ/PD Protocol for 12, 24, 48, 72 and 144 hours by Indirect Immunofluorescence Microscopy – C) GATA3

See main caption on page 177. Note nuclear expression of GATA3 in NHU cells, with clear upregulated expression associated with PPARγ activation.

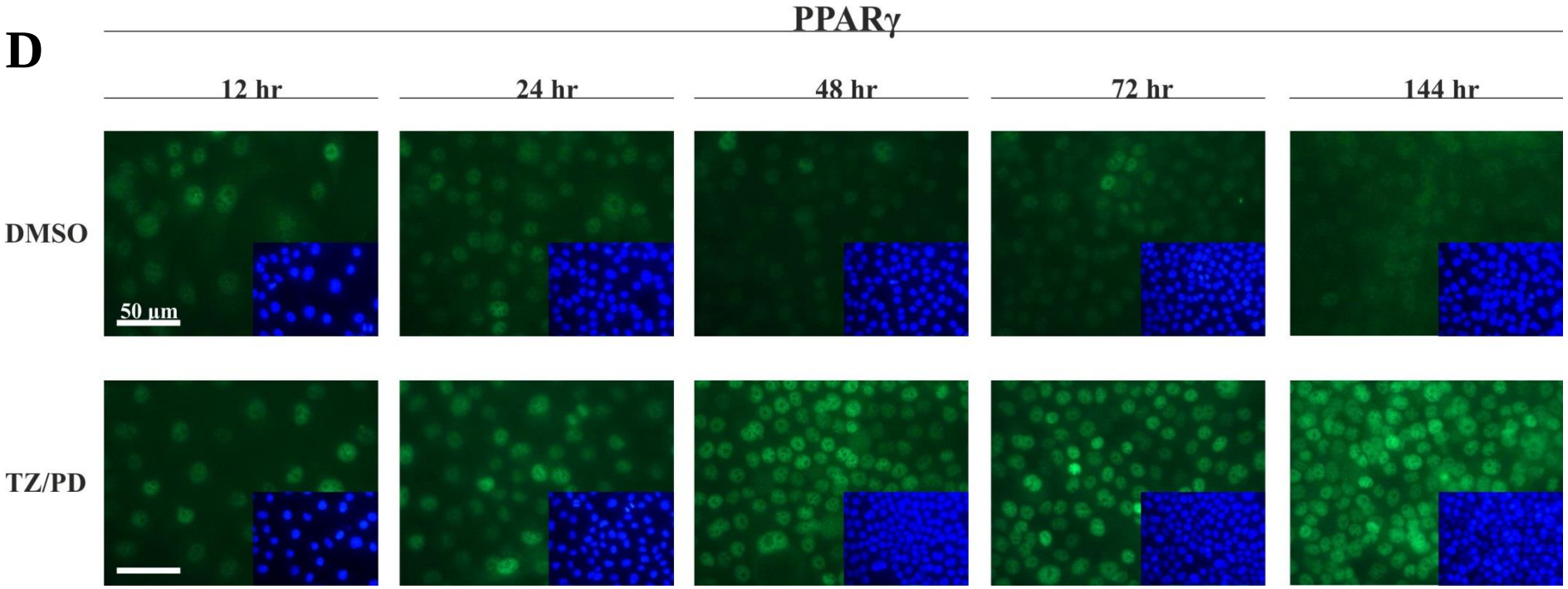

Figure 4.9. Evaluation of Transcription Factor Protein Expression in NHU Cells Following PPARγ Activation using the TZ/PD Protocol for 12, 24, 48, 72 and 144 hours by Indirect Immunofluorescence Microscopy – D) PPARγ

See main caption on page 177. Note nuclear expression of PPARγ in NHU cells, with upregulated expression associated with PPARγ activation.

4.5.5 PPARγ Protein Expression in Native Human Urothelium

By western blotting, freshly isolated urothelium from three independent human donor tissue samples (Urothelium-1, Y1772, Ureter; Urothelium-2, Y1773, Ureter; Urothelium-3, Y1774, Renal Pelvis) displayed abundant expression of PPARγ1 (Figure 4.10 A). Using the D69 antibody (Cell Signaling) a possible PPARγ2 band could be observed in each of the samples at approximately 57 kDa. Using the PPARγ2-specific antibody, N-19 (Santa Cruz), it was shown that this band was not PPARγ2, and that no PPARγ2 expression could be observed in any of the urothelium protein lysates (Figure 4.10 B & C).

4.5.6 PPARγ Protein Expression in Urothelial Carcinoma-Derived Cell Lines

The expression of PPARγ1 protein could be observed in UMUC9 cells, RT4 cells, RT112 cells, and 5637 cells grown in RPMI plus 5 % FBS, by western blotting (Figure 4.11). PPARγ1 protein expression was absent in EJ cells, as well as in 5637 cells that were grown in KSFM. Using the D69 antibody (Cell Signaling), a band corresponding to the appropriate height for PPARγ2 (approximately 57 kDa) could be observed in the 5637 cells grown in KSFM. Further assessment of PPARγ2 protein expression, using the N-19 antibody (Santa Cruz), revealed that this band in the 5637 cells was not PPARγ2. None of the urothelial carcinoma-derived cell lines evaluated displayed any detectable PPARγ2 protein.

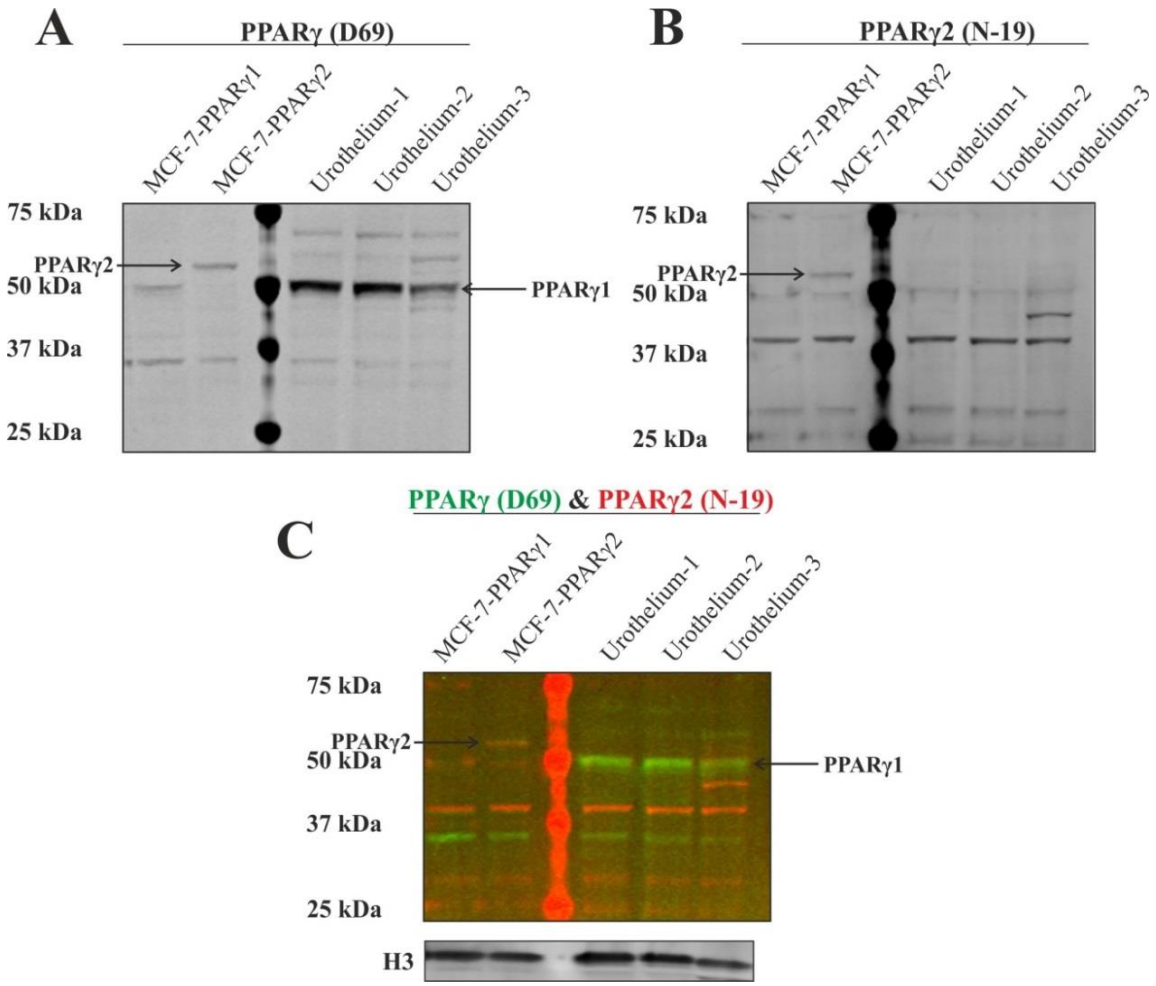

Figure 4.10 Evaluation of PPARγ Protein Expression in Native Urothelium by Western Blotting

The urothelium from three independent human donor tissue samples (Urothelium-1, Y1772, Ureter; Urothelium-2, Y1773, Ureter; Urothelium-3, Y1774, Renal Pelvis) was isolated; after removing the urothelium using forceps, the urothelium cell sheets were pelleted by centrifugation, and whole protein lysates were generated. Expression of **(A)** total PPARγ (Cell signaling, D69) and **(B)** PPARγ2 (Santa Cruz, N-19) was assessed by western blotting. The corresponding color images were overlaid for the two antibodies in **(C)**. Histone 3 (H3) expression was used as a loading control. MCF-7 cells overexpressing either PPARγ1 or PPARγ2 were included as positive controls for each antibody. 20 µg of protein was loaded into each well. Note clear PPARγ1 protein expression and an absence of PPARγ2 protein expression in native urothelium.

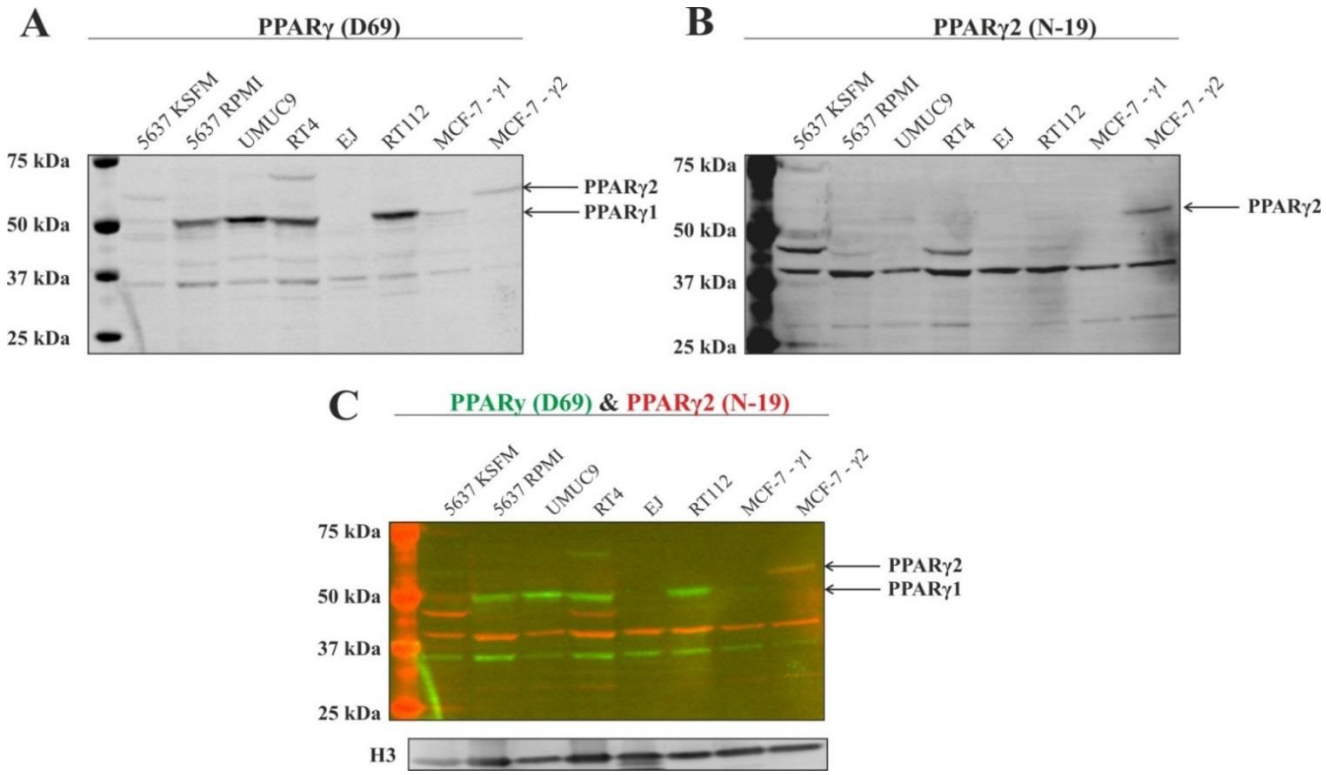

Figure 4.11 Assessment of PPARγ Protein Expression in Urothelial Carcinoma-Derived Cell Lines by Western Blotting

The expression of **(A)** total PPARγ (Cell Signaling, D69) and **(B)** PPARγ2 (Santa Cruz, N-19) was assessed in several urothelial carcinoma-derived cell lines by western blotting. The corresponding colour images were overlaid for the two antibodies in **(C)**. Histone 3 (H3) expression was used as a loading control. MCF-7 cells overexpressing either PPARγ1 or PPARγ2 were included as positive controls for each antibody. 20 μg of protein was loaded into each well. Note PPARγ1 protein expression in 5637 cells grown in RPMI plus 5 % FBS, UMUC9 cells, RT4 cells and RT112 cells. PPARγ2 expression was absent in all of the urothelial carcinoma-derived cell lines.

4.5.7 Expression of PPARγ Protein in NHU Cells Following Proteasome Inhibition

Since PPARγ1 protein expression appeared fairly weak in NHU cells, even following activation of PPARγ using TZ/PD, the proteasome inhibitor, MG132, was used to determine if PPARγ protein was being degraded by the proteasome.

By western blotting, it was shown that the addition of the proteasome inhibitor to NHU cells caused a dramatic increase in PPARγ1 expression in both control (0.1% DMSO) and TZ/PD treated cells (Figure 4.12). NHU cells from two independent cell lines (Y1390 and Y1691) were assessed for the purpose of this experiment, with both cell lines showing a similar trend in expression.

Treatment of UMUC9 cells with MG132 was also evaluated, for comparison. UMUC9 cells expressed high levels of PPARγ1 under normal growth conditions. After treatment with MG132, a slight increase in PPARγ1 expression was observed (Figure 4.12 B).

Proteasome inhibition did not result in any gain of PPARγ2 protein expression in either NHU cells or UMUC9 cells.

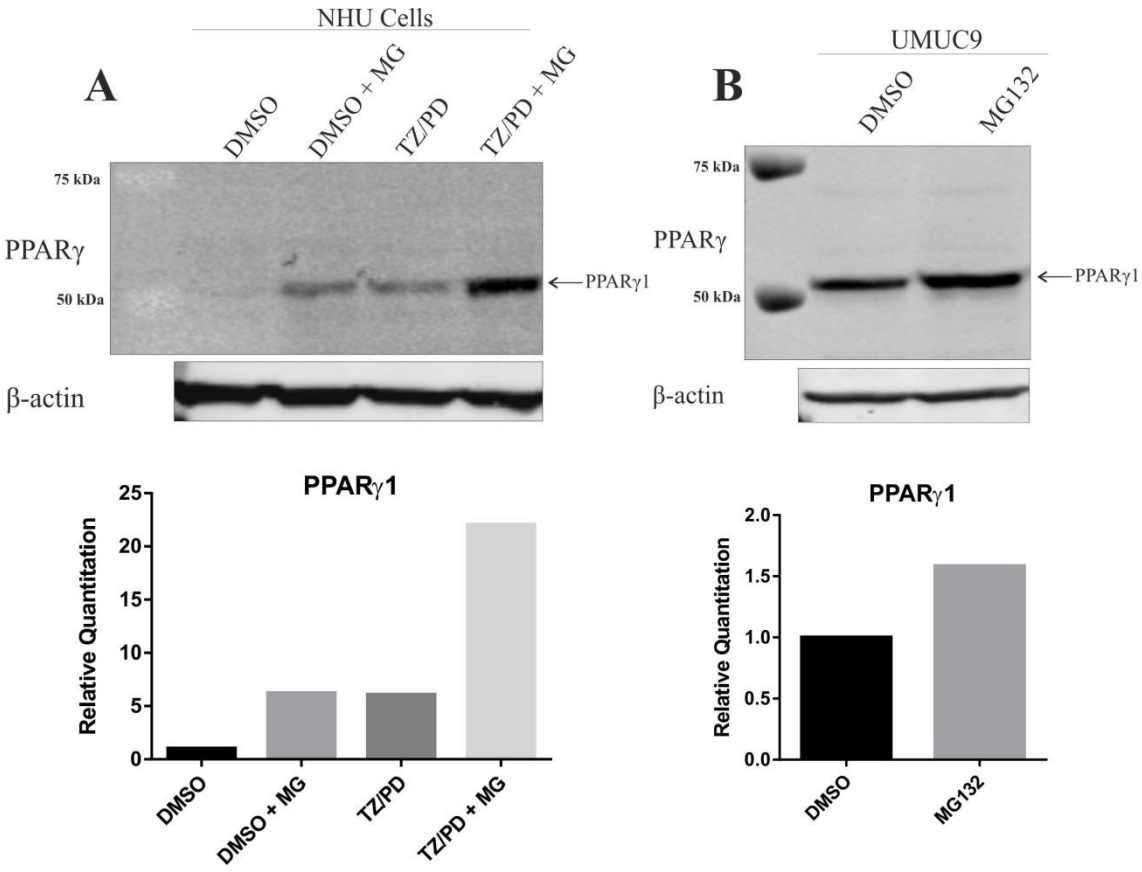

Figure 4.12 Evaluation of PPARγ Protein Expression by Western Blotting in NHU Cells and UMUC9 Cells Following Proteasome Inhibition

A) Western blot showing PPARγ protein expression (Cell Signaling, D69) in NHU cells (Y1390) treated with the proteasome inhibitor, MG132 (MG). NHU cells were first treated with either 0.1% DMSO (vehicle control) or TZ/PD for 72 hours. The medium was then changed, and the cells were either treated with 0.1% DMSO (vehicle control) or 12.5 μM MG132 for 6 hours.

B) Western blot showing PPARγ protein expression (Cell Signaling, D69) in UMUC9 cells treated with either 0.1% DMSO (vehicle control) or 12.5 μM MG132 for 6 hours.

The band corresponding to PPARγ1 (approximately 52 kDa) is indicated. β-actin was used as a loading control. 20 μg of protein was loaded into each well. The graphs shown represent densitometry analysis for the respective PPARγ1 protein expression. Data is shown relative to the DMSO treated cells. All values were first normalised to β-actin expression. An additional NHU cell line (Y1691) was completed for this experiment (see Appendix 7.6), which showed similar results to the NHU cell line shown above. Note clear upregulation of PPARγ1 protein expression in NHU cells following treatment with MG132. PPARγ2 expression was absent and not affected by proteasome inhibition in NHU cells or UMUC9 cells.

4.5.8 GATA3 Knockdown Using siRNA Prior to PPARγ Activation

4.5.8.1 GATA3 siRNA Titration

NHU cells (Y1752) displayed knockdown of GATA3 protein expression following transfection with either GATA3-siRNA1 or GATA3-siRNA2 at both the 50 nM and 100 nM concentrations (Figure 4.13 A). Densitometry analysis of the corresponding western blot revealed that GATA3-siRNA2 was more effective at GATA3 knockdown than GATA3-siRNA1 (Figure 4.13 B). At the 100 nM concentration both GATA3 siRNAs were able to reduce GATA3 protein expression by greater than 55%. 100 nM was chosen as the concentration to proceed with for the following experiments. At both siRNA concentrations, the cells survived and looked typical of being treated with TZ/PD alone.

4.5.8.2 Effect of GATA3 Knockdown on the Expression of Urothelial Differentiation-Associated Transcription Factors

GATA3 knockdown was shown to be significant using both of the GATA3 siRNAs relative to control siRNA, by RT-qPCR ($P \leq 0.001$) (Figure 4.14 A). By western blotting, GATA3-siRNA1 did not result in a significant knockdown of GATA3 protein, while GATA3-siRNA2 did cause a significant ($P \leq 0.01$) knockdown of GATA3 protein in NHU cells (Figure 4.15). There was no significant change ($P > 0.05$) in FOXA1 transcript (Figure 4.14 B) or protein expression (Figure 4.15), as a result of GATA3 knockdown. PPARγ expression was significantly ($P \leq 0.05$) downregulated at the transcript level (Figure 4.14 C), but this was not observed at the protein level (Figure 4.15); PPARγ protein expression appeared very weak in all of the NHU cell lines at the time point investigated (48 hr TZ/PD).

4.5.8.3 Effect of GATA3 Knockdown on the Expression of Urothelial Differentiation-Associated Genes

Knockdown of GATA3 resulted in a significant ($P \leq 0.01$) downregulation of CK13 protein expression by GATA3-siRNA2 (Figure 4.16 A & B). It also caused a significant ($P \leq 0.001$) downregulation of UPK2 gene expression, which was demonstrated by RT-qPCR analysis (Figure 4.16 C).

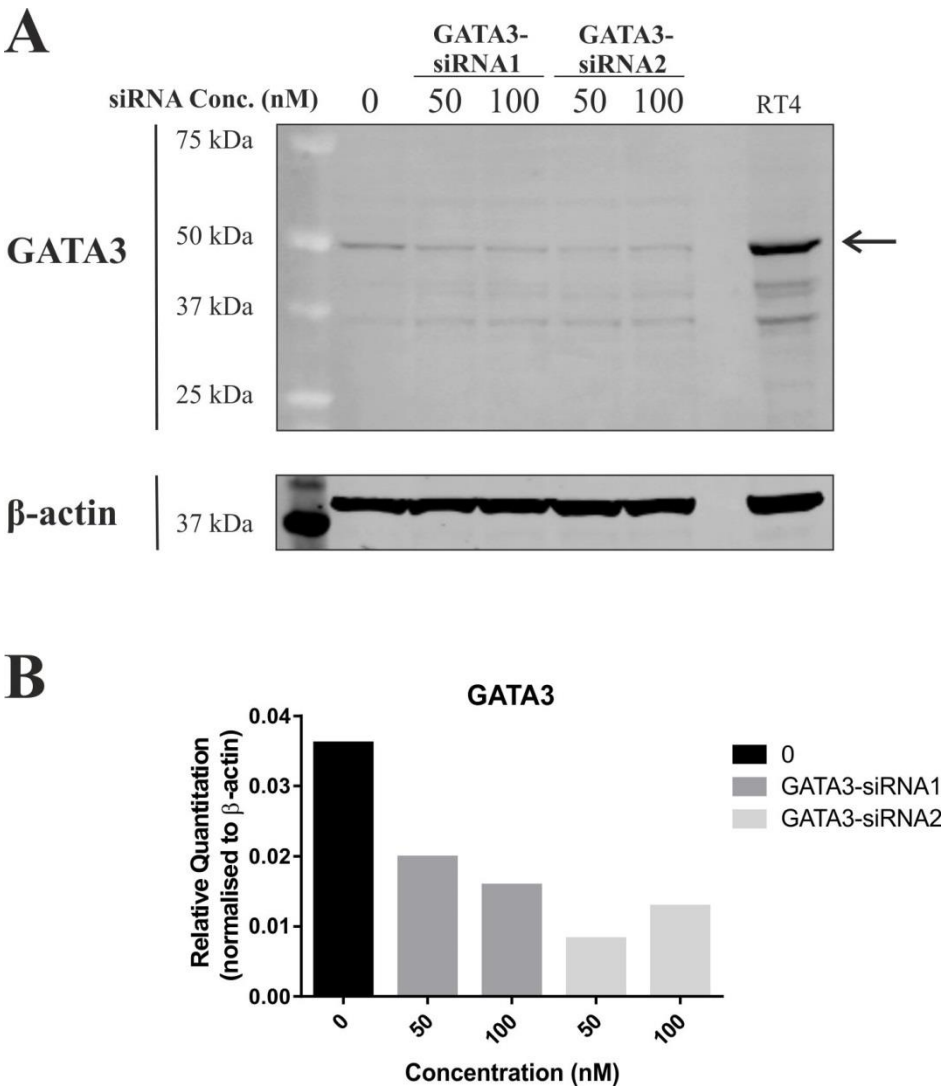

Figure 4.13. Effectiveness of GATA3 siRNA Evaluated by Western Blotting

NHU cells (Y1752) were transfected with 50 nM and 100 nM of either GATA3-siRNA1 or GATA3-siRNA2 for 4 hours, and then PPARγ was activated using the TZ/PD protocol for 48 hours. Control cells were treated with the transfection reagent only, followed by TZ/PD for 48 hours (denoted as 0 nM siRNA in the figures).

A) Western blot demonstrating GATA3 knockdown using both of the GATA3 siRNAs at 50 and 100 nM. RT4 cells were used as a positive control for GATA3 protein expression. β-actin was used as a loading control. 25 μg of protein was loaded into each well.

B) Densitometry analysis of the GATA3 protein expression (bands designated by arrow in **A**) shown relative to β-actin expression.

Note knockdown of GATA3 protein expression by both GATA3-siRNA1 and GATA3-siRNA2 at both the 50 nM and 100 nM concentrations.

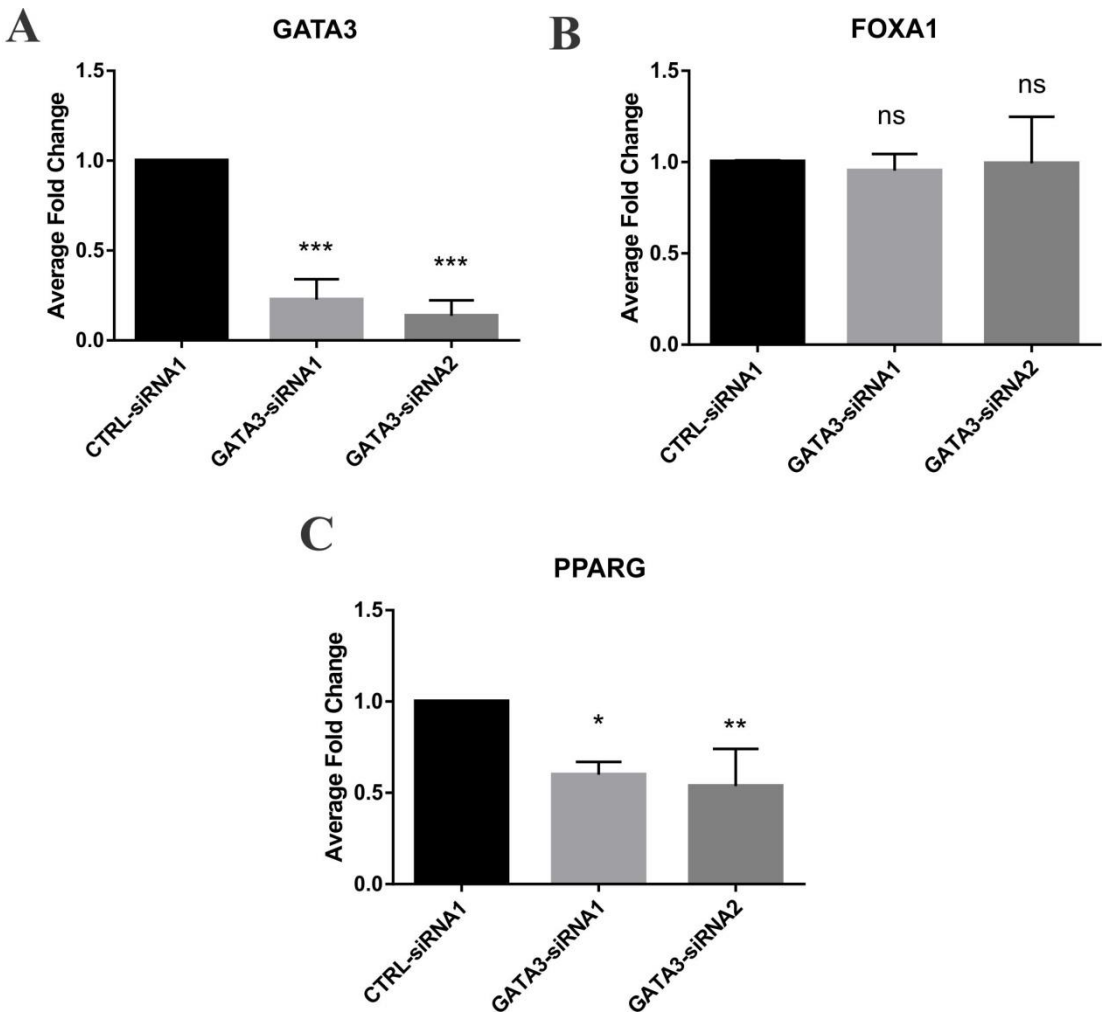

Figure 4.14. Effect of GATA3 Knockdown on Urothelial Differentiation-Associated Transcription Factor Expression Evaluated by RT-qPCR

RT-qPCR data was generated for **(A)** GATA3, **(B)** FOXA1, and **(C)** PPARγ gene expression using three independent NHU cell lines (Y1356, Y938, and Y1815) transfected with siRNA. Cultures were transfected with 100 nM of either CTRL-siRNA1, GATA3-siRNA1 or GATA3-siRNA2 for 4 hours, and then PPARγ was activated using TZ/PD for 48 hours. Values are shown as the mean of the three independent cell lines relative to CTRL-siRNA1. Error bars represent the standard deviation of the mean of the three independent NHU cell lines. All values were first normalised to GAPDH expression. Statistical analysis was performed using a one-way ANOVA test with a Dunnett's multiple comparisons post-hoc test. * represents $P \leq 0.05$. ** represents $P \leq 0.01$. *** represents $P \leq 0.001$. ns = not significant, $P > 0.05$. Note significant knockdown of GATA3 in NHU cells as a result of transfection with GATA3 siRNA. There was no effect on FOXA1 transcript expression. PPARγ transcript was significantly downregulated as a result of GATA3 knockdown.

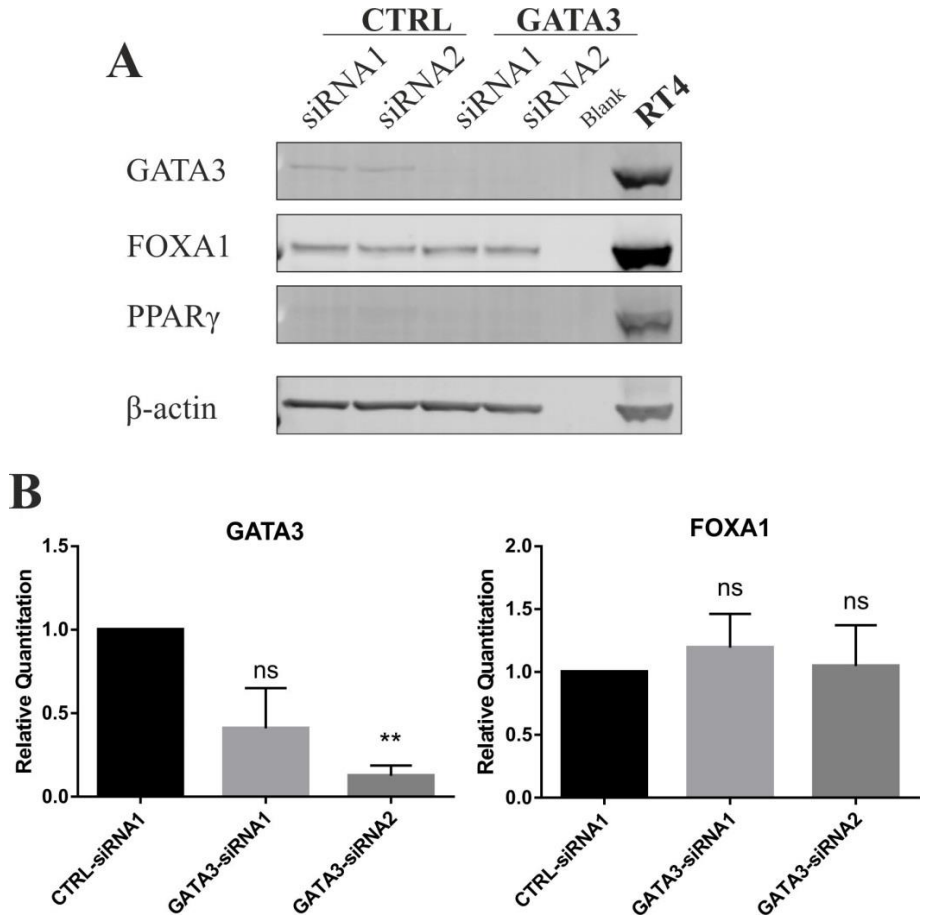

Figure 4.15. Effect of GATA3 Knockdown on Urothelial Cell Differentiation-Associated Transcription Factor Protein Expression Evaluated by Western Blotting

NHU cells from three independent cell lines (Y1356, Y938, and Y1815) were transfected with 100 nM of either CTRL-siRNA1, CTRL-siRNA2, GATA3-siRNA1 or GATA3-siRNA2 for 4 hours, and then PPARγ was activated using the TZ/PD protocol for 48 hours.

A) GATA3, FOXA1 (Santa Cruz, Q-6), and PPARγ (Cell Signaling, D69) expression was assessed by western blotting. β-actin was used as a loading control. RT4 cells were used as a positive control for each antibody. Western blots for the cell line Y1356 are shown. Western blots for the two additional NHU cell lines (Y938 and Y1815) can be found in Appendix 7.6. 30 μg of protein was loaded into each well.

B) Densitometry analysis of GATA3 and FOXA1 protein expression shown relative to CTRL-siRNA1. All values were first normalised to β-actin expression. Data is represented as the mean of the three independent transfected NHU cell lines (Y1356, Y938, and Y1815). Error bars represent the standard deviation of the mean of the three independent cell lines. Statistical analysis was performed using a one-way ANOVA test with a Dunnett's multiple comparisons post-hoc test. ** represents $P \leq 0.01$. ns = not significant, $P > 0.05$.

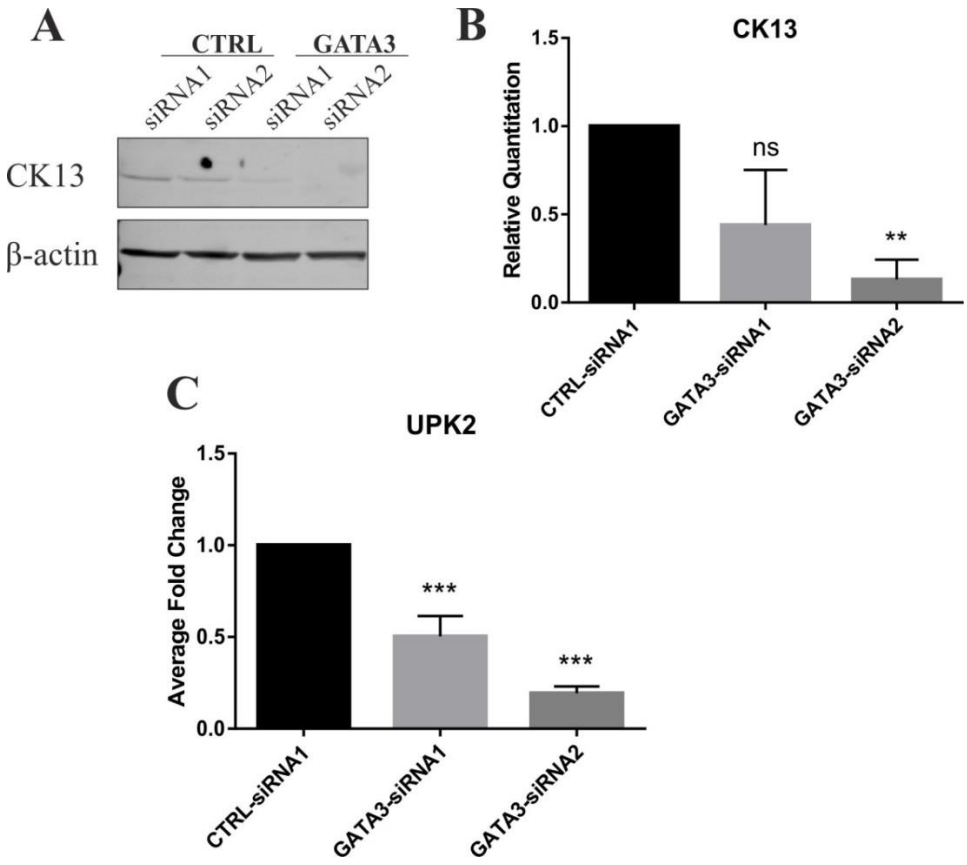

Figure 4.16. Effect of GATA3 Knockdown on the Expression of Urothelial Differentiation-Associated Genes Evaluated by Western Blotting and RT-qPCR

NHU cells from three independent cell lines (Y1356, Y938, and Y1815) were transfected with 100 nM of either CTRL-siRNA1, CTRL-siRNA2, GATA3-siRNA1 or GATA3-siRNA2 for 4 hours, and then PPARγ was activated using the TZ/PD protocol for 48 hours.

A) Representative western blot showing CK13 expression in NHU cells (Y1356) following GATA3 knockdown. β-actin was used as a loading control. 20 μg of protein was loaded into each well.

B) Densitometry analysis of CK13 protein expression in the three independent NHU cell lines (Y1356, Y938, and Y1815). All values were first normalised to β-actin.

C) RT-qPCR data generated for UPK2 gene expression using the three independent NHU cell lines (Y1356, Y938, and Y1815). All values were first normalised to GAPDH.

Data is shown as the mean of the three independent cell lines (Y1356, Y938, and Y1815) relative to CTRL-siRNA1. Error bars represent the standard deviation of the mean of the three independent NHU cell lines. Statistical analysis was performed using a one-way ANOVA test with a Dunnett's multiple comparisons post-hoc test. ** represents $P \leq 0.01$ *** represents $P \leq 0.001$. ns = not significant, $P > 0.05$.

4.6 Summary of Results

- GATA3 transcript and protein expression was upregulated in NHU cells as a result of TZ/PD treatment. This upregulation was likely attributed to PPARγ activation, as use of the PPARγ antagonist, T0070907, appeared to abrogate the upregulation.

- PPARγ expression could be shown at the transcript level by RT-PCR in NHU cells. Use of PPARγ2-specific PCR primers revealed weak/absent PPARγ2 expression even following activation of PPARγ using the TZ/PD protocol. This suggested that the PPARγ expression shown using the PCR primers that amplify 'total PPARγ' was almost entirely attributable to transcript variants encoding for the PPARγ1 protein. The potential for the expression of novel alternate transcript variants was also revealed using the 'total PPARγ' PCR primers.

- The primary PPARγ protein isoform detected in native human urothelium, cultured NHU cells, and several urothelial carcinoma-derived cell lines was PPARγ1. PPARγ2 protein expression could not be obviously detected in any of the cell types.

- Significant knockdown of GATA3 expression could be successfully demonstrated at both the transcript and protein levels in NHU cells following transfection with GATA3-targeted siRNAs.

- GATA3 was shown to have a potentially important regulatory role in the differentiation of urothelial cells. Knockdown of GATA3 expression by siRNA revealed a significant downregulation of both CK13 and UPK2 expression.

- GATA3 also appears to contribute to the regulation of key transcription factors involved in urothelial differentiation, as GATA3 knockdown also resulted in the significant downregulation of PPARγ transcript expression.

Chapter 5:
Overexpression of GATA3 and PPARγ1 in Buccal Epithelial Cells

5 Overexpression of GATA3 and PPARγ1 in Buccal Epithelial Cells

5.1 Rationale and Aims

Results presented in Chapter 3, comparing transcription factor expression between buccal epithelial cells and urothelial cells, saw noticeably weak expression of GATA3 and PPARγ. Use of the TZ/PD, atRA/PD or ABS/Ca^{2+} protocols with NHB cells did not cause any obvious upregulation of GATA3 or PPARγ expression. These observations suggested not only that abundant expression of GATA3 and PPARγ may be critical for maintaining the urothelial cell identity, but also that low expression of GATA3 and PPARγ expression may be important for maintaining a squamous epithelial cell phenotype. In Chapter 4, PPARγ1 was identified as the primary PPARγ protein isoform involved in urothelial cell differentiation. In addition to this, GATA3 was shown to have a potential role in regulating the differentiation of urothelial cells. As a result, GATA3 and PPARγ1 were chosen to overexpress in NHB cells in an initial attempt to transdifferentiate NHB cells into NHU cells.

The aim of this chapter was to assess the ability of individual GATA3 overexpression and PPARγ1 overexpression to cause urothelial-type transdifferentiation of NHB cells.

5.2 Hypothesis

The hypothesis was that individual overexpression of GATA3 or PPARγ1 in NHB cells would have the ability to upregulate urothelium-associated genes and downregulate squamous epithelial cell-associated genes.

5.3 Experimental Approach

The results portion of this chapter is separated into two sections (Chapter 5A and Chapter 5B), where Chapter 5A corresponds to results pertaining to GATA3 overexpression in NHB cells, and Chapter 5B corresponds to PPARγ1 overexpression in NHB cells.

To assess the propensity for either GATA3 overexpression or PPARγ1 overexpression to cause urothelial-type transdifferentiation of NHB cells, transduced NHB cells were assessed for their expression of urothelium-associated transcription factors, urothelium-associated differentiation markers, the squamous epithelial cell-associated protein (CK14), and barrier function, following use of the TZ/PD, atRA/PD and/or ABS/Ca^{2+} protocols. For urothelial-type transdifferentiation, the ultimate goal would be to upregulate urothelium-associated transcription factors and differentiation-associated genes, and promote barrier function. The expectation would also be to downregulate squamous epithelial cell-associated genes. A table outlining experiments which were performed on GATA3 overexpressing and PPARγ1 overexpressing cells, and the markers assessed can be found in Table 5.1. Based on the results presented in Chapter 3 and Chapter 4, the work in this chapter aimed to assess whether individual GATA3 overexpression or PPARγ1 overexpression in NHB cells could:

1. Upregulate and cause nuclear localisation of key urothelial differentiation-associated transcription factors, ELF3, FOXA1, GATA3 and PPARγ1.
2. Cause upregulation of the urothelium differentiation-associated uroplakin genes.
3. Cause downregulation of CK14 expression, a squamous epithelial cell-associated cytokeratin.
4. Cause an increase in barrier function, as measured by the TER. Various tight junction-associated proteins were also assessed to evaluate whether any changes in their expression had occurred.

Table 5.1 Summary of Experiments Performed to Assess the Transdifferentiation Potential of GATA3 Overexpression and PPARγ1 Overexpression in NHB Cells

Protocol	Makers Assessed		Technique Used
TZ/PD	Transcription Factors	ELF3 FOXA1 GATA3 PPARγ	RT-qPCR Western Blotting Immunofluorescence
	Uroplakin Genes	UPK1A UPK1B UPK2 UPK3A UPK3B	RT-qPCR
atRA/PD	Transcription Factors	ELF3 FOXA1 GATA3 IRF1 PPARγ	RT-PCR Immunofluorescence Western Blotting
	Cytokeratins	CK13 CK14	Immunofluorescence
ABS/Ca^{2+}	Transcription Factors	GATA3 PPARγ FOXA1	Western Blotting
	Tight Junction Proteins	CLDN3 CLDN4 CLDN5 CLDN7 ZO-1 ZO-3	Western Blotting
	Cytokeratins	CK13 CK14	Western Blotting
	Barrier Function		TER

5.3.1 GATA3 Overexpression and PPARγ1 Overexpression

NHB cells were transduced with retroviruses generated from PT67 cells transfected with either the empty pLXSN vector (control), the pLXSN vector containing the eGFP coding sequence (control), the pLXSN vector containing the GATA3 coding sequence, or the pLXSN vector containing the PPARγ1 coding sequence. Successfully transduced cells were maintained under antibiotic (0.025 mg/ml G418) selection. Details of the generation of the pLXSN-GATA3 vector and its subsequent transfection into PT67 cells can be found in Chapter 2 of this thesis.

The pLXSN-eGFP vector was previously generated, transfected into PT67 cells, and verified for use by Dr. Joanna Pearson, a research technician at the Jack Birch Unit. The PPARγ1 overexpression vector was previously generated, and transfected into PT67 cells by Ms. Jenny Hinley, a research technician at the Jack Birch Unit.

5.3.2 FOXA1 Antibodies for Immunofluorescence Microscopy

Two different antibodies were used to assess FOXA1 expression by immunofluorescence microscopy in this chapter, the C-20 antibody (Santa Cruz), which detects both FOXA1 and FOXA2 expression, and the Q-6 antibody (Santa Cruz), which is specific for FOXA1 expression. The C-20 antibody was used for immunofluorescence in the two previous chapters. The Q-6 antibody was used for FOXA1 detection by western blotting in all of the chapters. Its use for immunofluorescence was introduced in this chapter as a potentially more specific antibody for detecting FOXA1 expression than the C-20 antibody. The antibody used for each experiment is identified in the figure legends. Overall, both antibodies gave similar results.

5.4 Results – Part A (GATA3 Overexpression)

5.4.1 GATA3 Overexpression in NHB Cells

Forced overexpression of GATA3 in NHB cells resulted in no obvious changes to cell morphology by phase contrast microscopy (Figure 5.1 A). GATA3 overexpression could be successfully demonstrated in NHB cells by RT-PCR and immunofluorescence microscopy (Figure 5.1 B & C). GATA3 expression was nuclear in the GATA3 overexpressing cells. In control transduced cells (eGFP/Empty), GATA3 expression was weak/absent.

5.4.2 Evaluation of Transcription Factor Expression in Control and GATA3 Overexpressing NHB Cells Following TZ/PD Treatment

Forced overexpression of GATA3 in NHB cells resulted in an upregulation of ELF3 and FOXA1 transcript in two independent transduced NHB cell lines (AS008b and Y1590) following use of the TZ/PD protocol for 72 hours (Figure 5.2). PPARγ transcript expression was variable in the two cell lines assessed; one transduced cell line (AS008b) demonstrated an upregulation of PPARγ expression, while the other cell line (Y1590) showed a slight decrease in PPARγ expression as a result of GATA3 overexpression.

By western blotting, no obvious change in FOXA1 protein expression was observed as a result of GATA3 overexpression in two independent cell lines (Y1590 and Y1595) which had been treated with either 0.1 % DMSO or TZ/PD for 72 hours (Figure 5.3). PPARγ protein expression was absent in both control and GATA3 overexpressing cells even after use of the TZ/PD protocol. Clear GATA3 overexpression could be shown by western blotting in both DMSO and TZ/PD treated GATA3 overexpressing NHB cells.

By immunofluorescence, ELF3 expression appeared to have increased nuclear localisation as a result of GATA3 overexpression when the cells were treated with TZ/PD (Figure 5.4). There was no obvious change in localisation of FOXA1. PPARγ expression was weak/absent in all cases. GATA3 expression was clearly nuclear in the GATA3 overexpressing cells, and absent in control (Empty) cells.

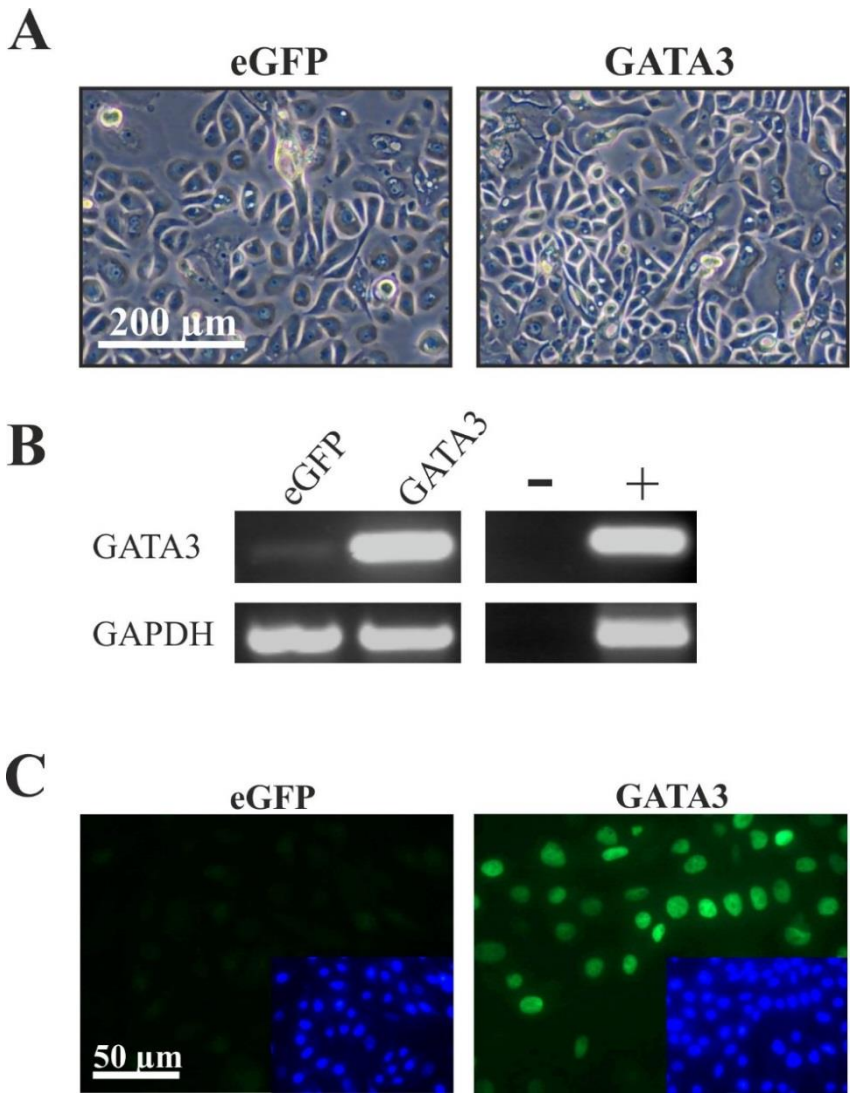

Figure 5.1 Demonstration of GATA3 Overexpression in NHB Cells (AS008b)

A) Phase contrast images of control (eGFP) and GATA3 overexpressing NHB cells (AS008b). Scale bar = 200 µm.

B) RT-PCR analysis of GATA3 gene expression in control (eGFP) and GATA3 overexpressing NHB cells (AS008b). GATA3 PCR was performed using 30 cycles. GAPDH was used as a loading control (25 cycles). H_2O (no template) was used as the negative control (-). Genomic DNA was used as a positive control for the PCR (+).

C) Immunofluorescence labelling for GATA3 was performed on formalin-fixed slides permeabilised with Triton X-100. Inset images represent the corresponding Hoechst 33258 staining to demonstrate cell density and nuclei location. Antibody labelled images were taken at the same exposure. Hoechst 33258 images were taken at optimal exposures. Note there was no obvious change in cell morphology as result of GATA3 overexpression. GATA3 overexpression could be clearly demonstrated by both RT-PCR and immunofluorescence microscopy.

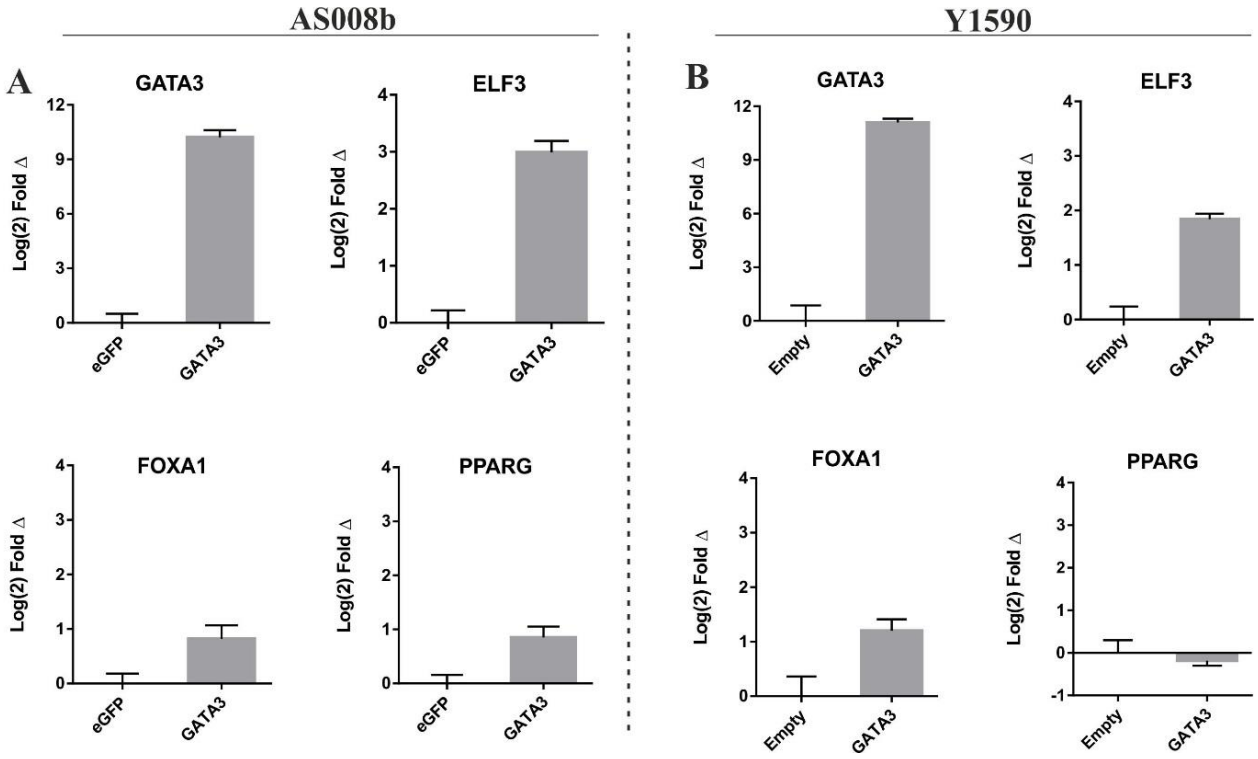

Figure 5.2 Analysis of ELF3, FOXA1, GATA3 and PPARG Transcript Expression by RT-qPCR in Control and GATA3 Overexpressing NHB Cells Following TZ/PD Treatment for 72 hours

Control (eGFP or Empty) and GATA3 overexpressing NHB cells **A)** AS008b and **B)** Y1590 were treated with TZ/PD for 72 hr. RNA was extracted and cDNA generated. qPCR data is shown for GATA3, ELF3, FOXA1, and PPARG gene expression. All values were normalised to GAPDH and are shown relative to the control (eGFP or Empty) cells for each gene. Data is shown as the mean of three technical replicates. Error bars represent the standard deviation of the three technical replicates. Note clear overexpression of GATA3 transcript. Also note upregulation of ELF3 and FOXA1 in two independent transduced NHB cell lines. PPARγ expression was variable between the two independent NHB cell lines.

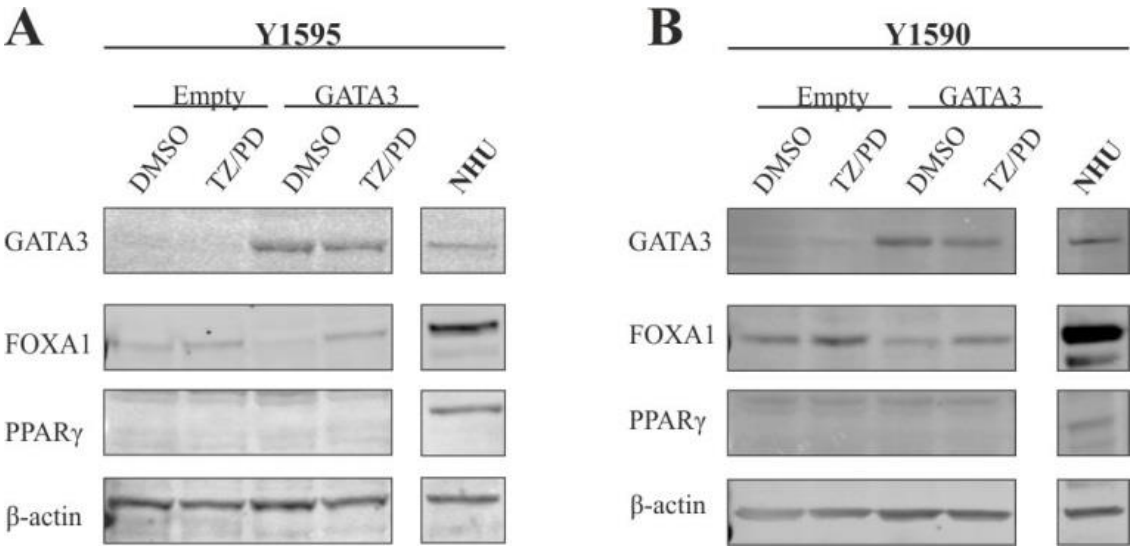

Figure 5.3 Evaluation of GATA3, FOXA1 and PPARγ Protein Expression by Western Blotting in Control and GATA3 Overexpressing NHB Cells Following Treatment with 0.1 % DMSO or TZ/PD for 72 hour

Control (Empty) and GATA3 overexpressing NHB cells **A)** Y1595 and **B)** Y1590, were treated with either 0.1% DMSO (vehicle control) or TZ/PD for 72 hr. Whole protein lysates were generated. GATA3, FOXA1 (Santa Cruz, Q-6), and PPARγ (Cell Signalling, D69) expression was assessed by western blotting. The band corresponding to PPARγ1 (approximately 52 kDa) is shown. NHU cells (Y1282 and Y1691 respectively), which were treated with TZ/PD for 72 hours, were included on each of the blots to act as positive controls. β-actin was used as a loading control. 25 μg of protein was loaded into each well. Note clear overexpression of GATA3 protein. Also note there was no obvious change in FOXA1 or PPARγ protein expression as a result of GATA3 overexpression in NHB cells even following use of the TZ/PD protocol.

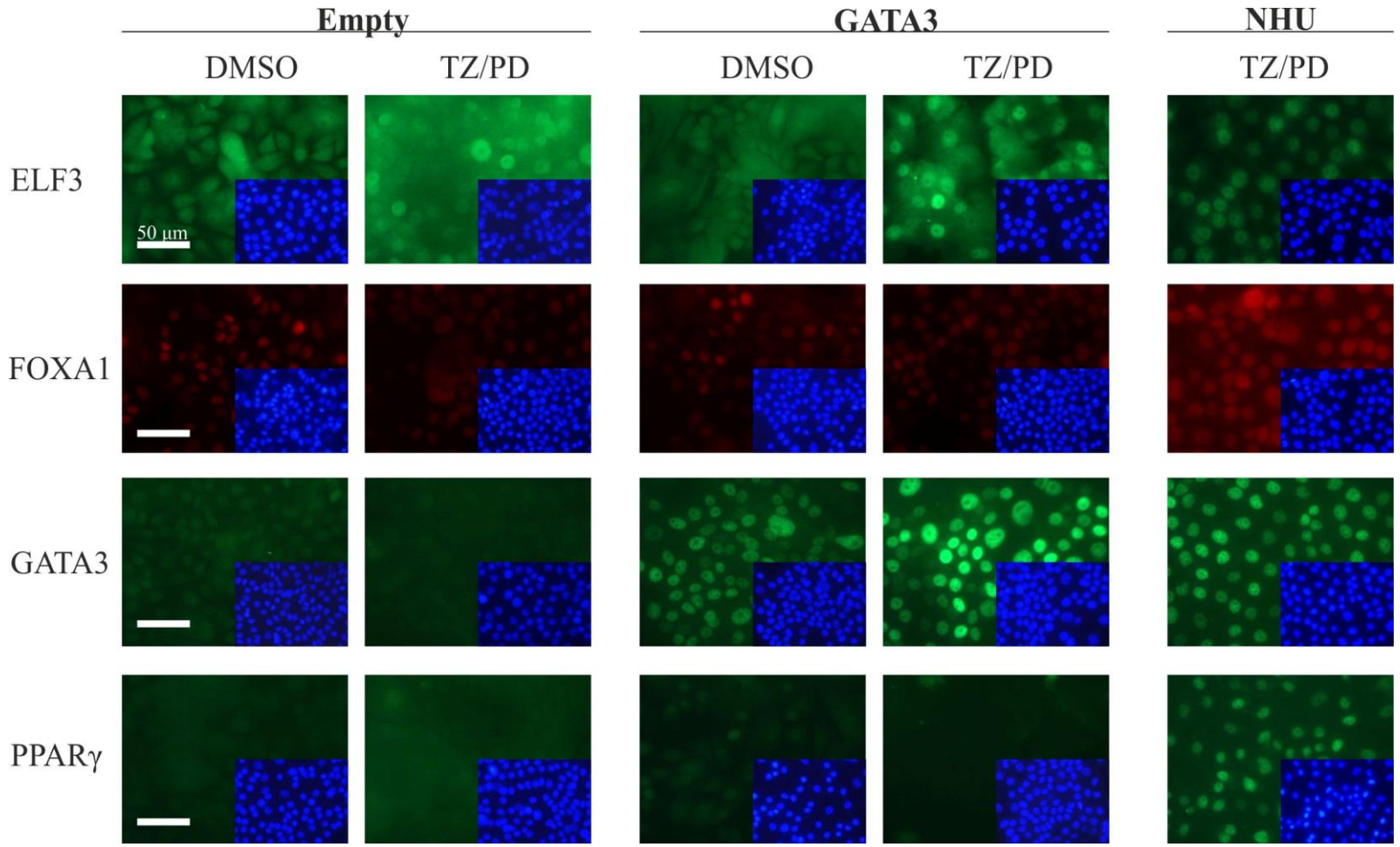

Figure 5.4 Evaluation of ELF3, FOXA1, GATA3, and PPARγ Expression by Indirect Immunofluorescence Microscopy in Control and GATA3 Overexpressing NHB Cells Treated with 0.1 % DMSO or TZ/PD for 72 Hours

Figure 5.4 Evaluation of ELF3, FOXA1, GATA3, and PPARγ Expression by Indirect Immunofluorescence Microscopy in Control and GATA3 Overexpressing NHB Cells Treated with 0.1 % DMSO or TZ/PD for 72 Hours

Control (Empty) and GATA3 overexpressing NHB cells (Y1595) were treated with either 0.1 % DMSO (vehicle control) or TZ/PD for 72 hours. Immunofluorescence labelling for ELF3, FOXA1 (Santa Cruz, Q-6), GATA3 and PPARγ (Cell Signaling, D69) was performed on formalin-fixed slides which had been permeabilised with Triton X-100. Inset images represent the corresponding Hoechst 33258 staining to demonstrate cell density and nuclei location. Antibody labelled images were taken at the same exposure for each antibody. Hoechst 33258 images were taken at optimal exposures. NHU cells (Y1752) which had been treated with TZ/PD for 48 hours were used as positive controls. An additional transduced cell line (Y1590) was also evaluated for the purpose of this experiment, and its figure can be found in Appendix 7.7. Note clear nuclear localisation of GATA3 in the GATA3 overexpressing cells, and absent GATA3 expression in control (Empty) cells. Also note possible increased nuclear localisation of ELF3 in the GATA3 overexpressing NHB cells following use of the TZ/PD protocol. FOXA1 and PPARγ expression were unchanged by GATA3 overexpression.

5.4.3 Evaluation of Uroplakin Gene Expression in Control and GATA3 Overexpressing NHB Cells Following use of the TZ/PD Protocol for 72 Hours

The expression of the five uroplakin genes was assessed by RT-qPCR in two independent transduced NHB cell lines (AS008b and Y1590) following use of the TZ/PD protocol for 72 hours (Figure 5.5). UPK1A and UPK3A gene expression was not detectable in either cell line. UPK1B expression was slightly increased in one of the NHB cell lines (AS008b), but had no obvious change in expression in the other cell line (Y1590), as a result of GATA3 overexpression. UPK2 and UPK3B expression was increased in both cell lines as a result of GATA3 overexpression following use of the TZ/PD protocol.

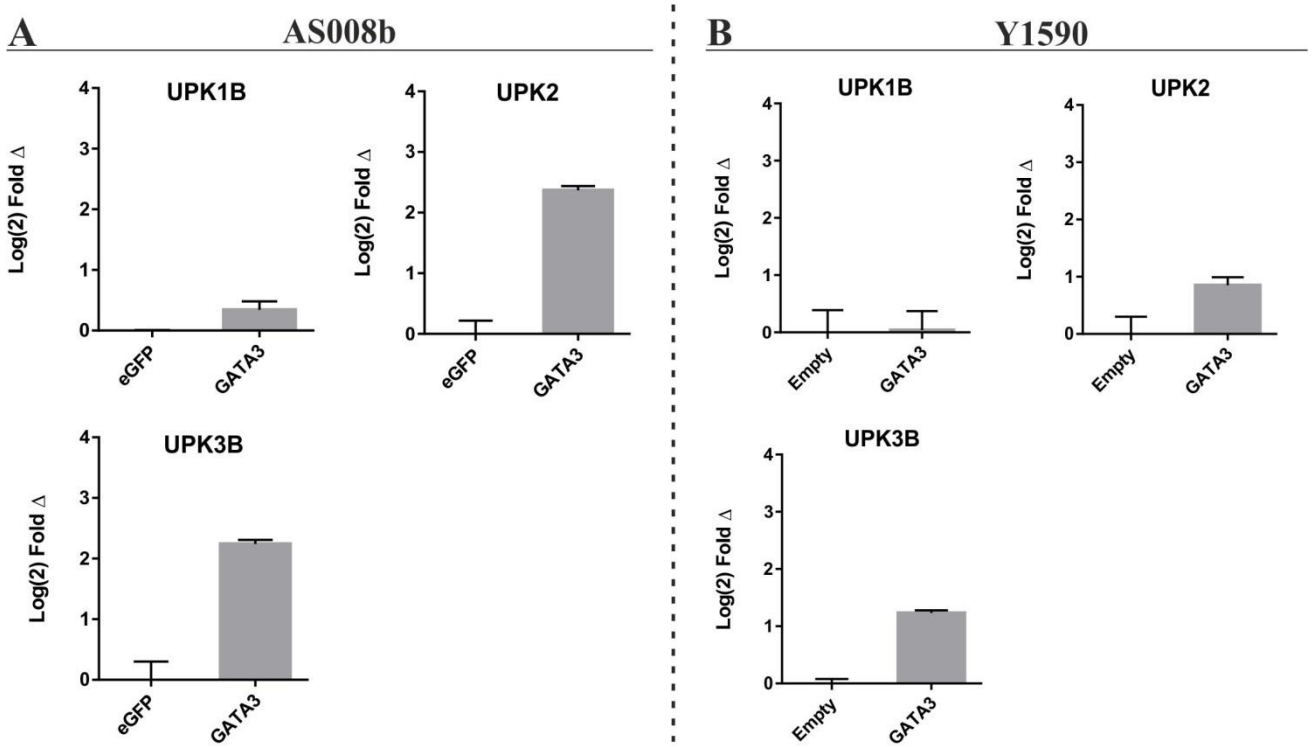

Figure 5.5 RT-qPCR analysis of Uroplakin Gene Expression in Control and GATA3 Overexpressing NHB Cells (AS008b) Following Treatment with TZ/PD for 72 Hours

Control (eGFP or Empty) and GATA3 overexpressing NHB cells, **A)** AS008b and **B)** Y1590, were treated with TZ/PD for 72 hr. RNA was extracted and cDNA generated. qPCR data was generated for UPK1A, UPK1B, UPK2, UPK3A, and UPK3B gene expression. UPK1A and UPK3A expression was absent in both cell lines and is therefore not shown. All values were normalised to GAPDH expression, and are shown relative to the control (eGFP or Empty) cells for each gene. Data is shown as the mean of three technical replicates. Error bars represent the standard deviation of the three technical replicates. Note increased UPK2 andUPK3B expression in the two independent NHB cells lines as a result of GATA3 overexpression.

5.4.4 Evaluation of Transcription Factor and Cytokeratin Protein Expression in Control and GATA3 Overexpressing NHB Cells Treated with the atRA/PD Protocol for 72 hours

Treatment of control (eGFP) and GATA3 overexpressing NHB cells with the atRA/PD protocol for 72 hours resulted in no obvious change in ELF3, FOXA1, IRF1 or PPARG transcript expression, as a result of GATA3 overxpression. An upregulation of FOXA1 expression was found in both the control (eGFP) and GATA3 overexpressing cells by both RT-PCR (Figure 5.6) and immunofluorescence microscopy (Figure 5.7).

No obvious change in CK13 or CK14 expression was observed in atRA/PD treated GATA3 overexpressing cells in comparison to control (eGFP) cells by immunofluorescence (Figure 5.7).

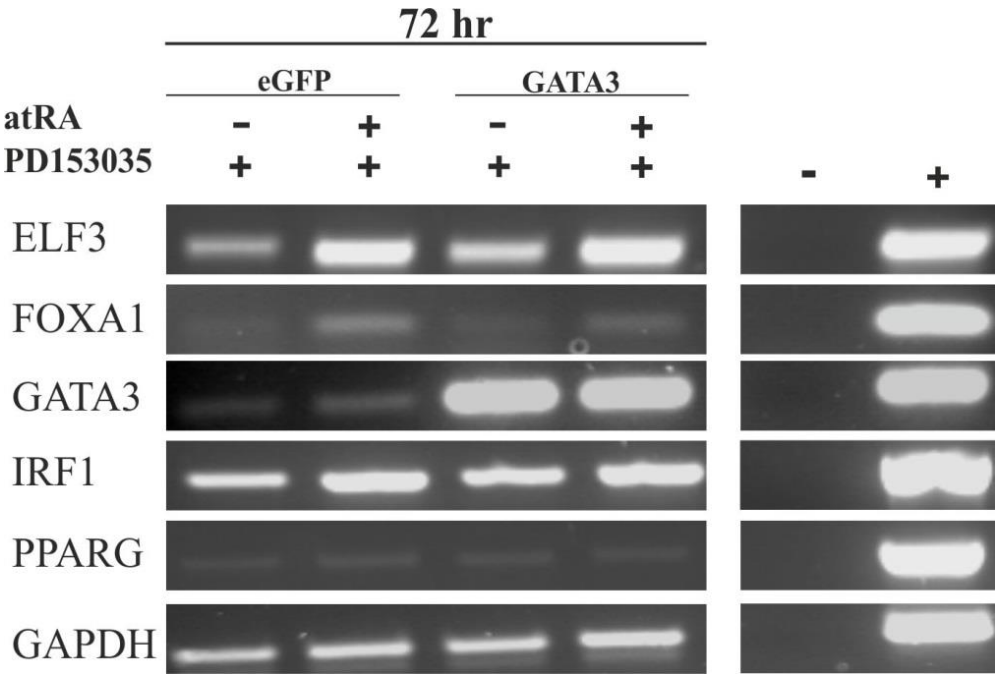

Figure 5.6 Analysis of Transcription Factor Expression by RT-PCR in Control and GATA3 Overexpressing NHB Cells Following use of the atRA/PD Protocol for 72 Hours

Control (eGFP) and GATA3 overexpressing NHB cells (AS008b) were treated with either 1 μM PD or 1 μM PD plus 100 nM atRA for 72 hours. RT-PCR was performed using 30 cycles for all target genes. GAPDH was used as a loading control (25 cycles). H_2O (no template) was used as the negative control (-). Genomic DNA was used as a positive control for the PCR (+). Note clear GATA3 overexpression. Also note no obvious change in ELF3, FOXA1, IRF1 or PPARG expression as a result of GATA3 overexpression even following treatment with atRA.

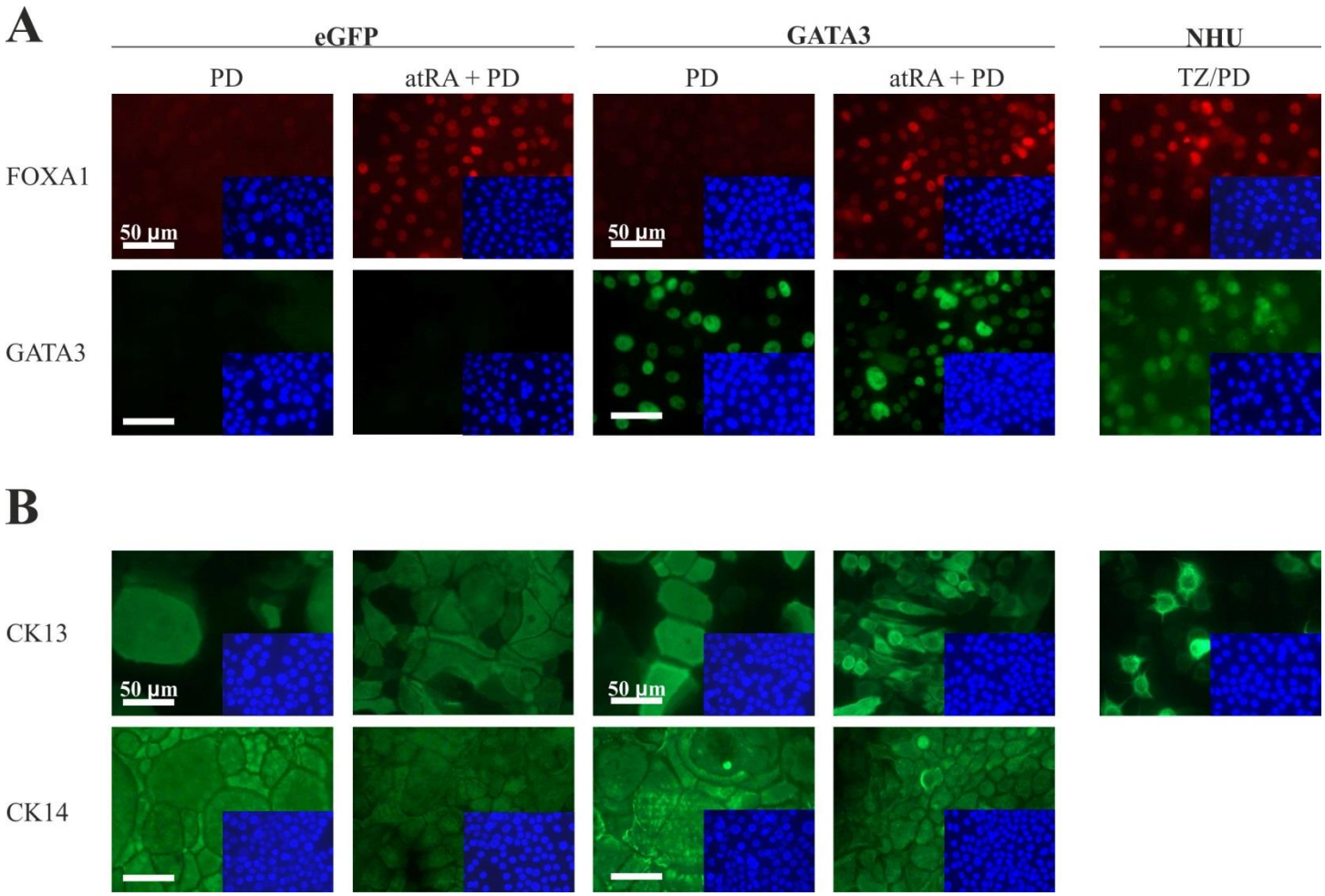

Figure 5.7 Evaluation of Transcription Factor and Cytokeratin Protein Expression by Indirect Immunofluorescence Microscopy in Control and GATA3 Overexpressing NHB Cells Following use of the atRA/PD Protocol for 72 Hours

Figure 5.7 Evaluation of Transcription Factor and Cytokeratin Protein Expression by Indirect Immunofluorescence Microscopy in Control and GATA3 Overexpressing NHB Cells Following use of the atRA/PD Protocol for 72 Hours

Control (Empty) and GATA3 overexpressing NHB cells (AS008b) were treated with either 1 μM PD or 1 μM PD plus 100 nM atRA for 72 hours. Immunofluorescence labelling for **A)** FOXA1 (Santa Cruz, Q-6), and GATA3, and **B)** CK13 and CK14, was performed on formalin-fixed slides which had been permeabilised with Triton X-100. Inset images represent the corresponding Hoechst 33258 staining to demonstrate cell density and nuclei location. Antibody labelled images were taken at the same exposure for each antibody. Hoechst 33258 images were taken at optimal exposures. NHU cells (Y1156) which had been treated with TZ/PD for 72 hours were used as positive controls for FOXA1, GATA3 and CK13 expression. Scale bar = 50 μm. Note no obvious change in FOXA1, CK13, or CK14 protein expression as a result of GATA3 overexpression and subsequent PD or atRA/PD treatment.

5.4.5 Assessment of Tight Junction-Associated Protein Expression in Control and GATA3 Overexpressing NHB Cells During use of the ABS/Ca^{2+} Protocol

The expression of several tight junction-associated proteins was assessed during use of the ABS/Ca^{2+} protocol in two independent transduced NHB cell lines (Y1595 and AS011b) by western blotting (Figure 5.8). A clear upregulation of CLDN3 protein expression was observed as a result of GATA3 overexpression at all of the time points. No obvious change in CLDN4, CLDN5 or CLDN7 protein expression was observed as a result of GATA3 overexpression; they were expressed at all of the time points in both cell types. ZO-1 expression varied between the two cell lines, but there was no clear trend in expression as a result of GATA3 overexpression. Overexpression of GATA3 was observed at all of the time points assessed in the GATA3 overexpressing cells.

5.4.6 Evaluation of CK14 Expression in Control and GATA3 Overexpressing NHB Cells During use of the ABS/Ca^{2+} Protocol

CK14 was strongly expressed at all of the time points assessed during use of the ABS/Ca^{2+} protocol, in both control and GATA3 overexpressing NHB cells (Y1595 and AS011b) (Figure 5.9). NHU cells (Y1336) which had been differentiated with ABS/Ca^{2+}, and included on the same western blots for comparison, showed a characteristic lack of CK14 expression.

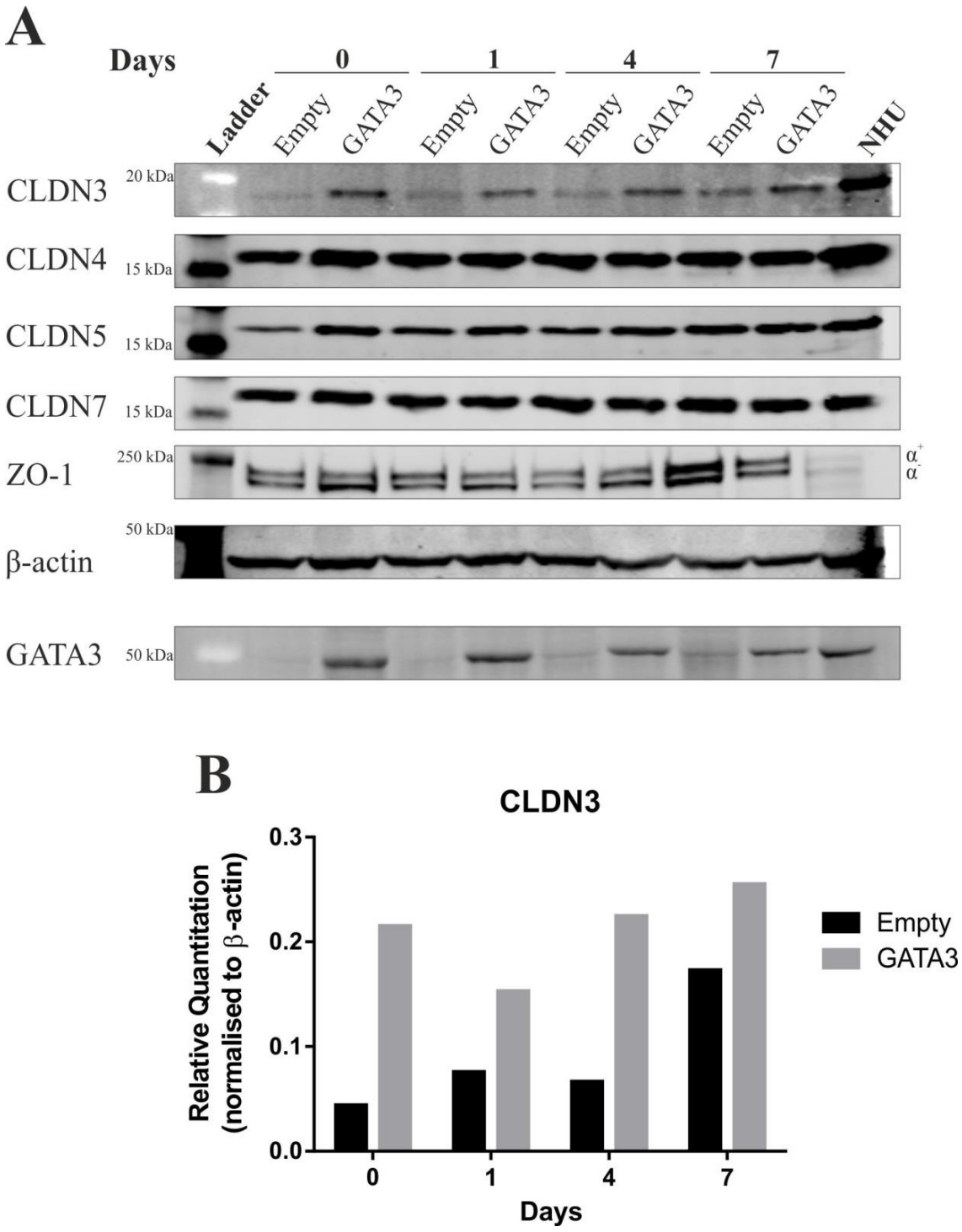

Figure 5.8 Assessment of Tight Junction-Associated Protein Expression by Western Blotting in Control and GATA3 Overexpressing NHB Cells During use of the ABS/Ca^{2+} Protocol

Figure 5.8 Evaluation of Tight Junction-Associated Protein Expression by Western Blotting in Control and GATA3 Overexpressing NHB Cells During use of the ABS/Ca^{2+} Protocol

Control (Empty) and GATA3 overexpressing NHB cells from two independent NHB cell lines (Y1595 and AS011b) were subjected to the ABS/Ca^{2+}protocol for up to 7 days. Whole protein lysates were generated on the days indicated.

A) CLDN3, CLDN4, CLDN5, CLDN7, and ZO-1 protein expression was assessed by western blotting. Evaluation of GATA3 expression demonstrated successful GATA3 overexpression at all of the time points. Western blots for the transduced NHB cell line, Y1595, are shown. β-actin was used as a loading control. Protein extracted from NHU cells (Y1336), which had been differentiated with ABS/Ca^{2+} for 5 days, was included on the same western blots, and used as a positive control. 25 μg of protein was loaded into each well.

B) Densitometry analysis of CLDN3 protein expression at each of the time points during use of the ABS/Ca^{2+} protocol. Data is shown for the western blot above, corresponding to Y1595. All values were normalised to β-actin expression.

The western blot figures for the additional cell line (AS011b), which showed similar results, can be found in Appendix 7.7.

Note clear upregulation of CLDN3 expression as a result of GATA3 overexpression in NHB cells at all time points during use of the ABS/Ca^{2+} protocol. The other tight junction-associated proteins examined were not obviously affected by GATA3 overexpression.

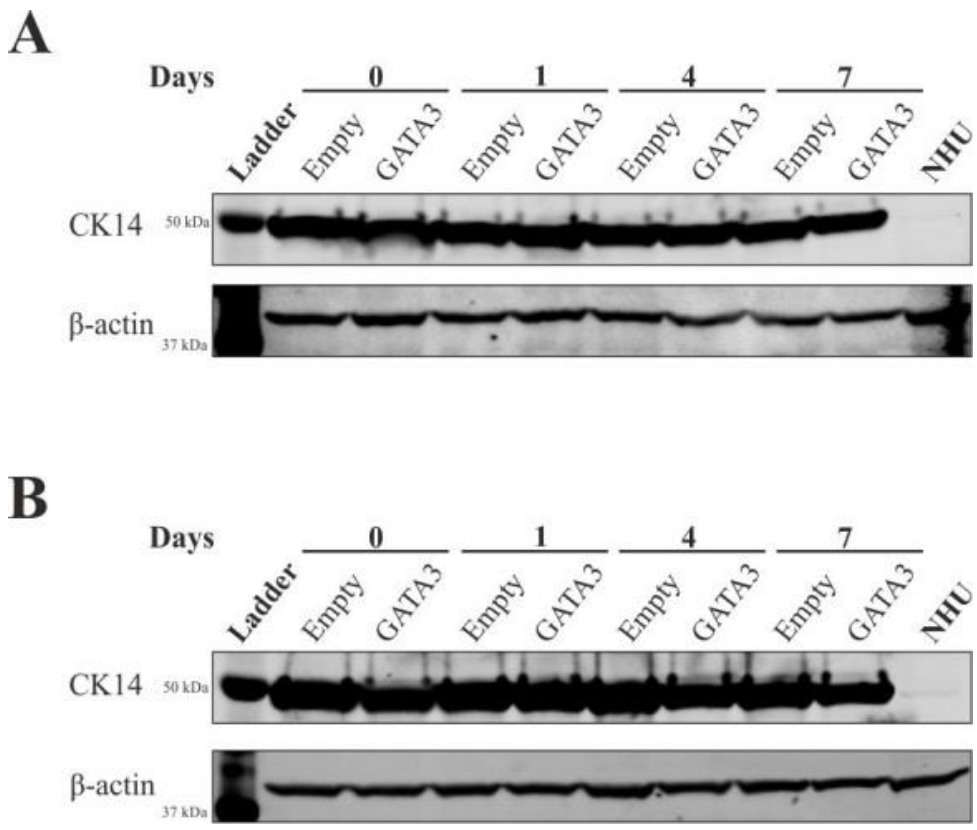

Figure 5.9 Analysis of CK14 Expression by Western Blotting in Control and GATA3 Overexpressing NHB Cells During use of the ABS/Ca^{2+} Protocol

Control (Empty) and GATA3 overexpressing NHB cells from two independent cell lines **A)** Y1595 and **B)** AS011b were subjected to the ABS/Ca^{2+}protocol for up to 7 days. Whole protein lysates were generated on the days indicated. CK14 expression was assessed by western blotting. β-actin was used as a loading control. A whole protein lystate from NHU cells (Y1336), which had been differentiated with ABS/Ca^{2+} for 5 days, was included on the same western blots for comparison. 25 μg of protein was loaded into each well. Note no reduction in CK14 expression (a squamous epithelial cell-associated protein) as a result of GATA3 overexpression in NHB cells during use of the ABS/Ca^{2+} protocol. The NHU cells showed a characteristic lack of CK14 expression.

5.4.7 Assessment of Barrier Function in Control and GATA3 Overexpressing NHB Cells During use of the ABS/Ca^{2+} Protocol

GATA3 overexpression had no obvious effect on the barrier function of NHB cells *in vitro* (Figure 5.10). Using a single transduced NHB cell line (AS011b), the TER was measured for seven days during use of the ABS/Ca^{2+} protocol. Control (eGFP) and GATA3 overexpressing cells maintained a TER below 150 $\Omega \cdot cm^2$ at all of the time points assessed.

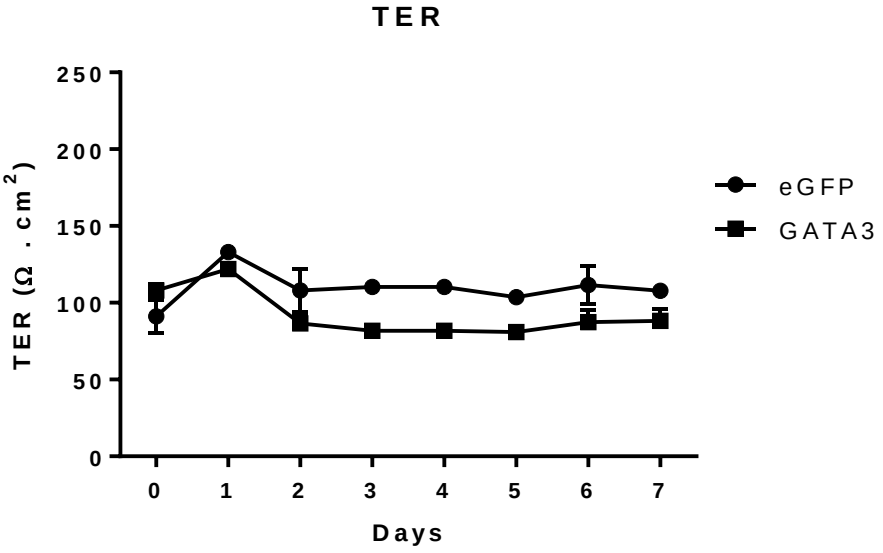

Figure 5.10 Transepithelial Electrical Resistance Measurement Time Course for Control and GATA3 Overexpressing NHB Cells During use of the ABS/Ca^{2+} Protocol
Control (eGFP) and GATA3 overexpressing NHB cells (AS011b) were pre-treated with 5% ABS for 5 days, and then passaged and seeded onto Greiner Bio-One 12-well ThinCert™ cell culture inserts. The calcium concentration was increased to 2 mM after 24 hours. The TER was measured every day for eight days. Data is shown as the mean of three technical replicates. Error bars represent the standard deviation from the mean of n = 3 technical replicates. Note there was no gain in barrier function as a result of GATA3 overexpression during use of the ABS/Ca^{2+} protocol.

5.5 Summary of Results (Chapter 5A)

- NHB cells were successfully transduced, using retrovirus, to overexpress GATA3. Successful GATA3 overexpression could be shown at both the transcript and protein levels.

- GATA3 overexpression resulted in an upregulation of ELF3 and FOXA1 (urothelium-associated transcription factors) transcript expression following treatment with TZ/PD for 72 hours. By western blotting, no obvious changes in ELF3, FOXA1 or PPARγ expression could be observed, but by immunofluorescence there appeared to be increased nuclear localisation of ELF3 as result of TZ/PD treatment in GATA3 overexpressing NHB cells.

- The expression of the urothelium-associated differentiation markers, UPK2 and UPK3B, was upregulated as a result of GATA3 overexpression, when the TZ/PD protocol was followed.

- Use of the atRA/PD protocol resulted in an increase in FOXA1 expression in both control (eGFP) and GATA3 overexpressing cells. There was no downregulation of CK14 expression as a result of GATA3 expression even when the atRA/PD protocol was followed.

- During use of the ABS/Ca^{2+} protocol, the expression of urothelial barrier function-associated tight junction protein, CLDN3, was upregulated as a result of GATA3 overexpression. The expression of other constitutively expressed tight junction proteins (CLDN4, CLDN5, CLDN7 and ZO-1) was not affected by GATA3 overexpression.

- GATA3 overexpression did not result in any gain of barrier function, as measured by TER, when the ABS/Ca^{2+} protocol was applied.

5.6 Results – Part B (PPARγ1 Overexpression)

5.6.1 PPARγ1 Overexpression in Human Buccal Epithelial Cells

NHB cells transduced to overexpress PPARγ1 had no obvious change in cell morphology in comparison to control cells (Empty) (Figure 5.11 A). Cultures grew as usual. Successful overexpression of PPARγ gene expression was demonstrated by RT-PCR (Figure 5.11 B) and RT-qPCR (Figure 5.12).

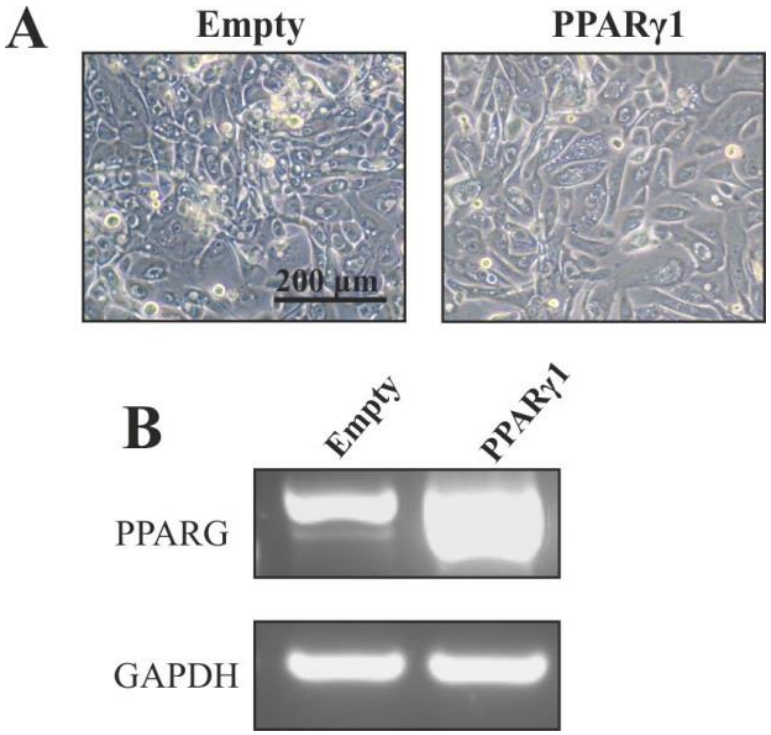

Figure 5.11 Phase Contrast Images and Analysis of PPARγ Expression by RT-PCR in Control and PPARγ1 Overexpressing NHB Cells

A) Phase contrast images of control (Empty) and PPARγ1 overexpressing NHB cells (AS011b). Scale bar = 200 µm

B) RT-PCR analysis of PPARγ gene expression in control (Empty) and PPARγ1 overexpressing NHB cells (AS011b). PPARγ PCR (primers in exon 1 and exon 6) was completed using 35 cycles. GAPDH was used as a loading control (25 cycles). Note overexpression of PPARγ transcript expression shown by RT-PCR.

5.6.2 Assessment of ELF3, FOXA1, GATA3 and PPARγ Expression after use of the TZ/PD Protocol for 72 Hours in Control and PPARγ1 Overexpressing NHB Cells

FOXA1 and GATA3 transcript expression was upregulated as a result applying the TZ/PD protocol in PPARγ1 overexpressing cells in three independent transduced cell lines (AS021b, Y1721 and AS011b) (Figure 5.12). ELF3 expression was assessed in two of the cell lines (AS021b and Y1721), and a clear upregulation of expression could be observed as a result of PPARγ1 overexpression. Overexpression of PPARγ transcript was evident in all three of the transduced NHB cell lines.

By western blotting, FOXA1 protein expression showed a dramatic, but not significant ($P > 0.05$), increase in expression in both DMSO and TZ/PD treated PPARγ1 overexpressing cells, from four independent transduced NHB cell lines (Y1600, AS027b, AS021b and AS011b) (Figure 5.13). GATA3 protein expression was weak to absent in all of the cell lines. There was no obvious change in ELF3 protein expression as a result of PPARγ1 overexpression even following use of the TZ/PD protocol.

By immunofluorescence, ELF3 expression appeared more intensely nuclear in the TZ/PD treated PPARγ1 overexpressing cells, in comparison to control (Empty) cells, in three independent transduced NHB cell lines (AS027b, Y1600, Y1656) (Figure 5.14). FOXA1 expression appeared nuclear, and a possible upregulation of expression was observed in the TZ/PD treated PPARγ1 overexpressing cells. Nuclear GATA3 expression was observed in the TZ/PD treated PPARγ1 overexpressing cells in two of the transduced cell lines (AS027b and Y1600); GATA3 expression was otherwise negative. Clear nuclear expression of PPARγ could be observed in both the DMSO and TZ/PD treated PPARγ1 overexpressing cells.

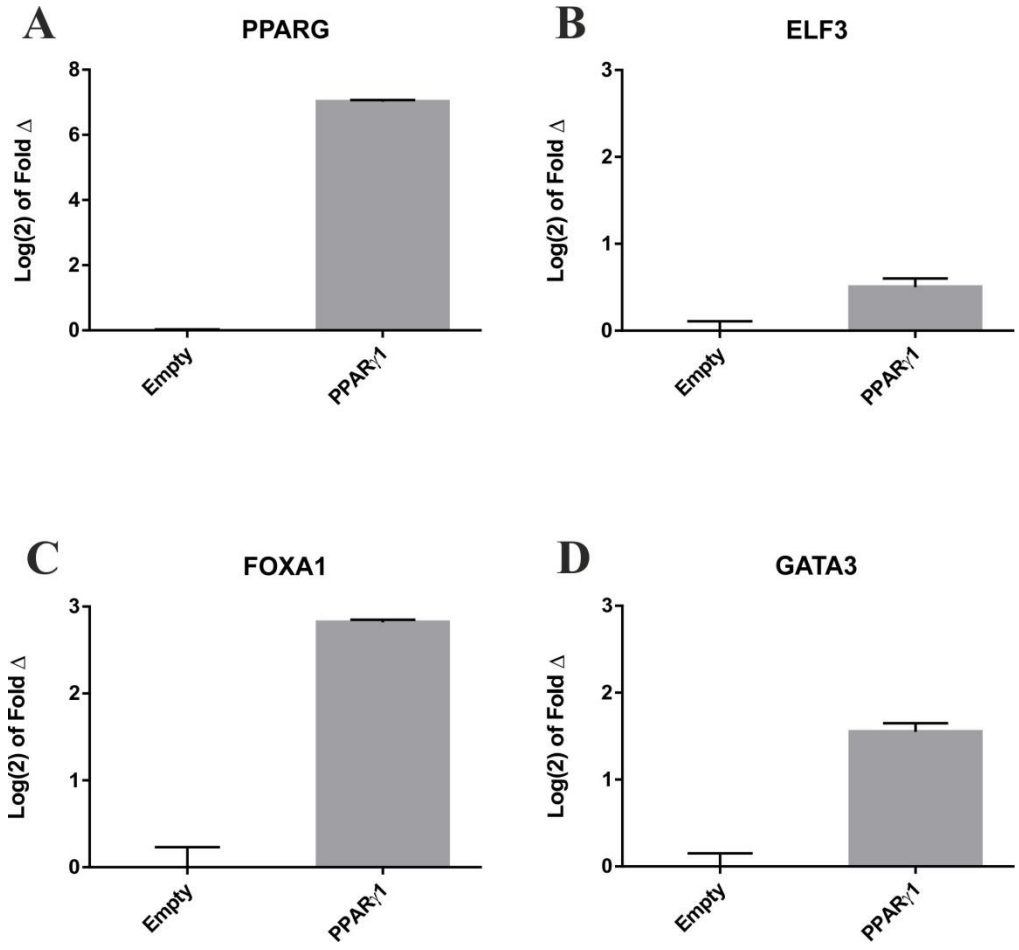

Figure 5.12 RT-qPCR Analysis of PPARG, ELF3, FOXA1 and GATA3 Transcript Expression in Control and PPARγ1 Overexpressing NHB Cells Treated with TZ/PD for 72 Hours

Control (Empty) and PPARγ1 overexpressing NHB cells (AS021b) were treated with TZ/PD for 72 hr. RNA was extracted and cDNA produced. qPCR data was generated to evaluate **A)** PPARγ, **B)** ELF3, **C)** FOXA1 and **D)** GATA3 expression. Values are shown relative to the control (Empty) cells. Gene expression was first normalised to GAPDH expression. Error bars represent the standard deviation of three technical replicates. Two additional transduced NHB cell lines (Y1721 and AS011b) were also evaluated for this experiment, and showed similar results. The figures can be found in Appendix 7.8. Note clear upregulation of ELF3, FOXA1, and GATA3 transcript expression as a result of PPARγ1 overexpression in NHB cells following use of the TZ/PD protocol.

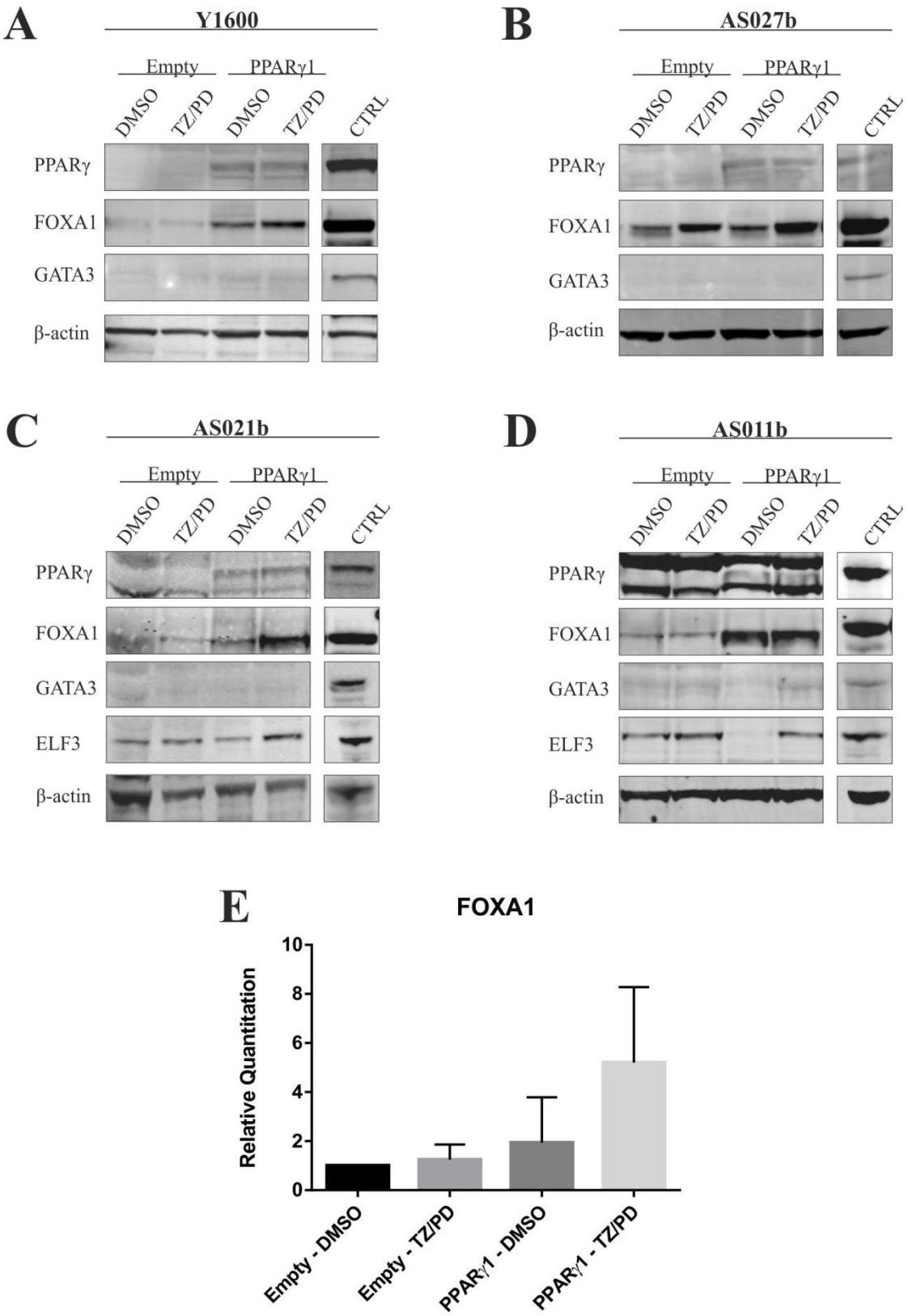

Figure 5.13 Analysis of ELF3, FOXA1, GATA3 and PPARγ Protein Expression by Western Blotting in Control and PPARγ1 Overexpressing NHB Cells Treated with either 0.1 % DMSO or TZ/PD for 72 Hours

Figure 5.13 Analysis of ELF3, FOXA1, GATA3 and PPARγ Protein Expression by Western Blotting in Control and PPARγ1 Overexpressing NHB Cells Treated with either 0.1 % DMSO or TZ/PD for 72 Hours

Control (Empty) and PPARγ1 overexpressing NHB cells, **A)** Y1600, **B)** AS027b, **C)** AS021b, **D)** AS011b, were treated with either 0.1% DMSO (vehicle control) or TZ/PD for 72 hr. Whole protein lysates were generated. ELF3, FOXA1 (Santa Cruz, Q-6), GATA3 and PPARγ (D69 for **A**, **B** and **C**; E-8 for **D**) expression was assessed by western blotting. The band corresponding to PPARγ1 (approximately 52 kDa) is shown. Various protein lysates were included on each of the blots to act as positive controls (CTRL) including RT4 cells, UMUC9 cells, and NHU cells treated with TZ/PD for 72 hours. β-actin was used as a loading control. Note clear PPARγ1 overexpression in all of the NHB cell lines. Also note the upregulation of FOXA1 expression as a result of PPARγ1 overexpression in NHB cells. ELF3 and GATA3 expression were not obviously affected by the PPARγ1 overexpression in DMSO or TZ/PD treated transduced NHB cells.
E) Densitometry analysis of FOXA1 protein expression shown relative to control cells (Empty-DMSO). All values were first normalised to β-actin. Data is shown as the mean of the four independent NHB cell lines shown above (Y1600, AS027b, AS021b, AS011b). Error bars represent the standard deviation of the mean of the four independent cell lines. Statistical analysis was completed using a one-way ANOVA test, but found no statistical difference ($P > 0.05$).

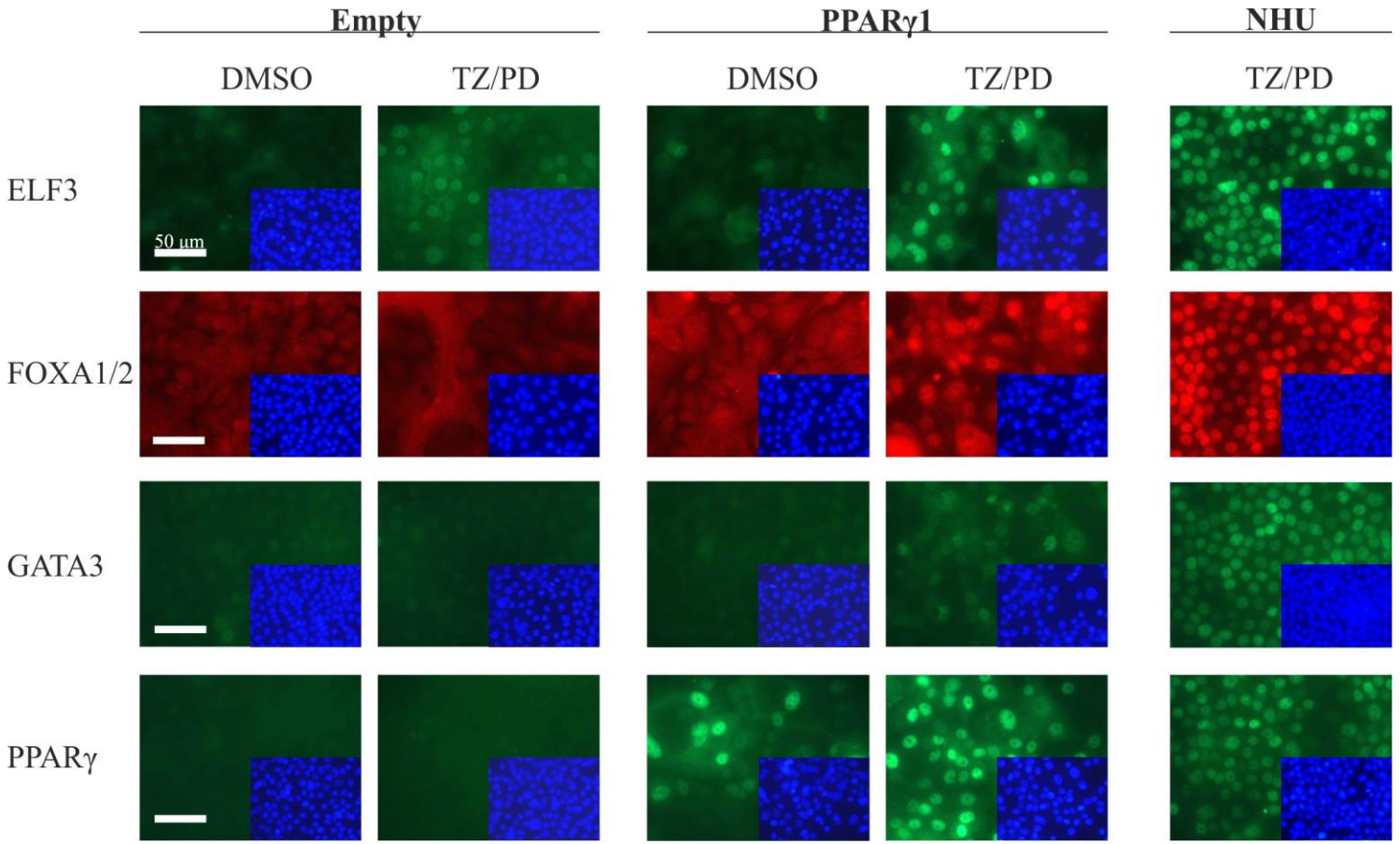

Figure 5.14 Evaluation of ELF3, FOXA1, GATA3 and PPARγ Protein Expression by Immunofluorescence Microscopy in Control and PPARγ1 Overexpressing NHB Cells Treated with 0.1 % DMSO or TZ/PD for 72 hours

Figure 5.14 Evaluation of ELF3, FOXA1, GATA3 and PPARγ Protein Expression by Immunofluorescence Microscopy in Control and PPARγ1 Overexpressing NHB Cells Treated with 0.1 % DMSO or TZ/PD for 72 hours

Control (Empty) and PPARγ1 overexpressing NHB cells (AS027b) were treated with either TZ/PD for 72 hours or 0.1% DMSO (vehicle control). Immunofluorescence labelling for ELF3, FOXA1/2 (Santa Cruz, C-20), GATA3, and PPARγ (Cell Signaling, D69) was performed on formalin-fixed slides which had been permeabilised with Triton X-100. Inset images represent the corresponding Hoechst 33258 staining to demonstrate cell density and nuclei location. Antibody labelled images were taken at the same exposure for each antibody. Hoechst 33258 images were taken at optimal exposures. NHU cells (Y1541) which had been treated with TZ/PD for 72 hours were used as a positive controls. Two additional transduced NHB cell lines (Y1600 and Y1656) were also evaluated for this experiment, and showed similar results; the figures can be found in Appendix 7.8. Note possible increased nuclear localisation of ELF3, FOXA1 and GATA3 as a result of TZ/PD treatment in PPARγ1 overexpressing cells.

5.6.3 Evaluation of Uroplakin Gene Expression in Control and PPARγ1 Overexpressing NHB Cells Treated with TZ/PD for 72 Hours

The expression of the five uroplakin genes was assessed by RT-qPCR in two independent transduced NHB cell lines (Y1721 and AS021b) following 72 hour TZ/PD treatment (Figure 5.15). The expression of UPK1A, UPK2 and UPK3B varied between the two cell lines. In one transduced cell line (Y1721), the expression of UPK1A, UPK2 and UPK3B was increased as a result of PPARγ1 overexpression, while in the other cell line (AS021b), the expression was decreased as a result of PPARγ1 overexpression. UPK1B was upregulated in both transduced cell lines as a result of PPARγ1 overexpression. UPK3A gene expression was not detectable in either cell line.

5.6.4 Evaluation of FOXA1, GATA3 and PPARγ1 Gene Expression in Control and PPARγ1 Overexpressing NHB Cells after using the atRA/PD Protocol for 72 Hours

Use of the atRA/PD protocol caused no obvious change in PPARγ1 protein expression in control or PPARγ1 overexpressing NHB cells (AS027b) (Figure 5.16). GATA3 expression appeared weak in all cases. FOXA1 expression was upregulated in PPARγ1 overexpressing cells which had been treated with either 1 μM PD153035 or 1 μM PD153035 plus 100 nM atRA.

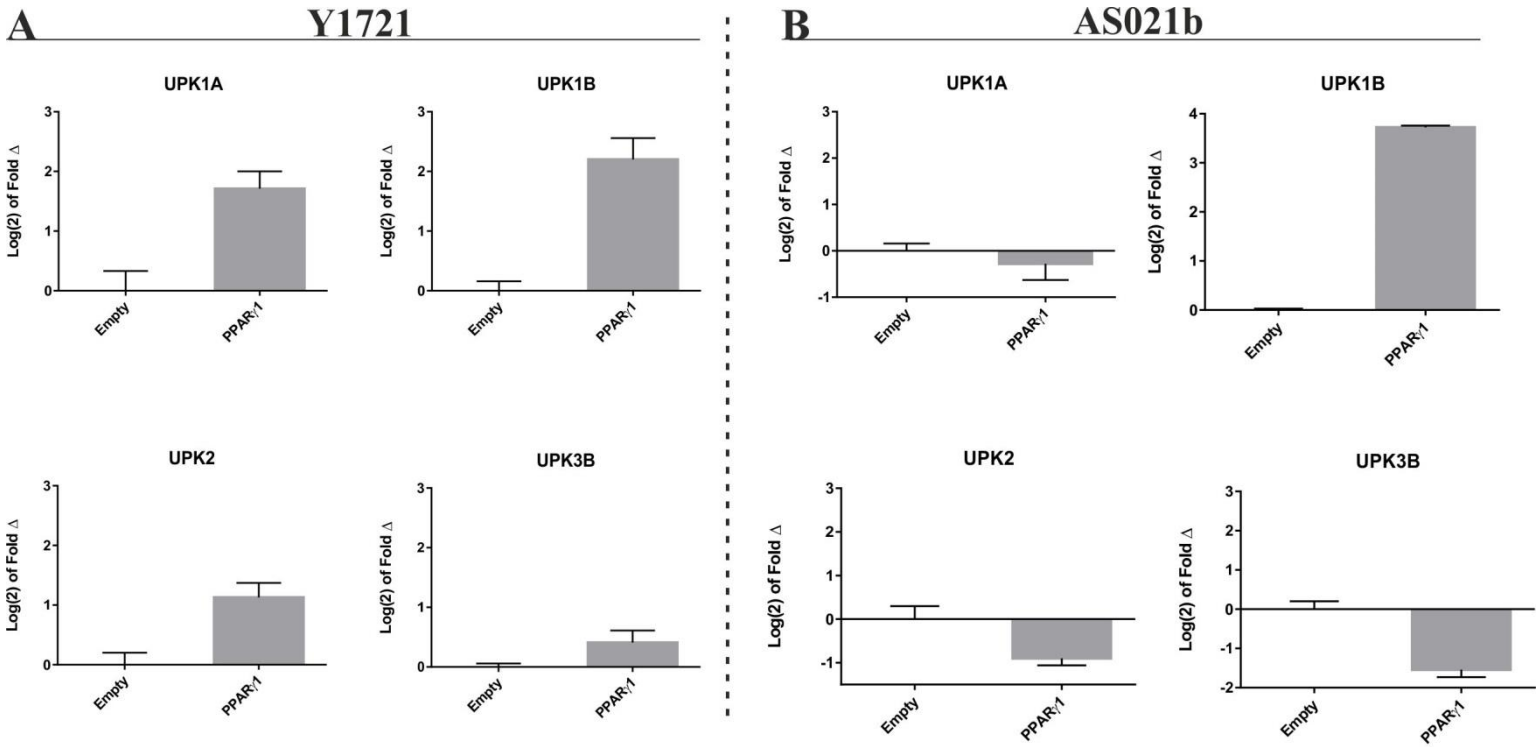

Figure 5.15 RT-qPCR Analysis of Uroplakin Gene Expression in Control and PPARγ1 Overexpressing NHB Cells treated with TZ/PD for 72 Hours

Control (Empty) and PPARγ1 overexpressing NHB cells, **A)** Y1721 and **B)** AS021b, were treated with TZ/PD for 72 hr. RNA was extracted and cDNA produced. qPCR data was generated to evaluate UPK1A, UPK1B, UPK2 and UPK3B expression. UPK3A was also evaluated but it was not expressed. Values are shown relative to the control (Empty) cells. Gene expression was first normalised to GAPDH expression. Error bars represent the standard deviation of three technical replicates. Note increased UPK1B expression in two independent transduced NHB cell lines as a result of PPARγ1 overexpression. Expression of UPK1A, UPK2 and UPK3B was variable between the two NHB cell lines.

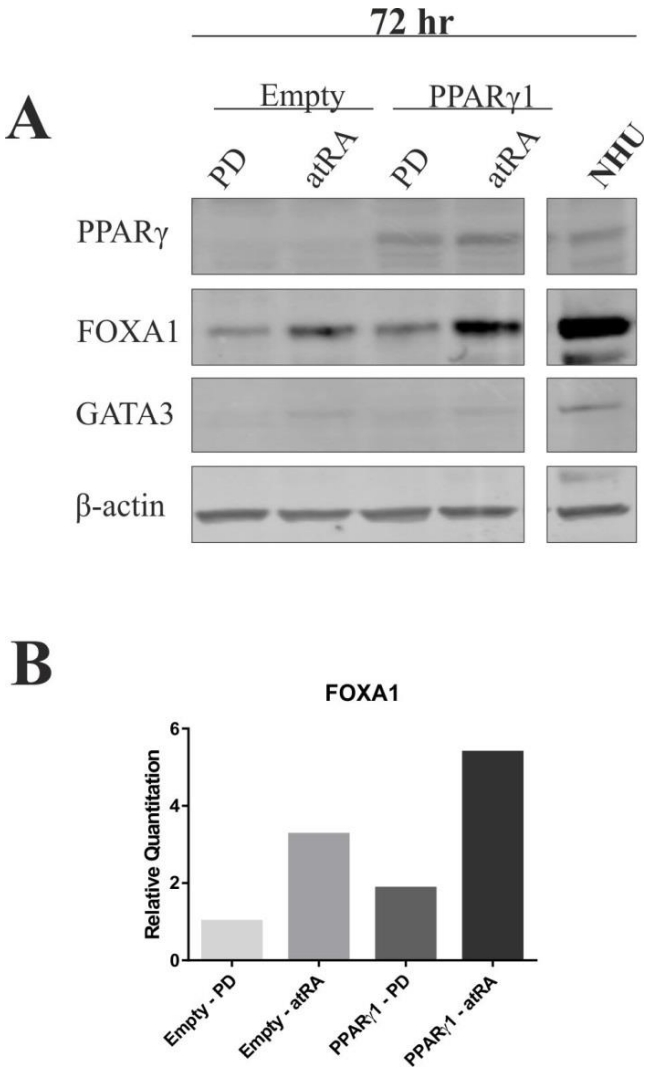

Figure 5.16 Evaluation of PPARγ, FOXA1, and GATA3 Protein Expression by Western Blotting in Control and PPARγ1 Overexpressing NHB Cells Treated with PD or atRA/PD for 72 hours

Control (Empty) and PPARγ1 overexpressing NHB cells (AS027b) were treated with either1 μM PD153035 (control) or 100 nM atRA plus 1 μM PD153035 for 72 hours.

A) PPARγ (Cell Signaling, D69), FOXA1 (Santa Cruz, Q-6), and GATA3 expression was assessed by western blotting. The band corresponding to PPARγ1 (approximately 52 kDa) is shown. β-actin was used as a loading control. NHU cells (Y1691) which had been treated with TZ/PD for 72 hours, were included on each of the western blots to act as a positive controls.

B) Densitometry analysis of FOXA1 protein expression shown relative to control cells (Empty-PD). All values were first normalised to β-actin expression.

Note upregulation of FOXA1 expression as a result of PPARγ1 overexpression in both PD and atRA/PD treated NHB cells. GATA3 expression was weak/absent in all cases.

5.6.5 Evaluation of Tight Junction Protein Expression in Control and PPARγ1 Overexpressing NHB Cells During use of the ABS/Ca^{2+} Protocol

Assessment of the expression of several tight junction proteins revealed that CLDN3 was significantly upregulated as a result of PPARγ1 overexpression during use of the ABS/Ca^{2+} protocol (Figure 5.17). CLDN4, CLDN5, CLDN7, ZO-1 and ZO-3 were all expressed in both control and PPARγ1 overexpressing cells; no obvious changes in expression were observed.

5.6.6 Evaluation FOXA1 Protein Expression in Control and PPARγ1 Overexpressing NHB Cells During use of the ABS/Ca^{2+} Protocol

Since FOXA1 expression was increased in PPARγ overexpressing cells following use of the TZ/PD and atRA/PD protocols, its expression was also assessed during use of the ABS/Ca^{2+} protocol. FOXA1 expression was also upregulated as a result of PPARγ1 overexpression during use of the ABS/Ca^{2+} protocol, although not significantly ($P > 0.05$) (Figure 5.18).

5.6.7 Assessment of CK13 and CK14 Protein Expression in Control and PPARγ1 Overexpressing NHB Cells During use of the ABS/Ca^{2+} Protocol

CK14 expression was assessed in control (Empty) and PPARγ1 overexpressing NHB cells by western blotting in three independent cell lines (AS027b, Y1721 and Y1600) differentiated with ABS/Ca^{2+} (Figure 5.19). PPARγ1 overexpression had no obvious effect on CK14 expression. Similarly, CK13 expression was assessed in two of the transduced cell lines (AS027b and Y1721) and showed no obvious change in expression as a result of PPARγ1 overexpression. NHU cells (Y1336) which had been differentiated with ABS/Ca^{2+} for 5 days were evaluated for comparison, and showed characteristic expression of CK13, and absent expression of CK14.

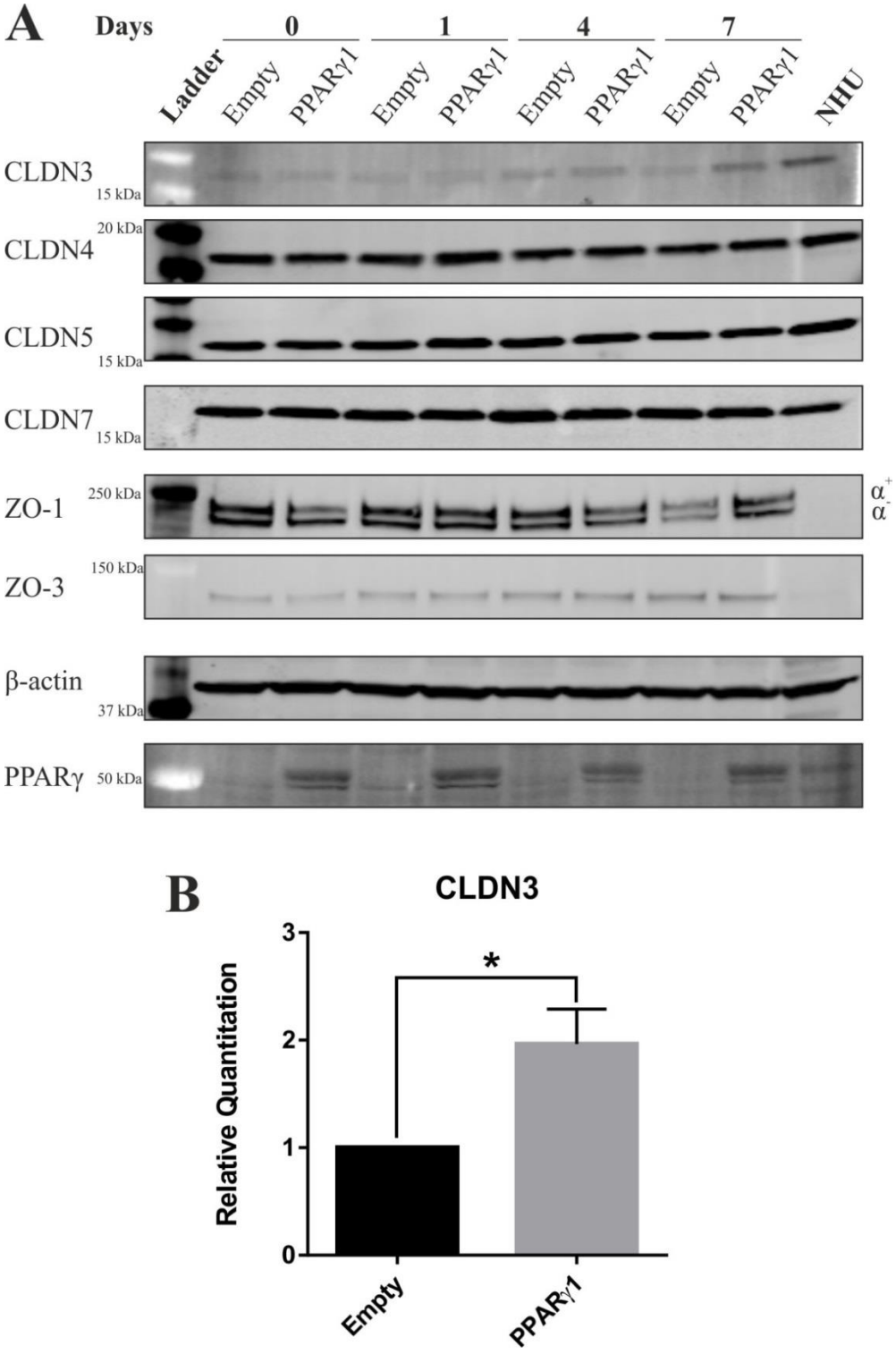

Figure 5.17 Evaluation of Tight Junction-Associated Protein Expression in Control and PPARγ1 Overexpressing NHB Cells by Western Blotting During use of the ABS/Ca^{2+} Protocol

Figure 5.17 Evaluation of Tight Junction-Associated Protein Expression in Control and PPARγ1 Overexpressing NHB Cells by Western Blotting During use of the ABS/Ca^{2+} Protocol

Control (Empty) and PPARγ1 overexpressing NHB cells from three independent cell lines (AS027b, Y1721 and Y1600) were subjected to the ABS/Ca^{2+} protocol for up to eight days. Whole protein lysates were generated on the days indicated.

A) CLDN3, CLDN4, CLDN5, CLDN7, ZO-1 and ZO-3 expression was assessed by western blotting. Western blots for the transduced NHB cell line, AS027b, are shown. β-actin was used as a loading control. Protein extracted from NHU cells (Y1336), which had been differentiated with ABS/Ca^{2+} for 5 days, was included on all of the western blots to act as a positive control/for comparison. 25 μg of protein was loaded into each well.

B) Densitometry analysis of CLDN3 protein expression at the **Day 7** time point. All values were normalised to β-actin. Expression is shown relative to control (Empty) cells. Data is shown as the mean of three independent transduced cell lines (AS027b, Y1721 and Y1600). Error bars represent the standard deviation of the mean of the three independent cell lines. Statistical analysis was performed using a two-tailed, paired t-test. * represents $P \leq 0.05$.

The western blot figures for the two additional cell lines can be found in Appendix 7.8. Note upregulation of CLDN3 protein expression at Day 4 and 7 in PPARγ1 overexpressing cells. All other tight junction-associated proteins assessed were unaffected by PPARγ1 overexpression in NHB cells during use of the ABS/Ca^{2+} protocol.

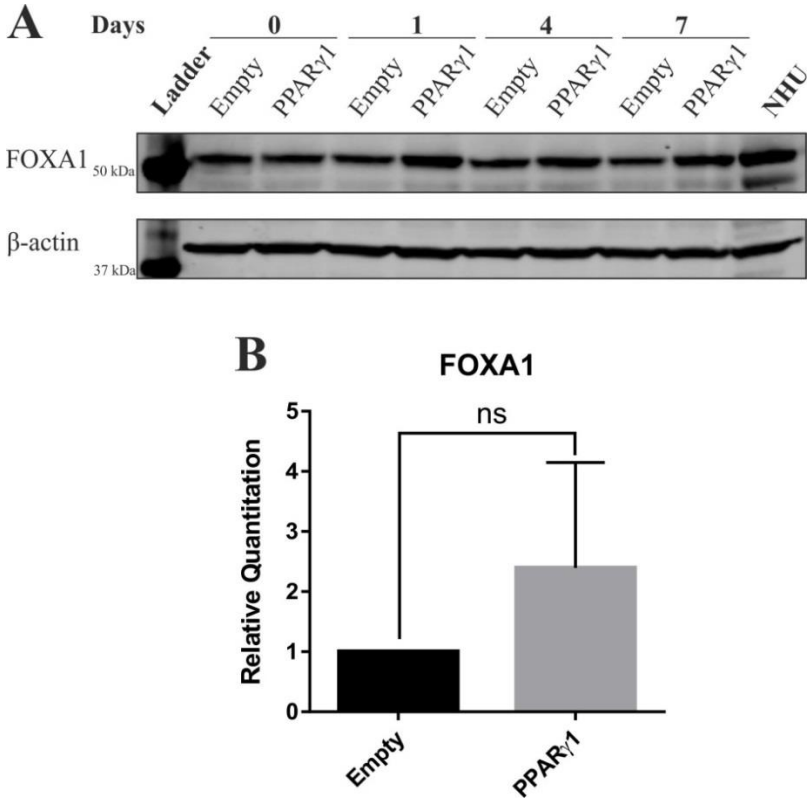

Figure 5.18 Evaluation of FOXA1 Expression in Control and PPARγ1 Overexpressing NHB Cells by Western Blotting During use of the ABS/Ca^{2+} Protocol

Control (Empty) and PPARγ1 overexpressing NHB cells from three independent cell lines (AS027b, Y1721 and Y1600) were subjected to the ABS/Ca^{2+} protocol for up to 7 days. Whole protein lysates were generated on the days indicated.

A) FOXA1 expression was assessed by western blotting. Western blots for the transduced NHB cell line, AS027b, are shown. β-actin was used as a loading control. Protein extracted from NHU cells (Y1336) which had been differentiated with ABS/Ca^{2+} for 5 days was included on all of the western blots, and used as a positive control. 25 μg of protein was loaded into each well.

B) Densitometry analysis of FOXA1 protein expression at the **Day 7** time point. All values were normalised to β-actin. Expression is shown relative to control (Empty) cells. Data is shown as the mean of three independent transduced cell lines (AS027b, Y1721 and Y1600). Error bars represent the standard deviation of the mean of the three independent transduced NHB cell lines. Statistical analysis was performed using a two-tailed, paired t-test. ns = not significant, $P > 0.05$. The western blot figures for the two additional cell lines can be found in Appendix 7.8.

Note upregulation of FOXA1 expression as a result of PPARγ1 overexpression during use of the ABS/Ca^{2+} protocol.

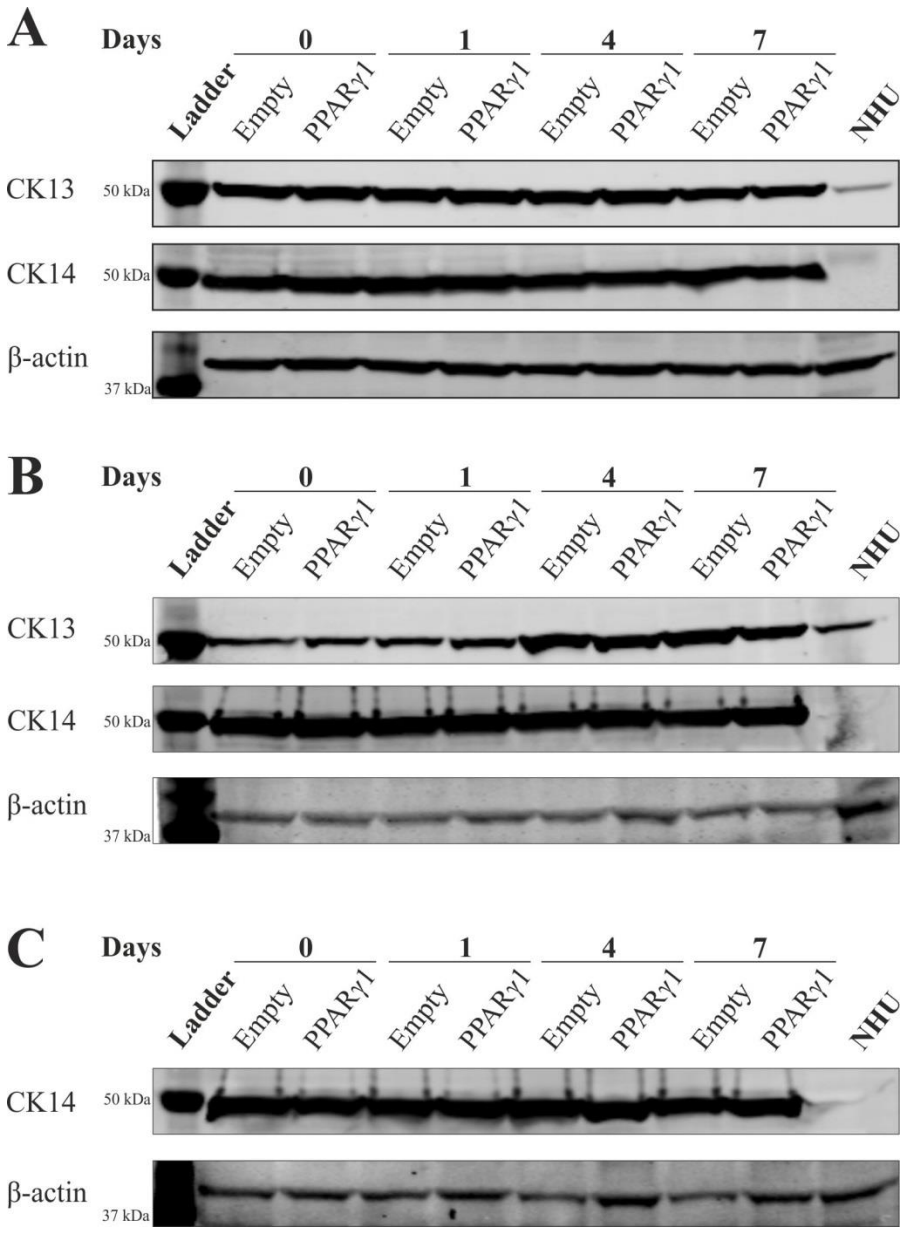

Figure 5.19 Analysis of CK13 and CK14 Expression in Control and PPARγ1 Overexpressing NHB Cells by Western Blotting During use of the ABS/Ca^{2+} Protocol

Control (Empty) and PPARγ1 overexpressing NHB cells from three independent NHB cell lines, **A)** AS027b, **B)** Y1721 and **C)** Y1600, were subjected to the ABS/Ca^{2+} protocol for up to eight days. Whole protein lysates were generated on the days indicated. CK13 and CK14 expression was assessed by western blotting. β-actin was used as a loading control. Protein extracted from NHU cells (Y1336) which had been differentiated with ABS/Ca^{2+} for 5 days were included on all of the western blots to act as a positive control/for comparison. 25 μg of protein was loaded into each well. Note there was no obvious change in CK13 or CK14 expression as a result of PPARγ1 overexpression.

5.6.8 Assessment of Barrier Function in Control and PPARγ1 Overexpressing NHB Cells

PPARγ1 overexpression had no obvious effect on the barrier function of NHB cells *in vitro* (Figure 5.20). Using a single transduced NHB cell line (Y1600), the TER was measured over seven days of the ABS/Ca^{2+} protocol. Control (Empty) and PPARγ1 overexpressing cells maintained TER measurements below 100 $\Omega \cdot cm^2$ at all of the time points assessed.

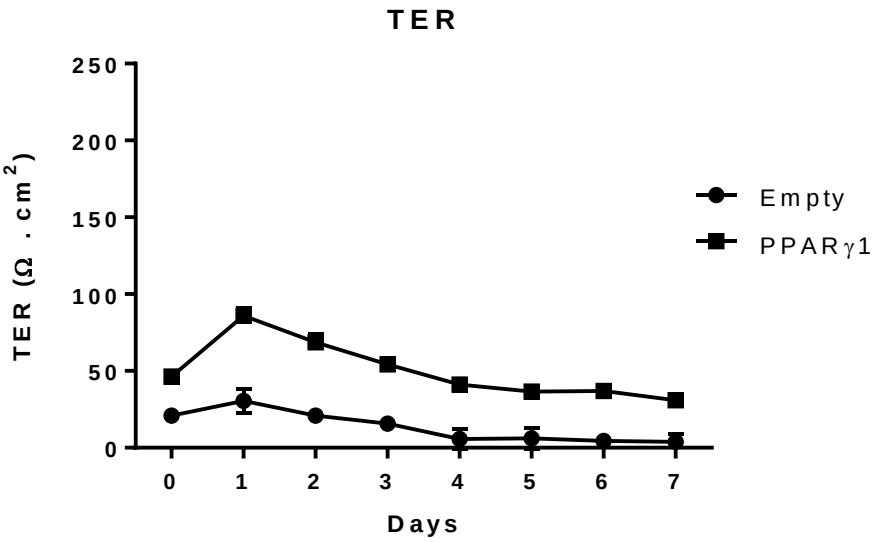

Figure 5.20 Transepithelial Electrical Resistance Measurement Time Course for Control and PPARγ1 Overexpressing NHB Cells During use of the ABS/Ca^{2+} Protocol

Control (Empty) and PPARγ1 overexpressing NHB cells (Y1600) were pre-treated with 5% ABS for 5 days, and then passaged and seeded onto Greiner Bio-One 12-well ThinCert™ cell culture inserts. The calcium concentration was increased to 2 mM following 24 hours. The TER was measured every day for eight days. Data is shown as the mean of n = 3 technical replicates. Error bars represent the standard deviation of the mean of the three technical replicates. Note no gain in barrier function as a result of PPARγ1 overexpression while using the ABS/Ca^{2+} protocol.

5.7 Summary of Results (Chapter 5B)

- NHB cells were successfully transduced, using retrovirus, to overexpress PPARγ1. Successful PPARγ1 overexpression could be shown at both the transcript and protein levels.

- PPARγ1 overexpression resulted in an upregulation of FOXA1 expression when the cells were treated with TZ/PD protocol, atRA/PD protocol, and during use of the ABS/Ca^{2+} protocol. This work suggested that when abundant PPARγ1 expression is present it acts upstream of FOXA1 expression in NHB cells.

- PPARγ1 overexpression resulted in an upregulation of ELF3 and GATA3 transcript expression in cultures treated with TZ/PD for 72 hours. By western blotting, GATA3 and ELF3 expression showed no increase in expression, but by immunofluorescence, some increased nuclear localisation was observed in the TZ/PD treated PPARγ1 overexpressing cells.

- UPK1B expression was upregulated as a result of PPARγ1 overexpression in the two transduced cell lines assessed.

- CLDN3 expression was significantly upregulated as a result of PPARγ1 overexpression during use of the ABS/Ca^{2+} protocol. The expression of other tight junction proteins (CLDN4, CLDN5, CLDN7, ZO-1 and ZO-3) was not affected.

- PPARγ1 overexpression had no effect on the squamous epithelial cell-associated protein, CK14, during use of the ABS/Ca^{2+} protocol.

- PPARγ1 overexpression did not result in any gain of barrier function, as measured by the TER, during use of the ABS/Ca^{2+} protocol.

Chapter 6:
Discussion

6 Discussion

6.1 Thesis Overview

The aim in this thesis was to investigate transcription factors involved in urothelial cell differentiation for the potential use of transdifferentiating human buccal epithelial cells into urothelial cells. To do this, first a set of transcription factors was identified which were differentially expressed between buccal epithelial cells and urothelial cells: ELF3, FOXA1, GATA3 and PPARγ. Since ELF3 and FOXA1 have been previously shown to act downstream of PPARγ in urothelial cells (Varley et al., 2009; Böck et al., 2014), PPARγ and GATA3 were identified as key upstream transcription factors to overexpress in buccal epithelial cells. The determined transcription factors (PPARγ and GATA3) were then investigated of their expression and/or role in urothelial cells to gain a better understanding of their importance to urothelial cell identity and differentiation. This work revealed that PPARγ1 was the primary PPARγ protein isoform involved in urothelial cell differentiation. Use of GATA3 knockdown in urothelial cells revealed that GATA3 likely has important regulatory roles in urothelial cell differentiation. In the final results chapter, the transcription factors GATA3 and PPARγ1 were individually overexpressed in human buccal epithelial cells, and evaluated for their ability to cause urothelial-type transdifferentiation. Although individual overexpression of the two transcription factors was unable to cause complete transdifferentiation, each were able to cause the upregulation of genes associated with urothelial cell differentiation and barrier formation.

This work has provided further evidence of the importance of ELF3, FOXA1 and PPARγ in maintaining the urothelial cell identity and promoting differentiation. It has also provided preliminary evidence in support of GATA3 as a key transcription factor in urothelial cell differentiation. Further to this, the work has provided evidence that buccal epithelial cells are likely capable of being transdifferentiated into urothelial cells, although this will probably require the combined overexpression of several of the identified transcription factors.

6.2 PPARγ Antibody Specificity

6.2.1 Western Blotting

An issue that arose with the use of the PPARγ antibodies tested in this thesis, was the presence of a number of additional proteins detected by western blotting, whether PPARγ-specific or not. Using the E-8 antibody (Santa Cruz) an obvious band could be observed directly below the PPARγ1-specific band at approximately 48 kDa in MCF-7 cells (see Appendix) and NHU cells (Chapter 4). Without appropriate positive controls, this band could easily be confused for PPARγ1 if no true PPARγ1 band was present. In addition to this lower 48 kDa band, the E-8 antibody also detected a band at approximately 58 kDa in NHU cells, which could be shown in control, TZ/PD and ABS/Ca^{2+} treated NHU cells (Figure 4.6). Georgopoulos et al. demonstrated the presence of these two additional bands, using the E-8 antibody, in control NHU cells and NHU cells which had been immortalised by the overexpression of hTERT. The authors did not draw any conclusions as to which of the protein bands corresponded to which of the PPARγ isoforms, due to lack of appropriate positive controls, and simply reported the presence of three PPARγ bands (Georgopoulos et al., 2011). The presence of this 58 kDa band detected by the E-8 antibody is very similar in height to that of anticipated full length PPARγ2. Work completed in Chapter 4 of this thesis using the PPARγ2-specific antibody (Santa Cruz, N-19) revealed that this 58 kDa band detected in NHU cells by the E-8 antibody did not correspond to PPARγ2 expression (Figure 4.7). The presence of additional bands detected by the E-8 antibody allows for possible misinterpretation of results, making it a poor choice of antibody to use in future for the detection of PPARγ expression by western blotting.

Although the D69 antibody (Cell Signaling) specifically identified both PPARγ1 and PPARγ2 in MCF-7 cells (see Appendix), with very minimal extra bands detected, when it was used on whole protein extracts from native urothelium and urothelial carcinoma-derived cell lines, several other protein bands could be detected (Figure 4.10 and Figure 4.11). Similar to the E-8 antibody, a band at approximately 58 kDa could be observed in some cell types. Use of the PPARγ2-specific antibody (Santa Cruz, N-19) again revealed that this band was not PPARγ2 protein.

The E-8 antibody is one of the most widely used antibodies for detecting PPARγ protein expression by western blotting, with data published in hundreds of papers. Its ability to detect additional protein bands at such similar heights to that of true PPARγ1 and PPARγ2 makes the ability to trust this antibody to convincingly detect PPARγ expression difficult. Similarly, the presence of this additional 58 kDa band, which could also be detected using the D69 antibody, proved that care must be taken in the interpretation of results. It became clear that in order to make use of the E-8, or D69 antibodies for detecting PPARγ by western blotting, two key additional conditions must be met: the use of rigorous positive controls for full length PPARγ1 and PPARγ2 expression, as well as the added use of a PPARγ2-specific antibody to confirm any PPARγ2 expression detected.

Interesting questions arise from this work as to the identity of these many additional bands detected by these PPARγ antibodies. Are these post-translationally modified versions of PPARγ? Are they alternative splice variants of PPARγ? Or, are they simply non-specific binding of the antibodies? A much more sophisticated analysis would need to be undertaken to answer these questions, but it is likely worth spending the time.

6.2.2 Immunofluorescence

Of the two reports demonstrating detection of PPARγ by immunofluorescence microscopy in NHU cells, both used methanol:acetone fixation and the E-8 antibody (Varley et al., 2004a; Varley et al., 2004b). Both reports demonstrated primarily cytoplasmic localisation of PPARγ in NHU cells grown at low confluence in KSFMc. When NHU cells were treated with 1 μM troglitazone, the localisation was also primarily cytoplasmic, but when the cells were treated with either 1 μM PD153035, or TZ/PD, PPARγ expression became nuclear (Varley et al., 2004a).

Work shown in the Appendix, suggested that the E-8 antibody may not be specific at detecting PPARγ expression by immunofluorescence. Using PT67 cells, a clear overexpression of PPARγ could be observed above control levels, but this could not be shown using the MCF-7 cells (see Appendix), where a similar nuclear and cytoplasmic expression was observed in all of the cell types. In addition to this, it was also shown,

using the PT67 cells, that formalin fixation of the cells was required to best observe PPARγ expression using the E-8 antibody (see Appendix). This work calls into question the observations previously made by Varley et al, and suggests that these experiments warrant being repeated using either the 81B8 or D69 antibodies, which did appear more specific to detecting PPARγ.

6.3 PPARγ Transcript Expression in Urothelial Cells

Evaluation of PPARγ expression at the transcript level in NHU cells revealed abundant expression (Figure 4.4). Use of the PPARγ2-specific PCR primers revealed very weak/absent expression (Figure 4.5), suggesting that the transcript identified using the 'total PPARγ' primers primarily contributes to PPARγ1 protein production. Of particular interest was the number of additional, smaller PCR products generated using the 'PPARγ total' primers. Since the forward primer was designed to a sequence in exon 1 and the reverse primer to a sequence in exon 6, it is possible that these smaller PCR products correspond to novel PPARγ transcript variants missing one or more internal exons. A more thorough investigation, which involves sequencing of these PCR products, would need to be undertaken to support this idea.

Several alternate PPARγ splice variants have been described in other cell types. Sabatino et al. described novel PPARγ transcript variants which were produced as the result of a read-through into intron 4. Due to an in-frame stop codon, the protein produced from the variants was missing the ligand binding domain (coded by exon 5 and 6). The authors determined that the protein acted as a dominant negative to wild-type PPARγ, and also showed that it was unable to elicit transcription using a PPRE-luciferase reporter assay (Sabatino et al., 2005). In a subsequent publication by the same group, the authors showed that expression of these novel transcript variants varied in a time-specific manner throughout human adipogenesis *in vitro* (Aprile et al., 2014). They suggested that PPARγ expression is likely heavily regulated through the expression of these alternate variants, but more work is needed to investigate this idea further.

Another truncated PPARγ variant has also been described, which is produced from the insertion of a novel exon 3' (Kim et al., 2006). Due to an in-frame stop codon, this results in the protein product missing the protein segment corresponding to exons 4, 5 and 6. The authors determined that the variant acted in a dominant negative fashion, and also showed that when it was overexpressed in Chinese hamster ovary (CHO) cells, it caused both an increase in proliferation and colony formation (Kim et al., 2006).

6.4 PPARγ Protein Expression in Urothelial Cells

Using the PPARγ total antibody, D69 (Cell Signaling), and the PPARγ2-specific antibody, N-19 (Santa Cruz), it was shown in this thesis that PPARγ1 was the most abundant PPARγ isoform present in native urothelium, cultured NHU cells, and several urothelial carcinoma-derived cell lines (Chapter 4). PPARγ2 protein expression could not be detected in any of these cell types.

In NHU cells grown in KSFMc, PPARγ1 expression was very weak, and could be difficult to detect by western blotting unless sufficient protein was loaded (typically a minimum of 25 μg) (Chapter 4). Expression was also weakly nuclear by immunofluorescence microscopy (Figure 4.9). Following induction to differentiate using TZ/PD (a PPARγ agonist and EGFR-TK inhibitor), PPARγ1 expression increased with a noticeable upregulation starting at 48 hours, and carrying on at the 72 and 144 hour TZ/PD time points, by western blotting (Figure 4.8). By immunofluorescence microscopy, treatment of the cells with TZ/PD increased the nuclear expression, with maximal expression observed at both the 72 and 144 hour time points. Treatment of NHU cells with the proteasome inhibitor, MG132, caused a striking upregulation of PPARγ1 protein expression (Figure 4.12).

The current prevailing view presented in the literature, suggests that PPARγ is highly expressed in NHU cells grown in KSFMc; two groups have previously demonstrated that NHU cells grown in KSFMc have clear and obvious PPARγ expression by western blotting (Kawakami et al., 2002; Varley et al., 2004a). As discussed in the previous section, it was also demonstrated that PPARγ expression in NHU cells grown at low

confluence in KSFMc is primarily cytoplasmic, and upon activation of PPARγ using TZ/PD, PPARγ translocates to the nucleus (Varley et al., 2004a).

Data presented in Chapter 4 supports an alternate theory, where PPARγ expression is largely labile, and is weakly nuclear in NHU cells grown to confluence in KSFMc. Following PPARγ activation using the TZ/PD protocol, PPARγ1 expression is strikingly upregulated, but due to a rapid turnover rate, caused by degradation by the proteasome, this is observed as only a slight upregulation in expression.

Georgopoulos et al. appear to have unknowingly demonstrated the upregulation of PPARγ1 protein expression in NHU cells treated with TZ/PD several years ago. Using the E-8 antibody for western blotting, the authors demonstrated the presence of three PPARγ protein bands, but did not identify which of the bands corresponded to which PPARγ isoform. Based on the results shown in this chapter, it is likely that the 'middle' band shown by Georgopoulos et al. correlates to PPARγ1 expression. If this is the case, the authors also demonstrated weak PPARγ1 expression in undifferentiated NHU cells, and showed that use of the TZ/PD protocol causes a 1.4-fold increase in expression. Their data would also suggest that in late passage NHU cells immortalised using hTERT overexpression, the upregulation of PPARγ1 as a result of TZ/PD treatment fails to occur.

Strand et al. have also published evidence which would support this alternative model of PPARγ expression in NHU cells. Using prostate epithelial cells, the authors showed that knockdown of PPARγ2 expression results in the de novo expression of CK20, a protein expressed only in the superficial cells of the urothelium, which suggested that the presence of PPARγ2 expression was inhibitory to urothelial-type differentiation (Strand et al., 2013). This result agrees with the observations shown in Chapter 4 which demonstrate a lack of PPARγ2 expression in native urothelium, in NHU cells grown in KSFMc, and in NHU cells induced to differentiate using the TZ/PD protocol. Strand et al. also demonstrated that the knockdown of both PPARγ1 and PPARγ2 resulted in the loss of differentiation-associated genes, and caused an increase in CK14 expression. This result also supports the work presented in Chapter 4, where it was shown that PPARγ expression is weak in NHU cells grown in KSFMc. It is well established that

NHU cells grown in KSFMc express CK14, are highly proliferative, and fail to express genes associated with urothelial differentiation (Varley et al., 2004a; Varley et al., 2004b; Varley et al., 2006).

6.5 The Involvement of GATA3 in Urothelial Cell Differentiation

GATA3 expression was upregulated upon activation of PPARγ in NHU cells using the TZ/PD protocol; this could be observed at the transcript level as early as 12 hours following the start of TZ/PD treatment (Figure 4.3). By western blotting, GATA3 expression was noticeably upregulated at the 72 and 144 hour TZ/PD time points (Figure 4.8). The PPARγ antagonist, T0070907, prior to TZ/PD, resulted in an inhibition of GATA3 upregulation, which was shown by RT-PCR (Figure 4.2). Together these results begin to suggest that GATA3 may act downstream of PPARγ in the transcription factor cascade that regulates urothelial differentiation; these results need further investigation in additional cell lines and using additional experimental methods (western blotting, RT-qPCR) to provide convincing evidence. In contrast to this, knockdown of GATA3 expression, prior to PPARγ activation, resulted in a significant downregulation of PPARγ transcript expression (Figure 4.14). This result suggested the opposite notion, where GATA3 acts upstream of PPARγ. GATA3 was also shown to have key roles in the differentiation of urothelial cells; both CK13 and UPK2 expression were significantly downregulated as a result of GATA3 knockdown (Figure 4.16).

Tong et al. have shown that during adipocyte differentiation, GATA3 is highly expressed in preadipocytes, but as the cells are induced to differentiate into mature adipocytes, GATA3 expression is lost while PPARγ expression is upregulated. Forced expression of GATA3 in murine adipocyte precursor cells prevented their ability to undergo adipocyte differentiation. In addition to this, the authors also demonstrated that embryonic stem (ES) cells, which were deficient in GATA3, had a greater propensity for adipocyte differentiation than control ES cells (Tong et al., 2000). This work suggested an inhibitory role for GATA3 in adipogenesis. The authors further demonstrated that this inhibitory role was, in part, due to direct binding of GATA3 to

the PPARγ2 promoter, preventing transcription (Tong et al., 2000). GATA3 has also been shown to have a positive regulatory role on PPARγ expression; work completed in murine T helper 2 (Th2) cells has shown that GATA3 was able to both bind to and positively regulate PPARγ gene expression, with expression of both genes being important for Th2 cell differentiation (Wei et al., 2011).

Work presented in this chapter provides evidence suggesting that neither PPARγ nor GATA3 is truly upstream of the other in urothelial cell differentiation, and that both PPARγ and GATA3 may be important for positively regulating each others expression.

6.6 Use of Buccal Epithelial Cells for Bladder Tissue Engineering

One of the possible methods that has been suggested for obtaining surrogate epithelial cells for bladder tissue engineering was to simply use another known barrier forming epithelial cell type. The main epithelial cell type suggested for this in the literature has been buccal epithelial cells (Lu et al., 2010; Watanabe et al., 2011), since buccal mucosa is already used as a grafted tissue for urology-based applications (reviewed in Markiewicz et al., 2007). The use of buccal epithelial cells for bladder tissue engineering has already been investigated by Watanabe et al., with some mixed results. The authors applied a composite cystoplasty approach, where autologous buccal epithelial cell sheets were produced, and then transplanted into the bladder of dogs. The authors found that direct transplant of the buccal epithelial cell sheets into the bladder resulted in loss of the cell sheets, with much of the grafts containing no epithelium after three weeks. This work suggested that direct use of buccal epithelial cell sheets in the bladder is not sufficient for bladder tissue-engineering. In order for the cell sheets to survive in the bladder, the authors demonstrated that the cell sheets must first be implanted in a latex poach in the abdomen for five days, before implantation in the bladder. This resulted in successful production of a stratified squamous epithelium in the bladder after three weeks.

Work presented in this thesis does not support or refute the use of buccal epithelial cells for bladder tissue engineering. What became clear throughout the work, was that major differences between buccal epithelial cells and urothelial cells exist. The most striking difference, which is likely most relevant for bladder tissue-engineering, was the inability of buccal epithelial cell sheets to form a functional barrier, as measured by TER (Figure 3.19). The work raises questions as to whether *in vitro* generated buccal epithelial cell sheets have the long term capacity to sustain barrier function and survive in the bladder. The result may provide a possible reason why the cell sheets produced by Watanabe et al. failed to survive in the bladder following direct implantation. Long term studies assessing the capacity for direct buccal mucosa grafts to survive in the bladder have shown relatively positive results, with no major adverse effects to the epithelium; this work suggested that the cells can survive in the bladder long term. It is therefore possible that the alternate approach taken by Watanabe et al., which relied on pre-implantation of the cell sheets in the abdomen, away from the bladder microenvironment, may be a key necessary step in preparing the cells for use, allowing them to develop a more mature barrier function. Long term studies using this alternate method of implantation are necessary to ascertain whether buccal epithelial cells on their own could be used for bladder tissue-engineering.

One of the groups studying the effect of the bladder microenvironment on direct buccal mucosa grafts, provided evidence of UPK2 expression in transplanted buccal mucosa following 6 and 12 months in the bladder of pigs. The authors suggested that this demonstrated the transdifferentiation potential of buccal epithelial cells. Work presented in this thesis demonstrated that human buccal epithelial cells *in vitro* are capable of expressing UPK2 (Figure 3.13), which suggested that UPK2 gene expression alone may not be an appropriate predictor of urothelial-type differentiation. It is probably unlikely that the bladder microenvironment itself would be capable of transdifferentiating buccal epithelial cells into urothelial cells, as urine has been shown to have no urothelial differentiation-associated signalling capacity (Stahlschmidt et al., 2005). Whether signalling from the underlying stroma and/or adjacent urothelial cells could have the capacity to cause urothelial-type transdifferentiation is not yet known. Based on the results shown by Lu et al. it appears most likely that the UPK2 expression observed is attributed to ingrowth of adjacent urothelium.

6.7 Identification of Differentially Expressed Transcription Factors Between Buccal Epithelial Cells and Urothelial Cells

The differentiation of urothelial cells is thought to be controlled by a tightly regulated cascade of transcription factor expression. In this thesis, the expression of seven transcription factors known to be important for urothelial cell differentiation (ELF3, FOXA1, GATA3, GRHL3, IRF1, KLF5 and PPARγ) was investigated in buccal epithelial cells (Figure 3.5). Of these transcription factors, PPARγ has been previously implicated as a key upstream transcription factor in human urothelial cell differentiation (Varley et al., 2004a; Varley et al., 2004b; Varley et al., 2006). Other key transcription factors, ELF3 and FOXA1, have been shown to act directly downstream of PPARγ in urothelial cell differentiation (Varley et al., 2009; Böck et al., 2014). Further to this, work presented in this thesis demonstrated that GATA3 may also act downstream of PPARγ, but that it is also capable of regulating PPARγ expression, suggesting that a feedback loop exists between PPARγ and GATA3 in urothelial cell differentiation. In addition to human *in vitro* work, previous work using mouse models identified GRHL3 and KLF5 as key transcription factors involved in urothelial cell differentiation and barrier function (Yu et al., 2009; Bell et al., 2011).

The work in this thesis evaluating the expression of transcription factors known to be important for urothelial cell identity and differentiation, revealed noticeably weak expression of ELF3, FOXA1, GATA3 and PPARγ in buccal epithelial cells. In addition to this, the expression of FOXA1, GATA3 and PPARγ could not be significantly upregulated as a result of using the TZ/PD protocol (Figure 3.6), suggesting that activation of PPARγ does not occur in human buccal epithelial cells. FOXA1 expression was able to be upregulated by other methods (atRA treatment) (Figure 3.10), indicating that at least FOXA1 is capable of being upregulated in buccal epithelial cells. These results highlighted key differences in the expression of transcription factors that play important roles in the differentiation of urothelial cells.

Previous work investigating the effect of PPARγ agonists on the differentiation of squamous epithelial cells from skin has shown that they are able to cause some upregulation of the squamous terminal differentiation-associated genes involucrin and transglutaminase-1 (Westergaard et al., 2001; Mao-Qiang et al., 2004). Neither of the groups investigated whether this was specifically as a result of PPARγ activation or due to off-target effects of the drugs. Westergaard et al. also investigated the expression of the three PPAR nuclear receptors (α, γ, δ) in normal human keratinocytes *in vitro,* when the cells were grown in KSFM with added bovine pituitary extract and epidermal growth factor. The authors found absent expression of PPARγ2, weak expression of PPARα and PPARγ1, and abundant expression of PPARδ (40 μg of protein was loaded). The work identified PPARδ as the predominant PPAR isoform in keratinocytes. Mao-Qiang demonstrated that knockout of PPARγ in the skin of mice did not result in any obvious changes to the epithelium. These results altogether suggesting that PPARγ likely does not play an essential role in squamous epithelial cell differentiation.

The results presented in this thesis also suggest that the combined weak expression of FOXA1, GATA3 and PPARγ may be a key indicator of the basal, squamous cell state. This is in agreement with the work presented in Chapter 4, which demonstrated that low expression of FOXA1, GATA3 and PPARγ was associated with urothelial cells in their undifferentiated, basal state (grown in KSFMc). This line of thinking is in further agreement with bladder cancer research, where low expression of FOXA1, GATA3 and PPARγ is associated with basal muscle invasive bladder cancers, as well as with squamous cell carcinoma of the bladder (Biton et al., 2014; Damrauer et al., 2014; Eriksson et al., 2015).

When GATA3 and PPARγ1 were individually overexpressed in human buccal epithelial cells, neither factor was able to cause significant upregulation of the other even when subjected to the TZ/PD or ABS/Ca^{2+} protocols. This work suggested that in buccal epithelial cells, either that GATA3 and PPARγ1 act independently of one another, or that both factors are heavily repressed and inaccessible to the other factor.

6.7.1 FOXA1 Expression

There were several interesting observations pertaining to FOXA1 expression observed in the results shown in this thesis, which are discussed below.

6.7.1.1 PPARγ1 and FOXA1

PPARγ has been shown to act directly upstream of FOXA1 in the regulation urothelial cell differentiation (Varley et al., 2009). Results from this thesis identified PPARγ1 as the primary PPARγ protein isoform involved in urothelial cell differentiation, which suggests that it is PPARγ1 which acts directly upstream of FOXA1.

Overexpression of PPARγ1 in buccal epithelial cells resulted in the upregulation of FOXA1 expression in both control (0.1 % DMSO) and TZ/PD treated cells (Figure 5.13). This work suggested that simply the presence of PPARγ1 expression (ie. without exogenous ligand activation) is able to transactivate FOXA1 expression in buccal epithelial cells. Upon attempts to activate PPARγ using the TZ/PD protocol, FOXA1 expression was further upregulated. This work demonstrated that when abundant PPARγ1 protein is present, it can transactivate the FOXA1 transcription factor pathway in human buccal epithelial cells.

6.7.1.2 GATA3 and FOXA1

Investigation into the effect of GATA3 knockdown on urothelial cell differentiation revealed that knockdown of GATA3 expression had no significant effect on FOXA1 transcript or protein expression (Figure 4.15). This was true even though knockdown of GATA3 appeared to downregulate PPARγ gene expression (Figure 4.14). These results indicated that in urothelial cell differentiation, GATA3 appears to act independently of FOXA1 expression. This was further shown in human buccal epithelial cells where overexpression of GATA3 failed to cause any upregulation of FOXA1 protein expression in any of the cell culture systems examined.

In breast epithelial cell differentiation and cancer progression, GATA3 has been shown to act directly upstream of FOXA1, and this interaction has been shown to be particularly important for mediating ESRα expression (Kouros-Mehr et al., 2006;

Theodorou et al., 2013). GATA3, FOXA1 and ESRα have also been shown to act as an 'enhanceosome' in order to elicit maximal expression from estrogen-responsive genes in ESRα-positive breast cancers (Kong et al., 2011). These results altogether indicate an essential role for the interaction of GATA3 and FOXA1 in breast epithelial cells.

The results presented in this thesis identify a striking difference between FOXA1 and GATA3 regulation in human buccal epithelial cells, urothelial cells, and those previously published in breast epithelial cells. These differences appear to be related to distinct differences in nuclear receptor signaling, since the estrogen receptors are not readily associated with squamous or urothelial-type differentiation. These differences in nuclear receptor usage appear to lead to major differences in transcription factor regulation.

6.7.1.3 Retinoic Acid and FOXA1

The retinoic acid receptors have been implicated as key upstream regulators of urothelium development, differentiation, and in particular in inhibiting squamous epithelial cell gene expression (Southgate et al., 1994; Mauney et al., 2010; Gandhi et al., 2013; Kang et al., 2014b). Results in this thesis demonstrated that FOXA1 transcript and protein expression could be upregulated in human buccal epithelial cells as a result of treatment with all-trans retinoic acid (Figure 3.9 and Figure 3.10). Previous work in murine embryonic carcinoma cell lines has shown the presence of a RARE in the FOXA1 promoter (Jacob et al., 1999). The authors also demonstrated that the RARs interact directly with the FOXA1 promoter to elicit gene expression.

Although this phenomenon was not investigated in urothelial cells in this thesis, questions arise as to whether retinoic acid could also be a key regulator of FOXA1 expression in urothelial cell differentiation, and in turn be a key transcription factor involved in preventing squamous-type differentiation. FOXA1 has previously been indicated as having a role in preventing squamous differentiation in a mouse model (Reddy et al., 2015), although a link to retinoic acid signalling was not discussed. Investigation into a link between retinoic acid signalling, FOXA1, and preventing squamous differentiation in human urothelial cells would be very interesting.

6.8 Uroplakins as Markers of Urothelial Cell Differentiation

The expression of the uroplakin genes has been primarily associated with urothelial cells, and they are known to be key protein components of the urothelium-specific asymmetric unit membrane (Sun et al., 1996; Deng et al., 2002). While the expression of UPK1B and UPK3B has been previously described in other cell types including corneal epithelium and mesothelium (Adachi et al., 2000; Kanamori-Katayama et al., 2011; Rudat et al., 2014), respectively, the prevailing view in the literature has been that expression of the uroplakin genes is the ultimate urothelium-specific marker. This is particularly true in studies which have aimed to convert multipotent or pluripotent stem cells into urothelial cells (Tian et al., 2010; Wu et al., 2013; Osborn et al., 2014).

The work presented in this thesis demonstrated low abundance transcript expression of UPK1A, UPK1B, and UPK2 in human buccal epithelial cells, along with considerable expression of UPK3B (Figure 3.13). Use of the TZ/PD protocol resulted in the upregulation of UPK1A, UPK1B, UPK2 and UPK3B gene expression in buccal epithelial cells, with UPK2 and UPK3B expression being significantly upregulated. Further to this, overexpression of GATA3 and PPARγ1 in human buccal epithelial cells resulted in additional upregulation of several of the uroplakin genes when the cells were treated with TZ/PD (Figure 5.5 and Figure 5.15). The ability to detect any uroplakin gene expression in buccal epithelial cells was a surprising and unexpected result, as there have only been a few reports of uroplakin gene expression in other cell types (Adachi et al., 2000; Kanamori-Katayama et al., 2011; Rudat et al., 2014). These results indicate that in addition to UPK1B and UPK3B expression being non-specific to urothelial cells, UPK1A and UPK2 are also able to be expressed in other cell types.

These results have particular implications for reprogramming and transdifferentiation-type experiments, when attempting to convert any cell type into urothelial cells. In recent years, many attempts have been made to convert various types of multipotent and pluripotent stem cells into urothelial cells. Of these attempts, the primary evidence used to demonstrate successful conversion to urothelial cells, as opposed to other epithelial cell types, has been to show upregulated expression of one or more of the uroplakin genes. The work presented in this thesis suggests that demonstrating upregulated expression of the uroplakin genes is not enough to distinguish urothelial cells from other

epithelial cell types. In particular, demonstrating the upregulation as relative fold-change RT-qPCR data, where low abundance expression can be made to look more impressive than it actually is. Since UPK3A expression could never be shown in buccal epithelial cells, the ability to demonstrate considerable UPK3A expression may be the most appropriate marker of urothelial cell specificity and differentiation.

One interesting question that arose from the work in this thesis, investigating uroplakin gene expression, was which aspect of the TZ/PD protocol was able to cause the upregulation of the uroplakin genes in buccal epithelial cells. In urothelial cells, uroplakin gene expression appears to be regulated specifically by PPARγ expression (Varley et al., 2004a), but work in this thesis suggested that PPARγ activation did not occur in buccal epithelial cells treated with TZ/PD. It is therefore plausible that the upregulation of the uroplakin genes may have been due to off-target effects of the drugs, or due to the effects of the PD153035, indicating that other transcription factors, in addition to those downstream of PPARγ, may be able to regulate uroplakin gene expression.

6.9 Barrier Function and Tight Junction-Associated Gene Expression

The urothelium is known to be one of the tightest barrier epithelia in the human body, with its primary function to act as a barrier to urine. The barrier function of the urothelium is attributed to two main features: highly specialised tight junctions and the presence of the AUM (reviewed in Khandelwal et al., 2009). The barrier function of buccal epithelium in contrast, is considered to be similar to that of skin, relying on the terminal differentiation of the epithelial cells, and the formation of a complex matrix of intracellular proteins and extracellular lipids (reviewed in Kalinin et al., 2002).

Cross et al. originally demonstrated that when NHU cells were induced to differentiate using the ABS/Ca^{2+} protocol, they were able to form a functional barrier epithelium as measured by TER and permeability assays. Barrier function in human urothelial cells

does not occur when the cells are grown in KSFMc (Cross et al., 2005) or during use of the TZ/PD protocol (Fleming, 2008), even though the TZ/PD protocol is able to upregulate key tight junction-associated proteins (Varley et al., 2006).

Work presented in this thesis demonstrated that human buccal epithelial cells fail to form a functional barrier, as measured by the TER, following use of the ABS/Ca^{2+} protocol (Figure 3.19); the TER values remained below 200 $\Omega \cdot cm^2$ at all of the time point assessed. This remained true even following the individual overexpression of GATA3 and PPARγ1 (Figure 5.10 and Figure 5.20). These result demonstrated an important functional difference between buccal epithelial cells and urothelial cells. The work has key implications for reprogramming and transdifferentiation-type experiments, where of the many attempts to convert multipotent and pluripotent stem cells into urothelial cells, only two of the groups demonstrated the measurement of barrier function as an assessment of successful differentiation to urothelial cells (Bharadwaj et al., 2013; Kang et al., 2014b). In both cases, permeability assays were performed, and the results were shown as relative change, making it difficult to infer whether barrier function was actually attained. Results from this thesis have identified gain of barrier function as a unique and important feature of urothelial cell differentiation, suggesting that assessment of barrier function may be a key test for successfully demonstrating urothelial cell differentiation.

The expression of key urothelium barrier-associated proteins, CLDN3, -4 and -5, has been previously shown to be regulated by PPARγ in human urothelial cells (Varley et al., 2006). Work shown in this thesis demonstrated a similar expression profile of claudins 1-10 in buccal epithelial cells treated with TZ/PD in comparison to urothelial cells (Figure 3.15). This work demonstrated that much of the same claudin genes are capable of being expressed in buccal epithelial cells and urothelial cells. Future work investigating the exact transcription factor regulatory networks governing claudin gene expression may be important for revealing key differences in barrier function. In particular, an assessment of whether PPARγ specifically plays a role in claudin gene expression in buccal epithelial cells is necessary.

Evaluation of the expression of CLDN4, -5 and -7 in the human buccal epithelial cell sheets revealed that while their expression was present at the intercellular borders, it was restricted to only the upper half of the cell layers (Figure 3.16). In contrast, expression of these same three claudin proteins in urothelial cell sheets was identified throughout all of the cell layers. This work identified that although each of the cell types express these claudin proteins, they have distinct localisations. This work demonstrated the importance of using immunohistochemical and/or immunofluorescence-based experiments for assessing protein localisation, as an additional tool to techniques like western blotting, which simply assess protein abundance. The work identified a potential reason for the lack of barrier function of the buccal epithelial cell sheets. Future work evaluating a wider panel of claudin proteins expressed may reveal even more striking differences by immunohistochemistry.

CLDN3 in particular has been shown to be critical for the barrier function of urothelial cells, as knockdown of CLDN3 resulted in complete ablation of barrier function in NHU cells *in vitro* (Smith et al., 2015). The authors also showed that gain of the ZO-1α+ protein isoform in urothelial cells appeared to be associated with urothelial cell differentiation and barrier function. Assessment of CLDN3 in human buccal epithelial cells revealed weak protein expression by western blotting during use of the ABS/Ca^{2+} protocol. Both GATA3 overexpression and PPARγ1 overexpression in human buccal epithelial cells appeared to upregulate CLDN3 expression (Figure 5.8 and Figure 5.17), although in both cases, the transduced buccal epithelial cells failed to form a functional barrier epithelium. Assessment of ZO-1 expression in human buccal epithelial cells during use of the ABS/Ca^{2+} protocol revealed that both of the ZO-1 protein isoforms were expressed at all of the time points assessed. This work further identified that although key barrier forming tight junction proteins can be expressed in buccal epithelial cells, their expression alone fails to result in barrier formation. This work further suggested that it is likely differences in the localisation of the tight junction proteins that may be critical for barrier formation.

6.10 Criteria for Demonstrating Successful Conversion of a Cell Type into Urothelial Cells

Work presented in this thesis identified many key differences between human buccal epithelial cells and urothelial cells, which have important implications for urothelial-type reprogramming and transdifferentiation experiments. The work made it clear that a more rigorous set of standards must be generated for assessing successful urothelial-type differentiation. This should likely include a more exhaustive panel of markers, as well as a set of functional assays assessing both the transcellular and paracellular barrier function.

Based on the work shown in this thesis, several key tests to consider for future urothelial-type reprogramming experiments have been identified:

1. **Demonstrating Considerable Expression of FOXA1, GATA3 and PPARγ**

ELF3, FOXA1, GATA3 and PPARγ expression was weak in buccal epithelial cells even upon use of the TZ/PD and/or ABS/Ca^{2+} protocols. The ability to demonstrate considerable expression of these four transcription factors is likely an important test for distinguishing squamous-type epithelial cells and urothelial cells.

2. **Demonstrating Loss of CK14 Protein Expression**

CK14 expression was always abundantly present in buccal epithelial cells, even following use of the ABS/Ca^{2+} protocol, where its expression is lost in urothelial cells. The ability to demonstrate absence of CK14 expression is clearly another important assessment for specifying urothelial cell differentiation.

3. **Demonstrating Gain of UPK3A Expression**

The ability to demonstrate considerable upregulation or de novo induction of expression of all five of the uroplakin genes should be a standard test used to evaluate conversion of a cell type into urothelial cells. Particular importance should be placed on demonstrating considerable UPK3A gene expression, as its expression was unable to be detected in buccal epithelial cells in any of the cell culture systems assessed. This work identified UPK3A as a key urothelium-specific marker.

4. Demonstrating Barrier Function

The ability to demonstrate functionality of a cell type is probably the most important aspect of reprogramming-type experiments. Therefore, when reprogramming to urothelial cells, the ability to demonstrate successful acquisition of barrier function is a vital test. Buccal epithelial cells were unable to form a functional barrier epithelium using the ABS/Ca^{2+} protocol, and this revealed an important difference between buccal epithelial cells and urothelial cells.

6.11 Conclusions and Future Work

In conclusion, the work presented in this thesis demonstrated that human buccal epithelial cells and urothelial cells do share several similar qualities when grown in basal conditions (KSFMc): they are both highly proliferative, express CK14, and have low expression of ELF3, FOXA1, GATA3 and PPARγ1. Major differences in the two cell types arose when the TZ/PD and ABS/Ca^{2+} protocols were investigated. The most striking difference was the inability of human buccal epithelial cells to form a functional barrier epithelium, which is a critical feature of urothelial cells. Further to this, at the molecular level, the inability of buccal epithelial cells to significantly upregulate FOXA1, GATA3 and PPARγ1 expression during use of the TZ/PD protocol, indicated that PPARγ activation is likely not occurring in buccal epithelial cells. Through this work, GATA3 and PPARγ were identified as key upstream transcription factors which could be used for urothelial-type reprogramming of buccal epithelial cells. A surprising result came with the investigation of uroplakin gene expression in buccal epithelial cells, where it was shown that four of the five uroplakin genes (UPK1A, UPK1B, UPK2 and UPK3B) were expressed, and further upregulated by using the TZ/PD protocol. This work identified UPK3A as a potentially key urothelium-specific marker, as it was the only uroplakin gene that was not expressed in buccal epithelial cells.

Future work in this area would aim to investigate whether GATA3 and PPARγ1 protein expression is truly absent in human buccal epithelial cells in culture. It is possible that, in a similar way to PPARγ1 expression in urothelial cells, they are rapidly degraded by the proteasome. Experiments performed using the proteasome inhibiting drug, MG132, could be used to examine this. An additional area of interest was the significant upregulation of ELF3, UPK2, UPK3B and TGM1 transcript expression observed following use of the TZ/PD protocol in buccal epithelia cells. Determining whether the upregulation of these gene was specifically as a result of PPARγ activation, or simply as a result of off-target effects of the drugs would be useful for deciphering a role for PPARγ in NHB cells. To investigate this, use of the PPARγ antagonist, T0070907, or PPARγ-specific siRNA could be employed.

Work in urothelial cells identified PPARγ1 as the primary PPARγ isoform involved in urothelial cell differentiation. Further to this, it was shown that PPARγ1 is only weakly expressed when human urothelial cells are grown in proliferative conditions (KSFMc). Only upon activation to differentiate, does PPARγ1 expression rapidly increase, but the expression appears to be largely labile; much of the PPARγ1 protein produced was rapidly degraded by the proteasome. PPARγ is clearly important for many aspects of urothelial cell identity and differentiation. Further research investigating the transient nature of PPARγ1 in normal human urothelial cells would be useful, as would identifying whether any novel variants or post-translationally modified versions of PPARγ are important in urothelial differentiation.

This study also provided preliminary evidence identifying an important role for GATA3 in the differentiation of normal human urothelial cells. In addition to this, the potential for GATA3 to have key roles in the regulation of urothelial differentiation-associated transcription factor expression was also identified. Further work to determine the exact role of GATA3 in normal urothelial differentiation is necessary, and has important implications for bladder cancer research, where GATA3 expression has already been identified as a key diagnostic and prognostic marker (Higgins et al., 2007; Miyamoto et al., 2012). Investigation into whether the GATA3 protein is primarily degraded by the proteasome in urothelial cells would also be of interest; similar to PPARγ1 protein expression, GATA3 protein expression was primarily weak, so it could be possible that it is also rapidly turned over in urothelial cells.

In the final results chapter, GATA3 and PPARγ1 were individually overexpressed in human buccal epithelial cells using retroviral transduction. Although neither gene was able to cause complete transdifferentiation on their own, each was able to upregulate key genes associated with urothelial cell differentiation and barrier function. Future work attempting to completely transdifferentiate squamous epithelial cells into urothelial cells should attempt combined overexpression of GATA3 and PPARγ1. In both individual GATA3 overexpression and PPARγ1 overexpression experiments neither PPARγ1 nor GATA3, respectively, were able to be upregulated, indicating that key regulatory pathways were still not activated.

Chapter 7:
Appendix

7 Appendix

7.1 Solution and Buffer Recipes

Solution	Recipe
10% (v/v) Formalin	100 ml of 37% Formaldehyde 900 ml of PBSc To make 1 L of PBSc: 1 L of 1x PBS, 0.5 ml of 1M $MgCl_2$ 0.9 ml of 1M $CaCl_2$
2x SDS Buffer	10 ml glycerol (20 % v/v), 1 g SDS (2 % w/v), 6.25 ml Tris-HCl (pH 6.8), 0.42 g NaF, 18.4 mg Na_3VO_4, 0.446 $Na_4P_2O_7$, 40 ml dH_2O.
Antifade (used for IF)	Dissolved 100 mg p-PhenylendiaminoDihydrochloride in 10 ml PBS and then adjusted to pH8.0. Added 90 ml glycerol.
Cell Freeze Mix	KSFMc (for buccal epithelial and urothelial cells) or Dulbecco's Modified Eagle's Medium (DMEM) (Gibco, 21969-035) (for cancer-derived cell lines) with 10% Fetal Bovine Serum (FBS) (SeraLab, EU-000) (batch selected) and 10% DMSO (Sigma, D2650).
Collagenase	Dissolved 10,000 U collagenase (Sigma, C5138) in 100 ml HBSS (with Ca^{2+} and Mg^{2+} ions) (Gibco, 24020-091). Then added 10 mM Hepes (Gibco, 15630-056). Filter sterilised using a 0.2 µm low protein-binding syringe filters (VWR, 514-4105).
DMEM10%	Dulbecco's Modified Eagle's Medium (DMEM) (Gibco®, 21969-035) with 10% Fetal Bovine Serum (FBS) (SeraLab, EU-000) (batch selected) and 1% L-glutamine (LG) (Gibco®, 25030-024).
dNTP Mix (10 mM)	Combined 10 µl ATP (100 mM), 10 µl TTP (100 mM), 10 µl CTP (100 mM), 10 µl GTP (100 mM) (Promega, U1240), and 60 µl dH_2O.
Dispase Solution (0.5 % or 2 %)	Dissolve dispase II powder (Sigma, D4693) in warm 1x DPBS (without Ca^{2+} and Mg^{2+} ions) (Gibco, 14185052) to 0.5 % or 2 %. Filter through Whatman 0 filter paper. Filter sterilise using a 0.2 µm low protein-binding syringe filters (VWR, 514-4105).
Haematoxylin	Solution 1: Dissolved 3 g haematoxylin in 20 ml ethanol. Solution 2: Dissolved 0.3 g sodium iodate, 1 g citric acid, 50 g chloral hydrate, and 50 g aluminium potassium sulphate in 850 ml dH_2O. Combined solutions 1 and 2 and added 120 ml glycerol.

Solution	Recipe
KSFMc	Keratinocyte Serum Free Medium (KSFM) (Gibco®, 17005-034) containing 0.05 mg/ml bovine pituitary extract (Gibco®, 37000-015), 5 ng/ml epidermal growth factor (Gibco®, 37000-015) and 30 ng/ml cholera toxin.
LB broth	Dissolve 5 g Yeast extract (Oxoid, LP0021), 10 g tryptone (Oxoid, LP0042), and 10 g sodium chloride in 1 L dH_2O, at pH to 7.0.
LB-Agar	Dissolve 5 g Yeast extract (Oxoid, LP0021), 10 g tryptone (Oxoid, LP0042), and 10 g sodium chloride in 1 L dH_2O and pH to 7.0. Then add 15 g agar (Oxoid, LP0013).
Phosphate Buffered Saline (PBS)	Dissolved 5 PBS tablets (Sigma, P4417) to 1 L ELGA-purified water and autoclaved.
Stripper Medium (Southgate et al., 1994)	444 ml of HBSS (without Ca^{2+} or Mg^{2+}) (Gibco®, 14170-088), 5 mL of 1 M Hepes (Gibco, 15630-056), 1 ml of Aprotonin (500,000 KIU) (Nordic Pharma Ltd), and 50 ml 1% EDTA (final concentration 0.1%).
Transfer Buffer (Western blotting)	1.45 g Tris, 7.2 g Glycine, 200 ml Methanol, 800 ml dH_2O.
Transport Medium (Southgate et al., 1994)	Hanks' Balanced Salt Solution (HBSS) (containing Ca^{2+} and Mg^{2+}) (Gibco®, 24020-091) with 10 mM HEPES (Gibco®, 15630-056), and 20 KIU/ml aprotonin (Nordic Pharma Ltd.).
Tris Buffered Saline (TBS) (recipe used for western blotting)	1.21 g Tris, 8.18 g NaCl, dH_2O to 1 L, pH 7.6
TBS-T (recipe used for western blotting)	TBS with 0.1% Tween-20 (Sigma, P1379)
Trypsin Inhibitor	Dissolved 100 mg of trypsin inhibitor (Sigma, T6522) in 5 ml of 1x DPBS (without Ca^{2+} or Mg^{2+}) (Gibco, 14200-067). Filter sterilised using a 0.2 µm low protein-binding syringe filters (VWR, 514-4105).
Trypsin-Versene (TV)	20 ml of 10x Trypsin (Sigma, T4549), 4 ml of 1% (w/v) EDTA and 176ml HBSS (without Ca^{2+} and Mg^{2+}) (Gibco®, 14170-088).

7.2 List of Companies

Company	Website
Abcam Plc.	http://www.abcam.com/
AbD Serotec®	https://abdserotec.com/
Abnova Corp.	http://www.abnova.com/
Agilent Technologies	http://www.agilent.com/
Bio-Rad Laboratories Inc.	http://www.bio-rad.com/
C A Hendley-Essex Ltd.	http://www.hendley-essex.com/
Cell Signaling Technology Inc.	http://www.cellsignal.com/
CellPath Ltd.	http://www.cellpath.co.uk/
Clontech Laboratories inc.	http://www.clontech.com/
Contained Air Solutions Ltd.	http://www.containedairsolutions.co.uk/
Dako	http://www.dako.com/
ELGA	http://www.elgalabwater.com/
Envair Ltd.	http://www.envair.co.uk/
Eurofins Genomics	https://www.eurofinsgenomics.eu/
Fisher Scientific Ltd.	http://www.fisher.co.uk/
Greiner Bio-One Ltd.	http://www.greinerbioone.com/
Hawksley	http://www.hawksley.co.uk/
Hettich Lab Technology	http://www.hettichlab.com/
Leica Biosystems • Novocastra	http://www.leicabiosystems.com/
Li-Cor Biosciences Ltd.	http://www.licor.com/
Life Technologies • Gibco® • Applied Biosystems® • Ambion® • Invitrogen™ • Zymed®	http://www.lifetechnologies.com/
Media Cybernetics inc.	http://www.mediacy.com/
Melford Laboratories Ltd.	http://melford.co.uk/
New England BioLabs (NEB)	https://www.neb.com/

Company	**Website**
Olympus	http://www.olympus.co.uk/
Priorclave ltd.	http://www.priorclave.co.uk/
Promega	https://www.promega.co.uk/
QIAGEN	https://www.qiagen.com/
R&D Systems Inc.	http://www.rndsystems.com/
Roche Products Ltd.	http://www.roche.co.uk/
Santa Cruz Biotechnology Inc.	http://www.scbt.com/
Sarstedt AG & Co.	https://www.sarstedt.com/
Scientific Industries Inc.	http://www.scientificindustries.com/
Scientific Laboratories Supplies Ltd. (SLS)	http://www.scientificlabs.co.uk/
SCIE-PLAS	http://www.scie-plas.com/
SciQuip Ltd.	http://www.sciquip.co.uk/
Sera Laboratories International Ltd. (SeraLab)	http://www.seralab.co.uk/
Sigma-Aldrich Co. LLC (Sigma)	http://www.sigmaaldrich.com/
Source Bioscience	http://www.sourcebioscience.com/
Syngene	http://www.syngene.co.uk/
Taylor-Wharton International LLC	http://www.taylorwharton.com/
The Binding Site Group Ltd.	http://www.thebindingsite.com/
Thermo Fisher Scientific Inc. • RA Lamb	http://www.thermoscientific.com/
Vector Laboratories Inc.	https://www.vectorlabs.com/
VMR International • Jencons • BDH	https://uk.vwr.com/
World Precision Instruments	http://www.wpiinc.com/

7.3 List of Acronyms

Acronym	**Meaning**
ABS	Adult Bovine Serum
AUM	Asymmetric Unit Membrane
cDNA	Complementary DNA
CK	Cytokeratin
CLDN	Claudin
DMEM10%	DMEM with 10% FBS and 1% LG
DNA	Deoxyribonucleic acid
ELF3	E74-like Factor 3
FBS	Fetal Bovine Serum
FOXA1	Forkhead Box Protein A1
GATA3	GATA Binding Protein 3
GRHL3	Grainyhead-like 3
KLF5	Kruppel-like Factor 5
KSFMc	Keratinocyte Serum Free Medium – Complete
LDS	Lithium dodecyl sulphate
LOR	Loricrin
NHB	Normal human buccal epithelial
NHU	Normal human urothelial
PBS	Phosphate Buffered Saline
PCR	Polymerase Chain Reaction
PCR	Polymerase Chain Reaction
PD	PD153035 (EGFR-TK inhibitor)
PPAR	Peroxisome Proliferator-Activated Receptor
RAR	Retinoic Acid Receptor
RNA	Ribonucleic acid
RT-qPCR	Reverse Transcriptase Quantitative Polymerase Chain Reaction
RXR	Retinoid X Receptor

Acronym	**Meaning**
SDS	Sodium dodecyl sulphate
SPRR4	Small Proline Rich Protein 4
TBS	Tris Buffered Saline
TBS-T	TBS with 0.1% Tween-20
TER	Trans-epithelial Electrical Resistance
TGM1	Transglutaminase 1
TZ	Troglitazone (PPARγ agonist)
UPK	Uroplakin
ZO	Zonula Occluden

7.4 PPARγ Antibody Optimisation

7.4.1 PPARγ Overexpression

One of the most commonly published antibodies used for the detection of PPARγ expression by western blotting has been the E-8 antibody clone (monoclonal) produced by Santa Cruz Biotechnology, Inc. Its use for evaluating PPARγ expression in normal human urothelial cells has been difficult because it detects several different protein bands at the approximate heights corresponding to PPARγ1 and PPARγ2; using the E-8 antibody, Georgopolous et al. described the detection of three PPARγ protein bands, but they did not identify which of the bands corresponded to which of the PPARγ protein isoforms. In order to evaluate the specificity of the E-8 and other PPARγ antibodies, it was decided to overexpress each of the PPARγ isoforms in an identified cell line with low PPARγ gene expression.

PPARγ1 and PPARγ2 overexpression vectors were previously generated and transfected into PT67 retroviral packaging cells by Jennifer Hinley, a research technician at the Jack Birch Unit, University of York. The retroviral vector backbone used was pLXSN (Clontech Laboratories Inc.). PT67 cells were also transfected with the pLXSN vector only, to act as an empty vector control, for comparison. Ms. Hinley also confirmed successful transfection and selection of all three vectors into PT67 cells by PCR.

To investigate the specificity of several PPARγ antibodies by western blotting and immunofluorescence, a cell line was identified with low PPARγ transcript abundance, in which to overexpress each of the two PPARγ isoforms. A search of the RNA-seq data generated for a range of commonly used cell lines on The Human Protein Atlas (proteinatlas.org) revealed that a number of cell lines had low PPARγ expression. MCF-7, a breast carcinoma-derived cell line, was chosen due to its relatively low abundance of PPARγ expression, and its availability as a cell line stock in the Jack Birch Unit. The MCF-7 cell stock had been previously genotyped upon arrival to the Jack Birch Unit MCF-7 cells were transduced with retroviruses generated from PT67 cells transfected with either the empty pLXSN vector, or the pLXSN vector containing either the PPARγ1 or PPARγ2 coding sequence. Successfully transduced cells were maintained under antibiotic selection (0.1 mg/ml G418). For western blotting, cells

were grown to confluence and whole cell protein lysates were taken. For immunofluorescence experiments, PT67 packaging cells, which had been transfected with either the empty pLXSN vector or the PPARγ overexpression vectors, were first evaluated to determine the appropriate fixation method required for each antibody (either methanol:acetone or 10 % (v/v) formalin followed by 0.1 % Triton X-100). Cells were seeded onto 12-well glass slides and grown to near confluence. MCF-7 cells were then evaluated for PPARγ expression by immunofluorescence microscopy using the fixation method determined using the transfected PT67 cells.

7.4.2 PPARγ Antibodies

The list of PPARγ antibodies which were evaluated for their specificity for either western blotting (WB) or immunofluorescence (IF) can be found below in Table 7.1. Several antibodies were tested that could detect both PPARγ1 and PPARγ2, and a single antibody was evaluated which was specific for PPARγ2. The respective binding locations for each of the PPARγ antibodies to the PPARγ proteins are shown in Figure 7.1.

Table 7.1 List of PPARγ Antibodies

Antibody Clone	PPARγ Specificity	Host (Production)	Supplier	Dilution*
E-8	PPARγ1 and PPARγ2	M (Monoclonal)	Santa Cruz	1:500 (WB) 1:200 (IF)
81B8	PPARγ1 and PPARγ2	Rb (Monoclonal)	Cell Signaling	1:500 (WB) 1:100 (IF)
D69	PPARγ1 and PPARγ2	Rb (Polyclonal)	Cell Signaling	1:500 (WB) 1:100 (IF)
P&A53.25	PPARγ1 and PPARγ2	M (Monoclonal)	GSK (gift)	- 1:1200 (IF)
N-19	PPARγ2 only	Gt (Polyclonal)	Santa Cruz	1:500 (WB) -

M – Mouse, Rb – Rabbit, Gt - Goat

* Dilutions were previously determined by titration.

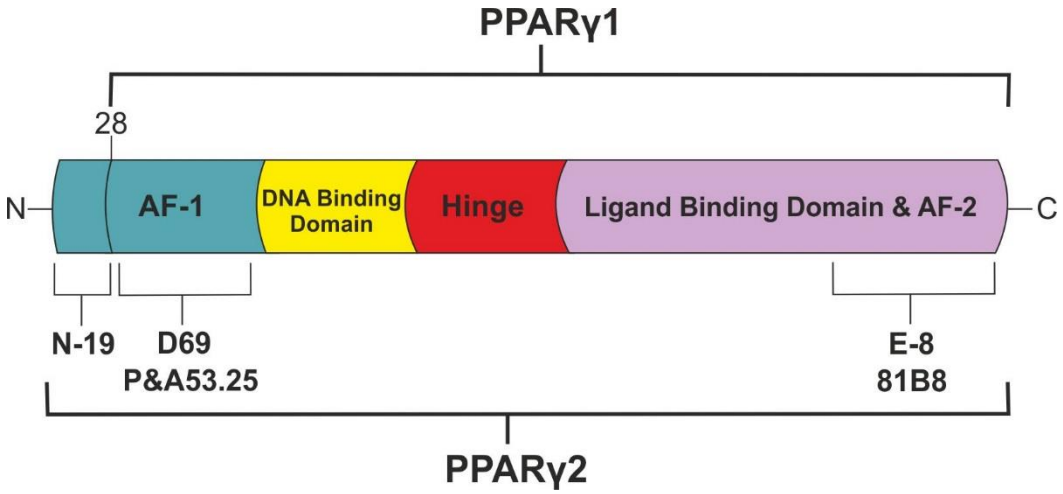

Figure 7.1 PPARγ Antibody Binding Locations

The 81B8, D69, E-8 and P&A53.25 antibodies all bind to both the human PPARγ1 and PPARγ2 proteins. The D69 and P&A53.25 antibodies bind to the more N-terminal portion of the proteins; the D69 antibody was raised against a peptide sequence surrounding the Asp69 residue of human PPARγ2. The E-8 and 81B8 antibodies bind to the C-terminal portion of the proteins; the E-8 antibody was raised against a peptide mapping to residues 480-505 of the human PPARγ2 sequence, while the 81B8 antibody was raised against a peptide sequence surrounding the His494 residue of human PPARγ2. The N-19 antibody only binds to PPARγ2, and was raised against a peptide sequence in the first 28 amino acids of human PPARγ2, which is not part of the PPARγ1 protein. Information regarding binding location for each antibody was obtained from the corresponding product data sheet. The information pertaining to the P&A53.25 antibody was obtained from (Su et al., 1999).

7.4.3 Assessment of PPARγ Antibodies for Western Blotting

The successful overexpression of PPARγ1 and PPARγ2 in MCF-7 cells was demonstrated by RT-PCR analysis (Figure 7.2 A). MCF-7 cells transfected with the empty vector only displayed weak total PPARγ expression and absent PPARγ2 gene expression.

All of the total PPARγ antibodies (E-8, 81B8, and D69) evaluated demonstrated reactivity to PPARγ (Figure 7.2 B, C & D) by western blotting. The western blots showed bands in the PPARγ1 overexpressing cells at approximately 52 kDa, and in the PPARγ2 overexpressing cells at approximately 57 kDa. The E-8 antibody gave a variety of additional bands including one band directly below the PPARγ1 protein band. The 81B8 and D69 antibodies also showed additional bands, but less than detected using the E-8 antibody. Based on these results, the D69 antibody was chosen to be the primary antibody used for detecting PPARγ expression by western blotting throughout this thesis; the antibody appeared to provided the most intense labelling, with the least amount of additional bands.

The N-19 antibody appeared to be specific for detecting PPARγ2 expression by western blotting (Figure 7.2 E). It detected a PPARγ2-specific band in only the PPARγ2 overexpressing cells at approximately 57 kDa. This band was equivalent to the one detected using the three PPARγ total antibodies.

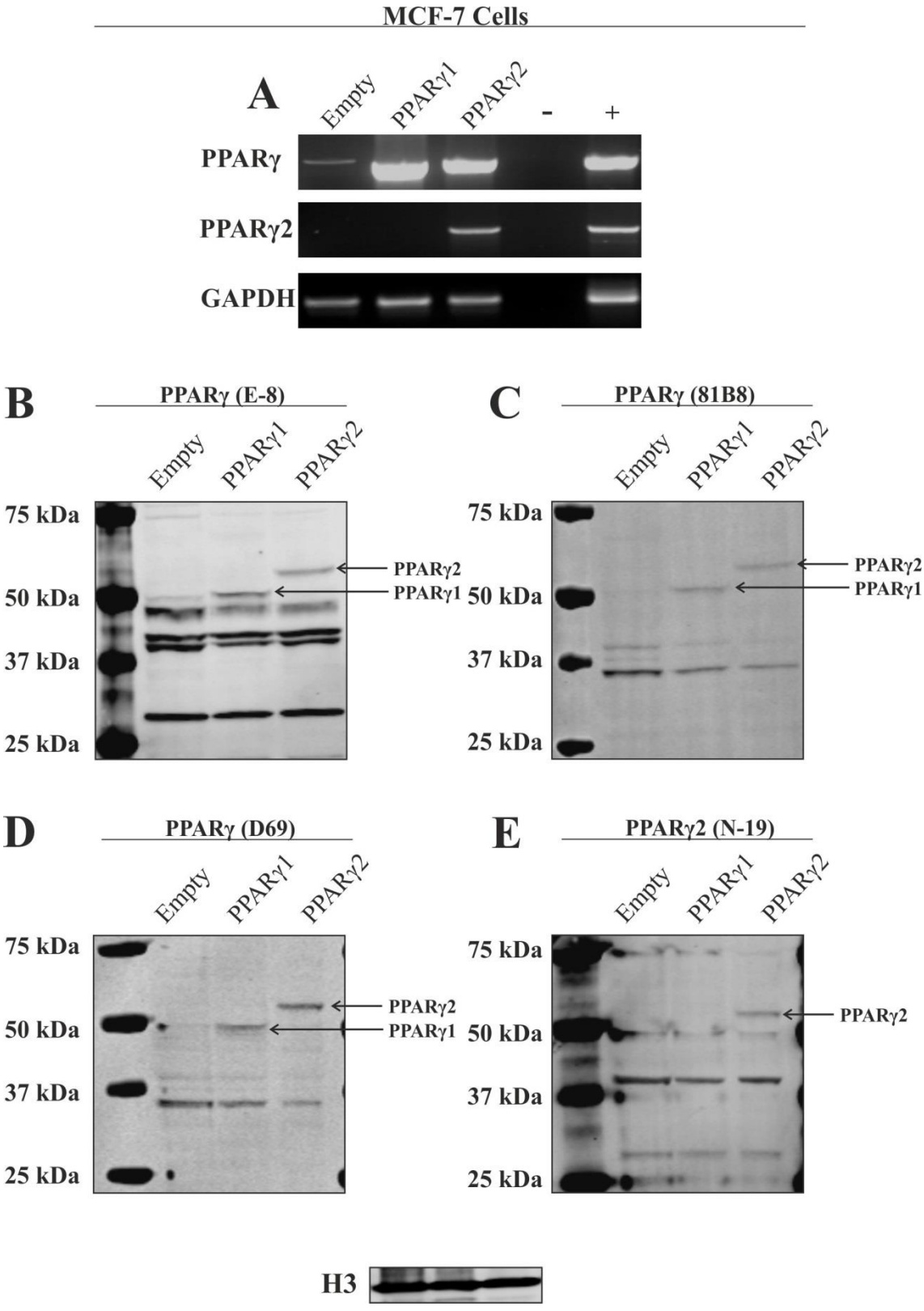

Figure 7.2 PPARγ Antibodies Evaluated for Western Blotting Using Transduced MCF-7 Cells

Figure 7.2 PPARγ Antibodies Evaluated for Western Blotting Using Transduced MCF-7 Cells

MCF-7 cells were transduced to either overexpress PPARγ1 or PPARγ2. Control cells were transduced with the antibiotic selection gene only, and are denoted in the figure as 'Empty'.

A) Successful overexpression was shown by RT-PCR for total PPARγ expression and PPARγ2 expression (30 cycles). GAPDH expression was used as loading control (25 cycles). H_2O (no template) was used as a negative control. cDNA from adipocyte differentiated mesenchymal stem cells (generated by Ros Duke and Jenny Hinley) was used as the positive control for the PCR.

Whole protein lysates were assessed by western blotting using total PPARγ antibodies **B)** E-8, **C)** 81B8, and **D)** D69 and a PPARγ2 specific antibody **E)** N-19. Histone 3 (H3) expression was used as a loading control. 20 μg of protein was loaded into each well. Note successful overexpression of PPARγ1 and PPARγ2 in MCF-7 cells. Also note detection of both PPARγ1 and PPARγ2 protein by the E-8, 81B8 and D69 antibodies. The PPARγ2-specific antibody, N-19, detected a unique band in the PPARγ2 overexpressing MCF-7 cells.

7.4.4 Assessment of PPARγ Antibodies for Immunofluorescence

Using PT67 cells, which had been transfected with either the empty pLXSN vector, or the pLXSN vector containing either the PPARγ1 or PPARγ2 coding sequences, it was shown that fixation of the cells with formalin plus permeabilisation with Triton X-100 was necessary to demonstrate specific PPARγ labelling. Fixation of the cells with Methanol:Acetone (50:50) resulted in only very weak nuclear expression in the cells, but no clear overexpression of PPARγ1 or PPARγ2 could be shown (Figure 7.3). Using formalin fixation, it was shown that the 81B8, D69 and E-8 antibodies demonstrated specificity to PPARγ, while the P&A53.25 antibody appeared non-specific to PPARγ (Figure 7.4).

In MCF-7 cells, only the 81B8 and D69 antibodies demonstrated specificity to PPARγ (Figure 7.5). The 81B8 antibody showed weak cytoplasmic/background labelling in the control (empty) cells, while the PPARγ1 and PPARγ2 overexpressing cells displayed clear nuclear expression. The D69 antibody showed weak background expression, with some possible cell membrane specific labelling. In the PPARγ1 and PPARγ2

overexpressing cells, the expression was clearly nuclear in all of the cells. Both the 81B8 and D69 antibody demonstrated clear overexpression of PPARγ in the PPARγ1 and PPARγ2 overexpressing cells, in comparison to the control cells.

The E-8 antibody appeared to be not specific at detecting PPARγ using the MCF-7 cells; a similar cytoplasmic and nuclear expression was detected in the control and PPARγ overexpressing cells. The P&A53.25 antibody demonstrated similar results to those observed using the PT67 cells, and detected high levels of background in all of the cell types, again suggesting a lack of specificity.

Based on the results described above, and consistent with western blotting, the D69 antibody was chosen to be used for all subsequent experiments for the detection of PPARγ expression by immunofluorescence in this thesis.

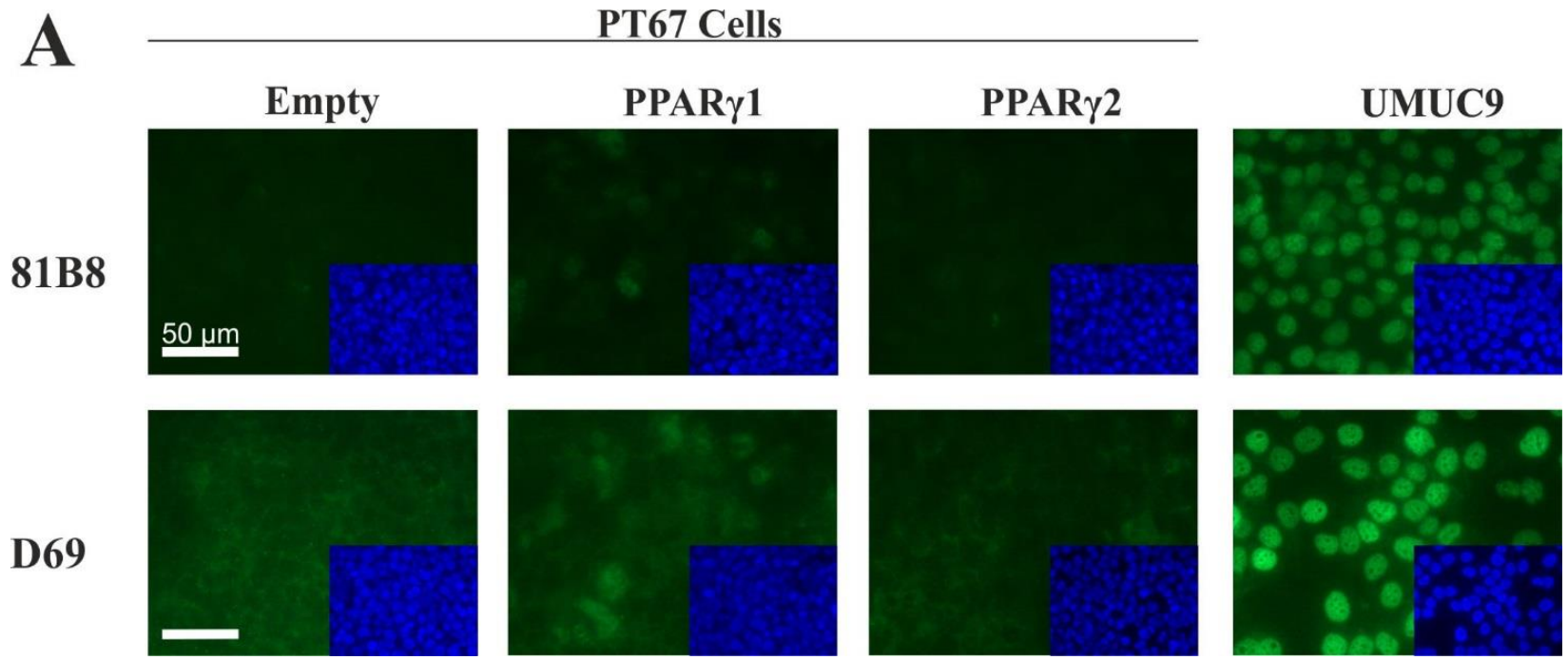

Figure 7.3 PPARγ Antibodies Evaluated for Indirect Immunofluorescence Microscopy Using Transfected PT67 Cells Fixed by Methanol:Acetone – A) 81B8 and D69

PT67 cells were transfected with either PPARγ1 or PPARγ2 overexpression vectors. Control cells were transfected with the empty vector only. Immunofluorescence labelling for the total PPARγ antibodies, **(A)** 81B8 and D69 and **(B)** E-8 and P&A53.25, was performed on methanol:acetone (50:50) fixed slides. UMUC9 cells were included as a positive control due to their known PPARγ expression. Inset images show the corresponding Hoechst 33258 staining to demonstrate cell density and nuclei location. Antibody labelled images were taken at the same exposure for each antibody. Hoechst 33258 images were taken at optimal exposures. Note the absence of PPARγ expression in all of the PT67 cells using either the 81B8 or D69 antibodies, with methanol:acetone fixation of the cells.

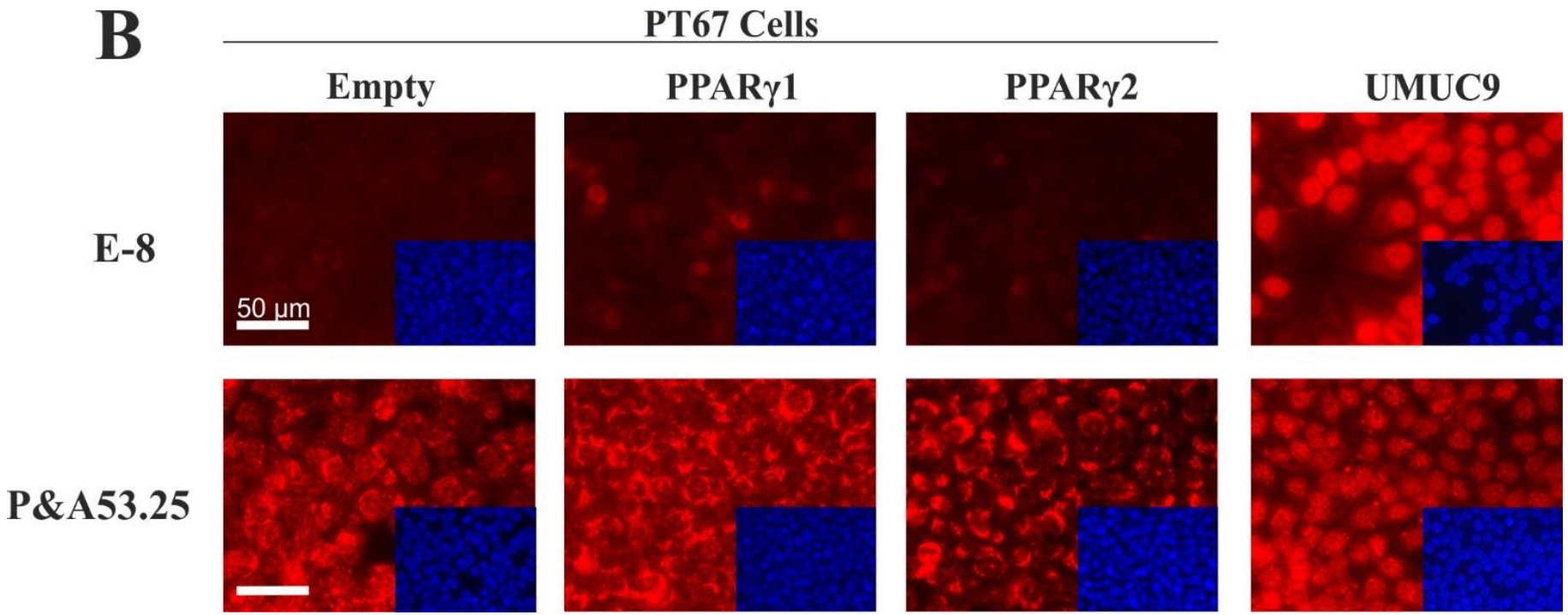

Figure 7.3 PPARγ Antibodies Evaluated for Indirect Immunofluorescence Microscopy Using Transfected PT67 Cells Fixed by Methanol:Acetone – B) E-8 and P&A53.25

See main caption on previous page. Note the absence of PPARγ expression in all of the PT67 cells using the E-8 antibody with methanol:acetone fixation. Use of the P&A53.25 antibody showed abundant PPARγ expression in all of the transfected PT67 cell types, suggesting that non-specific binding of the antibody may be occurring.

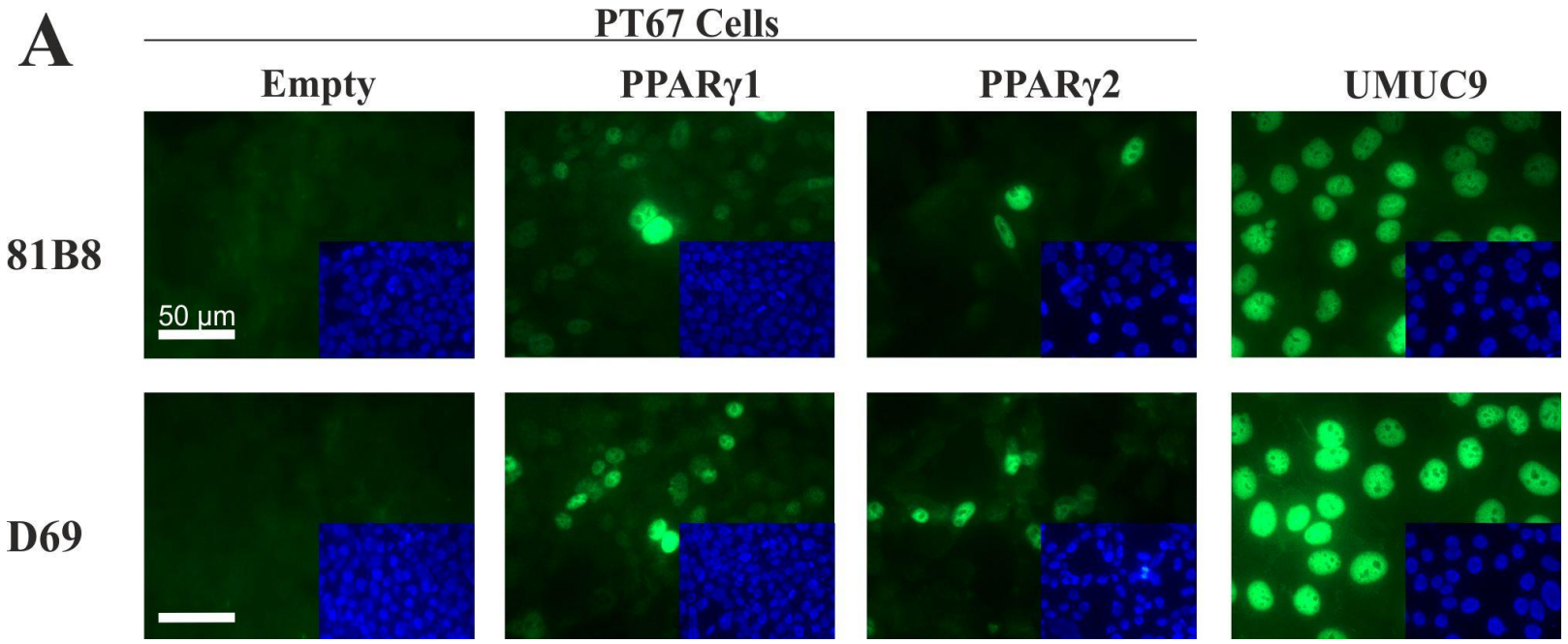

Figure 7.4 PPARγ Antibodies Evaluated for Indirect Immunofluorescence Microscopy Using Transfected PT67 Cells Fixed Using Formalin – A) 81B8 and D69

PT67 cells were transfected with either PPARγ1 or PPARγ2 overexpression vectors. Control cells were transfected with the empty vector only. Immunofluorescence labelling for the total PPARγ antibodies, **(A)** 81B8 and D69, and **(B)** E-8 and P&A53.25, was performed on formalin fixed slides which had been permeabilised with Triton X-100. UMUC9 cells were included as a positive control for PPARγ expression. Inset images show the corresponding Hoechst 33258 staining to demonstrate cell density and nuclei location. Antibody labelled images were taken at the same exposure. Hoechst 33258 images were taken at optimal exposures. Note clear nuclear expression of PPARγ in the PPARγ1 and PPARγ2 overexpressing PT67 cells using both the 81B8 and D69 antibodies. PPARγ expression was absent in the control (Empty) PT67 cells.

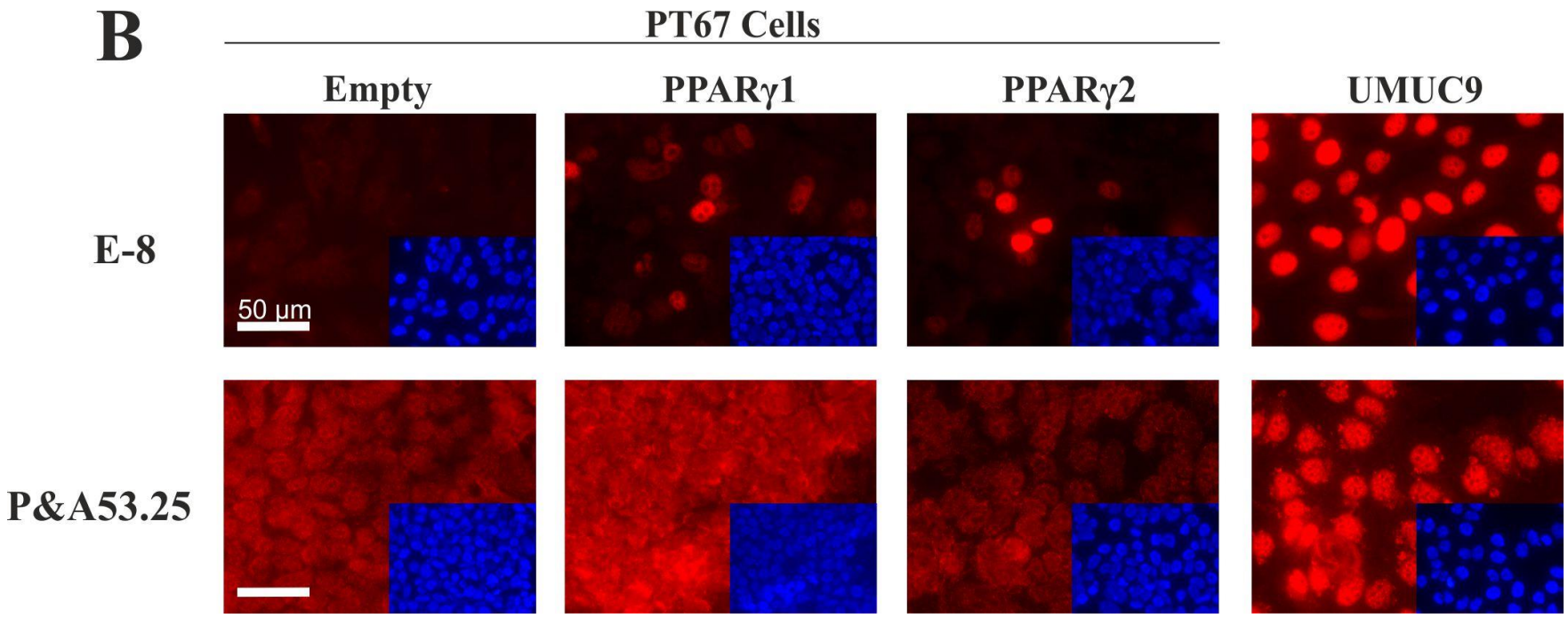

Figure 7.4 PPARγ Antibodies Evaluated for Indirect Immunofluorescence Microscopy Using Transfected PT67 Cells Fixed Using Formalin – B) E-8 and P&A53.25

See main caption on previous page. Note clear nuclear expression of PPARγ in the PPARγ1 and PPARγ2 overexpressing PT67 cells using the E-8 antibody and negative PPARγ expression in the control (Empty) PT67 cells. Use of the P&A53.25 antibody showed similar abundant PPARγ expression in all of the transfected PT67 cell types, again indicating that non-specific binding of the antibody may be occurring.

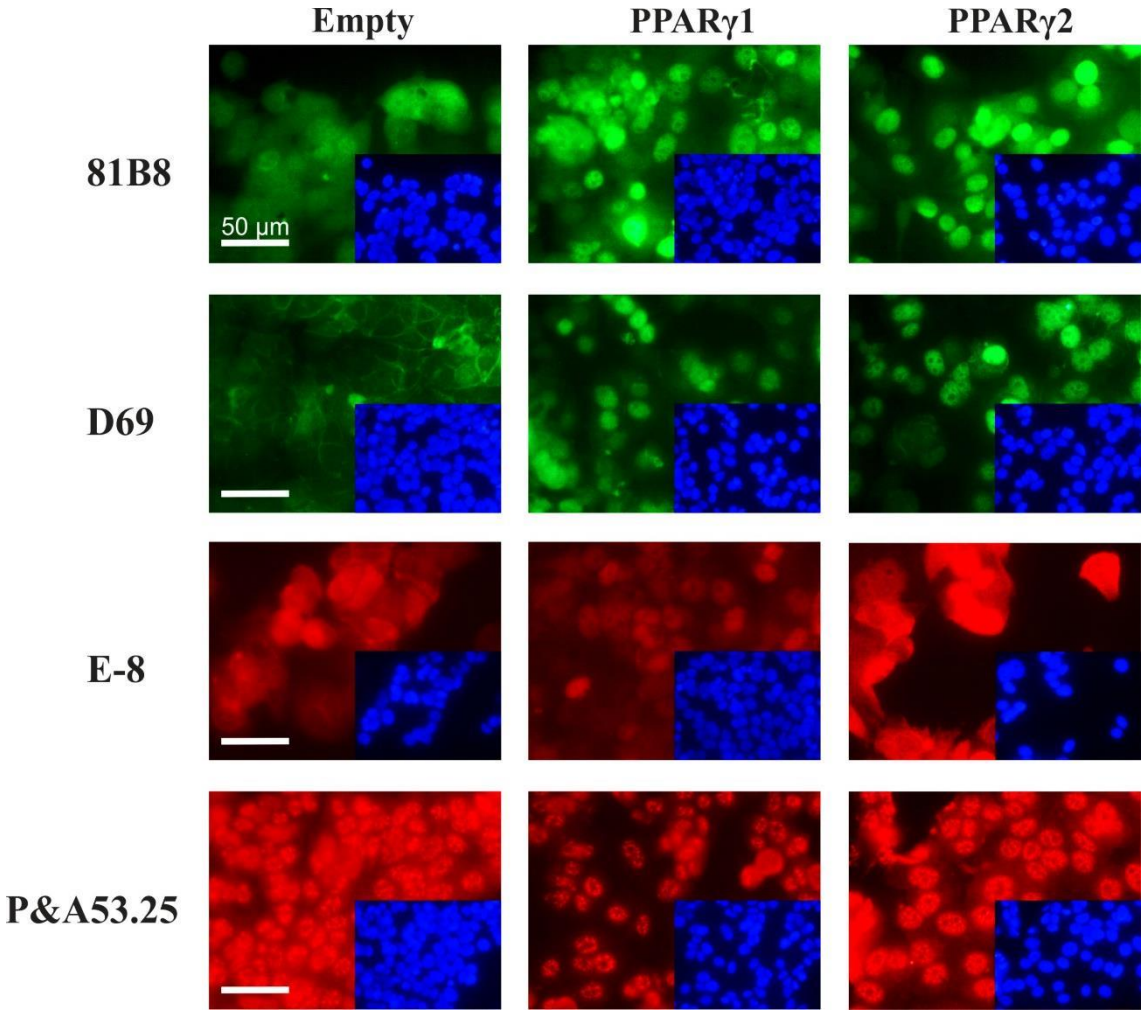

Figure 7.5 PPARγ Antibodies Evaluated for Immunofluorescence Using Transduced MCF-7 Cells Fixed using Formalin

MCF-7 cells were transduced to either overexpress PPARγ1 or PPARγ2. Control cells were transduced with the antibiotic selection gene only, and are denoted in the figure as 'Empty'. Immunofluorescence labelling for the total PPARγ antibodies E-8, 81B8, D69, P&A53.25 was performed on formalin fixed slides which had been permeabilised with Triton X-100. Inset images represent the corresponding Hoechst 33258 staining to demonstrate cell density and nuclei location. Antibody labelled images were taken at the same exposure for each antibody to allow for comparison with the control and PPARγ overexpressing cells. Hoechst 33258 images were taken at optimal exposures. Note clear nuclear PPARγ expression in the PPARγ1 and PPARγ2 overexpressing MCF-7 cells using the 81B8 and D69 antibodies. Use of the E-8 and P&A53.25 antibodies showed similar PPARγ expression in both the control (Empty) and PPARγ overexpressing MFC-7 cells.

7.5 In Vitro Characterisation of Buccal Epithelial Cells with Reference to Urothelial Cells

7.5.1 Buccal Epithelial Cell Isolation and Culture

Due to difficulty obtaining human buccal mucosa tissue samples, no direct experiments were performed to characterise their isolation or subsequent growth, in order to conserve the cells for other experiments. As a result, a description of the general observations pertaining to the isolation and culture of NHB cells can be found below.

Isolation of NHB cells was achieved as described in methods section 2.4.3.1. As a general observation, the isolation method yielded less than 10 % of the seeded cells adhering to the plastic ware following 24 hours of incubation at 37 ^{o}C with 5% CO_2 in air. The accumulation of dead cells was removed from the cultures following 24 hours and the cells were allowed to populate the dish, which typically took longer than one week due to the low initial plating density. NHU cells, by contrast, which were isolated using a different method (see method section 2.4.3.2), had an almost 100% adherence rate.

For general maintenance and culture, NHB cells were expanded using a method previously optimised for urothelial cells, which relied on the use of a serum-free, low calcium (0.09 mM) medium (KSFMc) (Figure 7.6). Cells were subcultured upon reaching confluence. Buccal epithelial cells proliferated comparably in this culture system to urothelial cells, although senesced much earlier (typically by passage 5). NHU cells, in contrast, could be passaged on average up to 10 times before reaching senescence.

In culture, buccal epithelial cells appeared more rounded in shape, while urothelial cells had a more elongated appearance (Figure 7.6). When buccal epithelial cells were treated with the TZ/PD (Figure 7.7), atRA/PD (Figure 7.8) or ABS/Ca^{2+} protocols (Figure 7.9), the cell appearance changed depending on the conditions. Using the TZ/PD and atRA/PD protocol, cultures grew to confluent monolayers. Use of the ABS/Ca^{2+} protocol on snapwell membranes produced multi-layered epithelia, of approximately 3-4 cell layers thick, similar to that which could be achieved with NHU cells.

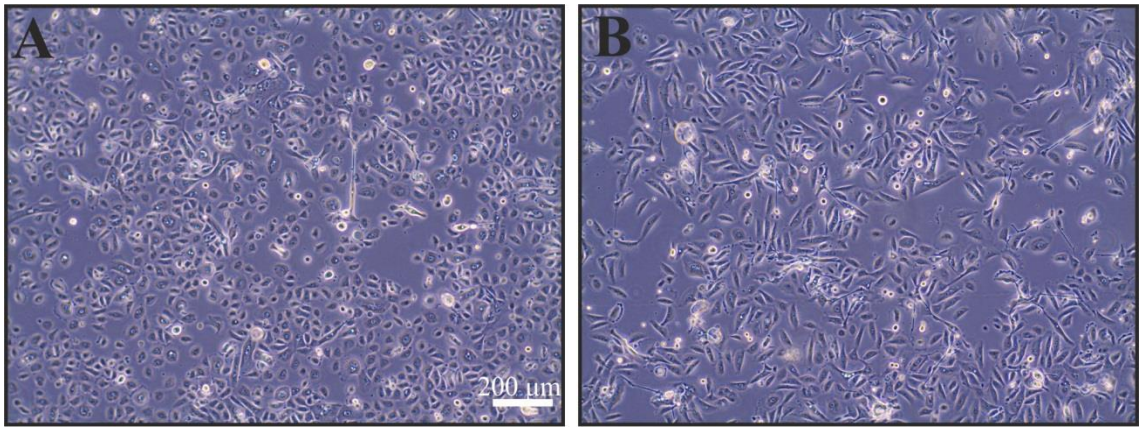

Figure 7.6 Phase Contrast Images of NHB Cells and NHU Cells Grown in a Serum-Free, Low Calcium Medium (KSFMc)

Buccal epithelial cells **A)** AS005b, and urothelial cells **B)** Y1334 grown in KSFMc. Scale bar = 200 µm. Note the rounded appearance of the NHB cells and the more elongated morphology of NHU cells.

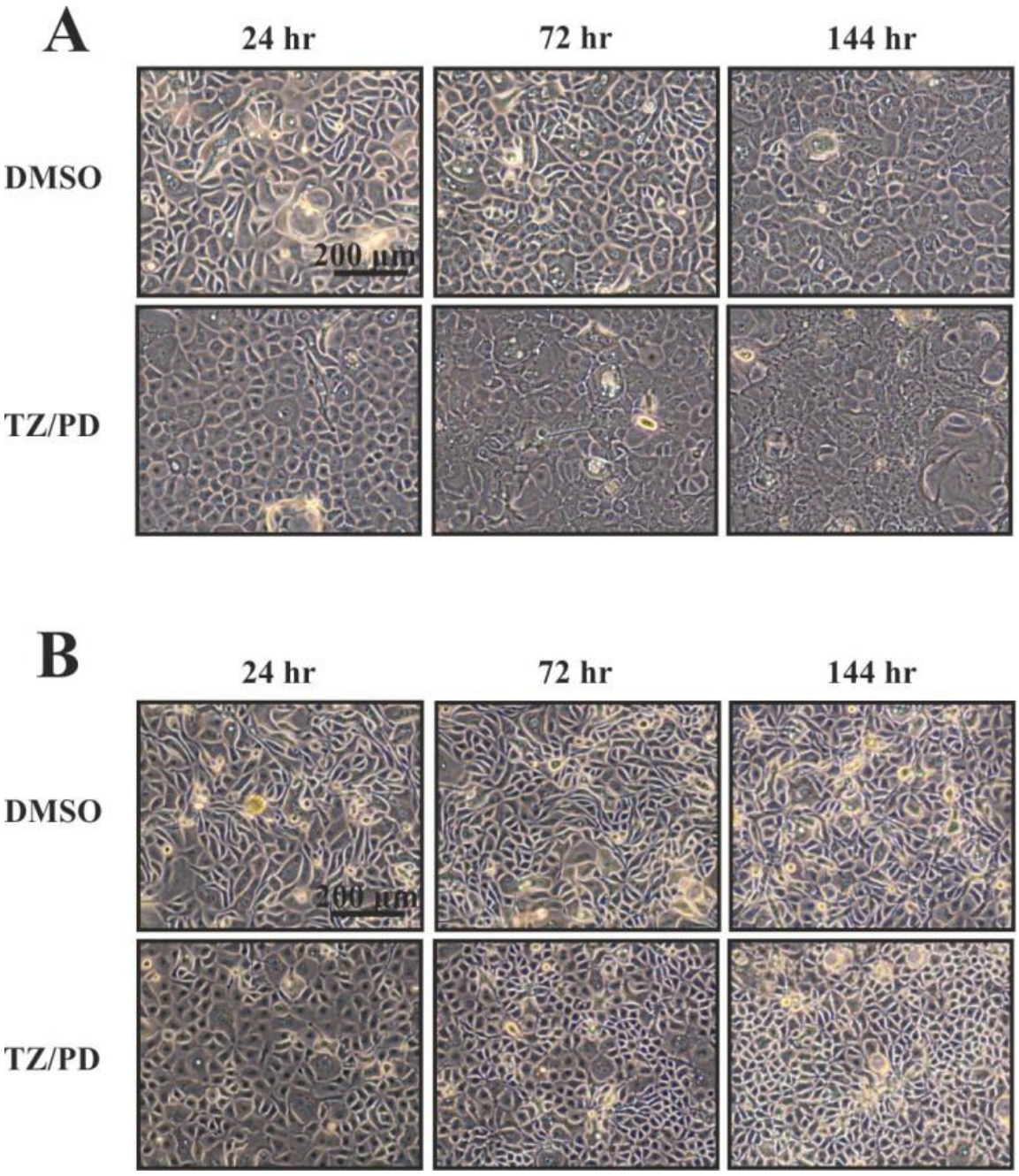

Figure 7.7 Phase Contrast Images of NHB Cells and NHU Cells Following use of the TZ/PD Protocol for 24, 72 and 144 hours

Buccal epithelial cells **A)** AS005b, and urothelial cells **B)** Y1453, which were treated with either 0.1% DMSO (vehicle control) or TZ/PD for 24, 72, or 144 hr. Scale bar = 200 µm. Note both cell types reaching extreme confluence by the 144 hour time point.

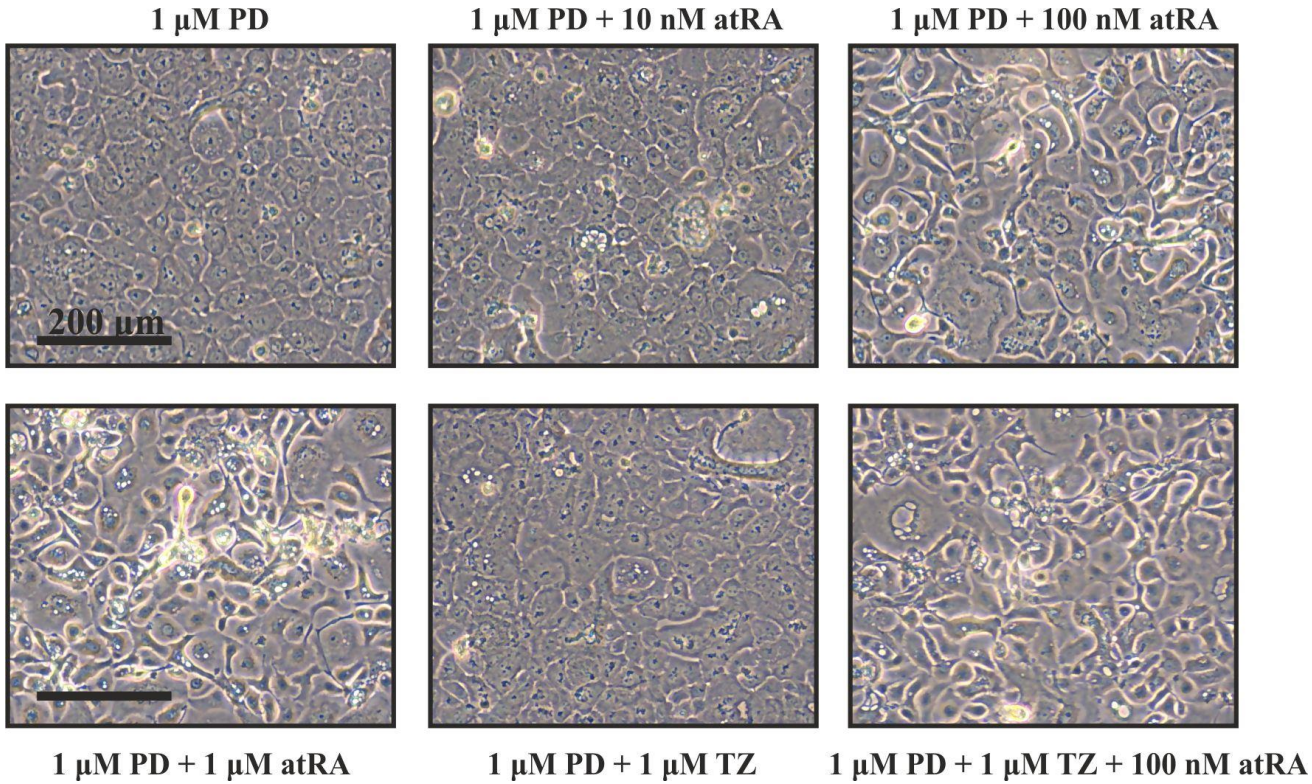

Figure 7.8 Phase Contrast Images of Buccal Epithelial Cells Treated with PD, atRA/PD, TZ/PD, or atRA/TZ/PD

Buccal epithelial cells (AS006b) were treated with either 1 µM PD (control) or 1 µM PD with 10 nM, 100 nM or 1 µM atRA. Additional cells were exposed to 1 µM PD and 1 µM TZ with and without 100 nM atRA. All protocols lasted for a total of 72 hours. Medium was changed following 24 hours; all treatments remained the same except the ones containing TZ, where the medium was changed to remove the TZ, following the standard TZ/PD protocol. Scale bar = 200 µm. Note the change in NHB cell appearance with increasing concentrations of atRA.

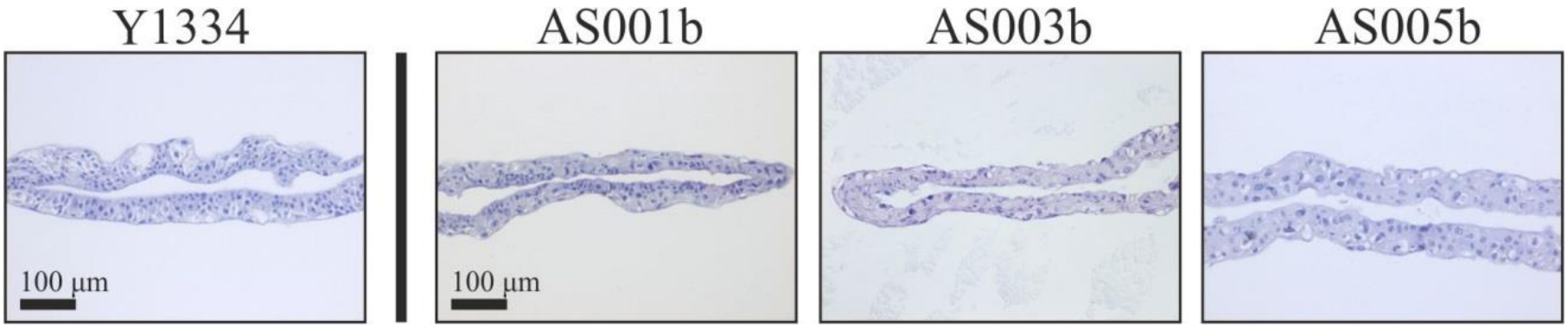

Figure 7.9 Haematoxylin and Eosin (H&E) Stained NHU and NHB Cell Sheets Generated using the ABS/Ca^{2+} Protocol

Following 8 days of the ABS/Ca^{2+} protocol on Snapwell inserts, cell sheets were harvested from the substrate using dispase, and fixed in 10 % (v/v) formalin. The cell sheets were then processed into paraffin wax, sectioned, and H&E stained. Images were generated using brightfield microscopy for a single urothelial cell line (Y1334) and three independent buccal epithelial cell lines (AS001b, AS003b, and AS005b). Note the similar appearance and number of cell layers between the NHB and NHU cell sheets.

7.5.2 Positive Control for CK20 Expression – Immunofluorescence Microscopy

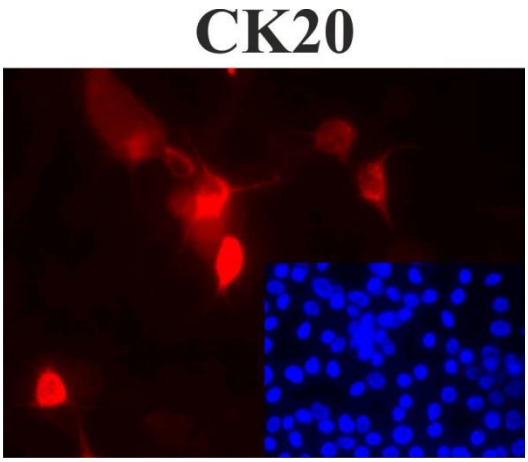

Figure 7.10 Positive Control for CK20 Expression for Immunofluorescence Microscopy

NHU cells (NHU4) were treated with the TZ/PD protocol for 6 days. CK20 expression was assessed by immunofluorescence microscopy. Inset image shows the corresponding Hoechst 33258 staining to demonstrate cell density and nuclei location

7.5.3 Additional Cell Line Results for Transcription Factor Gene Expression by RT-PCR in NHB Cells Treated with TZ/PD – (NHB5)

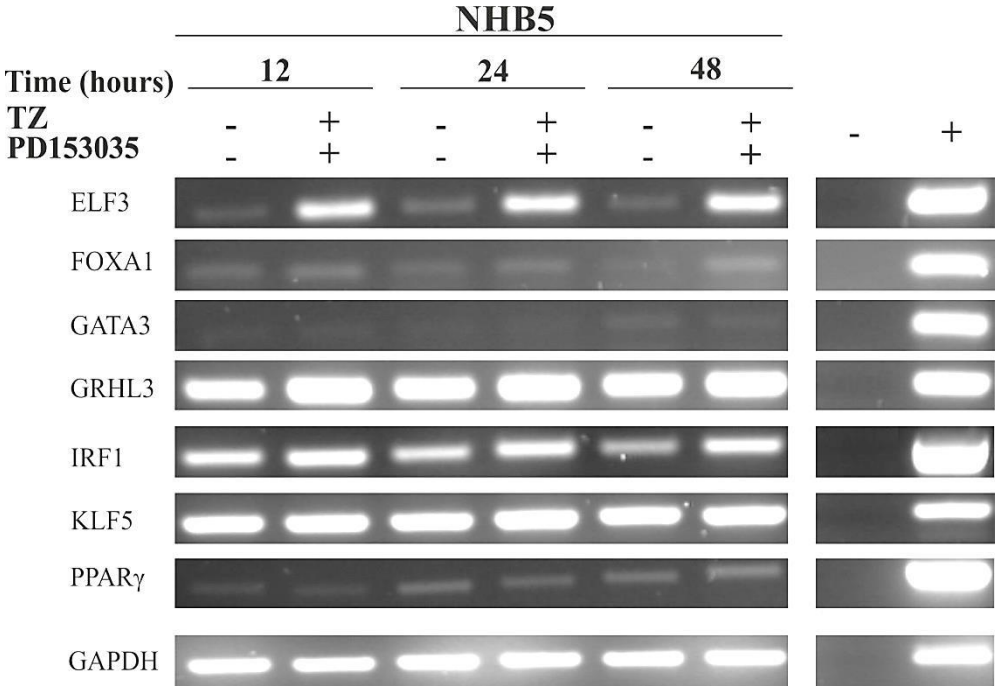

Figure 7.11 Expression of Urothelial Differentiation-Associated Transcription Factors in NHB Cells by RT-PCR Following TZ/PD Treatment – Additional Cell Line (NHB5)

Buccal epithelial cells (NHB5) were treated with TZ/PD for 24, 48 and 72 hours. The expression of ELF3, FOXA1, GATA3, GRHL3, IRF1, KLF5 and PPARγ (forward and reverse primers designed to sequences in exon 6) was assessed by RT-PCR. PCR was performed using 30 cycles. GAPDH was used as a loading control (25 cycles). H_2O (no template) was used as a negative control (-). Genomic DNA was used as the positive control for the PCR (+). Note weak/absent expression of FOXA1, GATA3 and PPARγ in NHB cells. Also note the apparent upregulation of ELF3 expression in NHB cells as a result of TZ/PD.

7.5.4 Full Length Western Blot Showing PPARγ Expression in NHB Cells Following Treatment with DMSO, PD or TZ/PD for 72 hours

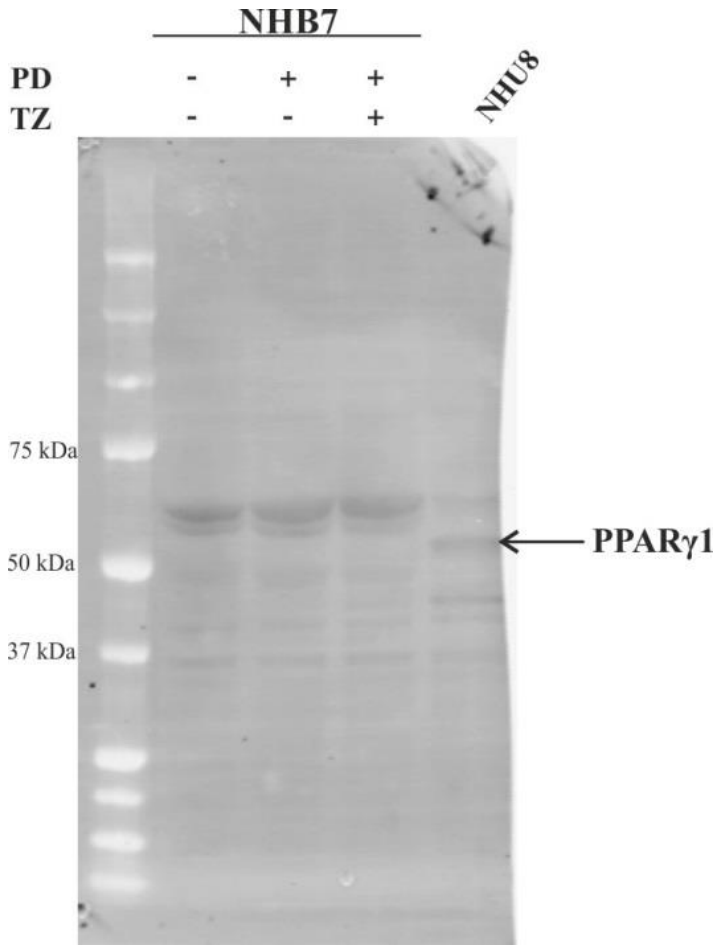

Figure 7.12 Full Length Western Blot Showing PPARγ Expression in NHB Cells (NHB7) Following Treatment with 0.1 % DMSO, PD and TZ/PD

Example full length western blot showing PPARγ expression in NHB cells (NHB7). NHB cells were treated with either 0.1% DMSO (vehicle control), 1 μM PD or TZ/PD for 72 hours. A single NHU cell line (NHU8) which had been treated with TZ/PD for 72 hours was included on all blots to act as a positive control/for comparison. Note PPARγ1 is not expressed in NHB cells. Additional possible non-specific bands were observed on the western blot.

7.5.5 Additional Cell Line Results for Evaluation of Transcription Factor Protein Expression by Immunofluorescence Microscopy in NHB Cells Treated with TZ/PD (NHB6)

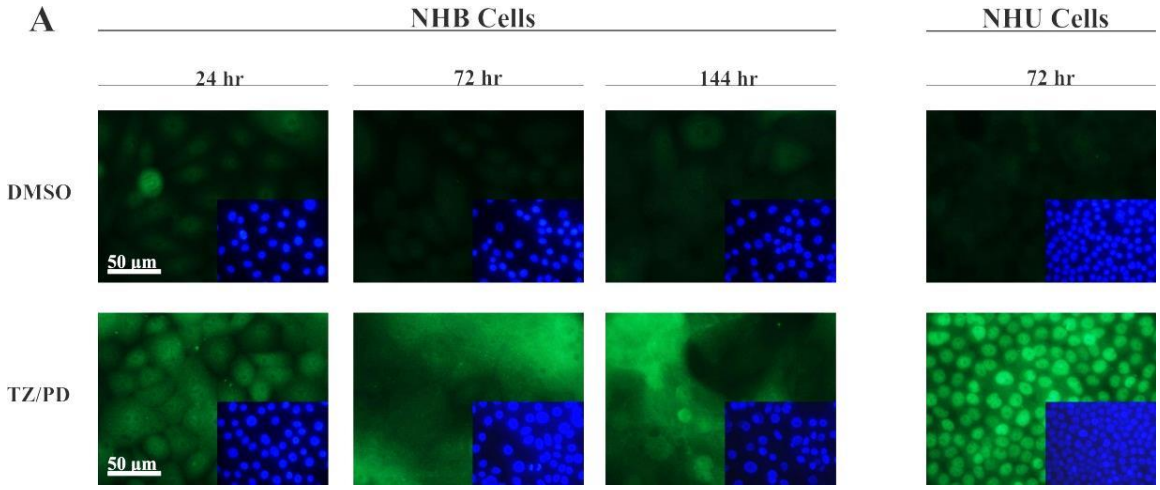

Figure 7.13 Evaluation of Transcription Factor Protein Expression by Immunofluorescence Microscopy in NHB Cells (NHB6) Treated with TZ/PD for 24, 72 and 144 hours – A) ELF3

NHB cells (NHB6) were treated with either 0.1% DMSO (vehicle control) or TZ/PD for 24, 72 and 144 hours. A single NHU cell line (NHU7) which had been treated with either 0.1 % DMSO or TZ/PD for 72 hours was used as a positive control for comparison. **A)** ELF3, **B)** FOXA1/2 (Santa Cruz, C-20), **C)** GATA3, and **D)** PPARγ (Cell Signaling, D69) expression was assessed by immunofluorescence on formalin-fixed slides which had been permeabilised using Triton X-100. Inset images show the corresponding Hoechst 33258 staining to demonstrate cell density and nuclei location. All antibody-labelled images were taken at the same exposure for both NHB cells and NHU cells. Hoechst 33258 images were taken at optimal exposures. Note weak expression of ELF3 in NHB cells at all time points.

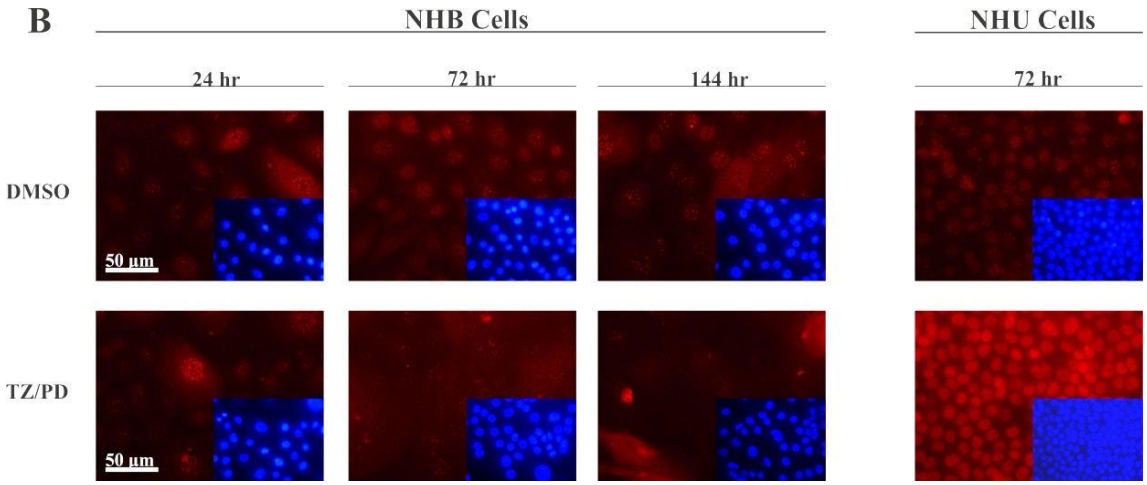

Figure 7.13 Evaluation of Transcription Factor Protein Expression by Immunofluorescence Microscopy in NHB Cells (NHB6) Treated with TZ/PD for 24, 72 and 144 hours - B) FOXA1/2

See main caption on page 280. Note weak/absent expression of FOXA1/2 in NHB cells even following use of the TZ/PD protocol for up to 144 hours.

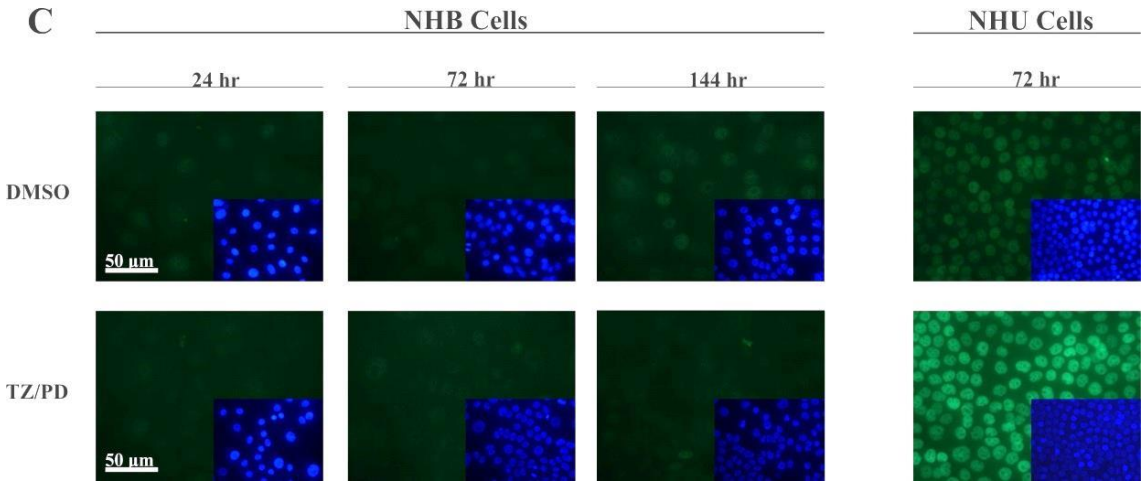

Figure 7.13 Evaluation of Transcription Factor Protein Expression by Immunofluorescence Microscopy in NHB Cells (NHB6) Treated with TZ/PD for 24, 72 and 144 hours - C) GATA3

See main caption on page 280. Note weak/absent expression of GATA3 in NHB cells even following use of the TZ/PD protocol for up to 144 hours.

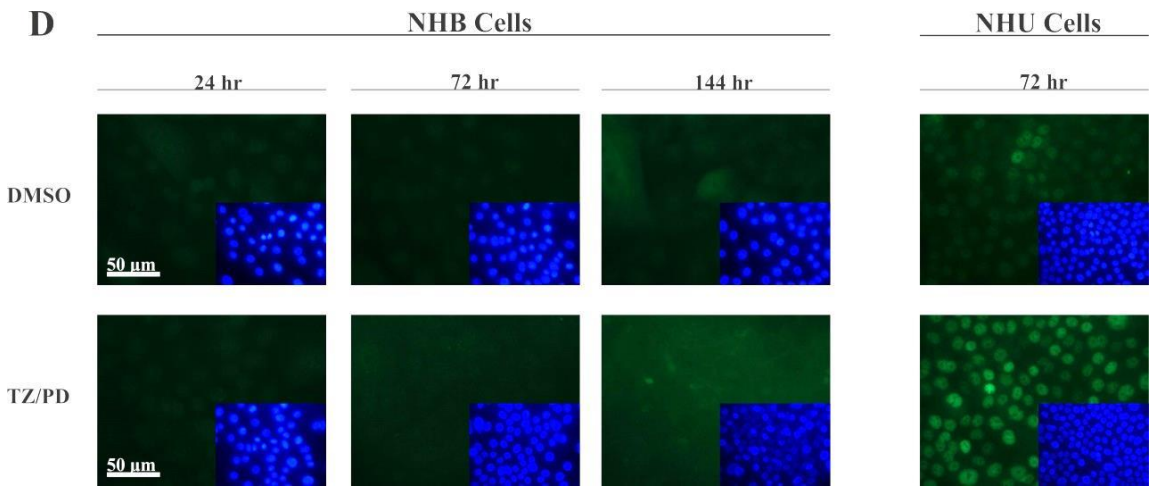

Figure 7.13 Evaluation of Transcription Factor Protein Expression by Immunofluorescence Microscopy in NHB Cells (NHB6) Treated with TZ/PD for 24, 72 and 144 hours - D) PPARγ

See main caption on page 280. Note weak/absent expression of PPARγ in NHB cells even following use of the TZ/PD protocol for up to 144 hours.

7.5.6 Additional Cell Line Results for Evaluation of Transcription Factor Expression by Immunofluorescence Microscopy in NHB Cells Treated with TZ/PD - (NHB8)

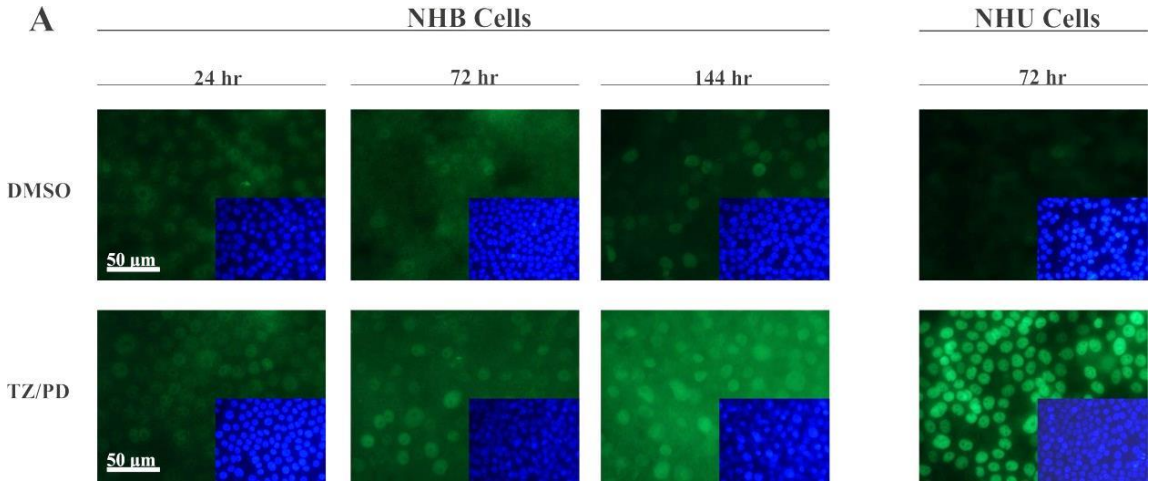

Figure 7.14 Evaluation of Transcription Factor Protein Expression by Immunofluorescence Microscopy in NHB Cells (NHB8) Treated with TZ/PD for 24, 72 and 144 hours – A) ELF3

NHB cells (NHB8) were treated with either 0.1 % DMSO (vehicle control) or TZ/PD for 24, 72 and 144 hours. A single NHU cell line (NHU6) which had been treated with either 0.1 % DMSO or TZ/PD for 72 hours was used as a positive control for comparison. **A)** ELF3, **B)** FOXA1/2 (Santa Cruz, C-20), and **C)** GATA3 expression was assessed by immunofluorescence on formalin-fixed slides which had been permeabilised using Triton X-100. Inset images show the corresponding Hoechst 33258 staining to demonstrate cell density and nuclei location. All antibody-labelled images were taken at the same exposure for both NHB cells and NHU cells. Hoechst 33258 images were taken at optimal exposures. Note weak nuclear expression of ELF3 in NHB cells at all time points, with some increased expression at the 144 hr TZ/PD time point.

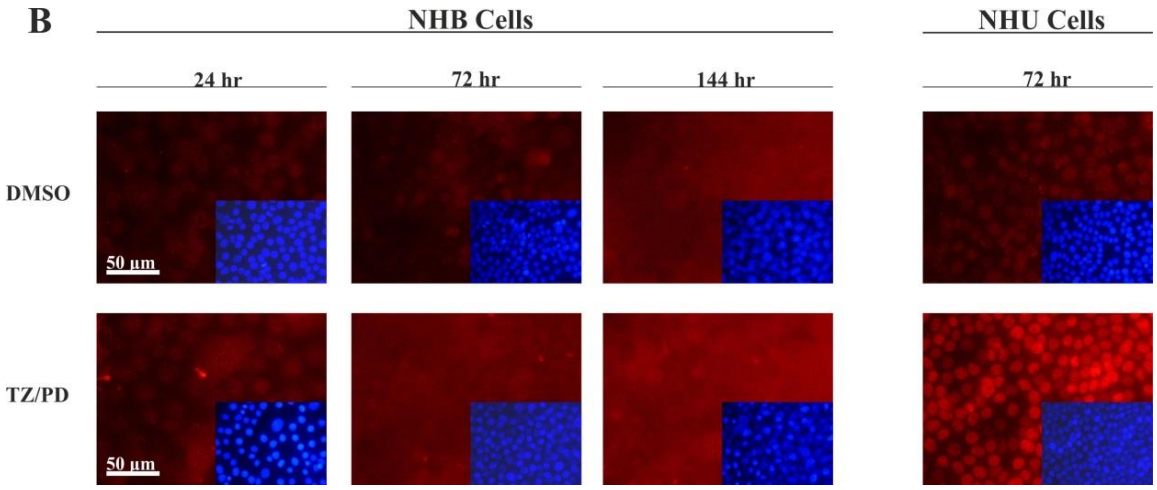

Figure 7.14 Evaluation of Transcription Factor Protein Expression by Immunofluorescence Microscopy in NHB Cells (NHB8) Treated with TZ/PD for 24, 72 and 144 hours – B) FOXA1/2

See main caption on page 283. Note weak/absent expression of FOXA1/2 in NHB cells even following use of the TZ/PD protocol for up to 144 hours.

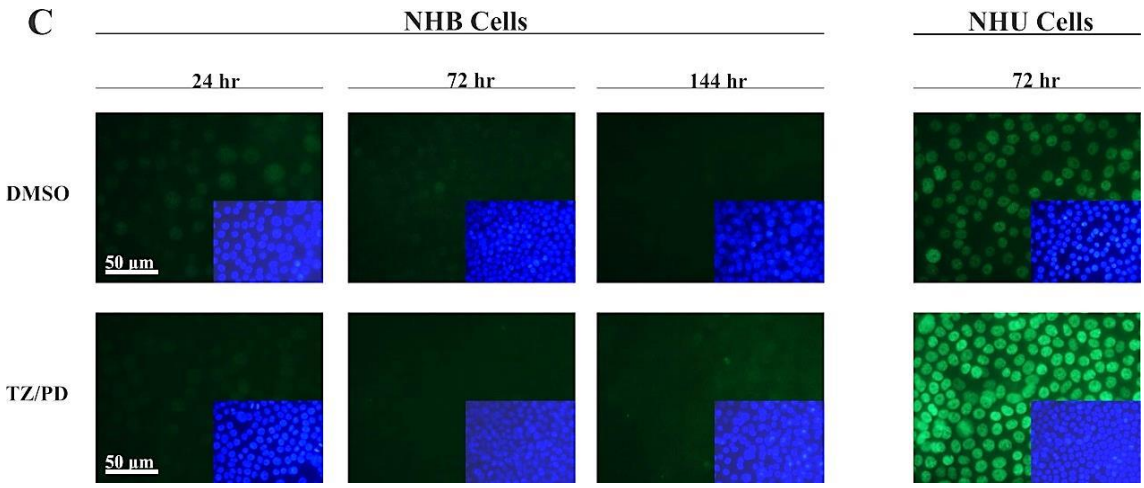

Figure 7.14 Evaluation of Transcription Factor Protein Expression by Immunofluorescence Microscopy in NHB Cells (NHB8) Treated with TZ/PD for 24, 72 and 144 hours – C) GATA3

See main caption on page 283. Note weak/absent expression of GATA3 in NHB cells even following use of the TZ/PD protocol for up to 144 hours.

7.5.7 Additional Cell Line Results for Evaluation of Uroplakin Gene Expression by RT-PCR in NHB Cells Treated with TZ/PD

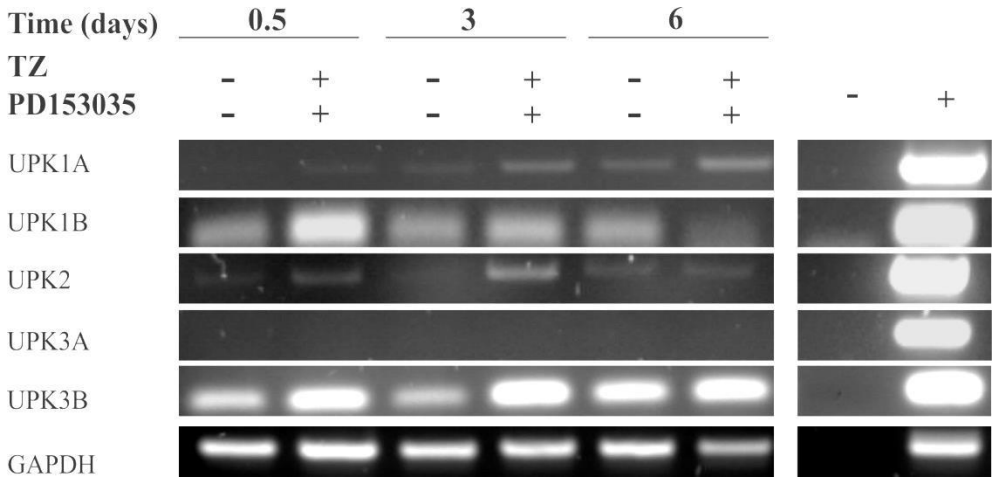

Figure 7.15 Evaluation of Uroplakin Gene Expression by RT-PCR in NHB Cells (NHB4) Following TZ/PD Treatment

Buccal epithelial cells (NHB4) were treated with either 0.1 % DMSO (vehicle control) or TZ/PD for 0.5, 3 or 6 days. The gene expression of the five uroplakin genes (UPK1A, UPK1B, UPK2, UPK3A, UPK3B) is shown by RT-PCR. PCR was performed using 30 cycles. GAPDH was used as a loading control (25 cycles). H_2O (no template) was used as a negative control (-). Genomic DNA was used as the positive control for the PCR (+). Note expression of UPK1A, UPK1B, UPK2 and UPK3B in NHB cells. UPK3A expression was absent.

7.5.8 Additional Cell Line Results for Assessment of Claudin Gene Expression by RT-PCR in NHB Cells Treated with TZ/PD

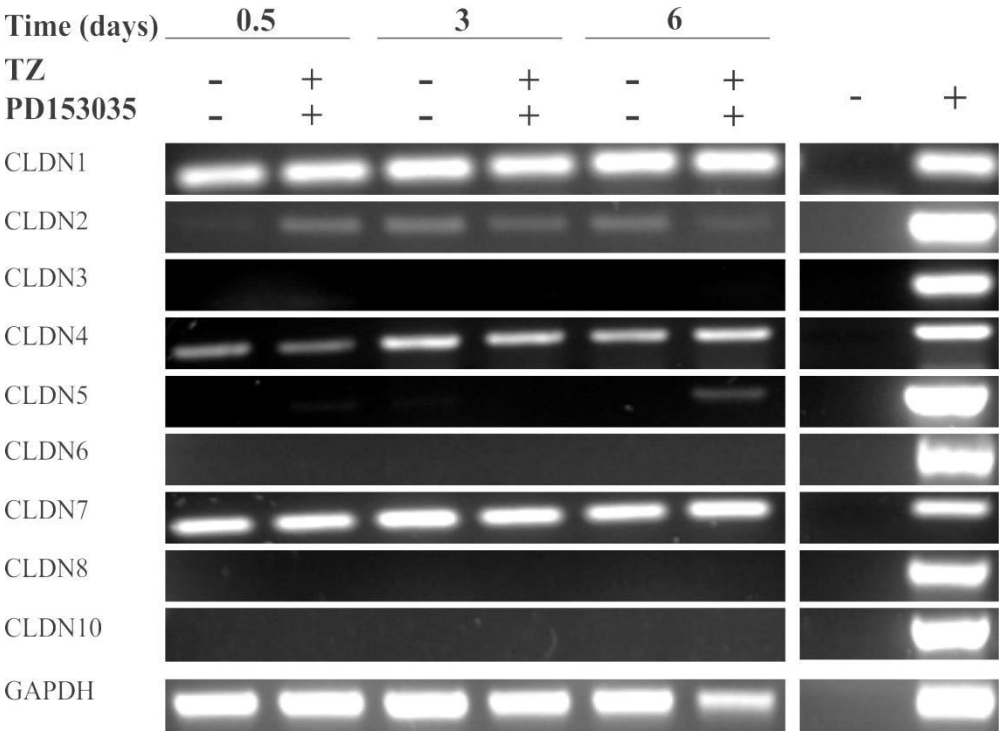

Figure 7.16 Evaluation of Claudin Gene Expression by RT-PCR in NHB Cells (NHB4) Following TZ/PD Treatment

NHB cells (NHB4) were treated with either 0.1 % DMSO (vehicle control) or TZ/PD for 0.5, 3 or 6 days. The gene expression of claudins (CLDNs) 1-10 is shown by RT-PCR. PCR was performed using either 30 or 35 cycles for a given gene. GAPDH was used as a loading control (25 cycles). H_2O (no template) was used as a negative control (-). Genomic DNA was used as the positive control for the PCR (+). Note expression of CLDN1, CLDN2, CLDN4, CLDN5 and CLDN7 in NHB cells.

7.5.9 Additional Cell Line Results for Evaluation of Stratified Squamous Differentiation-Associated Gene Expression by RT-PCR in NHB Cells Treated with TZ/PD

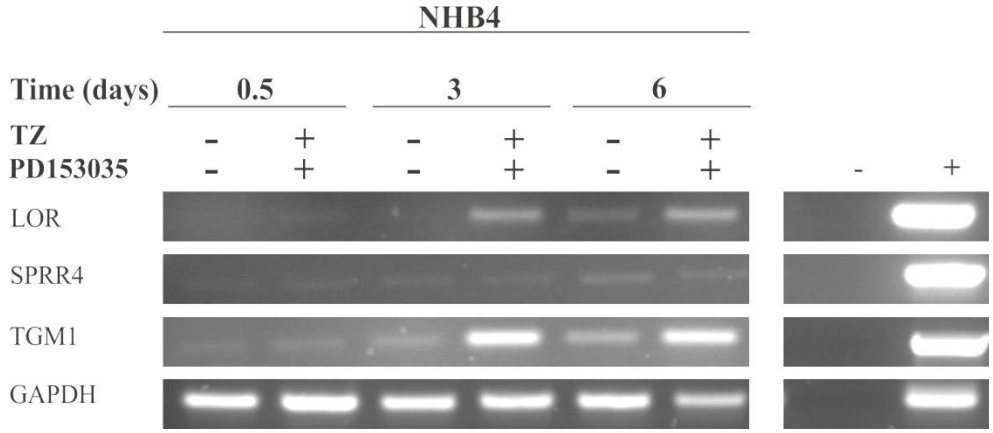

Figure 7.17 Assessment of Stratified Squamous Differentiation-Associated Gene Expression by RT-PCR in NHB Cells (NHB4) Following TZ/PD Treatment
Buccal epithelial cells (NHB4) were treated with either 0.1 % DMSO (vehicle control) or TZ/PD for 0.5, 3 or 6 days. The transcript expression of several stratified sqaumous differentiation-associated genes (LOR, SPRR4 and TGM1) is shown by RT-PCR. PCR was performed using either 25 or 30 cycles for a given gene. GAPDH was used as a loading control (25 cycles). H_2O was used as a negative control (-). Genomic DNA was used as the positive control for the PCR (+). Note expression of LOR, SPRR4 and TGM1 in NHB cells.

7.5.10 Positive Control Images and Example Negative Control Images for Immunohistochemistry

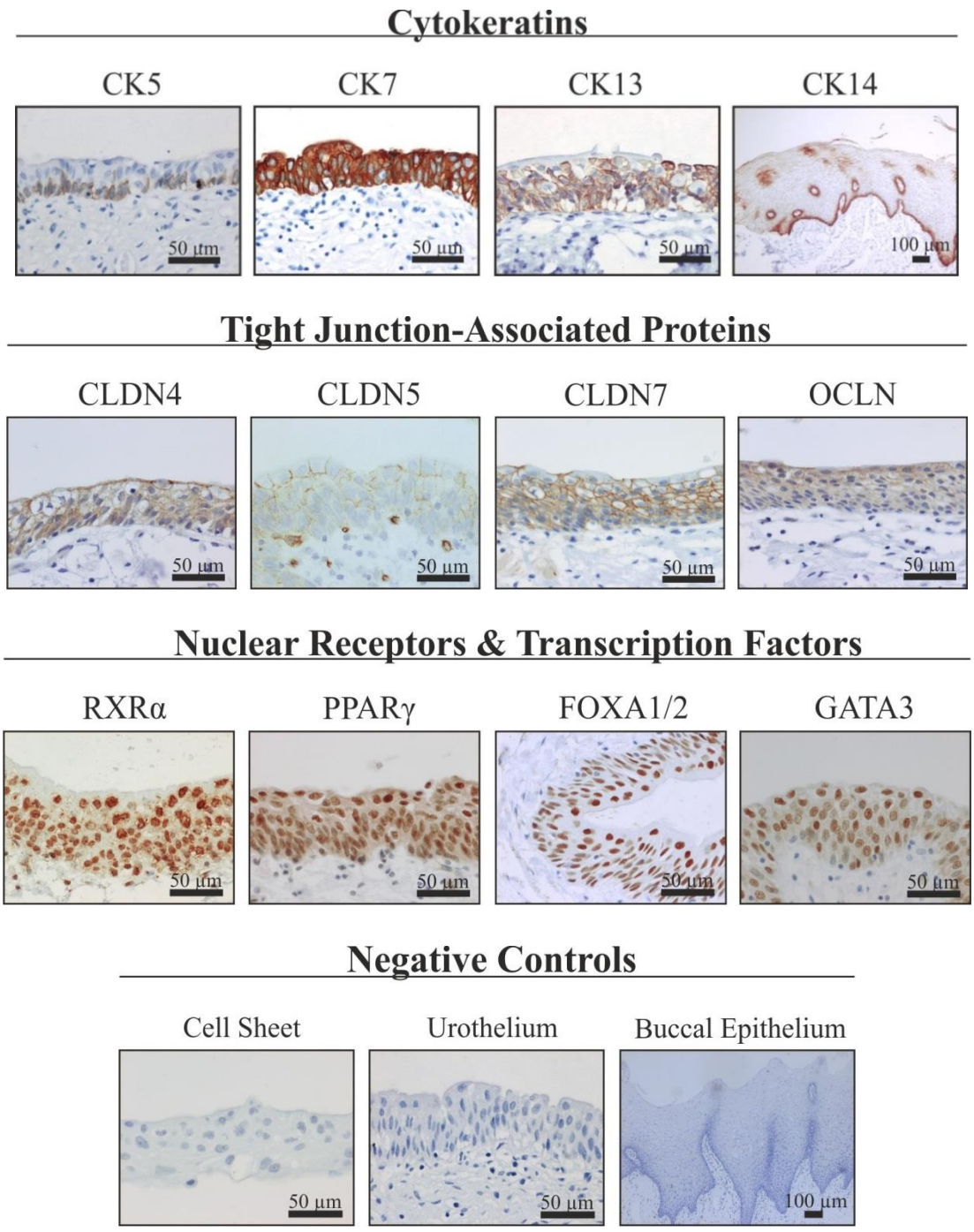

Figure 7.18 Positive Control Images and Example Negative Control Images For Immunohistochemistry

The urothelium of human bladder or ureter was used as positive controls for of the proteins examined, except CK14, where human buccal mucosa was used. An example negative control (no primary antibody) cell sheet is shown, as are example negative controls for urothelium and buccal epithelium.

7.6 Expression of PPARγ and GATA3 in Urothelial Cell Differentiation

7.6.1 Additional Cell Line Results for Evaluation of Transcription Factor Protein Expression by Western Blotting in NHU Cells Following PPARγ Activation

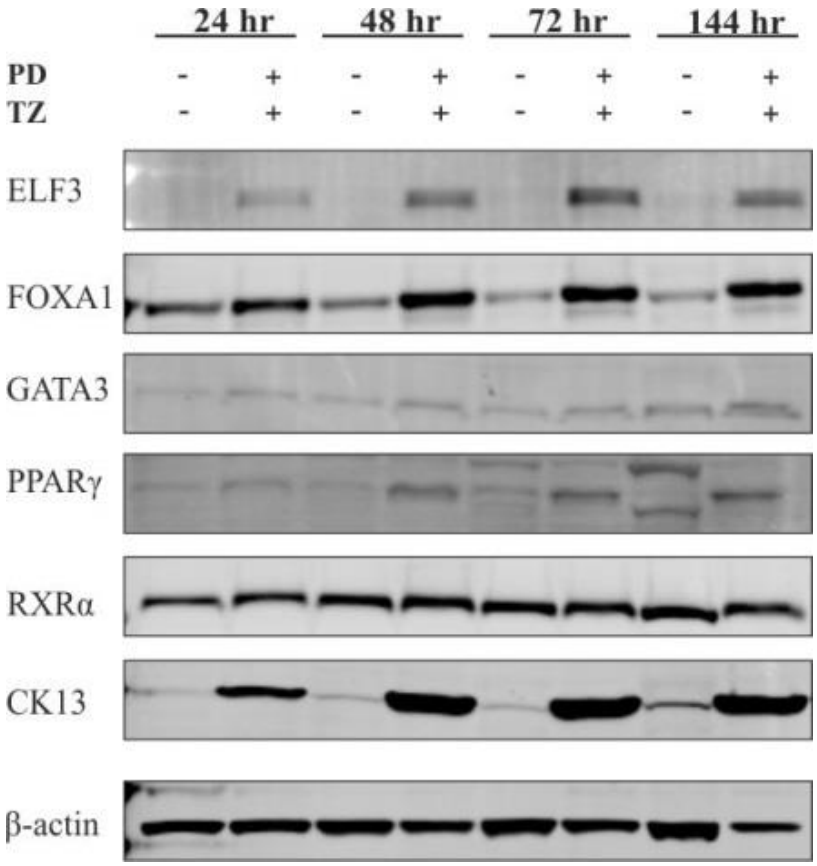

Figure 7.19 Evaluation of Transcription Factors, and Other Urothelial Cell-Associated Proteins in NHU Cells (Y1642) Following PPARγ Activation

NHU cells (Y1642) were treated with either 0.1 % DMSO (vehicle control) or TZ/PD for 24, 48, 72 or 144 hours. ELF3, FOXA1 (Santa Cruz, Q-6), GATA3, PPARγ (Cell Signaling, D69), and RXRα protein expression was assessed by western blotting. For PPARγ expression, the band corresponding to PPARγ1 (approximately 52 kDa) is shown. 25 μg of protein was loaded into each well and β-actin was used as a loading control. CK13 expression was evaluated to demonstrate induction of transitional-type differentiation. Note the clear upregulation of ELF3, FOXA1, GATA3 and PPARγ expression following PPARγ activation using the TZ/PD protocol.

7.6.2 Additional Cell Line Results for Evaluation of Transcription Factor Protein Expression by Immunofluorescence Microscopy in NHU Cells Following PPARγ – Y1642

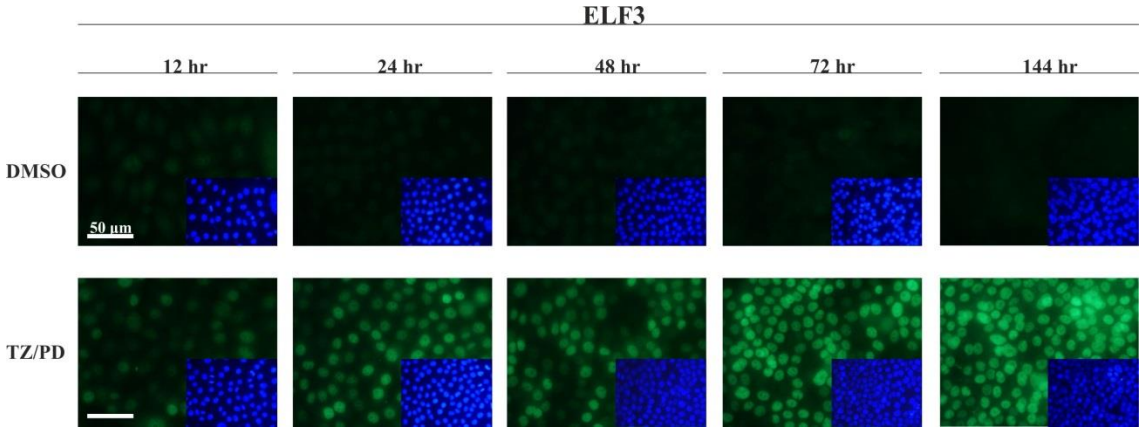

Figure 7.20 Evaluation of Transcription Factor Protein Expression by Immunofluorescence Microscopy in NHU Cells (Y1642) Following PPARγ Activation using the TZ/PD Protocol for 12, 24, 48, 72 and 144 hours – ELF3

NHU cells (Y1642) were treated with either 0.1 % DMSO (vehicle control) or TZ/PD for 12, 24, 48, 72 and 144 hours. Immunofluorescence labelling for **(A)** ELF3, **(B)** FOXA1/2 (Santa Cruz, C-20), and **(C)** GATA3 was performed on formalin-fixed slides which had been permeabilised with Triton X-100. Inset images represent the corresponding Hoechst 33258 staining to demonstrate cell density and nuclei location. All antibody labelled images were taken at the same exposure to enable for comparison of expression between the untreated and treated cells, and between the different time points. Hoechst 33258 images were taken at optimal exposures. Note the clear upregulation of expression and nuclear localisation of ELF3 as a result of PPARγ activation.

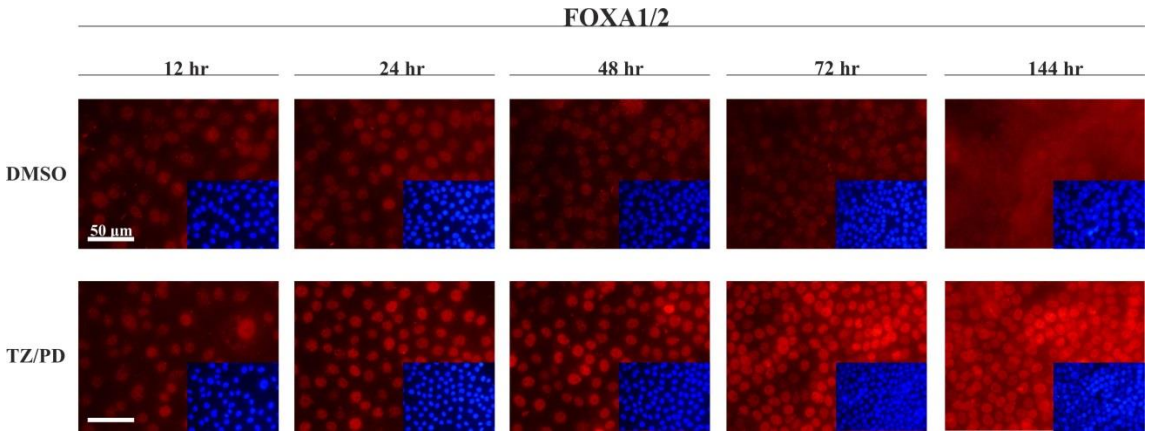

Figure 7.20 Evaluation of Transcription Factor Protein Expression by immunofluorescence Microscopy in NHU Cells (Y1642) Following PPARγ Activation using the TZ/PD Protocol for 12, 24, 48, 72 and 144 hours – FOXA1/2

See main caption on page 290. Note nuclear expression of FOXA1/2 in NHU cells, with upregulated expression associated with PPARγ activation.

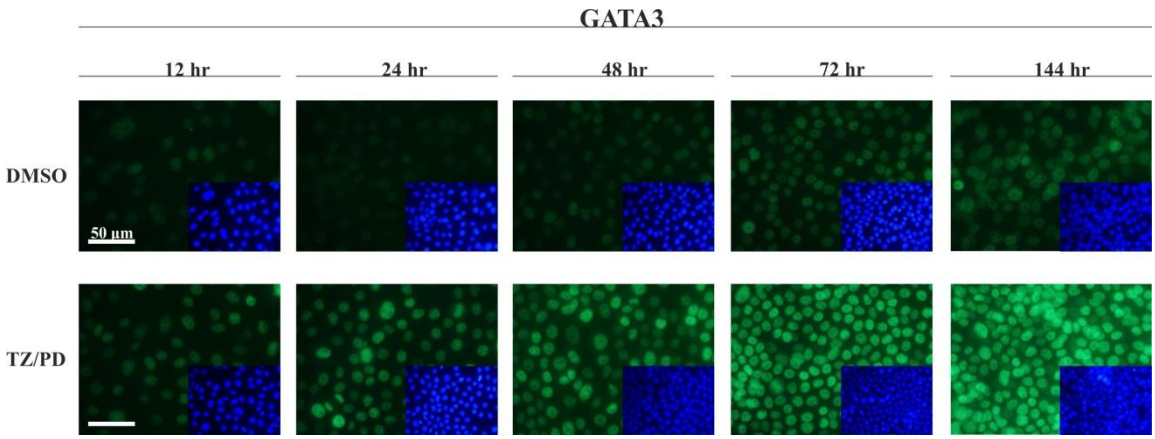

Figure 7.20 Evaluation of Transcription Factor Protein Expression by immunofluorescence Microscopy in NHU Cells (Y1642) Following PPARγ Activation using the TZ/PD Protocol for 12, 24, 48, 72 and 144 hours – GATA3

See main caption on page 290. Note nuclear expression of GATA3 in NHU cells, with upregulated expression associated with PPARγ activation as well as with increased confluence.

7.6.3 Additional Cell Line Results for Evaluation of Transcription Factor Protein Expression by Immunofluorescence Microscopy in NHU Cells Following PPARγ – Y1541

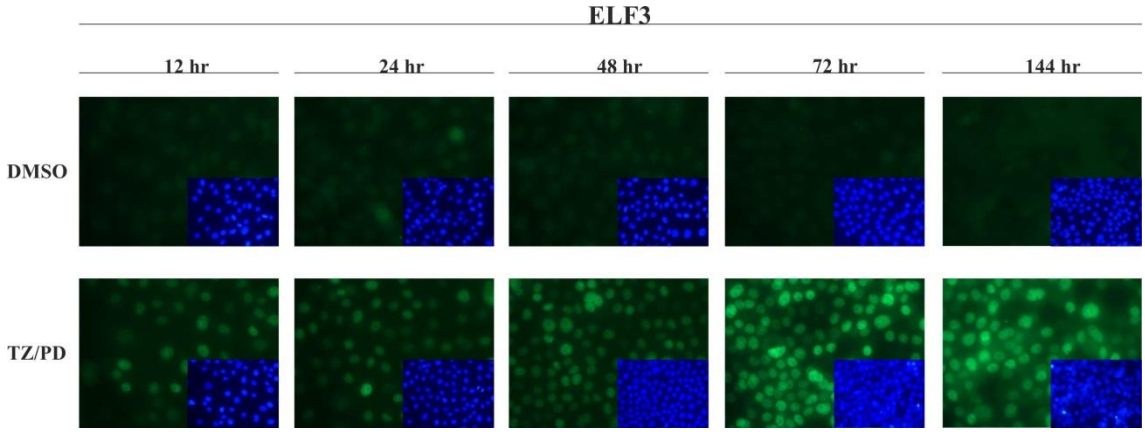

Figure 7.21 Evaluation of Transcription Factor Protein Expression by immunofluorescence Microscopy in NHU Cells (Y1541) Following PPARγ Activation using the TZ/PD Protocol for 12, 24, 48, 72 and 144 hours – ELF3

NHU cells (Y1541) were treated with either 0.1 % DMSO (vehicle control) or TZ/PD for 12, 24, 48, 72 and 144 hours. Immunofluorescence labelling for **(A)** ELF3, **(B)** FOXA1/2 (Santa Cruz, C-20), **(C)** GATA3 and **(D)** PPARγ (Cell, Signaling, D69) was performed on formalin-fixed slides which had been permeabilised with Triton X-100. Inset images represent the corresponding Hoechst 33258 staining to demonstrate cell density and nuclei location. All antibody labelled images were taken at the same exposure to enable for comparison of expression between the untreated and treated cells, and between the different time points. Hoechst 33258 images were taken at optimal exposures. Note the clear upregulation of expression and nuclear localisation of ELF3 as a result of PPARγ activation.

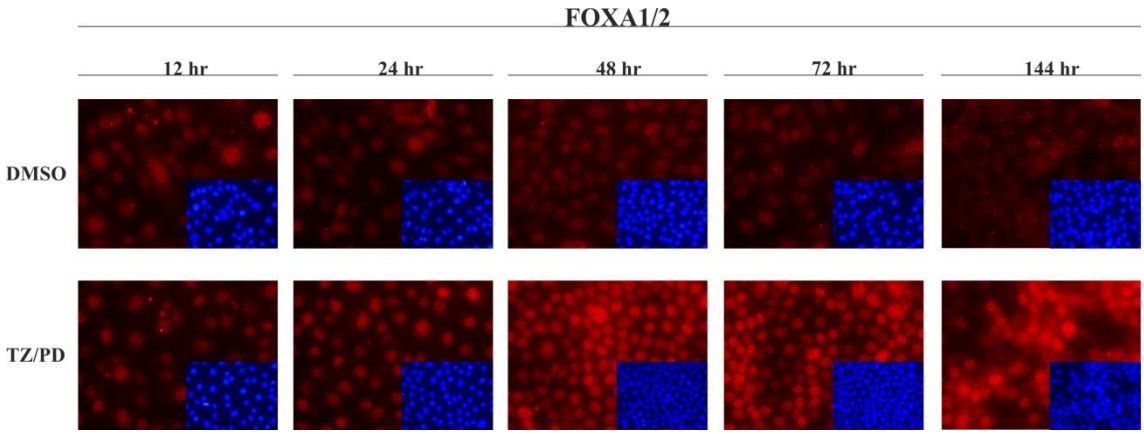

Figure 7.21 Evaluation of Transcription Factor Protein Expression by immunofluorescence Microscopy in NHU Cells (Y1541) Following PPARγ Activation using the TZ/PD Protocol for 12, 24, 48, 72 and 144 hours – FOXA1/2

See main caption on page 292. Note nuclear expression of FOXA1/2 in NHU cells, with upregulated expression associated with PPARγ activation.

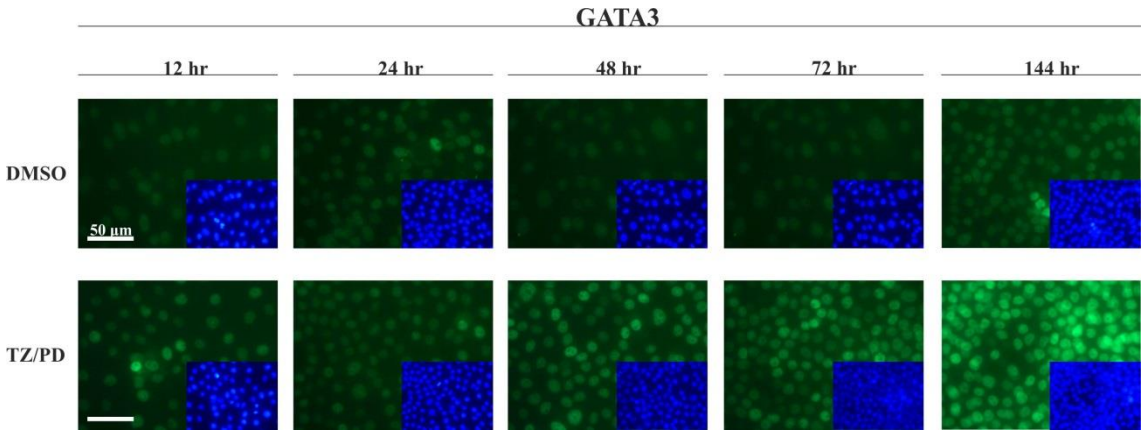

Figure 7.21 Evaluation of Transcription Factor Protein Expression by immunofluorescence Microscopy in NHU Cells (Y1541) Following PPARγ Activation using the TZ/PD Protocol for 12, 24, 48, 72 and 144 hours – GATA3

See main caption on page 292. Note nuclear expression of GATA3 in NHU cells, with upregulated expression associated with PPARγ activation and increased confluence.

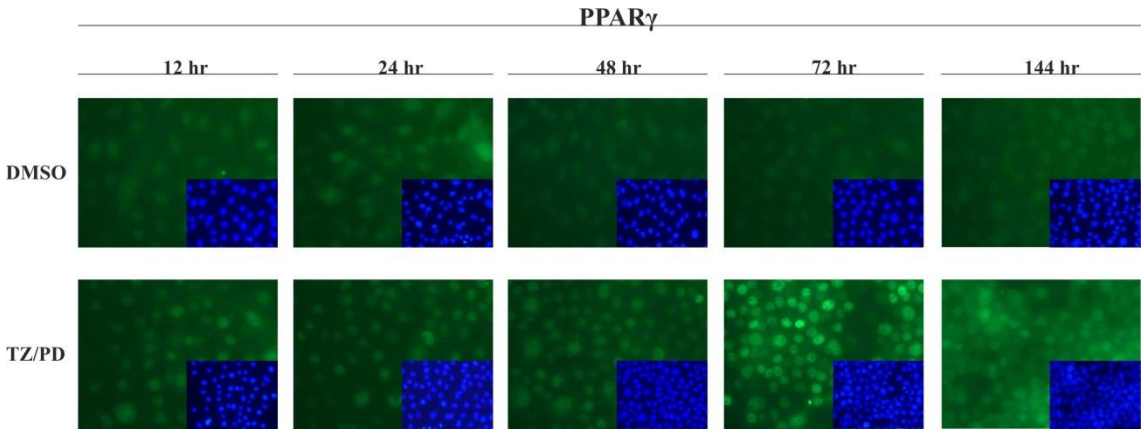

Figure 7.21 Evaluation of Transcription Factor Protein Expression by immunofluorescence Microscopy in NHU Cells (Y1541) Following PPARγ Activation using the TZ/PD Protocol for 12, 24, 48, 72 and 144 hours – PPARγ

See main caption on page 292. Note weak nuclear expression of PPARγ in NHU cells, with clear upregulated expression associated with PPARγ activation and 72 hours.

7.6.4 Example Positive Control (CK20 Expression) to Demonstrate Successful Differentiation of NHU Cells using TZ/PD

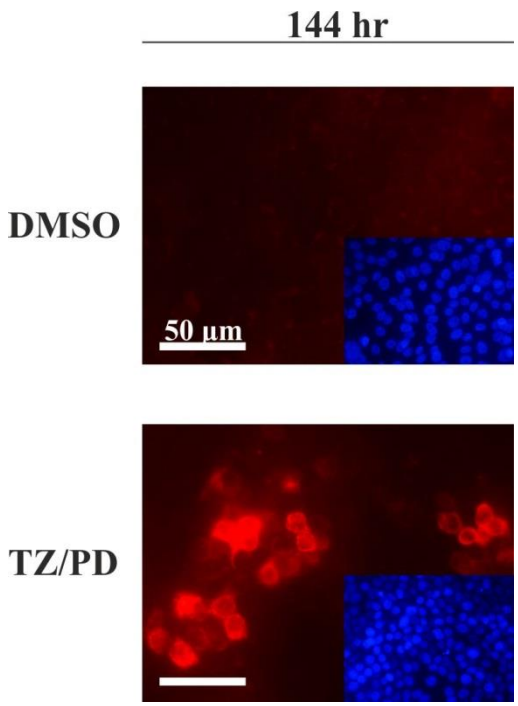

Figure 7.22 Example of CK20 Expression by immunofluorescence Microscopy in NHU Cells (Y1642) Treated with TZ/PD for 144 hours

CK20 expression was assessed in NHU cells (Y1642) to demonstrate successful differentiation of the cells using the TZ/PD protocol at the 144 hour time point.

7.6.5 Additional Cell Line Results for PPARγ Expression in MG132 Treated NHU Cells (Y1691)

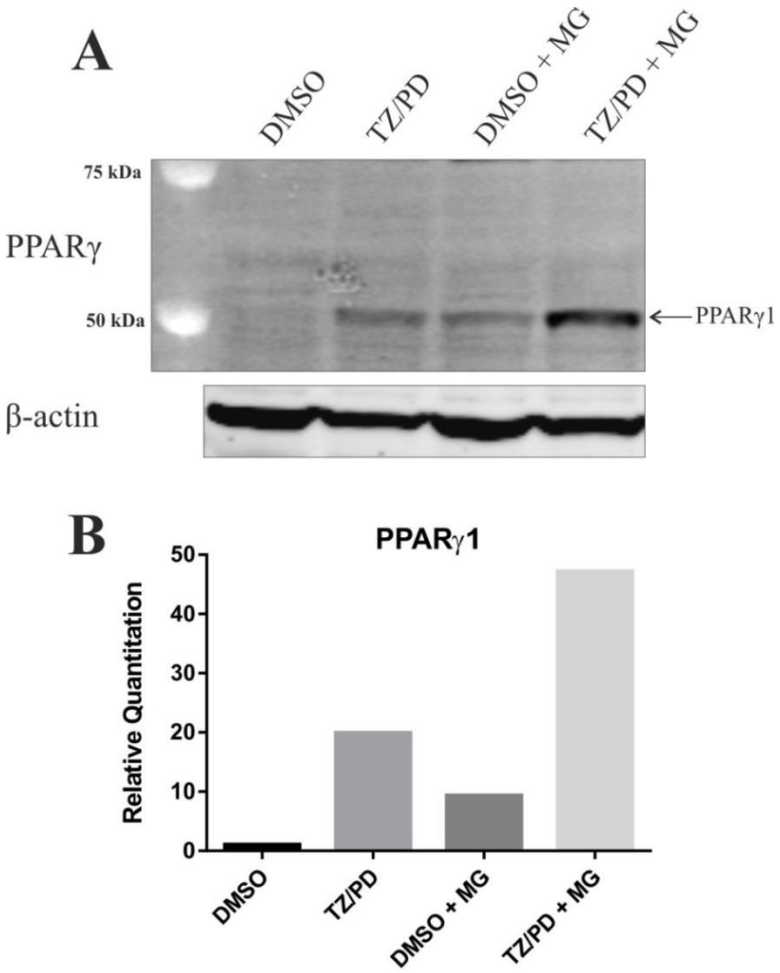

Figure 7.23 Evaluation of PPARγ Protein Expression by Western Blotting in NHU Cells (Y1691) Following Proteasome Inhibition

A) Western blot showing PPARγ protein expression (Cell Signaling, D69) in NHU cells (Y1691) treated with the proteasome inhibitor, MG132 (MG). NHU cells were first treated with either 0.1% DMSO (vehicle control) or TZ/PD for 72 hours. The medium was then changed, and the cells were either treated with 0.1 % DMSO (vehicle control) or 12.5 μM MG132 for 6 hours. β-actin was used as a loading control. 20 μg of protein was loaded into each well.

B) The graph showing densitometry analysis for PPARγ1 protein expression. Data is shown relative to the DMSO treated cells. All values were first normalised to β-actin.

Note clear upregulation of PPARγ1 protein expression in NHU cells following treatment with MG132. PPARγ2 expression was absent and not affected by proteasome inhibition in NHU cells.

7.6.6 Densitometry Analysis of Western Blots for MG132 Treated NHU Cells and UMUC9 Cells

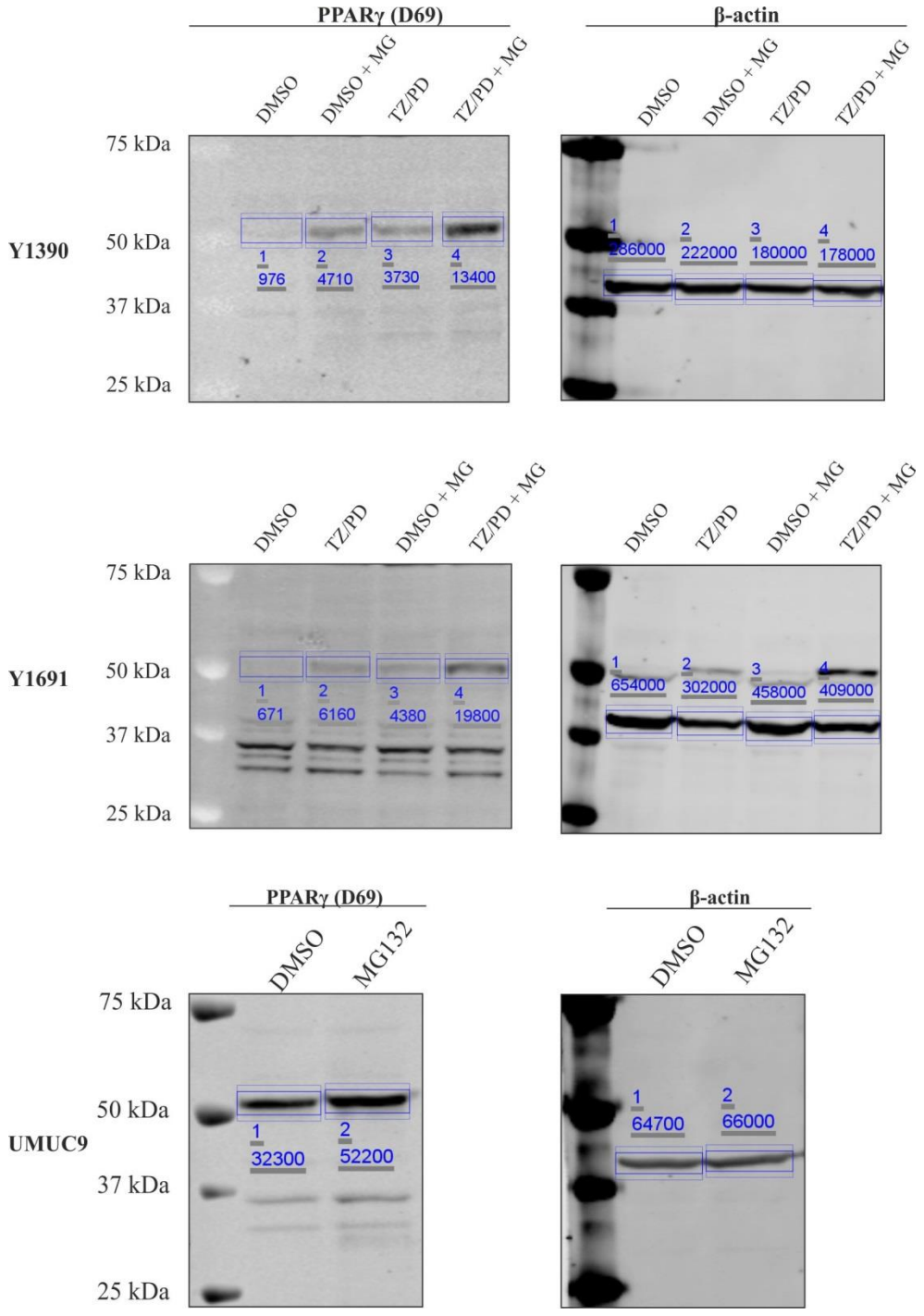

Figure 7.24 Densitometry Analysis for PPARγ1 and β-actin Expression in Two Independent NHU Cell Lines and UMUC9 Cells Treated with MG132

Western blots for PPARγ (Cell Signaling, D69) and β-actin expression are shown for the cells lines indicated. Densitometry is shown for the PPARγ1-specific band at approximately 52 kDa.

7.6.7 Densitometry Analysis of Western Blots for GATA3 Knockdown Experiments

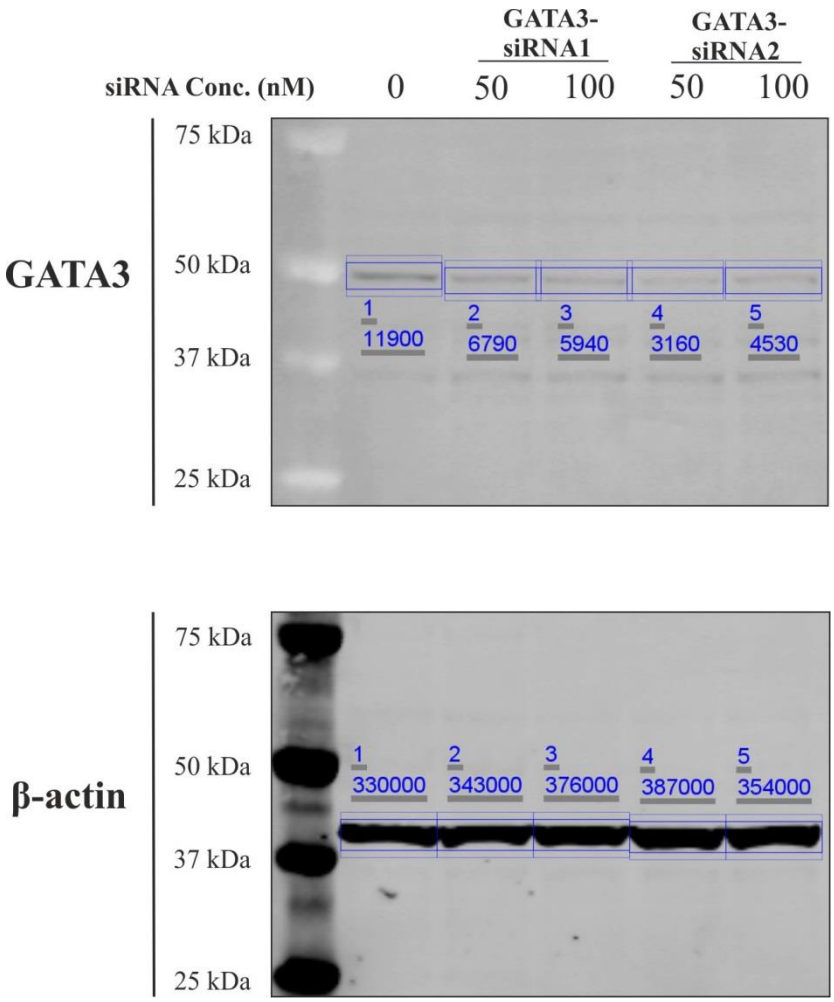

Figure 7.25. Densitometry Analysis for Western Blots for GATA3 and β-actin in NHU cells (Y1752) Transfected with Control and GATA3 siRNA – siRNA Titration

Densitometry analysis of western blots for GATA3 and β-actin expression are shown for the titration of GATA3 siRNA in NHU cells (Y1752).

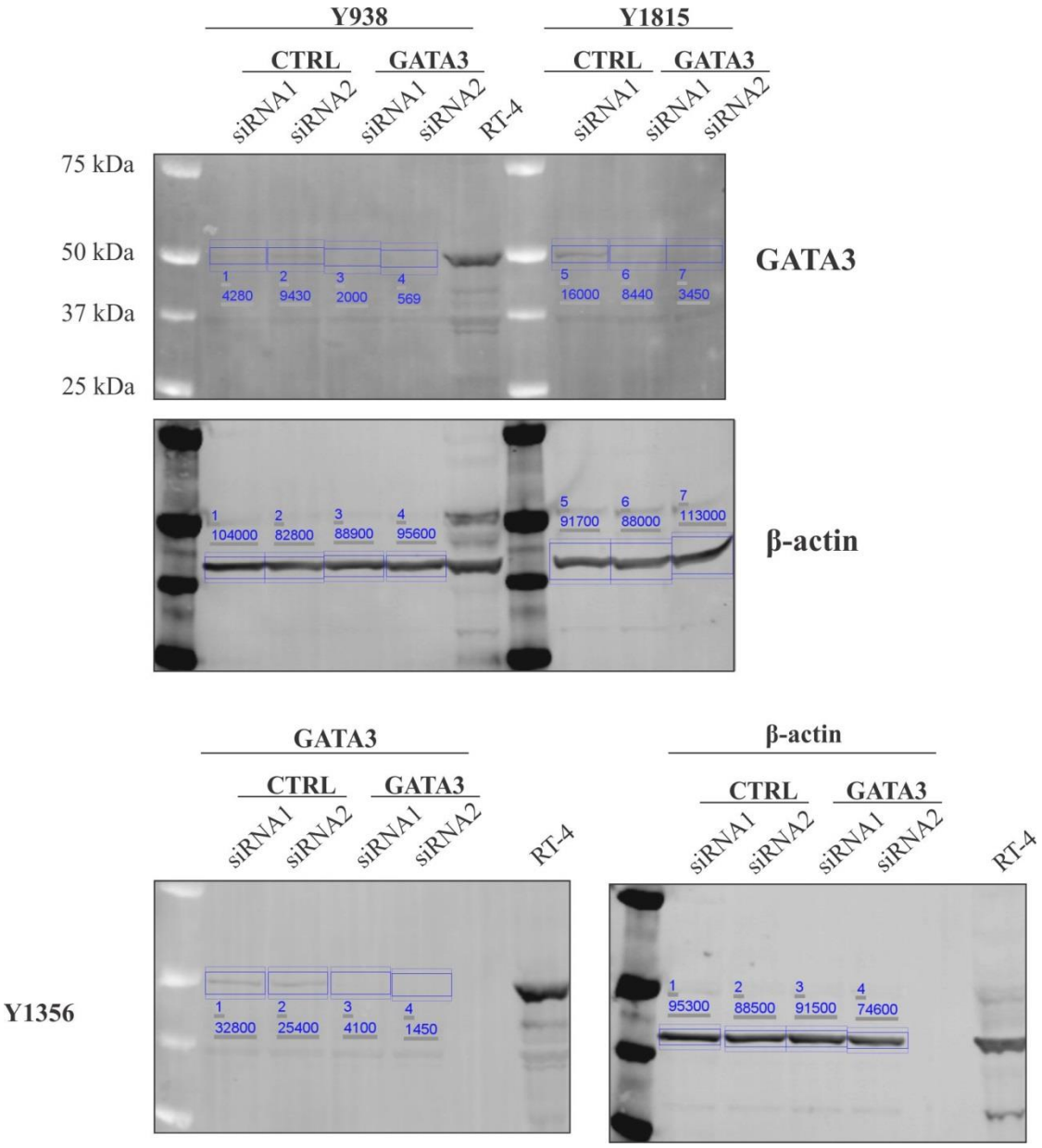

Figure 7.26. Densitometry Analysis for GATA3 and β-actin Expression in Three NHU Cell Lines Transfected with Control and GATA3 siRNA

Western blots for GATA3 and β-actin are shown for the three independent cell lines (Y1356, Y938 and Y1815), which were transfected with control and GATA3 siRNA.

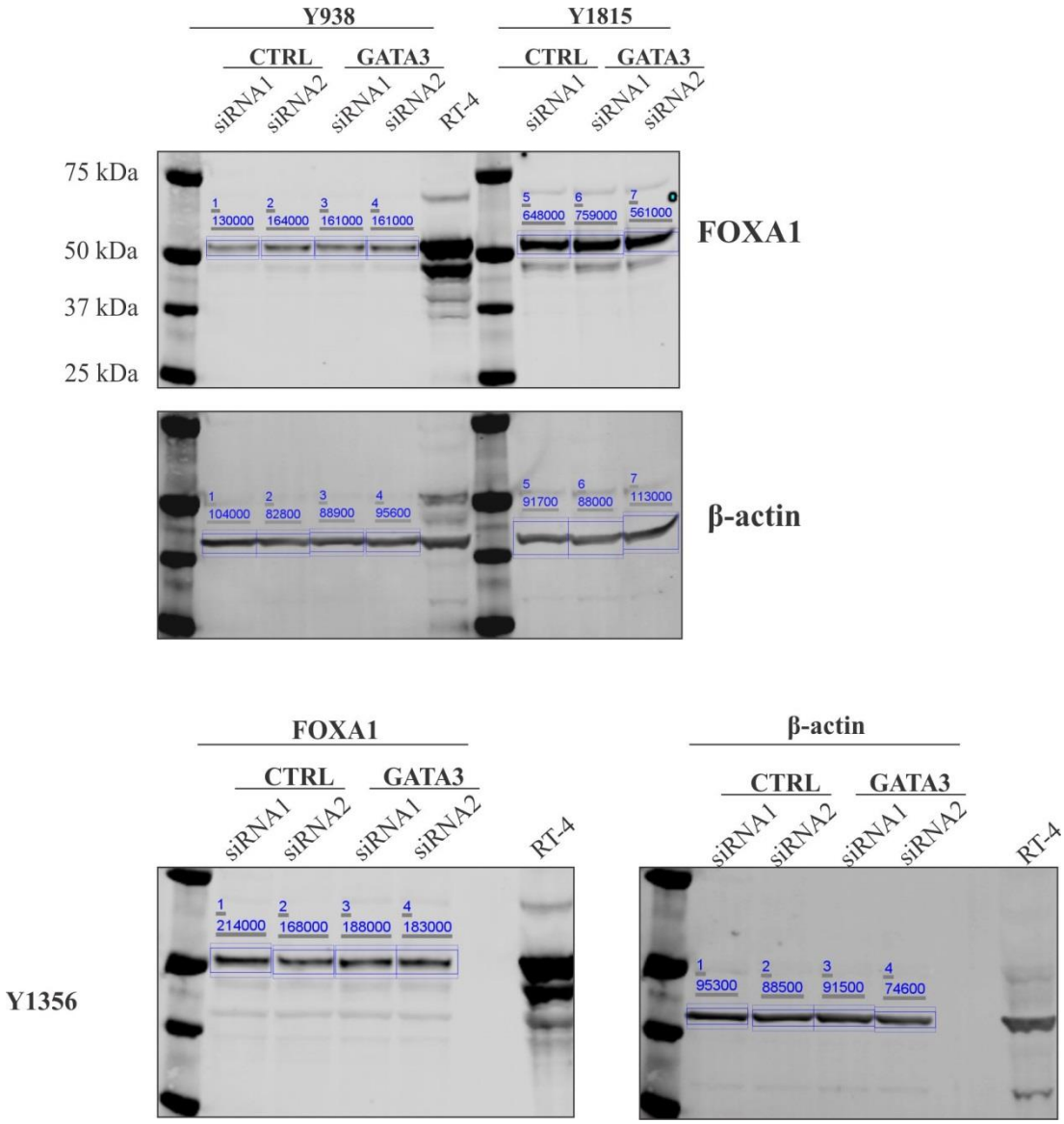

Figure 7.27. Densitometry Analysis for FOXA1 and β-actin Expression in Three NHU Cell Lines Transfected with Control and GATA3 siRNA

Western blots for FOXA1 (Santa Cruz, Q6) and β-actin are shown for the three independent cell lines (Y1356, Y938 and Y1815), which were transfected with control and GATA3 siRNA.

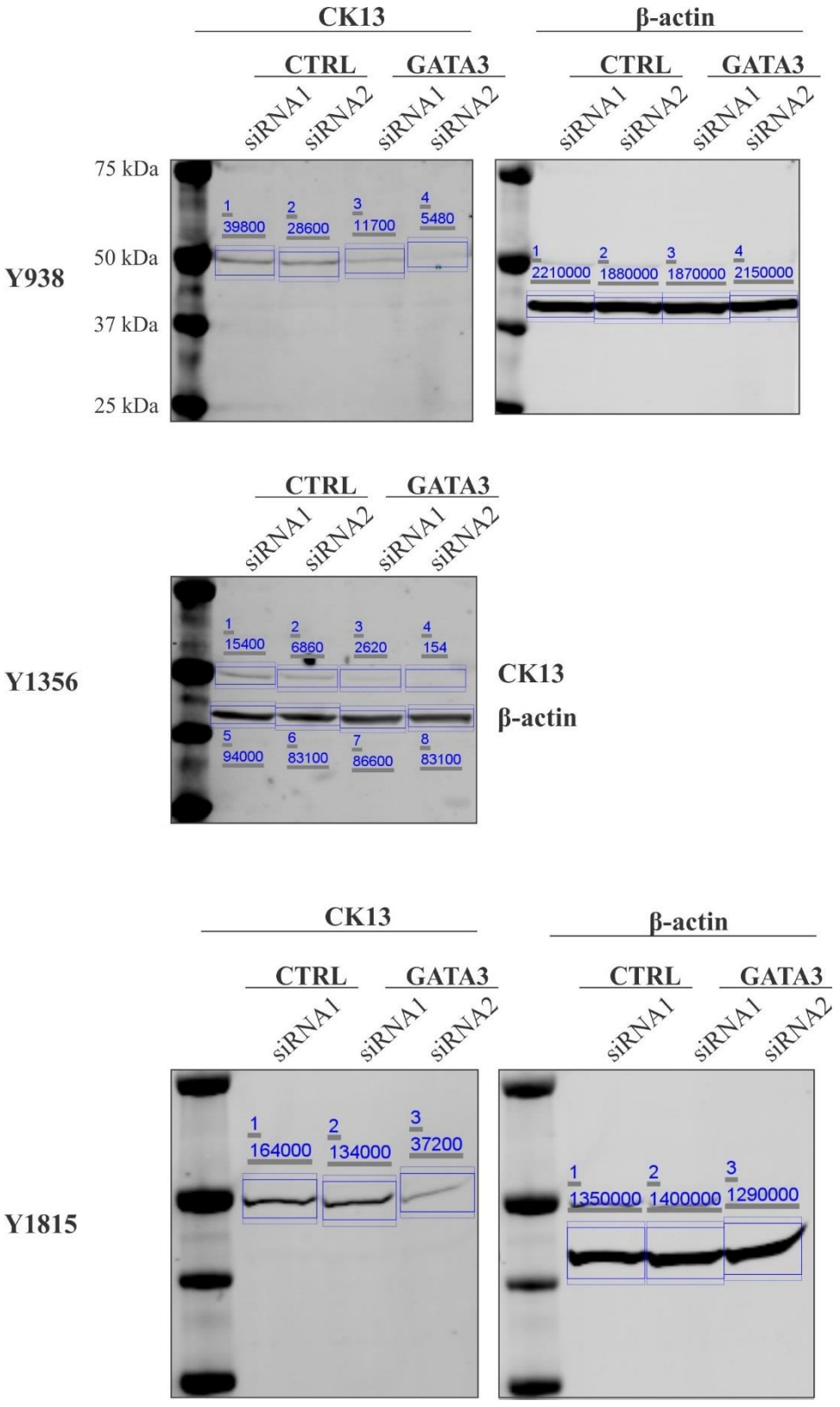

Figure 7.28. Densitometry Analysis for CK13 and β-actin Expression in Three NHU Cell Lines Transfected with Control and GATA3 siRNA

Western blots for CK13 and β-actin are shown for the three independent cell lines (Y1356, Y938 and Y1815), which were transfected with control and GATA3 siRNA.

7.7 Overexpression of GATA3 in Buccal Epithelial Cells

7.7.1 Additional Cell Line Result for Evaluation of Transcription Factor Expression by Immunofluorescence Microscopy in Control and GATA3 Overexpressing NHB Cells Following Use of the TZ/PD Protocol (Y1590)

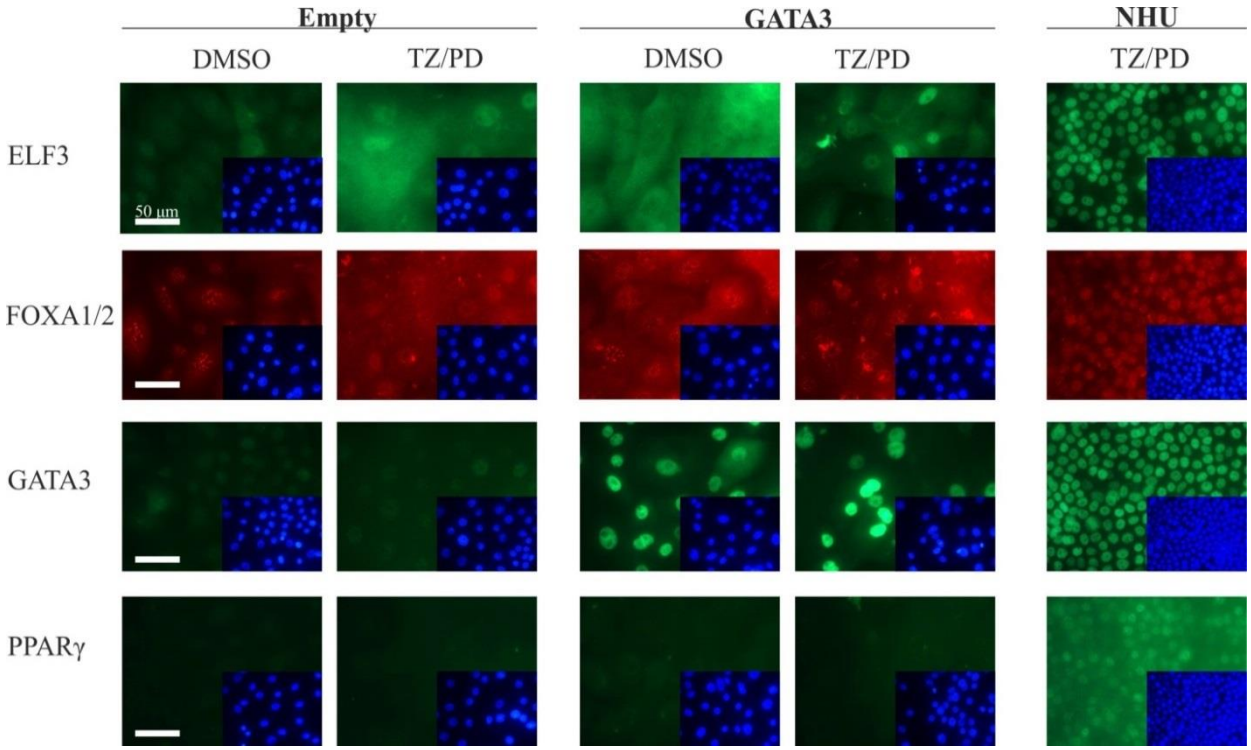

Figure 7.29 Evaluation of ELF3, FOXA1, FOXA1 GATA3, and PPARγ Expression by Immunofluorescence Microscopy in Control and GATA3 Overexpressing NHB Cells (Y1590) Treated with 0.1 % DMSO or TZ/PD for 72 Hours

Control (Empty) and GATA3 overexpressing NHB cells (Y1590) were treated with either 0.1 % DMSO (vehicle control) or TZ/PD for 72 hours. Immunofluorescence labelling for ELF3, FOXA1/2 (Santa Cruz, C-20), GATA3 and PPARγ (Cell Signaling, D69) was performed on formalin-fixed slides which had been permeabilised with Triton X-100. Inset images represent the corresponding Hoechst 33258 staining to demonstrate cell density and nuclei location. Antibody labelled images were taken at the same exposure for each antibody. Hoechst 33258 images were taken at optimal exposures. NHU cells (Y1642) which had been treated with TZ/PD for 72 hours were used as positive controls.

7.7.2 Additional Cell Line Results for Evaluation of Tight Junction Protein Expression by Western Blotting in Control and GATA3 Overexpressing NHB Cells During use of the ABS/Ca^{2+} Protocol (AS011b)

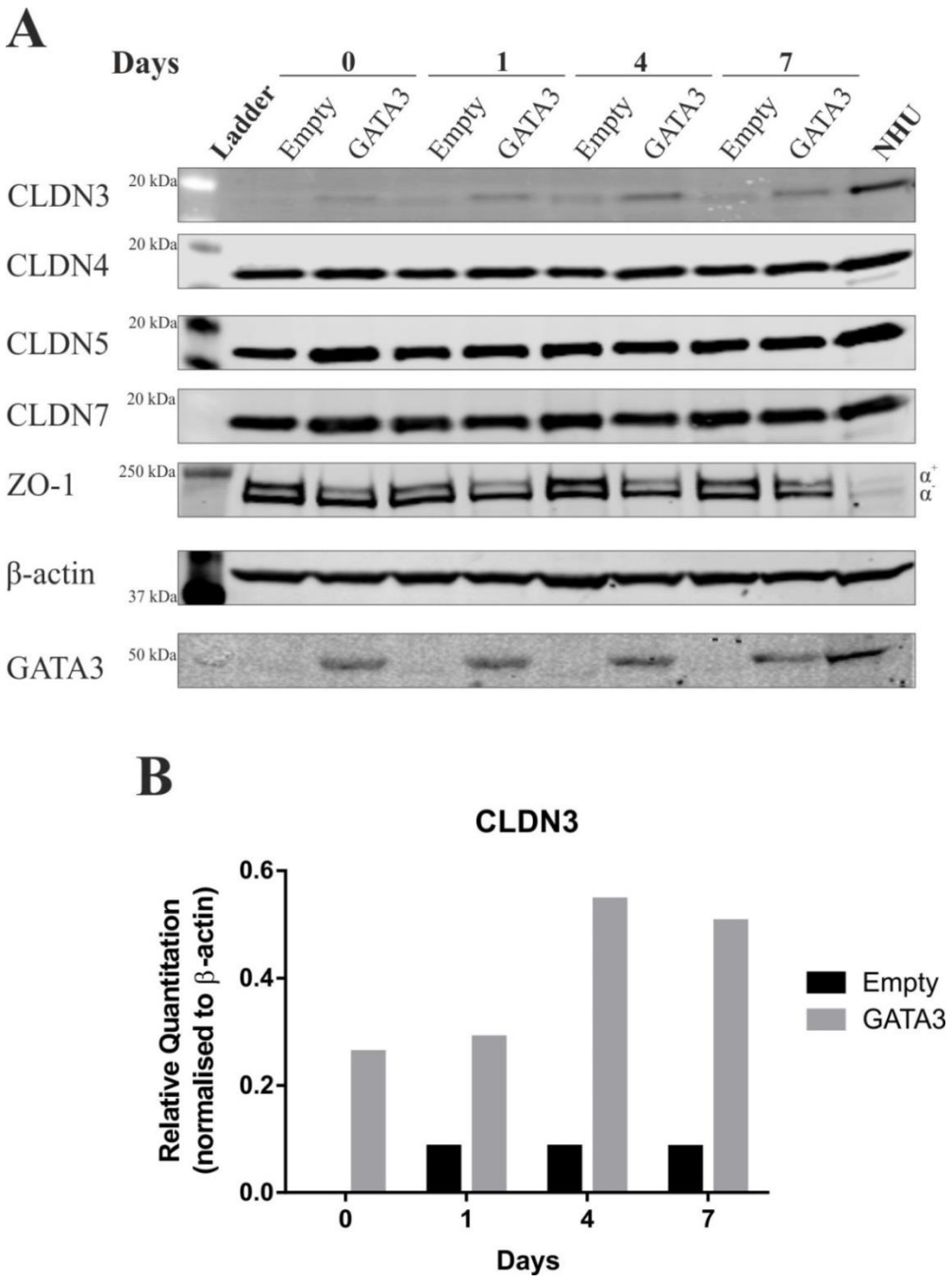

Figure 7.30 Evaluation of Tight Junction-Associated Protein Expression by Western Blotting in Control and GATA3 Overexpressing NHB Cells (AS011b) During use of the ABS/Ca^{2+} Protocol

Figure 7.30 Evaluation of Tight Junction-Associated Protein Expression by Western Blotting in Control and GATA3 Overexpressing NHB Cells (AS011b) During use of the ABS/Ca^{2+} Protocol

Control (Empty) and GATA3 overexpressing NHB cells (AS011b) were subjected to the ABS/Ca^{2+}protocol for up to 7 days. Whole protein lysates were generated on the days indicated.

C) CLDN3, CLDN4, CLDN5, CLDN7, and ZO-1 protein expression was assessed by western blotting. Evaluation of GATA3 expression demonstrated successful GATA3 overexpression at all of the time points. 25 μg of protein was loaded into each well and β-actin was used as a loading control. Protein extracted from NHU cells (Y1336), which had been differentiated with ABS/Ca^{2+} for 5 days, was included on the same western blots, and used as a positive control.

D) Densitometry analysis of CLDN3 protein expression at each of the time points during use of the ABS/Ca^{2+} protocol. Data is shown for the western blot above, corresponding to AS011b. All values were normalised to β-actin expression.

Note the clear upregulation of CLDN3 expression as a result of GATA3 overexpression in NHB cells at all time points during use of the ABS/Ca^{2+} protocol. The other tight junction-associated proteins examined were not obviously affected by GATA3 overexpression.

7.7.3 Densitometry Analysis of Western Blots for CLDN3 Expression in Control and GATA3 Overexpressing NHB Cells During use of the ABS/Ca^{2+} Protocol

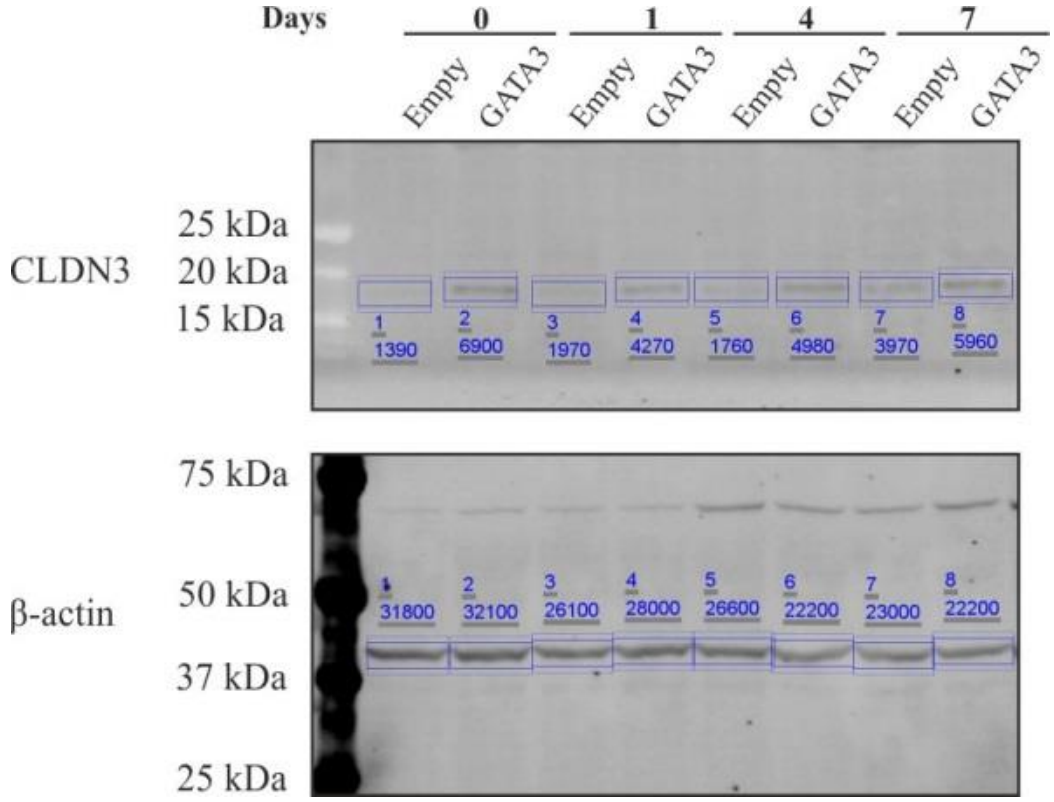

Figure 7.31 Densitometry Analysis of CLDN3 and β-actin Expression in Control and GATA3 Overexpressing NHB Cells (Y1595) During use of the ABS/Ca^{2+} Protocol
Western blots for CLDN3 and β-actin are shown for the transduced NHB cell line, Y1595.

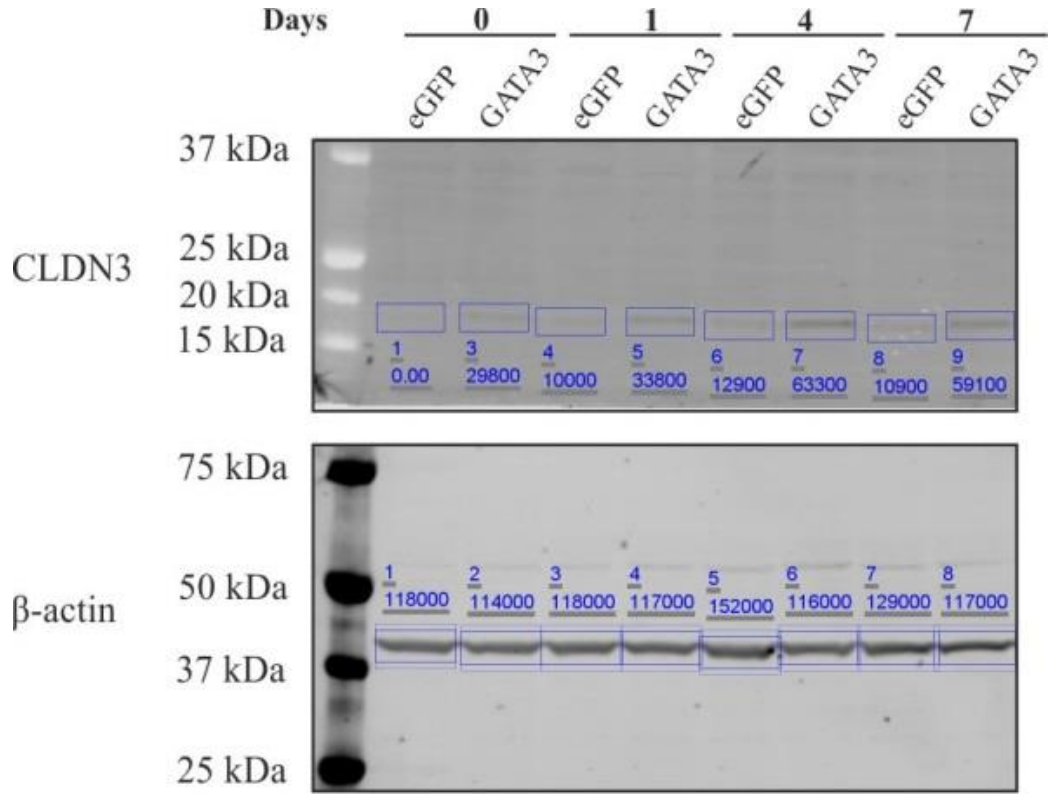

Figure 7.32 Densitometry Analysis of CLDN3 and β-actin Expression in Control and GATA3 Overexpressing NHB Cells (AS011b) During use of the ABS/Ca^{2+} Protocol

Western blots for CLDN3 and β-actin are shown for the transduced NHB cell line, AS011b.

7.8 Overexpression of PPARγ1 in Buccal Epithelial Cells

7.8.1 Additional Cell Line Results for Evaluation of Transcription Factor Expression by RT-qPCR in Control and PPARγ1 Overexpressing NHB Cells Following use of the TZ/PD Protocol (Y1721)

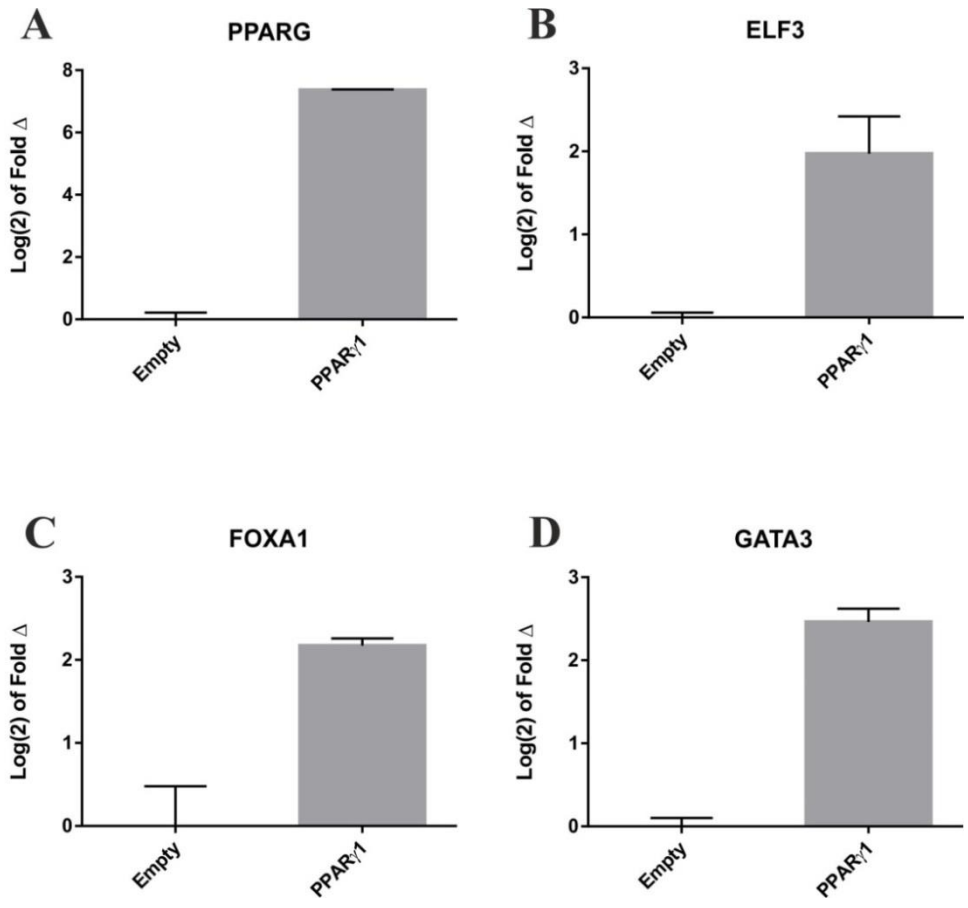

Figure 7.33 RT-qPCR Analysis of PPARG, ELF3, FOXA1 and GATA3 Expression in Control and PPARγ1 Overexpressing NHB Cells (Y1721) Treated with TZ/PD for 72 Hours

Control (Empty) and PPARγ1 overexpressing NHB cells (Y1721) were treated with TZ/PD for 72 hr. RNA was extracted and cDNA produced. qPCR data was generated to evaluate **A)** PPARγ, **B)** ELF3, **C)** FOXA1 and **D)** GATA3 expression. Values are shown relative to the control (Empty) cells. Gene expression was first normalised to GAPDH expression. Error bars represent the standard deviation of three technical replicates. Note clear upregulation of ELF3, FOXA1 and GATA3 transcript expression in PPARγ1 overexpressing cells.

7.8.2 Additional Cell Line Results for Evaluation of Transcription Factor Expression by RT-qPCR in Control and PPARγ1 Overexpressing NHB Cells Following use of the TZ/PD Protocol (AS011b)

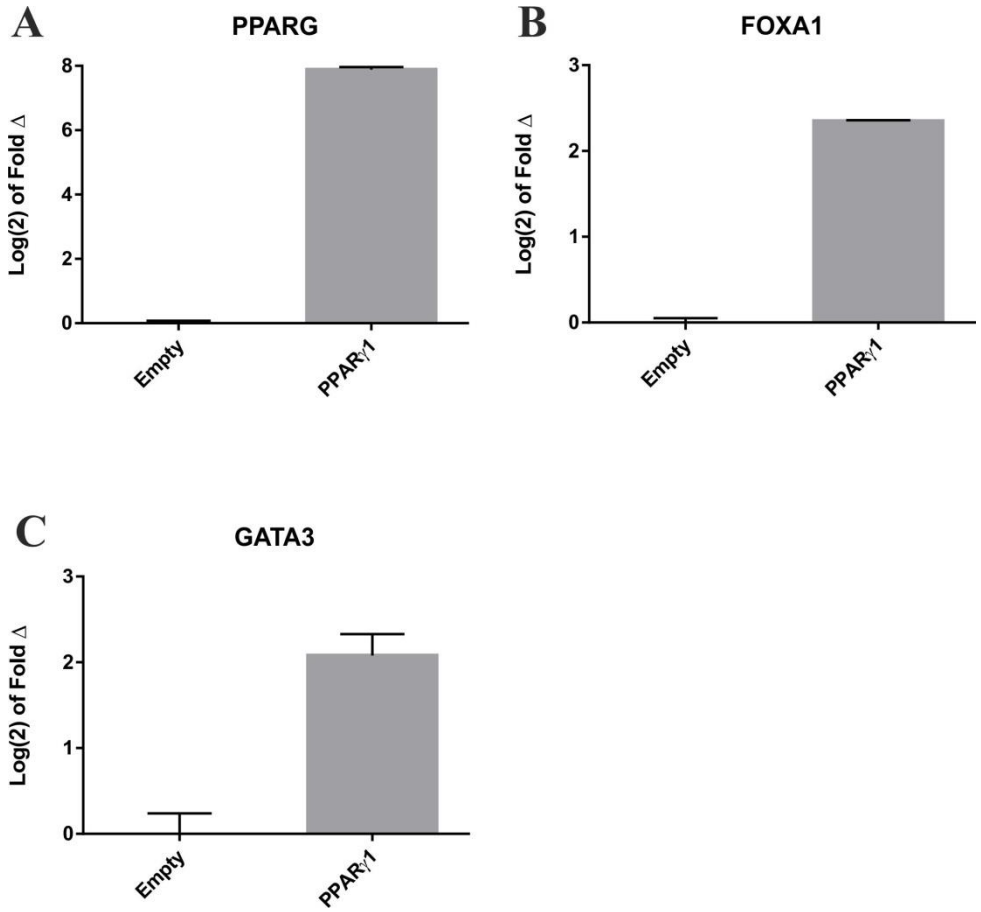

Figure 7.34 RT-qPCR Analysis of PPARG, ELF3, FOXA1 and GATA3 Expression in Control and PPARγ1 Overexpressing NHB Cells (AS011b) Treated with TZ/PD for 72 Hours

Control (Empty) and PPARγ1 overexpressing NHB cells (AS011b) were treated with TZ/PD for 48 hr. RNA was extracted and cDNA produced. qPCR data was generated to evaluate **A)** PPARγ, **B)** FOXA1 and **C)** GATA3 expression. Values are shown relative to the control (Empty) cells. Gene expression was first normalised to GAPDH expression. Error bars represent the standard deviation of three technical replicates. Note clear upregulation of FOXA1 and GATA3 transcript expression in PPARγ1 overexpressing cells.

7.8.3 Densitometry Analysis for Western Blots of FOXA1 Expression in Control and PPARγ1 Overexpressing NHB Cells Treated with 0.1 % DMSO or TZ/PD for 72 Hours

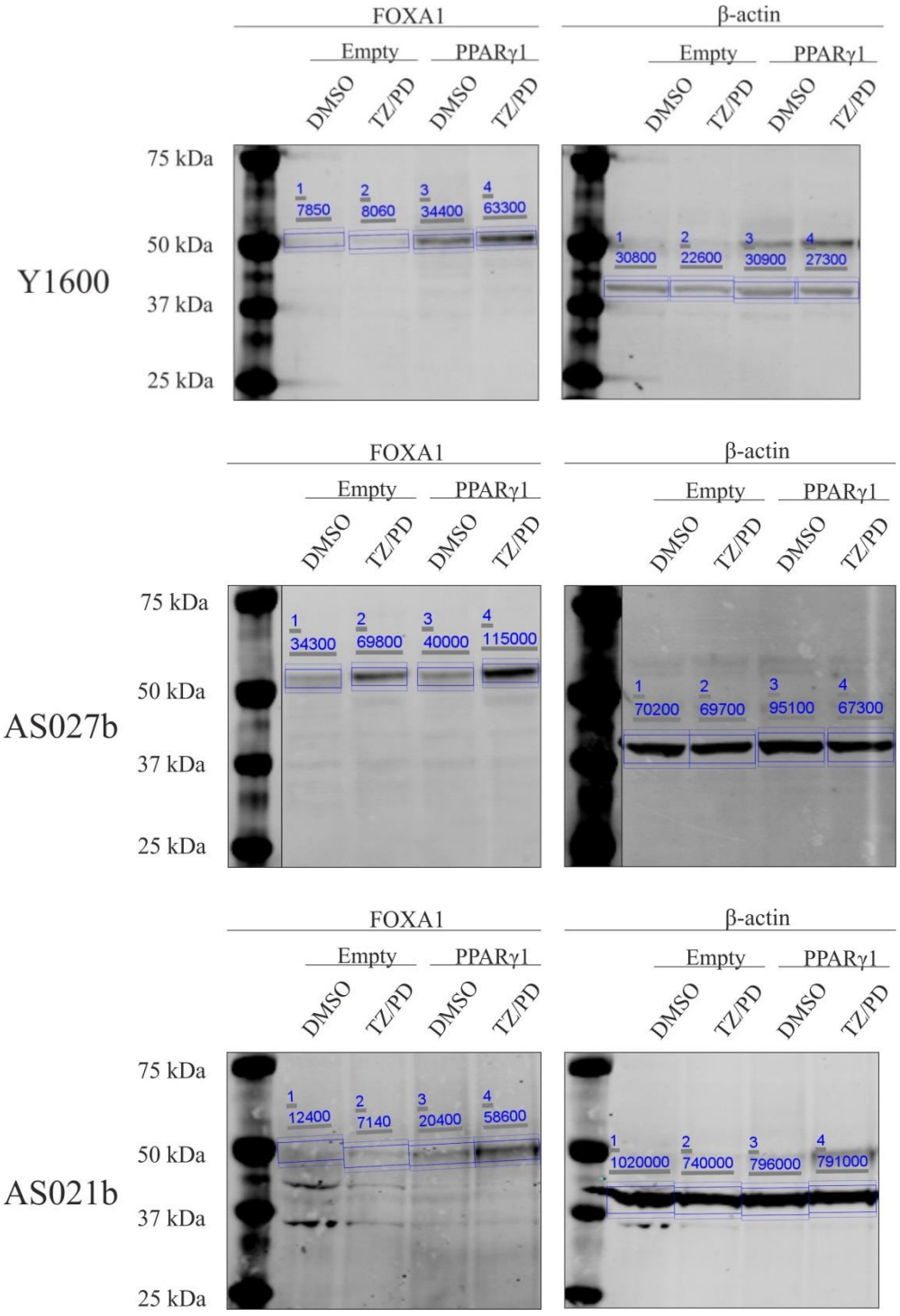

Figure 7.35 Densitometry Analysis of FOXA1 and β-actin Expression in Control and PPARγ1 Overexpressing NHB Cells (Y1600, AS027b, AS021b, and AS011b) Treated with TZ/PD for 72 hours

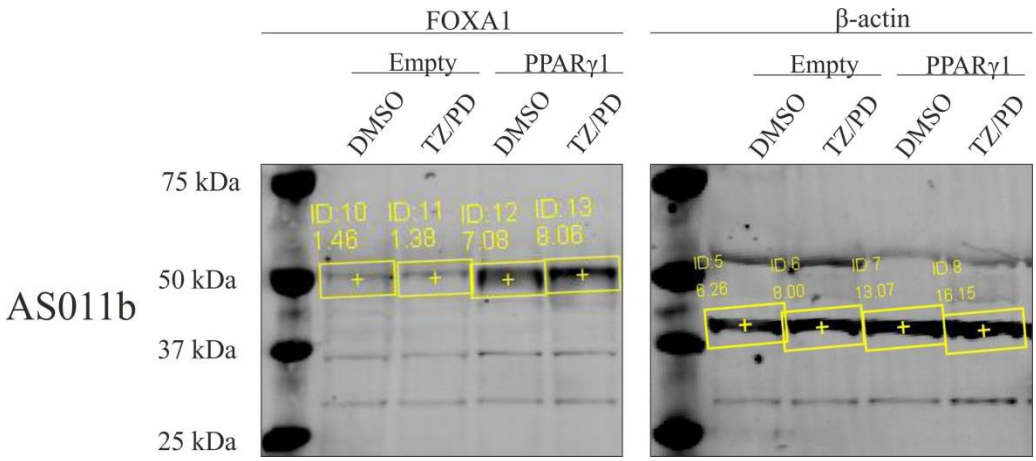

Figure 7.35 Continued.

Western blots for FOXA1 and β-actin are shown for the transduced NHB cell lines, Y1600, AS027b, AS021b and AS011b.

7.8.4 Additional Cell Line Results for Evaluation of ELF3, FOXA1, GATA3 and PPARγ Protein Expression by Immunofluorescence Microscopy in Control and PPARγ1 Overexpressing NHB Cells Treated with 0.1 % DMSO or TZ/PD for 72 hours (Y1600 and Y1656)

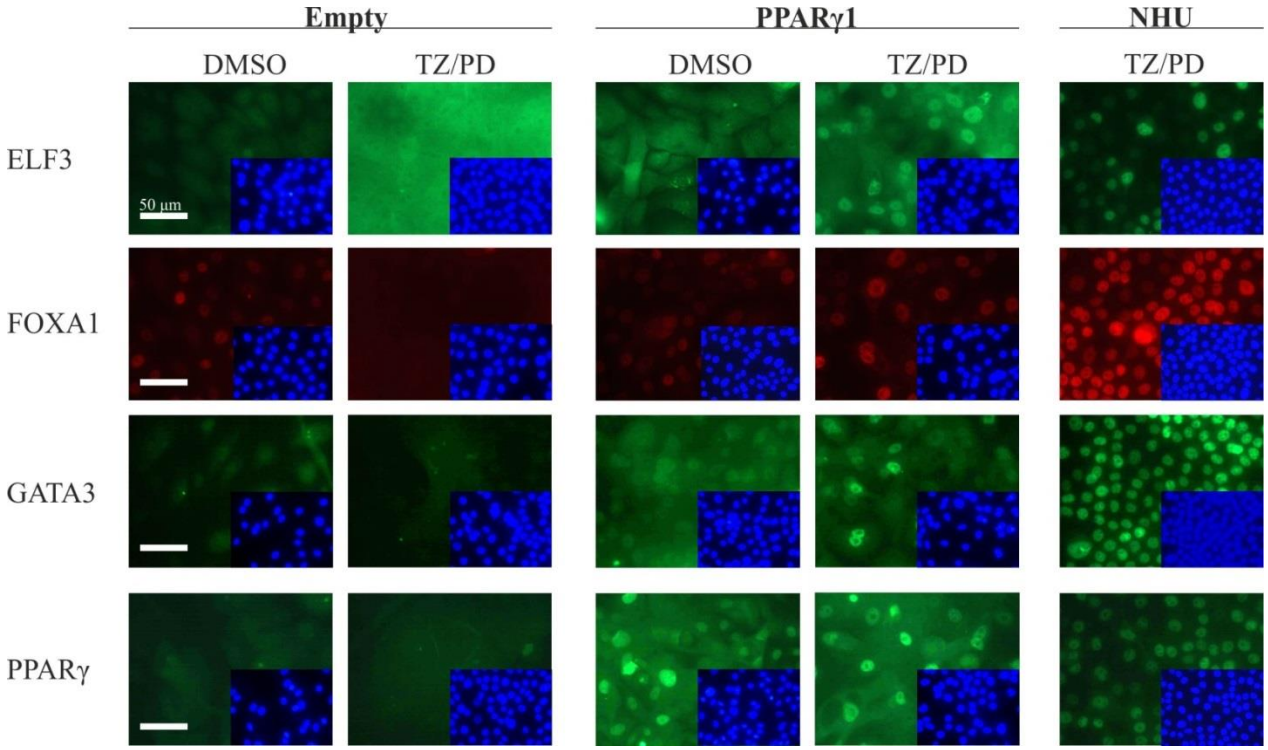

Figure 7.36 ELF3, FOXA1, GATA3 and PPARγ Protein Expression by Immunofluorescence Microscopy in Control and PPARγ1 Overexpressing NHB Cells (Y1600) Treated with TZ/PD for 72 hours

Control (Empty) and PPARγ1 overexpressing NHB cells (Y1600 and Y1656) were treated with either 0.1% DMSO (vehicle control) or TZ/PD for 72 hours. Immunofluorescence labelling for ELF3, FOXA1/2 (Santa Cruz, Q-6 or C-20), GATA3 and PPARγ (Cell Signaling, D69) was performed on formalin-fixed slides which had been permeabilised with Triton X-100. Inset images represent the corresponding Hoechst 33258 staining to demonstrate cell density and nuclei location. Antibody labelled images were taken at the same exposure for each antibody. Hoechst 33258 images were taken at optimal exposures. NHU cells (Y1642) which had been treated with TZ/PD for 72 hours were used as positive controls.

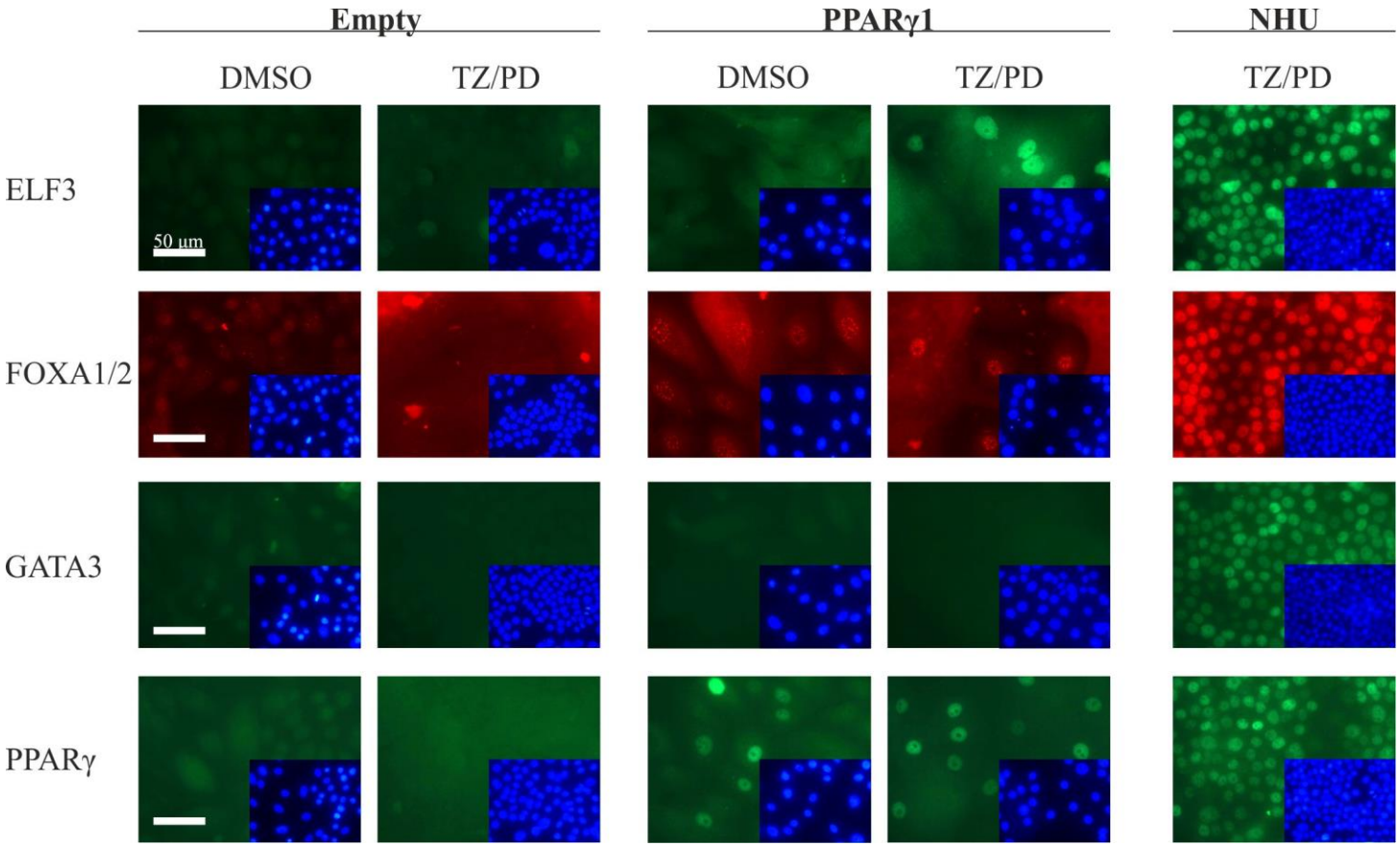

Figure 7.36 ELF3, FOXA1, GATA3 and PPARγ Protein Expression by Immunofluorescence Microscopy in Control and PPARγ1 Overexpressing NHB Cells (Y1656) Treated with TZ/PD for 72 hours

See main caption on previous page. Note increased nuclear localisation of ELF3and FOXA1/2 in the TZ/PD treated PPARγ1 overexpressing NHB cells.

7.8.5 Additional Cell Line Results for Evaluation of Tight Junction-Associated Protein Expression by Western Blotting in Control and PPARγ1 Overexpressing NHB Cells During use of the ABS/Ca^{2+} Protocol (Y1721 and Y1600)

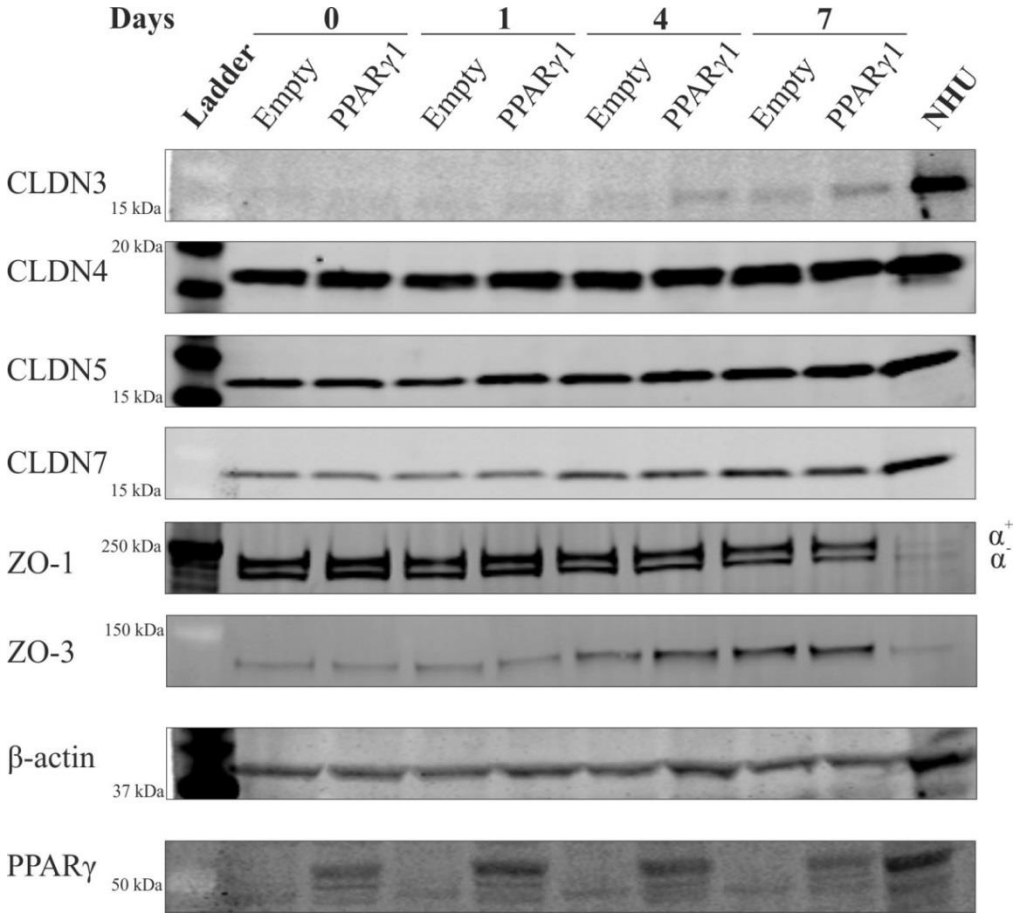

Figure 7.37 Evaluation of Tight Junction-Associated Protein Expression by Western Blotting in Control and PPARγ1 Overexpressing NHB Cells During use of the ABS/Ca^{2+} Protocol (Y1721 and Y1600)

Control (Empty) and PPARγ1 overexpressing NHB cells (Y1721 and Y1600) were subjected to the ABS/Ca^{2+} protocol for up to eight days. Whole protein lysates were generated on the days indicated. CLDN3, CLDN4, CLDN5, CLDN7, ZO-1 and ZO-3 expression was assessed by western blotting. β-actin was used as a loading control. Protein extracted from NHU cells (Y1336), which had been differentiated with ABS/Ca^{2+} for 5 days, was included on all of the western blots to act as a positive control/for comparison. 25 μg of protein was loaded into each well. Western blots for transduced NHB cell line, Y1721, are shown above. Note upregulation of CLDN3 protein expression at Day 4 and 7 in PPARγ1 overexpressing cells.

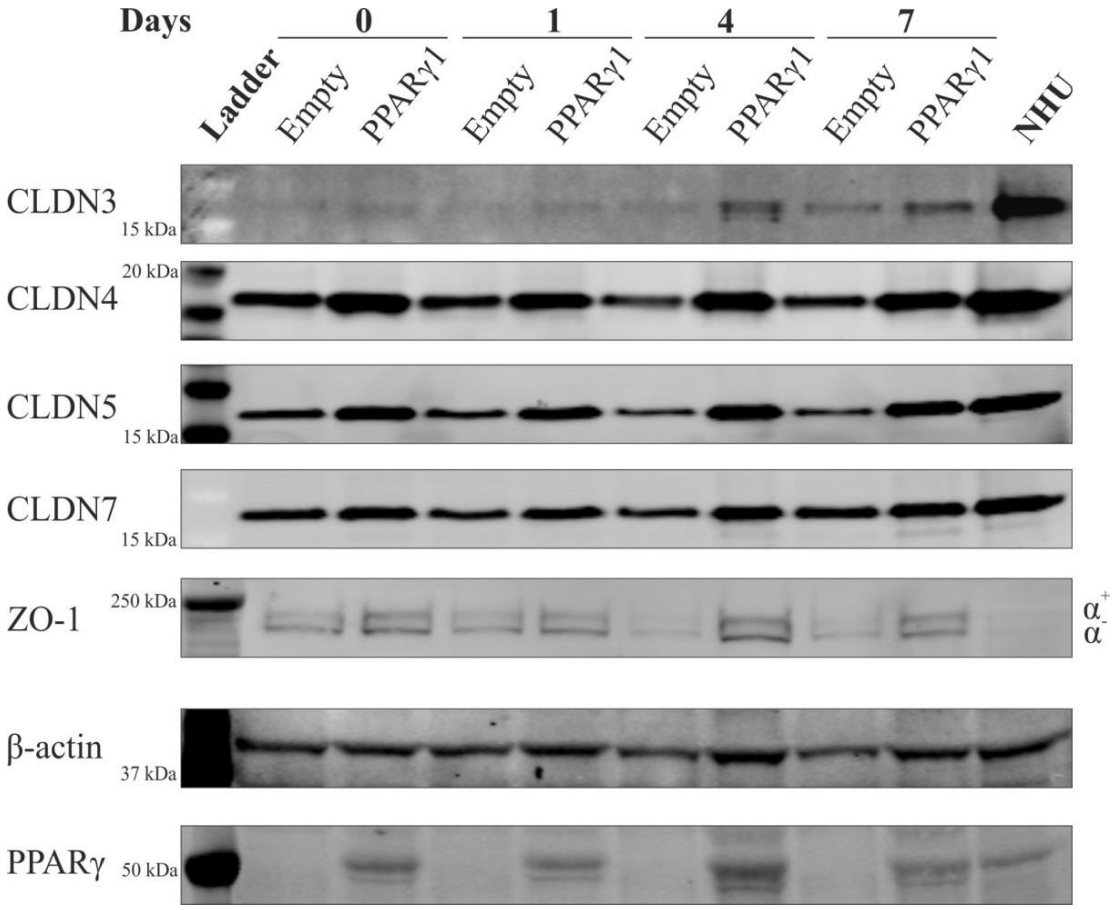

Figure 7.37 Evaluation of Tight Junction-Associated Protein Expression by Western Blotting in Control and PPARγ1 Overexpressing NHB Cells During use of the ABS/Ca^{2+} Protocol (Y1721 and Y1600)

See main caption on previous page. The western blots above correspond to transduced NHB cell line, Y1600. Note upregulation of CLDN3 protein expression at Day 4 and 7 in PPARγ1 overexpressing cells.

7.8.6 Densitometry Analysis of CLDN3 and FOXA1 Expression in Control and PPARγ1 Overexpressing NHB Cells Differentiated with ABS/Ca^{2+}

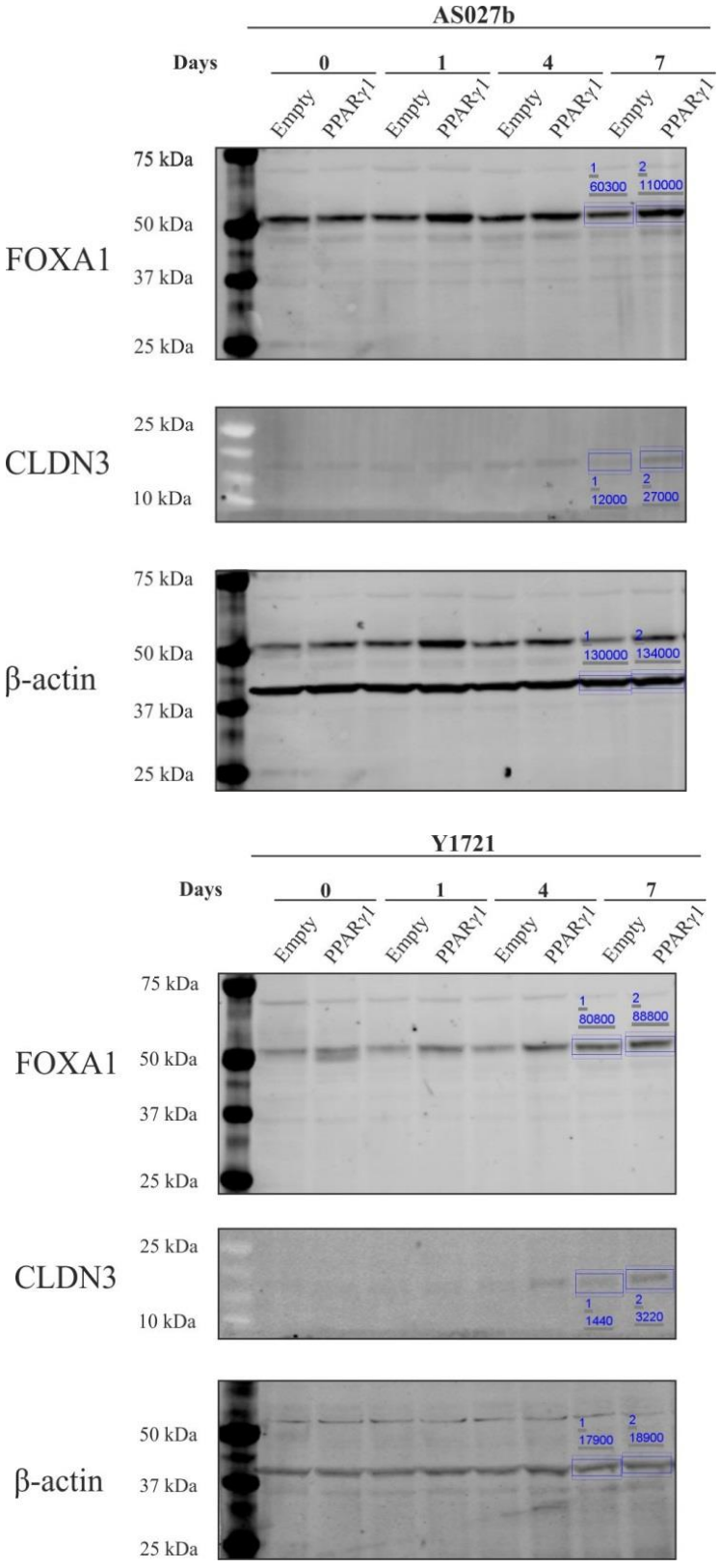

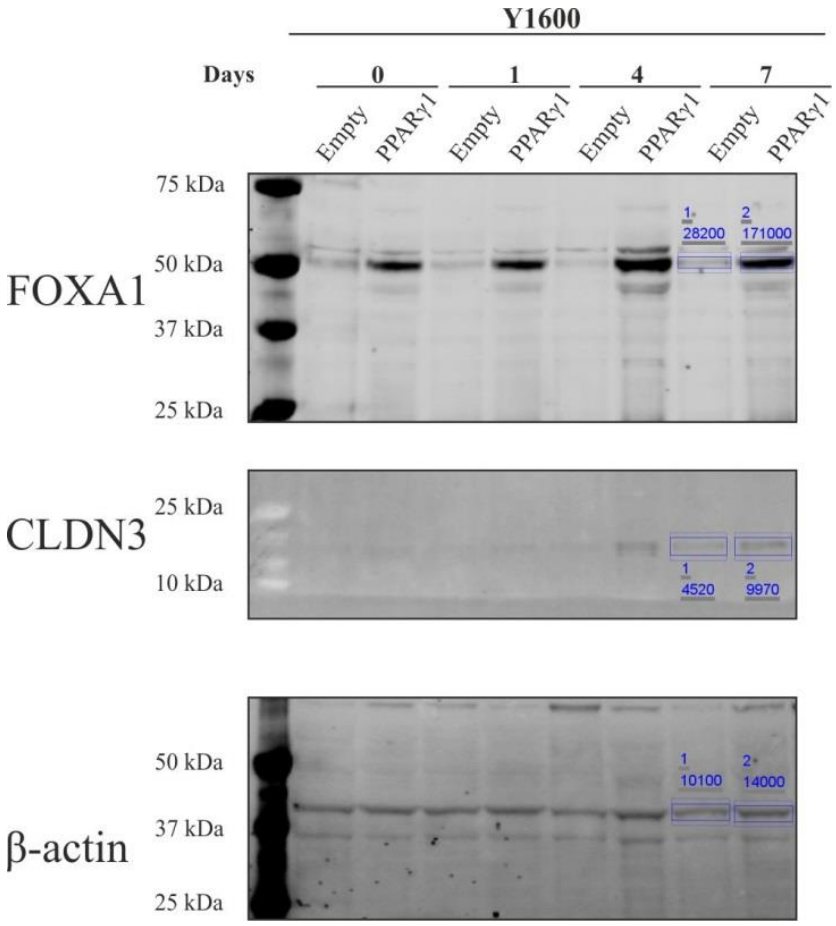

Figure 7.38 Densitometry Analysis of FOXA1, CLDN3 and β-actin Expression in Control and PPARγ1 Overexpressing NHB Cell Lines (AS027b, Y1721, and Y1600)
Western blots for FOXA1, CLDN3 and β-actin are shown for the transduced NHB cell lines, AS027b, Y1721 and Y1600.

8 References

Acharya, P., Beckel, J., Ruiz, W.G., Wang, E., Rojas, R., Birder, L., Apodaca, G., 2004. Distribution of the tight junction proteins ZO-1, occludin, and claudin-4, -8, and -12 in bladder epithelium. Am J Physiol Renal Physiol 287, F305-318.

Adachi, W., Okubo, K., Kinoshita, S., 2000. Human uroplakin Ib in ocular surface epithelium. Invest Ophthalmol Vis Sci 41, 2900-2905.

Adams, M., Reginato, M.J., Shao, D., Lazar, M.A., Chatterjee, V.K., 1997. Transcriptional activation by peroxisome proliferator-activated receptor gamma is inhibited by phosphorylation at a consensus mitogen-activated protein kinase site. J Biol Chem 272, 5128-5132.

Addis, R.C., Ifkovits, J.L., Pinto, F., Kellam, L.D., Esteso, P., Rentschler, S., Christoforou, N., Epstein, J.A., Gearhart, J.D., 2013. Optimization of direct fibroblast reprogramming to cardiomyocytes using calcium activity as a functional measure of success. J Mol Cell Cardiol 60, 97-106.

Ahmadian, M., Suh, J.M., Hah, N., Liddle, C., Atkins, A.R., Downes, M., Evans, R.M., 2013. PPARgamma signaling and metabolism: the good, the bad and the future. Nat Med 19, 557-566.

Amasheh, S., Meiri, N., Gitter, A.H., Schoneberg, T., Mankertz, J., Schulzke, J.D., Fromm, M., 2002. Claudin-2 expression induces cation-selective channels in tight junctions of epithelial cells. J Cell Sci 115, 4969-4976.

Aprile, M., Ambrosio, M.R., D'Esposito, V., Beguinot, F., Formisano, P., Costa, V., Ciccodicola, A., 2014. PPARG in Human Adipogenesis: Differential Contribution of Canonical Transcripts and Dominant Negative Isoforms. PPAR Res 2014, 537865.

Atala, A., Bauer, S.B., Soker, S., Yoo, J.J., Retik, A.B., 2006. Tissue-engineered autologous bladders for patients needing cystoplasty. Lancet 367, 1241-1246.

Azoulay, L., Yin, H., Filion, K.B., Assayag, J., Majdan, A., Pollak, M.N., Suissa, S., 2012. The use of pioglitazone and the risk of bladder cancer in people with type 2 diabetes: nested case-control study. BMJ 344, e3645.

Barak, Y., Nelson, M.C., Ong, E.S., Jones, Y.Z., Ruiz-Lozano, P., Chien, K.R., Koder, A., Evans, R.M., 1999. PPAR gamma is required for placental, cardiac, and adipose tissue development. Mol Cell 4, 585-595.

Bates, D.L., Chen, Y., Kim, G., Guo, L., Chen, L., 2008. Crystal structures of multiple GATA zinc fingers bound to DNA reveal new insights into DNA recognition and self-association by GATA. J Mol Biol 381, 1292-1306.

Bell, S.M., Zhang, L., Mendell, A., Xu, Y., Haitchi, H.M., Lessard, J.L., Whitsett, J.A., 2011. Kruppel-like factor 5 is required for formation and differentiation of the bladder urothelium. Dev Biol 358, 79-90.

Bernardo, G.M., Keri, R.A., 2012. FOXA1: a transcription factor with parallel functions in development and cancer. Biosci Rep 32, 113-130.

Bharadwaj, S., Liu, G., Shi, Y., Wu, R., Yang, B., He, T., Fan, Y., Lu, X., Zhou, X., Liu, H., Atala, A., Rohozinski, J., Zhang, Y., 2013. Multipotential differentiation of human urine-derived stem cells: potential for therapeutic applications in urology. Stem Cells 31, 1840-1856.

Bhargava, S., Patterson, J.M., Inman, R.D., MacNeil, S., Chapple, C.R., 2008. Tissue-engineered buccal mucosa urethroplasty - Clinical outcomes. European Urology 53, 1263-1271.

Biers, S.M., Venn, S.N., Greenwell, T.J., 2012. The past, present and future of augmentation cystoplasty. BJU Int 109, 1280-1293.

Bindels, E.M., van der Kwast, T.H., Izadifar, V., Chopin, D.K., de Boer, W.I., 2002. Functions of epidermal growth factor-like growth factors during human urothelial reepithelialization in vitro and the role of erbB2. Urol Res 30, 240-247.

Biton, A., Bernard-Pierrot, I., Lou, Y., Krucker, C., Chapeaublanc, E., Rubio-Perez, C., Lopez-Bigas, N., Kamoun, A., Neuzillet, Y., Gestraud, P., Grieco, L., Rebouissou, S., de Reynies, A., Benhamou, S., Lebret, T., Southgate, J., Barillot, E., Allory, Y., Zinovyev, A., Radvanyi, F., 2014. Independent component analysis uncovers the landscape of the bladder tumor transcriptome and reveals insights into luminal and basal subtypes. Cell Rep 9, 1235-1245.

Blasig, I.E., Winkler, L., Lassowski, B., Mueller, S.L., Zuleger, N., Krause, E., Krause, G., Gast, K., Kolbe, M., Piontek, J., 2006. On the self-association potential of transmembrane tight junction proteins. Cell Mol Life Sci 63, 505-514.

Böck, M., Hinley, J., Schmitt, C., Wahlicht, T., Kramer, S., Southgate, J., 2014. Identification of ELF3 as an early transcriptional regulator of human urothelium. Dev Biol 386, 321-330.

Bugge, A., Grontved, L., Aagaard, M.M., Borup, R., Mandrup, S., 2009. The PPARgamma2 A/B-domain plays a gene-specific role in transactivation and cofactor recruitment. Mol Endocrinol 23, 794-808.

Cahan, P., Li, H., Morris, S.A., Lummertz da Rocha, E., Daley, G.Q., Collins, J.J., 2014. CellNet: network biology applied to stem cell engineering. Cell 158, 903-915.

Camp, H.S., Tafuri, S.R., 1997. Regulation of peroxisome proliferator-activated receptor gamma activity by mitogen-activated protein kinase. J Biol Chem 272, 10811-10816.

Cancer Genome Atlas Research, N., 2014. Comprehensive molecular characterization of urothelial bladder carcinoma. Nature 507, 315-322.

Candi, E., Schmidt, R., Melino, G., 2005. The cornified envelope: a model of cell death in the skin. Nat Rev Mol Cell Biol 6, 328-340.

Candi, E., Terrinoni, A., Rufini, A., Chikh, A., Lena, A.M., Suzuki, Y., Sayan, B.S., Knight, R.A., Melino, G., 2006. p63 is upstream of IKK alpha in epidermal development. J Cell Sci 119, 4617-4622.

Chanda, S., Ang, C.E., Davila, J., Pak, C., Mall, M., Lee, Q.Y., Ahlenius, H., Jung, S.W., Sudhof, T.C., Wernig, M., 2014. Generation of induced neuronal cells by the single reprogramming factor ASCL1. Stem Cell Reports 3, 282-296.

Chandra, V., Huang, P., Hamuro, Y., Raghuram, S., Wang, Y., Burris, T.P., Rastinejad, F., 2008. Structure of the intact PPAR-gamma-RXR- nuclear receptor complex on DNA. Nature 456, 350-356.

Chen, Y., Jimenez, A.R., Medh, J.D., 2006. Identification and regulation of novel PPAR-gamma splice variants in human THP-1 macrophages. Biochim Biophys Acta 1759, 32-43.

Cheng, E.Y., 2014. Editorial comment. J Urol 191, 1395.

Cheng, L., Hu, W., Qiu, B., Zhao, J., Yu, Y., Guan, W., Wang, M., Yang, W., Pei, G., 2014. Generation of neural progenitor cells by chemical cocktails and hypoxia. Cell Res 24, 665-679.

Chikh, A., Sayan, E., Thibaut, S., Lena, A.M., DiGiorgi, S., Bernard, B.A., Melino, G., Candi, E., 2007. Expression of GATA-3 in epidermis and hair follicle: relationship to p63. Biochem Biophys Res Commun 361, 1-6.

Choi, W., Porten, S., Kim, S., Willis, D., Plimack, E.R., Hoffman-Censits, J., Roth, B., Cheng, T., Tran, M., Lee, I.L., Melquist, J., Bondaruk, J., Majewski, T., Zhang, S., Pretzsch, S., Baggerly, K., Siefker-Radtke, A., Czerniak, B., Dinney, C.P., McConkey, D.J., 2014. Identification of distinct basal and luminal subtypes of muscle-invasive bladder cancer with different sensitivities to frontline chemotherapy. Cancer Cell 25, 152-165.

Christoforou, N., Chellappan, M., Adler, A.F., Kirkton, R.D., Wu, T., Addis, R.C., Bursac, N., Leong, K.W., 2013. Transcription factors MYOCD, SRF, Mesp1 and SMARCD3 enhance the cardio-inducing effect of GATA4, TBX5, and MEF2C during direct cellular reprogramming. PLoS One 8, e63577.

Chung, J.H., Cho, K.H., Lee, D.Y., Kwon, O.S., Sung, M.W., Kim, K.H., Eun, H.C., 1997. Human oral buccal mucosa reconstructed on dermal substrates: a model for oral epithelial differentiation. Arch Dermatol Res 289, 677-685.

Chung, S.S., Koh, C.J., 2013. Bladder cancer cell in co-culture induces human stem cell differentiation to urothelial cells through paracrine FGF10 signaling. In Vitro Cell Dev Biol Anim 49, 746-751.

Colopy, S.A., Bjorling, D.E., Mulligan, W.A., Bushman, W., 2014. A population of progenitor cells in the basal and intermediate layers of the murine bladder urothelium contributes to urothelial development and regeneration. Dev Dyn 243, 988-998.

Cross, W.R., Eardley, I., Leese, H.J., Southgate, J., 2005. A biomimetic tissue from cultured normal human urothelial cells: analysis of physiological function. Am J Physiol Renal Physiol 289, F459-468.

Daher, A., de Boer, W.I., El-Marjou, A., van der Kwast, T., Abbou, C.C., Thiery, J.P., Radvanyi, F., Chopin, D.K., 2003. Epidermal growth factor receptor regulates normal urothelial regeneration. Lab Invest 83, 1333-1341.

Dai, X., Segre, J.A., 2004. Transcriptional control of epidermal specification and differentiation. Curr Opin Genet Dev 14, 485-491.

Damrauer, J.S., Hoadley, K.A., Chism, D.D., Fan, C., Tiganelli, C.J., Wobker, S.E., Yeh, J.J., Milowsky, M.I., Iyer, G., Parker, J.S., Kim, W.Y., 2014. Intrinsic subtypes of high-grade bladder cancer reflect the hallmarks of breast cancer biology. Proc Natl Acad Sci U S A 111, 3110-3115.

Davis, R.L., Weintraub, H., Lassar, A.B., 1987. Expression of a single transfected cDNA converts fibroblasts to myoblasts. Cell 51, 987-1000.

de Guzman Strong, C., Wertz, P.W., Wang, C., Yang, F., Meltzer, P.S., Andl, T., Millar, S.E., Ho, I.C., Pai, S.Y., Segre, J.A., 2006. Lipid defect underlies selective skin barrier impairment of an epidermal-specific deletion of Gata-3. J Cell Biol 175, 661-670.

DeGraff, D.J., Clark, P.E., Cates, J.M., Yamashita, H., Robinson, V.L., Yu, X., Smolkin, M.E., Chang, S.S., Cookson, M.S., Herrick, M.K., Shariat, S.F., Steinberg, G.D., Frierson, H.F., Wu, X.R., Theodorescu, D., Matusik, R.J., 2012. Loss of the urothelial differentiation marker FOXA1 is associated with high grade, late stage bladder cancer and increased tumor proliferation. PLoS One 7, e36669.

Deng, F.M., Liang, F.X., Tu, L., Resing, K.A., Hu, P., Supino, M., Hu, C.C., Zhou, G., Ding, M., Kreibich, G., Sun, T.T., 2002. Uroplakin IIIb, a urothelial differentiation marker, dimerizes with uroplakin Ib as an early step of urothelial plaque assembly. J Cell Biol 159, 685-694.

Du, Y., Wang, J., Jia, J., Song, N., Xiang, C., Xu, J., Hou, Z., Su, X., Liu, B., Jiang, T., Zhao, D., Sun, Y., Shu, J., Guo, Q., Yin, M., Sun, D., Lu, S., Shi, Y., Deng, H., 2014. Human hepatocytes with drug metabolic function induced from fibroblasts by lineage reprogramming. Cell Stem Cell 14, 394-403.

Duester, G., 2008. Retinoic acid synthesis and signaling during early organogenesis. Cell 134, 921-931.

Ellis, C.N., Varani, J., Fisher, G.J., Zeigler, M.E., Pershadsingh, H.A., Benson, S.C., Chi, Y., Kurtz, T.W., 2000. Troglitazone improves psoriasis and normalizes models of proliferative skin disease: ligands for peroxisome proliferator-activated receptor-gamma inhibit keratinocyte proliferation. Arch Dermatol 136, 609-616.

Eriksson, P., Aine, M., Veerla, S., Liedberg, F., Sjodahl, G., Hoglund, M., 2015. Molecular subtypes of urothelial carcinoma are defined by specific gene regulatory systems. BMC Med Genomics 8, 25.

Fajas, L., Auboeuf, D., Raspe, E., Schoonjans, K., Lefebvre, A.M., Saladin, R., Najib, J., Laville, M., Fruchart, J.C., Deeb, S., Vidal-Puig, A., Flier, J., Briggs, M.R., Staels, B., Vidal, H., Auwerx, J., 1997. The organization, promoter analysis, and expression of the human PPARgamma gene. J Biol Chem 272, 18779-18789.

Farhat, W.A., 2014. Editorial comment. J Urol 191, 1394.

Filipas, N., Fisch, M., Fichtner, J., Fitzpatrick, J., Berg, K., Storkel, S., Hohenfellner, R., Thuroff, J.W., 1999. The histology and immunohistochemistry of free buccal mucosa and full-skin grafts after exposure to urine. Bju International 84, 108-111.

Fleming, J., 2008. Regulation of Growth and Differentiation in Human Urothelium, Department of Biology. University of York.

Fraser, M., Thomas, D.F., Pitt, E., Harnden, P., Trejdosiewicz, L.K., Southgate, J., 2004. A surgical model of composite cystoplasty with cultured urothelial cells: a controlled study of gross outcome and urothelial phenotype. BJU Int 93, 609-616.

Fu, J.D., Stone, N.R., Liu, L., Spencer, C.I., Qian, L., Hayashi, Y., Delgado-Olguin, P., Ding, S., Bruneau, B.G., Srivastava, D., 2013. Direct reprogramming of human fibroblasts toward a cardiomyocyte-like state. Stem Cell Reports 1, 235-247.

Fu, M., Rao, M., Bouras, T., Wang, C., Wu, K., Zhang, X., Li, Z., Yao, T.P., Pestell, R.G., 2005. Cyclin D1 inhibits peroxisome proliferator-activated receptor gamma-mediated adipogenesis through histone deacetylase recruitment. J Biol Chem 280, 16934-16941.

Fujita, H., Hamazaki, Y., Noda, Y., Oshima, M., Minato, N., 2012. Claudin-4 deficiency results in urothelial hyperplasia and lethal hydronephrosis. PLoS One 7, e52272.

Furuse, M., Sasaki, H., Tsukita, S., 1999. Manner of interaction of heterogeneous claudin species within and between tight junction strands. J Cell Biol 147, 891-903.

Gandhi, D., Molotkov, A., Batourina, E., Schneider, K., Dan, H., Reiley, M., Laufer, E., Metzger, D., Liang, F., Liao, Y., Sun, T.T., Aronow, B., Rosen, R., Mauney, J., Adam, R., Rosselot, C., Van Batavia, J., McMahon, A., McMahon, J., Guo, J.J., Mendelsohn, C., 2013. Retinoid signaling in progenitors controls specification and regeneration of the urothelium. Dev Cell 26, 469-482.

Georgopoulos, N.T., Kirkwood, L.A., Varley, C.L., MacLaine, N.J., Aziz, N., Southgate, J., 2011. Immortalisation of normal human urothelial cells compromises differentiation capacity. Eur Urol 60, 141-149.

Gibbs, S., Ponec, M., 2000. Intrinsic regulation of differentiation markers in human epidermis, hard palate and buccal mucosa. Arch Oral Biol 45, 149-158.

Gilbert, S.M., Hensle, T.W., 2005. Metabolic consequences and long-term complications of enterocystoplasty in children: a review. J Urol 173, 1080-1086.

Han, D.W., Tapia, N., Hermann, A., Hemmer, K., Hoing, S., Arauzo-Bravo, M.J., Zaehres, H., Wu, G., Frank, S., Moritz, S., Greber, B., Yang, J.H., Lee, H.T.,

Schwamborn, J.C., Storch, A., Scholer, H.R., 2012. Direct reprogramming of fibroblasts into neural stem cells by defined factors. Cell Stem Cell 10, 465-472.

Harnden, P., Southgate, J., 1997. Cytokeratin 14 as a marker of squamous differentiation in transitional cell carcinomas. J Clin Pathol 50, 1032-1033.

Hatakeyama, S., Hayashi, S., Yoshida, Y., Otsubo, A., Yoshimoto, K., Oikawa, Y., Satoh, M., 2004. Retinoic acid disintegrated desmosomes and hemidesmosomes in stratified oral keratinocytes. J Oral Pathol Med 33, 622-628.

Hatakeyama, S., Ishida, K., Takeda, Y., 2010. Changes in cell characteristics due to retinoic acid; specifically, a decrease in the expression of claudin-1 and increase in claudin-4 within tight junctions in stratified oral keratinocytes. J Periodontal Res 45, 207-215.

Hauser, S., Adelmant, G., Sarraf, P., Wright, H.M., Mueller, E., Spiegelman, B.M., 2000. Degradation of the peroxisome proliferator-activated receptor gamma is linked to ligand-dependent activation. J Biol Chem 275, 18527-18533.

Heyman, R.A., Mangelsdorf, D.J., Dyck, J.A., Stein, R.B., Eichele, G., Evans, R.M., Thaller, C., 1992. 9-cis retinoic acid is a high affinity ligand for the retinoid X receptor. Cell 68, 397-406.

Higgins, J.P., Kaygusuz, G., Wang, L., Montgomery, K., Mason, V., Zhu, S.X., Marinelli, R.J., Presti, J.C., Jr., van de Rijn, M., Brooks, J.D., 2007. Placental S100 (S100P) and GATA3: markers for transitional epithelium and urothelial carcinoma discovered by complementary DNA microarray. Am J Surg Pathol 31, 673-680.

Hu, E., Kim, J.B., Sarraf, P., Spiegelman, B.M., 1996. Inhibition of adipogenesis through MAP kinase-mediated phosphorylation of PPARgamma. Science 274, 2100-2103.

Hu, E., Tontonoz, P., Spiegelman, B.M., 1995. Transdifferentiation of myoblasts by the adipogenic transcription factors PPAR gamma and C/EBP alpha. Proc Natl Acad Sci U S A 92, 9856-9860.

Hu, P., Deng, F.M., Liang, F.X., Hu, C.M., Auerbach, A.B., Shapiro, E., Wu, X.R., Kachar, B., Sun, T.T., 2000. Ablation of uroplakin III gene results in small urothelial plaques, urothelial leakage, and vesicoureteral reflux. J Cell Biol 151, 961-972.

Hu, P., Meyers, S., Liang, F.X., Deng, F.M., Kachar, B., Zeidel, M.L., Sun, T.T., 2002. Role of membrane proteins in permeability barrier function: uroplakin ablation elevates urothelial permeability. Am J Physiol Renal Physiol 283, F1200-1207.

Ieda, M., Fu, J.D., Delgado-Olguin, P., Vedantham, V., Hayashi, Y., Bruneau, B.G., Srivastava, D., 2010. Direct reprogramming of fibroblasts into functional cardiomyocytes by defined factors. Cell 142, 375-386.

Itoh, M., Furuse, M., Morita, K., Kubota, K., Saitou, M., Tsukita, S., 1999. Direct binding of three tight junction-associated MAGUKs, ZO-1, ZO-2, and ZO-3, with the COOH termini of claudins. J Cell Biol 147, 1351-1363.

Jacob, A., Budhiraja, S., Reichel, R.R., 1999. The HNF-3alpha transcription factor is a primary target for retinoic acid action. Exp Cell Res 250, 1-9.

Jayawardena, T.M., Egemnazarov, B., Finch, E.A., Zhang, L., Payne, J.A., Pandya, K., Zhang, Z., Rosenberg, P., Mirotsou, M., Dzau, V.J., 2012. MicroRNA-mediated in vitro and in vivo direct reprogramming of cardiac fibroblasts to cardiomyocytes. Circ Res 110, 1465-1473.

Jin, L., Li, Y., 2010. Structural and functional insights into nuclear receptor signaling. Adv Drug Deliv Rev 62, 1218-1226.

Jones, K.B., Klein, O.D., 2013. Oral epithelial stem cells in tissue maintenance and disease: the first steps in a long journey. Int J Oral Sci 5, 121-129.

Joseph, D.B., Borer, J.G., De Filippo, R.E., Hodges, S.J., McLorie, G.A., 2014. Autologous cell seeded biodegradable scaffold for augmentation cystoplasty: phase II study in children and adolescents with spina bifida. J Urol 191, 1389-1395.

Jost, S.P., Gosling, J.A., Dixon, J.S., 1989. The morphology of normal human bladder urothelium. J Anat 167, 103-115.

Jpenberg, A., Jeannin, E., Wahli, W., Desvergne, B., 1997. Polarity and specific sequence requirements of peroxisome proliferator-activated receptor (PPAR)/retinoid X receptor heterodimer binding to DNA. A functional analysis of the malic enzyme gene PPAR response element. J Biol Chem 272, 20108-20117.

Kalinin, A.E., Kajava, A.V., Steinert, P.M., 2002. Epithelial barrier function: assembly and structural features of the cornified cell envelope. Bioessays 24, 789-800.

Kanamori-Katayama, M., Kaiho, A., Ishizu, Y., Okamura-Oho, Y., Hino, O., Abe, M., Kishimoto, T., Sekihara, H., Nakamura, Y., Suzuki, H., Forrest, A.R., Hayashizaki, Y., 2011. LRRN4 and UPK3B are markers of primary mesothelial cells. PLoS One 6, e25391.

Kang, H.H., Kang, J.J., Kang, H.G., Chung, S.S., 2014a. Urothelial differentiation of human amniotic fluid stem cells by urothelium specific conditioned medium. Cell Biol Int 38, 531-537.

Kang, M., Kim, H.H., Han, Y.M., 2014b. Generation of bladder urothelium from human pluripotent stem cells under chemically defined serum- and feeder-free system. Int J Mol Sci 15, 7139-7157.

Kato, H., Izumi, K., Saito, T., Ohnuki, H., Terada, M., Kawano, Y., Nozawa-Inoue, K., Saito, C., Maeda, T., 2013. Distinct expression patterns and roles of aldehyde dehydrogenases in normal oral mucosa keratinocytes: differential inhibitory effects of a pharmacological inhibitor and RNAi-mediated knockdown on cellular phenotype and epithelial morphology. Histochem Cell Biol 139, 847-862.

Katsuno, T., Umeda, K., Matsui, T., Hata, M., Tamura, A., Itoh, M., Takeuchi, K., Fujimori, T., Nabeshima, Y., Noda, T., Tsukita, S., Tsukita, S., 2008. Deficiency of zonula occludens-1 causes embryonic lethal phenotype associated with defected yolk sac angiogenesis and apoptosis of embryonic cells. Mol Biol Cell 19, 2465-2475.

Kautsky, M.B., Fleckman, P., Dale, B.A., 1995. Retinoic acid regulates oral epithelial differentiation by two mechanisms. J Invest Dermatol 104, 546-553.

Kawakami, S., Arai, G., Hayashi, T., Fujii, Y., Xia, G., Kageyama, Y., Kihara, K., 2002. PPARgamma ligands suppress proliferation of human urothelial basal cells in vitro. J Cell Physiol 191, 310-319.

Khandelwal, P., Abraham, S.N., Apodaca, G., 2009. Cell biology and physiology of the uroepithelium. Am J Physiol Renal Physiol 297, F1477-1501.

Kim, H.J., Woo, I.S., Kang, E.S., Eun, S.Y., Kim, H.J., Lee, J.H., Chang, K.C., Kim, J.H., Seo, H.G., 2006. Identification of a truncated alternative splicing variant of human PPARgamma1 that exhibits dominant negative activity. Biochem Biophys Res Commun 347, 698-706.

Kliewer, S.A., Lenhard, J.M., Willson, T.M., Patel, I., Morris, D.C., Lehmann, J.M., 1995. A prostaglandin J2 metabolite binds peroxisome proliferator-activated receptor gamma and promotes adipocyte differentiation. Cell 83, 813-819.

Kliewer, S.A., Sundseth, S.S., Jones, S.A., Brown, P.J., Wisely, G.B., Koble, C.S., Devchand, P., Wahli, W., Willson, T.M., Lenhard, J.M., Lehmann, J.M., 1997. Fatty acids and eicosanoids regulate gene expression through direct interactions with peroxisome proliferator-activated receptors alpha and gamma. Proc Natl Acad Sci U S A 94, 4318-4323.

Ko, L.J., Engel, J.D., 1993. DNA-binding specificities of the GATA transcription factor family. Mol Cell Biol 13, 4011-4022.

Kong, S.L., Li, G., Loh, S.L., Sung, W.K., Liu, E.T., 2011. Cellular reprogramming by the conjoint action of ERalpha, FOXA1, and GATA3 to a ligand-inducible growth state. Mol Syst Biol 7, 526.

Kong, X.T., Deng, F.M., Hu, P., Liang, F.X., Zhou, G., Auerbach, A.B., Genieser, N., Nelson, P.K., Robbins, E.S., Shapiro, E., Kachar, B., Sun, T.T., 2004. Roles of uroplakins in plaque formation, umbrella cell enlargement, and urinary tract diseases. J Cell Biol 167, 1195-1204.

Kouros-Mehr, H., Bechis, S.K., Slorach, E.M., Littlepage, L.E., Egeblad, M., Ewald, A.J., Pai, S.Y., Ho, I.C., Werb, Z., 2008. GATA-3 links tumor differentiation and dissemination in a luminal breast cancer model. Cancer Cell 13, 141-152.

Kouros-Mehr, H., Slorach, E.M., Sternlicht, M.D., Werb, Z., 2006. GATA-3 maintains the differentiation of the luminal cell fate in the mammary gland. Cell 127, 1041-1055.

Krug, S.M., Schulzke, J.D., Fromm, M., 2014. Tight junction, selective permeability, and related diseases. Semin Cell Dev Biol 36, 166-176.

Kurzrock, E.A., Lieu, D.K., Degraffenried, L.A., Chan, C.W., Isseroff, R.R., 2008. Label-retaining cells of the bladder: candidate urothelial stem cells. Am J Physiol Renal Physiol 294, F1415-1421.

Ladewig, J., Mertens, J., Kesavan, J., Doerr, J., Poppe, D., Glaue, F., Herms, S., Wernet, P., Kogler, G., Muller, F.J., Koch, P., Brustle, O., 2012. Small molecules enable highly efficient neuronal conversion of human fibroblasts. Nat Methods 9, 575-578.

Lam Van Ba, O., Aharony, S., Loutochin, O., Corcos, J., 2015. Bladder tissue engineering: a literature review. Adv Drug Deliv Rev 82-83, 31-37.

Landay, M.A., Schroeder, H.E., 1979. Differentiation in normal human buccal mucosa epithelium. J Anat 128, 31-51.

Lang, R., Liu, G., Shi, Y., Bharadwaj, S., Leng, X., Zhou, X., Liu, H., Atala, A., Zhang, Y., 2013. Self-renewal and differentiation capacity of urine-derived stem cells after urine preservation for 24 hours. PLoS One 8, e53980.

Larsson, H.M., Gorostidi, F., Hubbell, J.A., Barrandon, Y., Frey, P., 2014. Clonal, self-renewing and differentiating human and porcine urothelial cells, a novel stem cell population. PLoS One 9, e90006.

Lefterova, M.I., Haakonsson, A.K., Lazar, M.A., Mandrup, S., 2014. PPARgamma and the global map of adipogenesis and beyond. Trends Endocrinol Metab 25, 293-302.

Lehmann, J.M., Moore, L.B., Smith-Oliver, T.A., Wilkison, W.O., Willson, T.M., Kliewer, S.A., 1995. An antidiabetic thiazolidinedione is a high affinity ligand for peroxisome proliferator-activated receptor gamma (PPAR gamma). J Biol Chem 270, 12953-12956.

Lesch, C.A., Squier, C.A., Cruchley, A., Williams, D.M., Speight, P., 1989. The permeability of human oral mucosa and skin to water. J Dent Res 68, 1345-1349.

Li, C., Xu, Y.M., Song, L.J., Fu, Q., Cui, L., Yin, S., 2008. Urethral reconstruction using oral keratinocyte seeded bladder acellular matrix grafts. Journal of Urology 180, 1538-1542.

Li, Y., Fanning, A.S., Anderson, J.M., Lavie, A., 2005. Structure of the conserved cytoplasmic C-terminal domain of occludin: identification of the ZO-1 binding surface. J Mol Biol 352, 151-164.

Li, Y., Ishiguro, H., Kawahara, T., Kashiwagi, E., Izumi, K., Miyamoto, H., 2014a. Loss of GATA3 in bladder cancer promotes cell migration and invasion. Cancer Biol Ther 15, 428-435.

Li, Y., Ishiguro, H., Kawahara, T., Miyamoto, Y., Izumi, K., Miyamoto, H., 2014b. GATA3 in the urinary bladder: suppression of neoplastic transformation and down-regulation by androgens. Am J Cancer Res 4, 461-473.

Liang, F.X., Bosland, M.C., Huang, H., Romih, R., Baptiste, S., Deng, F.M., Wu, X.R., Shapiro, E., Sun, T.T., 2005. Cellular basis of urothelial squamous metaplasia: roles of lineage heterogeneity and cell replacement. J Cell Biol 171, 835-844.

Liang, F.X., Riedel, I., Deng, F.M., Zhou, G., Xu, C., Wu, X.R., Kong, X.P., Moll, R., Sun, T.T., 2001. Organization of uroplakin subunits: transmembrane topology, pair formation and plaque composition. Biochem J 355, 13-18.

Limas, C., 1993. Proliferative state of the urothelium with benign and atypical changes. Correlation with transferrin and epidermal growth factor receptors and blood group antigens. J Pathol 171, 39-47.

Lin, J.H., Wu, X.R., Kreibich, G., Sun, T.T., 1994. Precursor sequence, processing, and urothelium-specific expression of a major 15-kDa protein subunit of asymmetric unit membrane. J Biol Chem 269, 1775-1784.

Liu, J., Huang, J., Lin, T., Zhang, C., Yin, X., 2009. Cell-to-cell contact induces human adipose tissue-derived stromal cells to differentiate into urothelium-like cells in vitro. Biochem Biophys Res Commun 390, 931-936.

Lu, M.J., Zhou, G.D., Liu, W., Wang, Z., Zhu, Y.J., Yu, B., Zhang, W.J., Cao, Y.L., 2010. Remodeling of Buccal Mucosa by Bladder Microenvironment. Urology 75.

Lujan, E., Chanda, S., Ahlenius, H., Sudhof, T.C., Wernig, M., 2012. Direct conversion of mouse fibroblasts to self-renewing, tripotent neural precursor cells. Proc Natl Acad Sci U S A 109, 2527-2532.

Lutz, N., Frey, P., 1995. Enterocystoplasty using modified pedicled, detubularized, de-epithelialized sigmoid patches in the mini-pig model. J Urol 154, 893-898.

Mader, S., Chen, J.Y., Chen, Z., White, J., Chambon, P., Gronemeyer, H., 1993. The patterns of binding of RAR, RXR and TR homo- and heterodimers to direct repeats are dictated by the binding specificites of the DNA binding domains. EMBO J 12, 5029-5041.

Mao-Qiang, M., Fowler, A.J., Schmuth, M., Lau, P., Chang, S., Brown, B.E., Moser, A.H., Michalik, L., Desvergne, B., Wahli, W., Li, M., Metzger, D., Chambon, P.H., Elias, P.M., Feingold, K.R., 2004. Peroxisome-proliferator-activated receptor (PPAR)-gamma activation stimulates keratinocyte differentiation. J Invest Dermatol 123, 305-312.

Markiewicz, M.R., Lukose, M.A., Margarone, J.E., 3rd, Barbagli, G., Miller, K.S., Chuang, S.K., 2007. The oral mucosa graft: a systematic review. J Urol 178, 387-394.

Mascre, G., Dekoninck, S., Drogat, B., Youssef, K.K., Brohee, S., Sotiropoulou, P.A., Simons, B.D., Blanpain, C., 2012. Distinct contribution of stem and progenitor cells to epidermal maintenance. Nature 489, 257-262.

Matter, K., Aijaz, S., Tsapara, A., Balda, M.S., 2005. Mammalian tight junctions in the regulation of epithelial differentiation and proliferation. Curr Opin Cell Biol 17, 453-458.

Mauney, J.R., Ramachandran, A., Yu, R.N., Daley, G.Q., Adam, R.M., Estrada, C.R., 2010. All-trans retinoic acid directs urothelial specification of murine embryonic stem cells via GATA4/6 signaling mechanisms. PLoS One 5, e11513.

Medina-Gomez, G., Virtue, S., Lelliott, C., Boiani, R., Campbell, M., Christodoulides, C., Perrin, C., Jimenez-Linan, M., Blount, M., Dixon, J., Zahn, D., Thresher, R.R., Aparicio, S., Carlton, M., Colledge, W.H., Kettunen, M.I., Seppanen-Laakso, T., Sethi, J.K., O'Rahilly, S., Brindle, K., Cinti, S., Oresic, M., Burcelin, R., Vidal-Puig, A., 2005. The link between nutritional status and insulin sensitivity is dependent on the adipocyte-specific peroxisome proliferator-activated receptor-gamma2 isoform. Diabetes 54, 1706-1716.

Mehra, R., Varambally, S., Ding, L., Shen, R., Sabel, M.S., Ghosh, D., Chinnaiyan, A.M., Kleer, C.G., 2005. Identification of GATA3 as a breast cancer prognostic marker by global gene expression meta-analysis. Cancer Res 65, 11259-11264.

Mikami, H., Kuwahara, G., Nakamura, N., Yamato, M., Tanaka, M., Kodama, S., 2012. Two-Layer Tissue Engineered Urethra Using Oral Epithelial and Muscle Derived Cells. Journal of Urology 187, 1882-1889.

Miura, K., Okada, Y., Aoi, T., Okada, A., Takahashi, K., Okita, K., Nakagawa, M., Koyanagi, M., Tanabe, K., Ohnuki, M., Ogawa, D., Ikeda, E., Okano, H., Yamanaka, S., 2009. Variation in the safety of induced pluripotent stem cell lines. Nat Biotechnol 27, 743-745.

Miyamoto, H., Izumi, K., Yao, J.L., Li, Y., Yang, Q., McMahon, L.A., Gonzalez-Roibon, N., Hicks, D.G., Tacha, D., Netto, G.J., 2012. GATA binding protein 3 is down-regulated in bladder cancer yet strong expression is an independent predictor of poor prognosis in invasive tumor. Hum Pathol 43, 2033-2040.

Moad, M., Pal, D., Hepburn, A.C., Williamson, S.C., Wilson, L., Lako, M., Armstrong, L., Hayward, S.W., Franco, O.E., Cates, J.M., Fordham, S.E., Przyborski, S., Carr-Wilkinson, J., Robson, C.N., Heer, R., 2013. A novel model of urinary tract differentiation, tissue regeneration, and disease: reprogramming human prostate and bladder cells into induced pluripotent stem cells. Eur Urol 64, 753-761.

Molloy, C.J., Laskin, J.D., 1988. Effect of retinoid deficiency on keratin expression in mouse bladder. Exp Mol Pathol 49, 128-140.

Mueller, E., Drori, S., Aiyer, A., Yie, J., Sarraf, P., Chen, H., Hauser, S., Rosen, E.D., Ge, K., Roeder, R.G., Spiegelman, B.M., 2002. Genetic analysis of adipogenesis through peroxisome proliferator-activated receptor gamma isoforms. J Biol Chem 277, 41925-41930.

Muto, S., Hata, M., Taniguchi, J., Tsuruoka, S., Moriwaki, K., Saitou, M., Furuse, K., Sasaki, H., Fujimura, A., Imai, M., Kusano, E., Tsukita, S., Furuse, M., 2010. Claudin-2-deficient mice are defective in the leaky and cation-selective paracellular permeability properties of renal proximal tubules. Proc Natl Acad Sci U S A 107, 8011-8016.

Negrete, H.O., Lavelle, J.P., Berg, J., Lewis, S.A., Zeidel, M.L., 1996. Permeability properties of the intact mammalian bladder epithelium. Am J Physiol 271, F886-894.

Neumann, A., Weill, A., Ricordeau, P., Fagot, J.P., Alla, F., Allemand, H., 2013. Pioglitazone and risk of bladder cancer: clarification of the design of the French study. Reply to Perez AT [letter]. Diabetologia 56, 228-229.

Nguyen, M.M., Lieu, D.K., deGraffenried, L.A., Isseroff, R.R., Kurzrock, E.A., 2007. Urothelial progenitor cells: regional differences in the rat bladder. Cell Prolif 40, 157-165.

Ning, J., Li, C., Li, H., Chang, J., 2011. Bone marrow mesenchymal stem cells differentiate into urothelial cells and the implications for reconstructing urinary bladder mucosa. Cytotechnology 63, 531-539.

Nolte, R.T., Wisely, G.B., Westin, S., Cobb, J.E., Lambert, M.H., Kurokawa, R., Rosenfeld, M.G., Willson, T.M., Glass, C.K., Milburn, M.V., 1998. Ligand binding and co-activator assembly of the peroxisome proliferator-activated receptor-gamma. Nature 395, 137-143.

Oberpenning, F., Meng, J., Yoo, J.J., Atala, A., 1999. De novo reconstitution of a functional mammalian urinary bladder by tissue engineering. Nat Biotechnol 17, 149-155.

Oda, D., Watson, E., 1990. Human oral epithelial cell culture I. Improved conditions for reproducible culture in serum-free medium. In Vitro Cell Dev Biol 26, 589-595.

Ohshima, T., Koga, H., Shimotohno, K., 2004. Transcriptional activity of peroxisome proliferator-activated receptor gamma is modulated by SUMO-1 modification. J Biol Chem 279, 29551-29557.

Oottamasathien, S., Wang, Y., Williams, K., Franco, O.E., Wills, M.L., Thomas, J.C., Saba, K., Sharif-Afshar, A.R., Makari, J.H., Bhowmick, N.A., DeMarco, R.T., Hipkens, S., Magnuson, M., Brock, J.W., 3rd, Hayward, S.W., Pope, J.C.t., Matusik, R.J., 2007. Directed differentiation of embryonic stem cells into bladder tissue. Dev Biol 304, 556-566.

Osborn, S.L., Kurzrock, E.A., 2015. Production of urothelium from pluripotent stem cells for regenerative applications. Curr Urol Rep 16, 466.

Osborn, S.L., Thangappan, R., Luria, A., Lee, J.H., Nolta, J., Kurzrock, E.A., 2014. Induction of human embryonic and induced pluripotent stem cells into urothelium. Stem Cells Transl Med 3, 610-619.

Pang, Z.P., Yang, N., Vierbuchen, T., Ostermeier, A., Fuentes, D.R., Yang, T.Q., Citri, A., Sebastiano, V., Marro, S., Sudhof, T.C., Wernig, M., 2011. Induction of human neuronal cells by defined transcription factors. Nature 476, 220-223.

Pascual, G., Fong, A.L., Ogawa, S., Gamliel, A., Li, A.C., Perissi, V., Rose, D.W., Willson, T.M., Rosenfeld, M.G., Glass, C.K., 2005. A SUMOylation-dependent pathway mediates transrepression of inflammatory response genes by PPAR-gamma. Nature 437, 759-763.

Pedone, P.V., Omichinski, J.G., Nony, P., Trainor, C., Gronenborn, A.M., Clore, G.M., Felsenfeld, G., 1997. The N-terminal fingers of chicken GATA-2 and GATA-3 are independent sequence-specific DNA binding domains. EMBO J 16, 2874-2882.

Pignon, J.C., Grisanzio, C., Geng, Y., Song, J., Shivdasani, R.A., Signoretti, S., 2013. p63-expressing cells are the stem cells of developing prostate, bladder, and colorectal epithelia. Proc Natl Acad Sci U S A 110, 8105-8110.

Piontek, J., Winkler, L., Wolburg, H., Muller, S.L., Zuleger, N., Piehl, C., Wiesner, B., Krause, G., Blasig, I.E., 2008. Formation of tight junction: determinants of homophilic interaction between classic claudins. FASEB J 22, 146-158.

Powell, D.W., 1981. Barrier function of epithelia. Am J Physiol 241, G275-288.

Presland, R.B., Dale, B.A., 2000. Epithelial structural proteins of the skin and oral cavity: function in health and disease. Crit Rev Oral Biol Med 11, 383-408.

Pust, R., Butz, M., Rost, A., Ogbuihi, S., Riedel, B., 1976. Denudation of the urinary bladder mucosa in the cat by formaldehyde. Urol Res 4, 55-61.

Reddy, O.L., Cates, J.M., Gellert, L.L., Crist, H.S., Yang, Z., Yamashita, H., Taylor, J.A., 3rd, Smith, J.A., Jr., Chang, S.S., Cookson, M.S., You, C., Barocas, D.A., Grabowska, M.M., Ye, F., Wu, X.R., Yi, Y., Matusik, R.J., Kaestner, K.H., Clark, P.E., DeGraff, D.J., 2015. Loss of FOXA1 Drives Sexually Dimorphic Changes in Urothelial Differentiation and Is an Independent Predictor of Poor Prognosis in Bladder Cancer. Am J Pathol 185, 1385-1395.

Ricote, M., Li, A.C., Willson, T.M., Kelly, C.J., Glass, C.K., 1998. The peroxisome proliferator-activated receptor-gamma is a negative regulator of macrophage activation. Nature 391, 79-82.

Ring, K.L., Tong, L.M., Balestra, M.E., Javier, R., Andrews-Zwilling, Y., Li, G., Walker, D., Zhang, W.R., Kreitzer, A.C., Huang, Y., 2012. Direct reprogramming of mouse and human fibroblasts into multipotent neural stem cells with a single factor. Cell Stem Cell 11, 100-109.

Rosen, E.D., Hsu, C.H., Wang, X., Sakai, S., Freeman, M.W., Gonzalez, F.J., Spiegelman, B.M., 2002. C/EBPalpha induces adipogenesis through PPARgamma: a unified pathway. Genes Dev 16, 22-26.

Rosen, E.D., Spiegelman, B.M., 2001. PPARgamma : a nuclear regulator of metabolism, differentiation, and cell growth. J Biol Chem 276, 37731-37734.

Rudat, C., Grieskamp, T., Rohr, C., Airik, R., Wrede, C., Hegermann, J., Herrmann, B.G., Schuster-Gossler, K., Kispert, A., 2014. Upk3b is dispensable for development and integrity of urothelium and mesothelium. PLoS One 9, e112112.

Sabatino, L., Casamassimi, A., Peluso, G., Barone, M.V., Capaccio, D., Migliore, C., Bonelli, P., Pedicini, A., Febbraro, A., Ciccodicola, A., Colantuoni, V., 2005. A novel peroxisome proliferator-activated receptor gamma isoform with dominant negative activity generated by alternative splicing. J Biol Chem 280, 26517-26525.

Segre, J.A., Bauer, C., Fuchs, E., 1999. Klf4 is a transcription factor required for establishing the barrier function of the skin. Nat Genet 22, 356-360.

Shi, J.G., Fu, W.J., Wang, X.X., Xu, Y.D., Li, G., Hong, B.F., Hu, K., Cui, F.Z., Wang, Y., Zhang, X., 2012. Transdifferentiation of human adipose-derived stem cells into urothelial cells: potential for urinary tract tissue engineering. Cell Tissue Res.

Shin, K., Lee, J., Guo, N., Kim, J., Lim, A., Qu, L., Mysorekar, I.U., Beachy, P.A., 2011. Hedgehog/Wnt feedback supports regenerative proliferation of epithelial stem cells in bladder. Nature 472, 110-114.

Slack, J.M., 2007. Metaplasia and transdifferentiation: from pure biology to the clinic. Nat Rev Mol Cell Biol 8, 369-378.

Smith, N.J., Hinley, J., Varley, C.L., Eardley, I., Trejdosiewicz, L.K., Southgate, J., 2015. The human urothelial tight junction: claudin 3 and the ZO-1alpha switch. Bladder (San Franc) 2, e9.

Southgate, J., Harnden, P., Trejdosiewicz, L.K., 1999. Cytokeratin expression patterns in normal and malignant urothelium: a review of the biological and diagnostic implications. Histol Histopathol 14, 657-664.

Southgate, J., Hutton, K.A., Thomas, D.F., Trejdosiewicz, L.K., 1994. Normal human urothelial cells in vitro: proliferation and induction of stratification. Lab Invest 71, 583-594.

Squier, C.A., 1977. Membrane coating granules in nonkeratinizing oral epithelium. J Ultrastruct Res 60, 212-220.

Staack, A., Hayward, S.W., Baskin, L.S., Cunha, G.R., 2005. Molecular, cellular and developmental biology of urothelium as a basis of bladder regeneration. Differentiation 73, 121-133.

Stahlschmidt, J., Varley, C.L., Toogood, G., Selby, P.J., Southgate, J., 2005. Urothelial differentiation in chronically urine-deprived bladders of patients with end-stage renal disease. Kidney Int 68, 1032-1040.

Steed, E., Balda, M.S., Matter, K., 2010. Dynamics and functions of tight junctions. Trends Cell Biol 20, 142-149.

Strand, D.W., DeGraff, D.J., Jiang, M., Sameni, M., Franco, O.E., Love, H.D., Hayward, W.J., Lin-Tsai, O., Wang, A.Y., Cates, J.M., Sloane, B.F., Matusik, R.J., Hayward, S.W., 2013. Deficiency in metabolic regulators PPARgamma and PTEN cooperates to drive keratinizing squamous metaplasia in novel models of human tissue regeneration. Am J Pathol 182, 449-459.

Su, J.L., Winegar, D.A., Wisely, G.B., Sigel, C.S., Hull-Ryde, E.A., 1999. Use of a PPAR gamma-specific monoclonal antibody to demonstrate thiazolidinediones induce PPAR gamma receptor expression in vitro. Hybridoma 18, 273-280.

Subramaniam, R., Hinley, J., Stahlschmidt, J., Southgate, J., 2011. Tissue engineering potential of urothelial cells from diseased bladders. J Urol 186, 2014-2020.

Sugasi, S., Lesbros, Y., Bisson, I., Zhang, Y.Y., Kucera, P., Frey, P., 2000. In vitro engineering of human stratified urothelium: analysis of its morphology and function. J Urol 164, 951-957.

Sun, T.T., Zhao, H., Provet, J., Aebi, U., Wu, X.R., 1996. Formation of asymmetric unit membrane during urothelial differentiation. Mol Biol Rep 23, 3-11.

Sun, W., Wilhelmina Aalders, T., Oosterwijk, E., 2014. Identification of potential bladder progenitor cells in the trigone. Dev Biol 393, 84-92.

Tamori, Y., Masugi, J., Nishino, N., Kasuga, M., 2002. Role of peroxisome proliferator-activated receptor-gamma in maintenance of the characteristics of mature 3T3-L1 adipocytes. Diabetes 51, 2045-2055.

Tanaka, T., Yoshida, N., Kishimoto, T., Akira, S., 1997. Defective adipocyte differentiation in mice lacking the C/EBPbeta and/or C/EBPdelta gene. EMBO J 16, 7432-7443.

Thangappan, R., Kurzrock, E.A., 2009. Three clonal types of urothelium with different capacities for replication. Cell Prolif 42, 770-779.

Theodorou, V., Stark, R., Menon, S., Carroll, J.S., 2013. GATA3 acts upstream of FOXA1 in mediating ESR1 binding by shaping enhancer accessibility. Genome Res 23, 12-22.

Thier, M., Worsdorfer, P., Lakes, Y.B., Gorris, R., Herms, S., Opitz, T., Seiferling, D., Quandel, T., Hoffmann, P., Nothen, M.M., Brustle, O., Edenhofer, F., 2012. Direct conversion of fibroblasts into stably expandable neural stem cells. Cell Stem Cell 10, 473-479.

Thomas, J.C., Oottamasathien, S., Makari, J.H., Honea, L., Sharif-Afshar, A.R., Wang, Y., Adams, C., Wills, M.L., Bhowmick, N.A., Adams, M.C., Brock, J.W., 3rd, Hayward, S.W., Matusik, R.J., Pope, J.C.t., 2008. Temporal-spatial protein expression in bladder tissue derived from embryonic stem cells. J Urol 180, 1784-1789.

Tian, H., Bharadwaj, S., Liu, Y., Ma, P.X., Atala, A., Zhang, Y., 2010. Differentiation of human bone marrow mesenchymal stem cells into bladder cells: potential for urological tissue engineering. Tissue Eng Part A 16, 1769-1779.

Ting, S.B., Caddy, J., Hislop, N., Wilanowski, T., Auden, A., Zhao, L.L., Ellis, S., Kaur, P., Uchida, Y., Holleran, W.M., Elias, P.M., Cunningham, J.M., Jane, S.M., 2005. A homolog of Drosophila grainy head is essential for epidermal integrity in mice. Science 308, 411-413.

Tong, Q., Dalgin, G., Xu, H., Ting, C.N., Leiden, J.M., Hotamisligil, G.S., 2000. Function of GATA transcription factors in preadipocyte-adipocyte transition. Science 290, 134-138.

Tontonoz, P., Hu, E., Graves, R.A., Budavari, A.I., Spiegelman, B.M., 1994. mPPAR gamma 2: tissue-specific regulator of an adipocyte enhancer. Genes Dev 8, 1224-1234.

Tsukita, S., Furuse, M., Itoh, M., 2001. Multifunctional strands in tight junctions. Nat Rev Mol Cell Biol 2, 285-293.

Turner, A., Subramanian, R., Thomas, D.F., Hinley, J., Abbas, S.K., Stahlschmidt, J., Southgate, J., 2011. Transplantation of autologous differentiated urothelium in an experimental model of composite cystoplasty. Eur Urol 59, 447-454.

Umeda, K., Ikenouchi, J., Katahira-Tayama, S., Furuse, K., Sasaki, H., Nakayama, M., Matsui, T., Tsukita, S., Furuse, M., Tsukita, S., 2006. ZO-1 and ZO-2 independently determine where claudins are polymerized in tight-junction strand formation. Cell 126, 741-754.

Van Itallie, C.M., Anderson, J.M., 2014. Architecture of tight junctions and principles of molecular composition. Semin Cell Dev Biol 36, 157-165.

Varley, C., Hill, G., Pellegrin, S., Shaw, N.J., Selby, P.J., Trejdosiewicz, L.K., Southgate, J., 2005. Autocrine regulation of human urothelial cell proliferation and migration during regenerative responses in vitro. Exp Cell Res 306, 216-229.

Varley, C.L., Bacon, E.J., Holder, J.C., Southgate, J., 2009. FOXA1 and IRF-1 intermediary transcriptional regulators of PPARgamma-induced urothelial cytodifferentiation. Cell Death Differ 16, 103-114.

Varley, C.L., Garthwaite, M.A., Cross, W., Hinley, J., Trejdosiewicz, L.K., Southgate, J., 2006. PPARgamma-regulated tight junction development during human urothelial cytodifferentiation. J Cell Physiol 208, 407-417.

Varley, C.L., Southgate, J., 2008. Effects of PPAR agonists on proliferation and differentiation in human urothelium. Exp Toxicol Pathol 60, 435-441.

Varley, C.L., Stahlschmidt, J., Lee, W.C., Holder, J., Diggle, C., Selby, P.J., Trejdosiewicz, L.K., Southgate, J., 2004a. Role of PPARgamma and EGFR signalling in the urothelial terminal differentiation programme. J Cell Sci 117, 2029-2036.

Varley, C.L., Stahlschmidt, J., Smith, B., Stower, M., Southgate, J., 2004b. Activation of peroxisome proliferator-activated receptor-gamma reverses squamous metaplasia and induces transitional differentiation in normal human urothelial cells. Am J Pathol 164, 1789-1798.

Vierbuchen, T., Ostermeier, A., Pang, Z.P., Kokubu, Y., Sudhof, T.C., Wernig, M., 2010. Direct conversion of fibroblasts to functional neurons by defined factors. Nature 463, 1035-1041.

Wada, R., Muraoka, N., Inagawa, K., Yamakawa, H., Miyamoto, K., Sadahiro, T., Umei, T., Kaneda, R., Suzuki, T., Kamiya, K., Tohyama, S., Yuasa, S., Kokaji, K., Aeba, R., Yozu, R., Yamagishi, H., Kitamura, T., Fukuda, K., Ieda, M., 2013. Induction of human cardiomyocyte-like cells from fibroblasts by defined factors. Proc Natl Acad Sci U S A 110, 12667-12672.

Wan, Y.Y., 2014. GATA3: a master of many trades in immune regulation. Trends Immunol 35, 233-242.

Watanabe, E., Yamato, M., Shiroyanagi, Y., Tanabe, K., Okano, T., 2011. Bladder Augmentation Using Tissue-Engineered Autologous Oral Mucosal Epithelial Cell Sheets Grafted on Demucosalized Gastric Flaps. Transplantation 91, 700-706.

Wei, G., Abraham, B.J., Yagi, R., Jothi, R., Cui, K., Sharma, S., Narlikar, L., Northrup, D.L., Tang, Q., Paul, W.E., Zhu, J., Zhao, K., 2011. Genome-wide analyses of transcription factor GATA3-mediated gene regulation in distinct T cell types. Immunity 35, 299-311.

Wertz, P.W., Cox, P.S., Squier, C.A., Downing, D.T., 1986. Lipids of epidermis and keratinized and non-keratinized oral epithelia. Comp Biochem Physiol B 83, 529-531.

Westergaard, M., Henningsen, J., Svendsen, M.L., Johansen, C., Jensen, U.B., Schroder, H.D., Kratchmarova, I., Berge, R.K., Iversen, L., Bolund, L., Kragballe, K., Kristiansen, K., 2001. Modulation of keratinocyte gene expression and differentiation by PPAR-selective ligands and tetradecylthioacetic acid. J Invest Dermatol 116, 702-712.

Wezel, F., Pearson, J., Southgate, J., 2014. Plasticity of in vitro-generated urothelial cells for functional tissue formation. Tissue Eng Part A 20, 1358-1368.

Winning, T.A., Townsend, G.C., 2000. Oral mucosal embryology and histology. Clin Dermatol 18, 499-511.

Wu, S., Cheng, Z., Liu, G., Zhao, X., Zhong, L., Zhu, Y., Zhu, J., 2013. Urothelial differentiation of human umbilical cord-derived mesenchymal stromal cells in vitro. Anal Cell Pathol (Amst) 36, 63-69.

Wu, X.R., Medina, J.J., Sun, T.T., 1995a. Selective interactions of UPIa and UPIb, two members of the transmembrane 4 superfamily, with distinct single transmembrane-domained proteins in differentiated urothelial cells. J Biol Chem 270, 29752-29759.

Wu, X.R., Sun, T.T., 1993. Molecular cloning of a 47 kDa tissue-specific and differentiation-dependent urothelial cell surface glycoprotein. J Cell Sci 106 (Pt 1), 31-43.

Wu, Z., Xie, Y., Bucher, N.L., Farmer, S.R., 1995b. Conditional ectopic expression of C/EBP beta in NIH-3T3 cells induces PPAR gamma and stimulates adipogenesis. Genes Dev 9, 2350-2363.

Xie, H., Ye, M., Feng, R., Graf, T., 2004. Stepwise reprogramming of B cells into macrophages. Cell 117, 663-676.

Xu, J., Du, Y., Deng, H., 2015. Direct lineage reprogramming: strategies, mechanisms, and applications. Cell Stem Cell 16, 119-134.

Xu, J., Kausalya, P.J., Phua, D.C., Ali, S.M., Hossain, Z., Hunziker, W., 2008. Early embryonic lethality of mice lacking ZO-2, but Not ZO-3, reveals critical and nonredundant roles for individual zonula occludens proteins in mammalian development. Mol Cell Biol 28, 1669-1678.

Xu, Y.M., Sa, Y.L., Qiao, Y., Zhang, H.Z., Zhang, X.R., Zhang, J., Chen, Z., Xie, H., Si, J.M., Li, T., 2005. Histopathological changes of free buccal mucosa and colonic mucosa grafts after translation to dog bladder. Chinese Medical Journal 118, 337-339.

Xue, Y., Ouyang, K., Huang, J., Zhou, Y., Ouyang, H., Li, H., Wang, G., Wu, Q., Wei, C., Bi, Y., Jiang, L., Cai, Z., Sun, H., Zhang, K., Zhang, Y., Chen, J., Fu, X.D., 2013. Direct conversion of fibroblasts to neurons by reprogramming PTB-regulated microRNA circuits. Cell 152, 82-96.

Yang, A., Schweitzer, R., Sun, D., Kaghad, M., Walker, N., Bronson, R.T., Tabin, C., Sharpe, A., Caput, D., Crum, C., McKeon, F., 1999. p63 is essential for regenerative proliferation in limb, craniofacial and epithelial development. Nature 398, 714-718.

Yoo, A.S., Sun, A.X., Li, L., Shcheglovitov, A., Portmann, T., Li, Y., Lee-Messer, C., Dolmetsch, R.E., Tsien, R.W., Crabtree, G.R., 2011. MicroRNA-mediated conversion of human fibroblasts to neurons. Nature 476, 228-231.

Yoo, J.J., Meng, J., Oberpenning, F., Atala, A., 1998. Bladder augmentation using allogenic bladder submucosa seeded with cells. Urology 51, 221-225.

Yu, J., Lin, J.H., Wu, X.R., Sun, T.T., 1994. Uroplakins Ia and Ib, two major differentiation products of bladder epithelium, belong to a family of four transmembrane domain (4TM) proteins. J Cell Biol 125, 171-182.

Yu, Z., Mannik, J., Soto, A., Lin, K.K., Andersen, B., 2009. The epidermal differentiation-associated Grainyhead gene Get1/Grhl3 also regulates urothelial differentiation. EMBO J 28, 1890-1903.

Zaret, K.S., Carroll, J.S., 2011. Pioneer transcription factors: establishing competence for gene expression. Genes Dev 25, 2227-2241.

Zhang, B., Berger, J., Zhou, G., Elbrecht, A., Biswas, S., White-Carrington, S., Szalkowski, D., Moller, D.E., 1996. Insulin- and mitogen-activated protein kinase-mediated phosphorylation and activation of peroxisome proliferator-activated receptor gamma. J Biol Chem 271, 31771-31774.

Zhang, H., Lin, G., Qiu, X., Ning, H., Banie, L., Lue, T.F., Lin, C.S., 2012. Label retaining and stem cell marker expression in the developing rat urinary bladder. Urology 79, 746 e741-746.

Zhang, J., Fu, M., Cui, T., Xiong, C., Xu, K., Zhong, W., Xiao, Y., Floyd, D., Liang, J., Li, E., Song, Q., Chen, Y.E., 2004. Selective disruption of PPARgamma 2 impairs the development of adipose tissue and insulin sensitivity. Proc Natl Acad Sci U S A 101, 10703-10708.

Zhang, Y., McNeill, E., Tian, H., Soker, S., Andersson, K.E., Yoo, J.J., Atala, A., 2008. Urine derived cells are a potential source for urological tissue reconstruction. J Urol 180, 2226-2233.

Zhao, J., Zeiai, S., Ekblad, A., Nordenskjold, A., Hilborn, J., Gotherstrom, C., Fossum, M., 2014. Transdifferentiation of autologous bone marrow cells on a collagen-

poly(epsilon-caprolactone) scaffold for tissue engineering in complete lack of native urothelium. J R Soc Interface 11, 20140233.

Zhao, L., Antic, T., Witten, D., Paner, G.P., Taxy, J.B., Husain, A., Gwin, K., Mirza, M.K., Lingen, M.W., Tretiakova, M.S., 2013. Is GATA3 expression maintained in regional metastases?: a study of paired primary and metastatic urothelial carcinomas. Am J Surg Pathol 37, 1876-1881.